Gorachand Dutta *Editor*

Next-Generation Nanobiosensor Devices for Point-Of-Care Diagnostics

Springer

Next-Generation Nanobiosensor Devices for Point-Of-Care Diagnostics

Gorachand Dutta
Editor

Next-Generation Nanobiosensor Devices for Point-Of-Care Diagnostics

Springer

Editor
Gorachand Dutta
School of Medical Science and
Technology
Indian Institute of Technology Kharagpur
Kharagpur, West Bengal, India

ISBN 978-981-19-7129-7 ISBN 978-981-19-7130-3 (eBook)
https://doi.org/10.1007/978-981-19-7130-3

This Springer imprint is published by the registered company Springer Nature Singapore Pte Ltd.
The registered company address is: 152 Beach Road, #21-01/04 Gateway East, Singapore 189721, Singapore

Preface

The modern era makes our life more complex. This emergence of dynamic complexity even in healthcare sectors makes the world to come up with a smart solution. The evolution of point-of-care testing provides medical diagnosis within and outside the laboratory. Such bench-to-bedside diagnosis advances patient management to a great extent. To cater to the needs, a significant amount of focus has been dedicated to developing an inexpensive, accurate, sensitive point-of-care device at an affordable price to reach the common people.

Rapid detection and point-of-care (POC) diagnostics have become very crucial especially after the life-threatening coronavirus pandemic. The pandemic has proved that despite tremendous advances in medical sciences and technology, sorely we are lagging in healthcare research. Detection schemes can be realized with an electrochemical platform, thanks to its promising advantages like low-to-moderate cost, high sensitivity, and selectivity with a lower limit of detection (LOD), rapid response, and easy integration with microfluidic systems. A variety of signal amplification methods based on electrochemical-chemical-chemical (ECC) redox cycling and rolling circle amplification (RCA) have been explored. Integration of these systems opens a new horizon to fabricate miniaturized devices, disposability, need for less sample volume, multiplex, and POC sensing ability.

Our motto is to fabricate a label-free, wash-free, and portable electrochemical biosensor for point-of-care application and early detection of disease. It will be in the form of a handheld or bench-top instrument which will accept a sample with very little or no pre-preparation and can provide a comprehensible result in seconds to hours for easy interpretation. *Next-Generation Nanobiosensor Devices for Point-of-Care Diagnostics* was prepared for beginning and experienced authors to explore the challenges for the development of next-generation point-of-care test platform using nanobiotechnology.

In this book, we address these challenges for the development of a point-of-care test platform. The book also describes printed chip-based assays (Lab-on-a-Chip, Lab-on-a-PCB) for rapid, inexpensive, biomarkers detection in real samples. The main challenges of point-of-care testing require implementing complex analytical methods into low-cost technologies. This is particularly true for countries with less developed healthcare infrastructure. Wash-free, Lab-on-a-Chip, and Lab-on-a-PCB techniques are very simple and innovative for point-of-care device development.

The redox cycling technology can detect several interesting targets at the same time on a printed chip. The areas are inherently cross-disciplinary, combining expertise in biosensing, electrochemistry, electronics and electrical engineering, healthcare, and manufacturing. Other focus audience includes physical and chemical science scientists who are involved in the development of an analytical device for the easy and early detection of chronic diseases. Furthermore, other than research purposes, this book can potentially also be helpful for nanobiotechnology and biomedical engineering teachers and students. Besides, chapters are organized in such a way that the reader can easily understand the emphasis of each chapter's focus to select appropriate biosensors of interest. The title covers a very vast audience from basic science to engineering and technology experts and learners. This could eventually work as a textbook for engineering and biomedical students or science master's programs and for researchers. This title also serves the common public interest by presenting new methods for data evaluation and medical diagnosis to improve the quality of life in general, with a better integration into society.

Kharagpur, India Gorachand Dutta

Contents

About the Editor

Gorachand Dutta PhD is an Assistant Professor with the School of Medical Science and Technology, Indian Institute of Technology Kharagpur. His research interests include the design and characterization of portable biosensors, biodevices, and sensor interfaces for miniaturized systems and biomedical applications for point-of-care testing. He received his Ph.D. in Biosensor and Electrochemistry from Pusan National University, South Korea, where he developed different classes of electrochemical sensors. He completed his postdoctoral fellowships in the Department of Mechanical Engineering, Michigan State University, USA, and the Department of Electronic and Electrical Engineering at the University of Bath, UK. He has expertise on label-free multichannel electrochemical biosensors, electronically addressable biosensor arrays, aptamer- and DNA-based sensors and surface bio-functionalization.

He is recipient of many prestigious awards and fellowships, such as the prestigious Pusan National University Research Fellowship, BK-21 Fellowship South Korea.

Recent Development in Detection Systems for Human Viral Pathogens from Clinical Samples with Special Reference to Biosensors

Kamal Shokeen, Purvita Chowdhury, and Sachin Kumar

Abstract

Over the last few decades, the emergence and re-emergence of various pathogenic viruses have significantly impacted human health. The continuous rise in cases with increasing mortality rates has driven the chase for effective treatment options and early diagnosis to combat this global health issue. Currently, used laboratory techniques for virus detection require complex equipment, trained personnel, and, most importantly, are time-consuming. In times of outbreaks and epidemics like COVID-19 and Ebola, easy-to-use and point-of-care tests, especially for developing and underdeveloped countries, are indispensable.

This chapter explicitly discusses the availability of the detection methods for various human viral pathogens with their shortcomings and recent advancements in biosensors. With the ongoing improvement in biosensors, these hold important avenues for rapid, sensitive, and scalable devices for viral diagnostic purposes. The effectiveness of previously known and current approaches/devices/methods that utilize different principles for detection has also been reviewed here, with the listing of all the available tests for various human pathogens.

Keywords

Virus · Biosensor · Viral protein · Viral nucleic acid · Diagnosis

K. Shokeen · P. Chowdhury · S. Kumar (✉)
Department of Biosciences and Bioengineering, Indian Institute of Technology Guwahati, Guwahati, India
e-mail: sachinku@iitg.ac.in

G. Dutta (ed.), *Next-Generation Nanobiosensor Devices for Point-Of-Care Diagnostics*, https://doi.org/10.1007/978-981-19-7130-3_1

1 Preamble

Viral infections are a considerable threat to global health despite numerous efforts that have been made for their prevention and control. We constantly witness the emergence of new viruses and sometimes appearances of previously known viral diseases, which can infect and cause disease with fatal consequences [1]. Presently, humans are known to be infected with 219 reported virus species, and newer species are still being found every year [2, 3], and all are adept at causing devastating diseases. As the more contemporary species will continue to emerge and cause devastation to the global population, an efficient detection, and prevention system for early diagnosis and proper treatment is required to control the fatalities [4, 5]. These viral species are genetically diverse with varying pathogenicity and genotypes; therefore, the need for detection and differentiation systems with higher accuracy and sensitivity has increased significantly in the last few years. Proper attention must be bestowed to detect more efficiently to avoid future epidemics and outbreaks. There has been a sudden emergence of many viral infections over the last few decades, including human immunodeficiency virus (HIV) [6], influenza A virus [7], severe acute respiratory syndrome coronavirus (SARS-CoV), middle east respiratory syndrome coronavirus (MERS-CoV) [8], and most recently, Ebola [9, 10], Zika [11], and SARS-CoV-2 [12] throughout the world [13]. The ease with which the viruses can spread worldwide within days apprises that a global-level surveillance system is essential to detect novel viruses rapidly.

To prevent the deaths and rapid spreading of the disease, performing an accurate screening for early detection is vital. Diagnosis methods for viruses have progressed rapidly from animal inoculation to computer automation. There has been a continuous development of new detection methods based on molecular and cellular approaches. Some of the available techniques detect viral genomes or proteins, while others detect viable virions. Presently, several detection methods are available associated with PCR, CRISPR/Cas system, immunoassays, cell-based assays, and next-generation sequencing (NGS) [14]. Each screening test provides complementary advantages and disadvantages. No one system can provide a rapid and reliable method for detection in the real world; thus, improved screening systems are urgently needed. Identifying the viral agents is essential to managing patients while reducing the risk of spread appropriately. Presently, all the recent technological advancements focusing on the technical fallacies of traditional approaches are yet to be resolved in this field.

2 Direct Cultivation Approach

Cell culture inoculation is the conventional approach for detecting and identifying many human viral pathogens [15]. Cell cultures have provided a suitable environment for isolation and culturing the viruses; however, the process is slow, technologically sophisticated, and needs the expertise to read cytopathic effects [16]. Generally, several different cell lines are being used for the culture and

detection of viruses with differences in efficiency and specificity. The most extensively used cell lines used for viral detection are Madin-Darby canine kidney (MDCK) cells, primary rhesus monkey kidney (RhMK) cells, primary rabbit kidney (RK13) cells, human foreskin fibroblasts (hFFs), human lung fibroblasts (MRC-5), Vero cells, human epidermoid carcinoma (HEp-2) cells, and human lung carcinoma (A549) cells [17]. Studying the growth patterns usually require maintaining a variety of cells, then inoculating the pathogens followed by a minimum of 24 h of incubation to yield observable outcomes. Culturing the viruses in cell lines helps determine viral particles and characterize their properties and behavior, which ultimately helps develop various treatment methods.

Additionally, the viruses propagated in the cell can further be used to study morphology by electron microscopy. The approach has more limitations for non-culturable viruses than advantages [18]. Thus, it was quickly replaced by a nucleic acid-based amplification approach, mainly polymerase chain reaction (PCR), which helped rapidly detect unculturable or fastidious pathogens directly from clinical samples [19, 20].

3 Nucleic Acid-Based Approach

The idea of sequence analysis by PCR offered better identification and characterization of the pathogen with more reliable, reproducible, and specific outcomes for a broader panel of viruses [21]. The assertive approach of PCR helps synthesize millions of copies of the particular segment in vitro from a modicum amount, which is undetectable by any other method. Detection of the pathogen by PCR requires the knowledge of unique nucleotide segments on the DNA to synthesize the primers complementary to the sequences flanking the distinctive region. Generally, two primers are used for annealing the sense and antisense strand simultaneously; further, a thermostable DNA polymerase extends the primers simply by adding complementary nucleotides [22]. From time to time, advancements in conventional methodology were made to make them easy to use, precise, and efficient in virus detection even at the early stages of the disease [23–26]. The cell culture methods are often coupled with PCR to yield robust results [27]. A better understanding of viral genomes and their pathogenicity has helped us develop upgraded amplification systems to detect them [28, 29].

3.1 Real-Time PCR

Real-time Polymerase Chain Reaction (RT-PCR)-based detection system was considered the gold standard for detecting all types of viruses for a very long time [30–33]. This approach has been used to successfully diagnose dengue infection, Japanese encephalitis virus, SARS-CoV-2, and many other viruses [34–36]. It produced the most sensitive quantification by determining the viral load level in symptomatic and non-symptomatic individuals [37]. It also offered noninvasive sampling and

easy collection methods from patients' saliva and other bodily fluids. However, the process requires total RNA isolation from the samples, then the synthesis of complementary first strand DNA followed by RT-PCR amplification, making it time consuming [38]. Additionally, the outputs were also linked with false negatives, and they only detect the presence of viral genomes and not the live infectious viral particle [39–41]. Other significant problems associated are detecting only known viruses, difficulty in identifying viruses with high genome variability, and the inability to differentiate between infectious and noninfectious viruses. Despite all the necessary changes and improvements, they have not been suitable for large-scale use. They are relatively expensive, labor intensive, and require equipment, making them incompatible with use in remote locations. All these fallacies accentuated the need to direct our efforts toward working on low-cost and accessible diagnostic procedures.

3.2 Isothermal PCR

The RT-PCR test is usually performed in a thermal cycler, which requires a constant power supply. A proper temperature is needed for amplification by polymerase enzyme, making the process impossible to carry out on fields. Recent advancements have made the process temperature independent by utilizing enzymes to separate the strand. This powerful diagnostic tool offers nucleic acid amplification at a stable temperature without the need for expensive instruments or reagents [42]. The fluorescence dye can visualize the outcome surpassing the endpoint detection limitations. Loop-mediated isothermal amplification-based assay (LAMP) is one widely used approach to detecting several human viruses [43, 44]. The primers are responsible for accurate results, as several pairs are required with the optimized location. Several refinements, the addition of quencher or replacement of fluorescent dye, have also been made to make the system more efficient but still failed to produce accurate results for low viral load samples. Due to the complexity of primer designing and false negatives, this approach could not satisfy the urgent need for an effective diagnostic method. Still, it has been considered to diagnose the SARS-CoV-2 virus [45, 46].

3.3 Droplet Digital PCR

The digital droplet PCR (ddPCR) is the new generation absolute quantification assay for nucleic acids, an improvement of the conventional PCR technique. Due to its high sensitivity for absolute viral load concentrations, robustness against PCR inhibitors, and reproducibility, ddPCR is a promising technique for viral identification. In this technique, the nucleic acid is quantified through numerous partitioned reactions where the sample is captured inside an oil and immiscible fluid droplet. After amplification, the concentration of the sample is determined using Poisson's

statistics. Several platforms have been commercialized for ddPCR, and tests for detecting SARS-CoV-2, HIV, and Herpes virus have been reported [47–49].

3.4 Nucleic Acid Sequencing

Sequencing is the rapidly growing approach that helps pathogen identification and determines the circulating strain's pathogenic nature. Sanger sequencing is the widely used method based on the principle of chain termination during DNA amplification. This approach involves using fluorophores labeled dideoxynucleotides (ddNTPs), leading to chain termination during amplification when incorporated into the newly synthesized strand. Significant limitations of the classical technique are their speed, read length, and low throughput, due to template preparation and the enzymatic reactions [50]. The evolution of sequencing technologies has drastically reduced the rate at which multiple samples can be simultaneously analyzed [51]. Developing a high-throughput version of the classical method helped quickly obtain first-hand information about the viral genome and its pathogenicity.

NGS-based testing provides a comprehensive and feasible approach to determining the genomic sequence, even more than one million base pairs in a single experiment [52]. The NGS platform's key factors are read length, throughput, read accuracy, read depth, and cost per base. Several NGS-based sequencing platforms, including pyrosequencing, Ion torrent technology, Illumina/Solexa, and SOLiD (Sequencing by Oligonucleotide Ligation and Detection) have revolutionized sequencing [53]. The identification of viruses by the NGS method includes sample preparation, sequencing, processing raw data using bioinformatics tools, and finally, analysis and interpretation. It has excellent prominence for identifying unknown pathogen and differentiating circulating strains by incorporating mutations. Still, the massive cost of the equipment and reagents required restricts its application in routine diagnostic laboratories. The prime problem associated with this approach is generating a large amount of data, which requires an efficient data interpretation procedure. Recent studies have shown the usage of NGS-based methods for discovering the newly emerging and circulating strains of SARS-CoV-2 [53]. The rapid screening and accumulation of sequence of all the strains have immensely helped generate phylogenetic trees revealing all the closely related variants and their origin. Even the slightest difference in the nucleotide sequence in the spike protein could be detected rapidly through genome sequencing to identify the variants and for evolutionary analysis [54, 55].

3.5 CRISPR/Cas-Based Systems

The discovery and growing research on clustered regularly interspaced short palindromic repeats (CRISPR) and CRISPR-associated proteins (Cas) have paved the way for a novel molecular diagnostic platform for viral detection. Their high

programmability and specificity make them ideal molecular sensors for detecting target DNA in vitro. These sequences are essentially present in bacteria as their adaptive immune response mechanism [56]. Thus, the RNA-guided nucleases cleaved the foreign nucleic acid attacking the bacterial cell. Among these systems, CRISPR/Cas12a and CRISPR/Cas13a have been the most widely explored for nucleic acid detection [57]. A CRISPR/Cas13a-based point-of-care platform was proposed, known as SHERLOCK, to detect Zika and dengue virus nucleic acid [58].

4 Protein-Based Approach

Serological assays were also developed to detect virus-specific antibody responses offering faster and hassle-free detection [59]. The available tests include virus neutralization, hemagglutination, single radial hemolysis, complement fixation, and indirect immunofluorescence. They directly determine viral proteins and indirect determination of Immunoglobulin G (IgG) and IgM antibodies in the serum samples without preprocessing. The enzyme-linked immunoassay (ELISA) is the most commonly performed immunoassay in most laboratories to detect virus antigen-specific antibodies. Generally, the antigen is bound to absorbent polypropylene plates for this technique. When the unknown serum sample is added, it forms an antigen-antibody complex which is further attached to specific conjugated antibodies. The reaction is detected with an indicator to evaluate the amount of response [60].

4.1 Hemagglutination Assay

An inexpensive and classical screening technique is commonly used to detect influenza virus from isolates harvested from embryonated chicken allantoic fluid or cell culture. The surface hemagglutinin protein of influenza virus binds to the N-acetyl neuraminic acid of avian erythrocytes, resulting in an agglutination reaction where the erythrocytes form a lattice and precipitate. A quantitative assay denotes that one hemagglutinating unit is equivalent to 5–6 logs of the virus [61].

4.2 Hemagglutination Inhibition Assay

It is one of the primary and most reliable assays to quantify the antibodies and subtype determination for influenza virus. The hemagglutination inhibition assay (HI) principle depends on the Hemagglutination Assay (HA) activity of the virus, and serial dilutions of serum with virus and erythrocytes are incubated for the test. If antibodies against the virus are present in the serum, the binding of erythrocytes to the influenza hemagglutinin protein, i.e., hemagglutination, is inhibited. The highest dilution of serum that ultimately shows HI is considered the HI titer [62]. This test is feasible for influenza viruses, parainfluenza viruses, and arthropod-borne viruses like West Nile and the Japanese encephalitis virus [63–65].

4.3 Virus Neutralization Assay

The serological virus neutralization assay is performed to assess the presence and magnitude of functional antibodies that can prevent virus infectivity in vitro. Conventionally, the antibody titer is determined based on the presence of a cytopathic effect or immunoreactive test. This method detects antibodies in serum against several viruses like Influenza, Dengue, and SARS-CoV-2, which are detected by this method [66–68].

4.4 Lateral Flow Immunoassay

One of the most commonly used technologies for rapidly detecting viral antigens is the lateral flow immunoassay or immunochromatographic assay. When a clinical sample is put into the absorbent chromatographic paper, it is drawn toward the conjugate paper by capillary action. The conjugate paper has immobilized specific monoclonal antibodies conjugated with a colored particle (colloidal gold) and primarily reacts with the viral antigen. The antigen–antibody complex, if formed, is carried by the capillary flow effect to an immobilized specific antibody bound to a reaction membrane and can be observed as a colored line [69]. Numerous rapid antigen detection kits have been developed using this technology for diagnosing diseases like COVID-19, Dengue, Zika, and Influenza [70–72].

The immunological approach not only helps in identifying the viral protein but also in characterizing the virus properties. However, such serological methods are limited in their diagnostic value due to cross-reactivity among different viruses belonging to the same family. There are also some chances of obtaining false results due to the failure of antibody attachment. The detectable IgM and IgG antibodies are only produced after a few days of onset of symptoms; therefore, the test sometimes fails to give a positive outcome in patients with mild infection or who fail to develop antibodies. These problems pose barriers to early diagnosis as the present situation demands rapid and point-of-care testing assays.

5 Biosensor-Based Approach

Biosensors are independent consolidated devices with three major components: i) a bioreceptor, ii) a transducer, and iii) a digital output detector. Biosensors produce quantitative or semiquantitative-specific analytical information. Primarily, an immobilized biological element like a DNA probe, enzyme, or antibody acts as a bioreceptor that recognizes and interacts with a target biological analyte like complementary DNA, enzyme–substrate, or antigen [73]. The changes produced from the interaction are thus converted to measurable signals by the transducers and then quantified by the digital detectors.

The essential features for the performance of a biosensor are:

1. The primary characteristic is the selective recognition of a specific biological analyte in a sample composed of a mixture of components. Therefore, depending on the need, a particular bioreceptor is determined [74].
2. Secondly, the reproducibility of signal output for the same experimental set-up is another crucial criterion for a biosensor.
3. The stability of a biosensor is its endurance capacity against environmental conditions like pH, temperature, or ions and can affect the precision of the device [75]. Therefore, biosensors need to be stable.
4. Limit of detection (LOD) or sensitivity is one of the essential criteria for biosensors, determining the least amount of biological analyte that the biosensor can analyze.

A biosensor is distinct from the regularly used bioprobe or bioanalytical devices. As opposed to bioprobes, biosensors are reusable and detect analyte concentration uninterruptedly. Biosensors are easy to operate, unlike bioanalytical devices, as they do not require added processing phases or reagents [75]. Biosensors offer a variety of advantages over traditional methods, providing rapid results with high specificity and sensitivity. Moreover, a portable and compact device with real-time analysis and point-of-care testing (POCT) is suitable for biosensors, making it an attractive alternative to traditional methods [76]. Researchers are now developing strategies to enhance biosensors' signal amplification and sensitivity using nanomaterials, namely, nanoparticles, nanofilm, and quantum dots [77–79]. Based on the transducing module, biosensors may be categorized as optical, electrochemical, thermal, piezoelectric, magnetic, and micromechanical to diagnose various viruses (Table 1) [80, 81].

1. ***Optical Biosensors***: When the biological analyte and recognition element on the transducer surface react to form optical changes, it is then measured by an optical biosensor. In the past decade, advances in optical biosensors have picked up the pace for more sensitive optical platforms like surface plasma resonance (SPR), ring resonators, fiber optics, interferometers, photonic crystals, and planar optical wavelength [82] (Fig. 1).
   Virus Detection Examples:
   (a) Dengue: Researchers have developed optical biosensors to detect anti-Dengue envelope protein antibodies using tapered optical fiber as a polyamidoamine (PAMAM) dendrimer sensor. This PAMAM enhances the adhesion of the biorecognition element, i.e., the Dengue E protein antigen and LOD of the sensor were found to be 1.0 pM [83]. Another approach for Dengue diagnostic was developed using the spin coating method where Dengue monoclonal antibody was immobilized on a thin film of gold/Fe-MPA-NCC-CTAB/EDC-NHS. This thin film's interaction with Dengue protein generated an SPR signal with 39.96° nM^{-1} sensitivity [84].
   (b) Hepatitis: In a study, Hepatitis B surface antigen (HBsAg) with secondary antibody was used to detect human Hepatitis B virus (HBV) antibody using the SPR technique, and the LOD was found as 10 nmol [85]. Another group

Table 1 Biosensor platforms proposed for detection of various human viruses. HAU, hemagglutinating unit; pfu, plaque forming unit

Type of biosensor	Virus	Biorecognition component	Detection limit	References
Optical	Ebola	Fluorescence nucleic acid	0.2 pfu/mL	[126]
	Zika	Envelope protein	5 pfu	[127]
	Influenza	Anti-H5N1 aptamer	0.128 HAU	[128]
	Norovirus	Monoclonal antibody	0.01 ng/mL	[129]
	Adenovirus	DNA	10^1 copies/reaction	[130]
Electrochemical	Ebola	DNA probe	4.7 nM	[131]
	Zika	DNA probe	25.0 ± 1.7 nM	[132]
	Influenza	DNA probe	1 pM	[133]
	Norovirus	Recognition peptides	7.8 copies/mL (clinical sample	[134]
	Adenovirus	Anti-adenoviral monoclonal antibody	30 copies/mL	[135]
Piezoelectric	Ebola	Anti-Ebola monoclonal antibody	1.9×10^4 pfu/mL	[136]
	Zika	Anti-Zika antibody	Not mentioned	[118]
	Influenza	Synthetic sialylglycoconjugates	10^5 virions/mL	[118]
	Human papilloma virus	Synthetic biotinylated oligonucleotides	50 nM	[137]
	Human rhinovirus virus	Molecular imprinted "artificial antibody"	100 μg/mL	[138]
Magnetic	Ebola	Biotinylated capture probes	33 cDNA molecules	[139]
	Zika	Fluorescent tagged magnetic beads	13 ng/L	[140]
	Influenza	Erythrocyte membrane covered magnetic nanoparticles	Not mentioned	[141]
	Norovirus	Au/M nanoparticles-Graphene conjugated with anti-Norovirus antibody	1.16 pg/mL	[142]
	Ebola	Biotinylated capture probes	33 cDNA molecules	[139]
Micromechanical	Ebola	Anti-Ebola probe	1 ng/mL	[143]
	Zika	QCM biosensor with aptamers	1 ng	[144]
	Influenza	Au nanoparticles conjugated with antibodies	1×10^3PFU/mL	[145]

(continued)

Table 1 (continued)

Type of biosensor	Virus	Biorecognition component	Detection limit	References
	Norovirus	Graphene-Au nanoparticle with ferrocene tagged aptasensor	100 pM	[146]

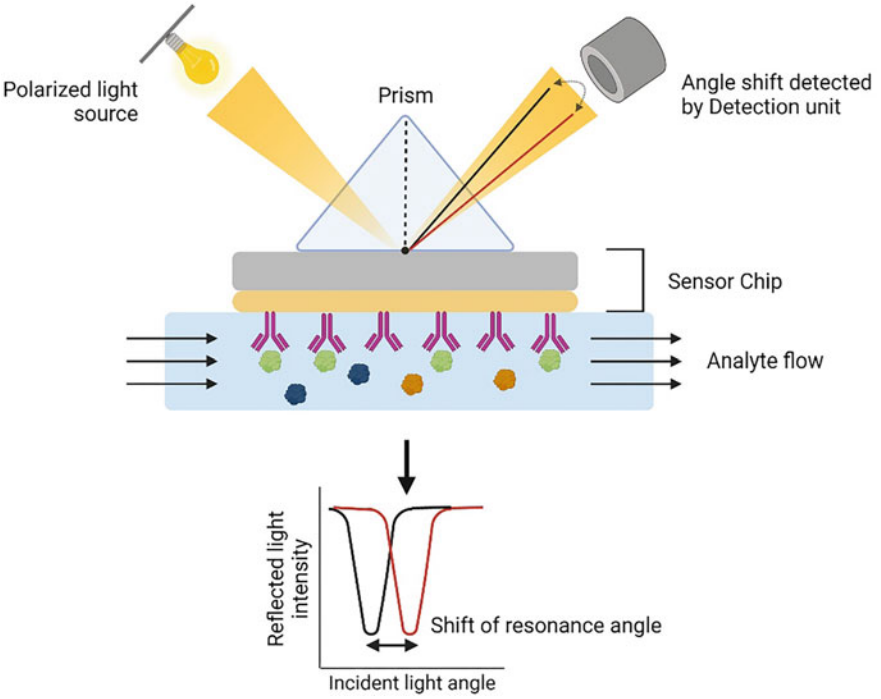

Fig. 1 Optical biosensor: Schematic representation of the basic operation of optical biosensor with detection of angle shift. Created with biorender.com

of researchers used the surface-enhanced Raman scattering method to develop a biosensor on a gold nanoparticle chip to detect HBV DNA. The LOD was observed to be 0.44 fm [86].

(c) HIV: For HIV detection, label-free photonic crystal nanostructures have been used. The researchers reported that intact RNA of HIV from biological samples, when immobilized on the nanostructured surface, produces a resonant peak wavelength shift. This biosensor could detect 10^4 to 10^8 copies/mL [87]. Another approach for the detection of HIV was reported using multiple modified layers of poly-l-lysine, gold, and anti-HIV antibody. This technique detected ~100 copies/mL of the clinical sample across subtypes of HIV [88]. This nanoplasmonic electrical field-enhanced resonating platform has been recently developed into a portable device [89].

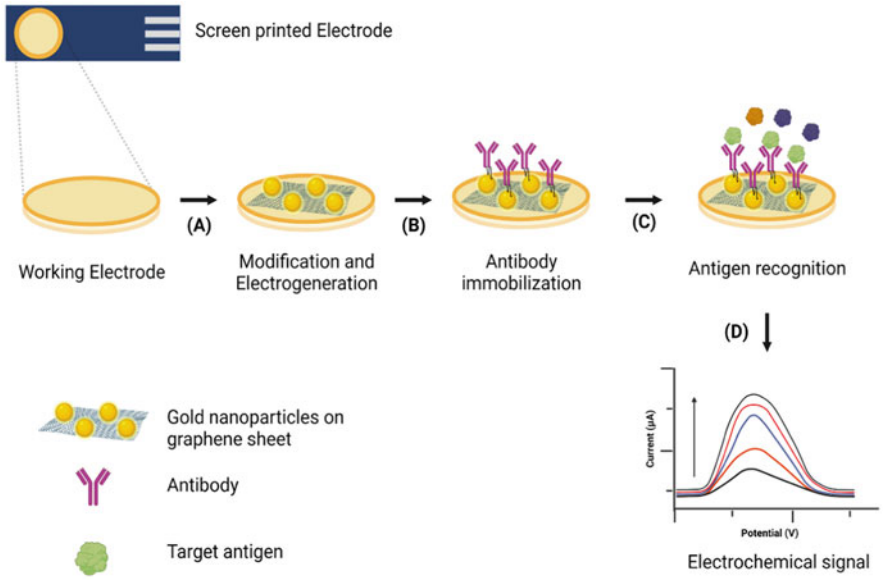

Fig. 2 Electrochemical Biosensor: Schematic diagram of a screen-printed electrochemical biosensor. (**a**) Modification and fabrication of the electrochemical biosensor. (**b**) Immobilization of antibody. (**c**) Binding of target antigen with the specific immobilized antibody. (**d**) Measurement of the electrochemical detection. Created with biorender.com

(d) SARS-CoV-2: With the recent COVID-19 pandemic caused by the SARS-CoV-2 virus, research for rapid detection techniques, especially on biosensors, are ongoing rapidly. A very contemporary approach using a plastic optical fiber-based probe to detect different variants of SARS-CoV-2 has been developed. The probe fitted with a laser source can be directly inserted into the patients' nasopharyngeal or oropharyngeal tract, which detects the signal received by the photodetector [90]. Another study proposed a multilayer of TiO_2–Ag–$MoSe_2$ graphene combined with a BK7 prism where recombinant monoclonal anti-SARS-CoV-2 antibodies were immobilized in the sensor. The antigen–antibody interaction results in an angular shift in the SPR and is thus detected by the biosensor [91].

2. ***Electrochemical Biosensors***: The platform for electrochemical biosensors contains electrochemical transducers that may be either gas, metal, carbon, or glass electrodes [92]. Principally an electrochemical biosensor has two components: (i) Biorecognition element, which detects the analyte, and (ii) Transducer, which converts electrochemical data into a signal proportional to the concentration of the analyte. Electrochemical biosensors may be classified as potentiometry, amperometry, conductometric, and ion charge or field-effect based on the detection mode. The transducing electrodes are modified with virus-specific probes or antibodies for virus detection (Fig. 2).
   Virus Detection Examples:

(a) Dengue: Numerous studies have developed an electrochemical biosensor to detect the dengue virus [93]. A recent study developed a gold electrode biosensor with gold nanoparticles and carbon nanotubes to improve the electrochemical signal. Dengue NS1 protein-specific antibodies were immobilized on the nanoparticles, and upon recombinant Dengue antigen–antibody interaction, the LOD was observed to be 3×10^{-13} g/mL [94]. Similarly, in another study, functionalized gold electrodes were immobilized with chemically synthesized peptides against Dengue NS1 protein. The LOD of this biosensor was 1.49 μg/mL [95].

(b) Hepatitis: To detect Hepatitis C, screen-printed electrodes have been used as an electrochemical biosensor. Linear peptides against the E2 protein of Hepatitis C were functionalized on the peptides, and the binding of the analyte was evaluated using differential pulse voltammetry. The LOD for this device was 2.1×10^{-5} mg/mL in simulated blood plasma [96]. To detect Hepatitis E, quantum dots of graphene fabricated with gold polyaniline nanowire were used as an electrochemical biosensor. The results of this study report an exceptionally low LOD of 0.8 fg/mL [97].

(c) HIV: A glass carbon electrode functionalized with polyaniline and graphene was used as an electrochemical biosensor to detect HIV. This study used single-stranded DNA probes immobilized on the electrode, and the sensor showed a LOD of 1.0×10^{-16} M [98]. Another study described label-free electrochemical biosensors using gold-sputtered electrodes and screen-printed electrodes. Specific DNA probes against HIV-1 and HIV-2 were fabricated on the electrode surface, and analyte interaction was monitored by square wave voltammetry. The LOD of this device was found to be 0.1 nM [99].

(d) SARS-CoV-2: Several researchers have explored electrochemical biosensors to detect SARS-CoV-2. An ultrasensitive electrochemical biosensor for detecting SARS-CoV-2 was reported using screen-printed carbon electrodes. The probes were immobilized with redox-active labels hybridized and isothermal rolling circle amplification product in this device. The electrochemical biosensor further detected it, and the minimum detection limit was observed to be one copy/μl [100]. The field-effect transistor-based biosensor was also developed using anti-spike antibodies to detect SARS-CoV-2, which showed LOD as low as 1–100 fM from clinical samples [101].

3. ***Piezoelectric biosensors*:** When certain natural and artificial materials are subjected to mechanical strain or stress, they generate an internal oscillating electric field known as piezoelectric materials [102]. Some of the best-known and understood piezoelectric materials are quartz, silicon dioxide, and ferroelectric ceramics. Thus, these materials have gained importance as biomaterials can be functionalized on the surface and used as diagnostic biosensors. In a piezoelectric biosensor, the piezoelectric material is the transducer; when there is an interaction between the immobilized probe on the electrode placed on the piezoelectric material and the analyte, Masson, the electrode changes resulting in current variation and is detected by crystal microbalance [103] (Fig. 3).

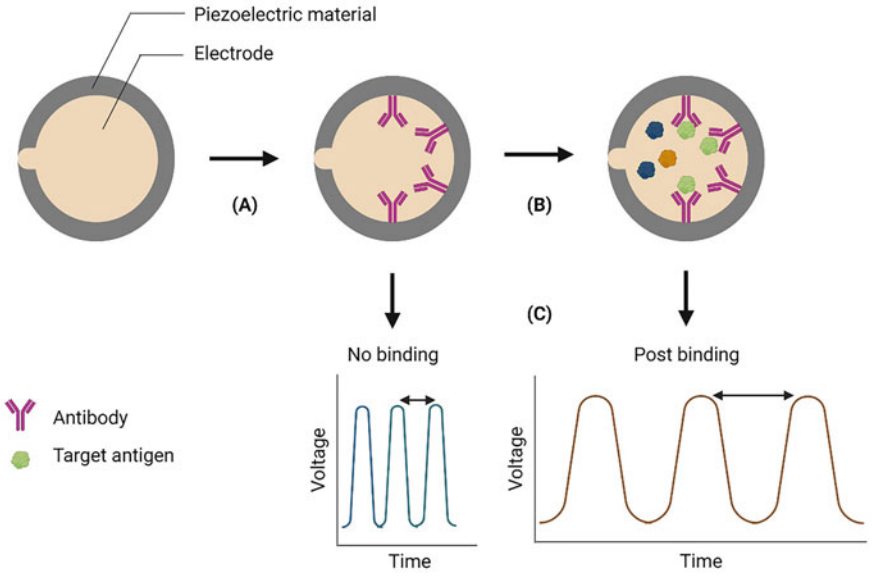

Fig. 3 Piezoelectric biosensor: Schematic representation of the basic operation of piezoelectric biosensor. (**a**) Immobilization of specific antibodies. (**b**) Binding of a target antigen to the specific antibody. (**c**) Detection of time-dependent frequency shift post-antibody–antigen binding. Created with biorender.com

Virus Detection Examples:

(a) Dengue: Several piezoelectric biosensor devices have been proposed to detect the Dengue virus. Among the reported studies, an immune chip of QCM was developed by immobilizing monoclonal antibodies against Dengue E and NS1 proteins from clinical samples. The detection limit was 1.7 μg/mL and 0.7 μg/mL for E and NS1 proteins, respectively [104]. At the same time, another study proposed bacterial cellulose nanocrystals as a thin-film coating on QCM to detect dengue. According to the authors, this coating enhanced the sensitivity and attachment of the specific monoclonal antibody to detect dengue NS1 protein from clinical serum samples. The LOD was observed to be 0.1–0.32 μg/mL [105].

(b) Hepatitis: A novel piezoelectric device was proposed by a team of Chinese scientists to detect the Hepatitis B virus. The apparatus comprises a gold electrode with polyethyleneimine adhesion on piezoelectric quartz material. The Hepatitis B DNA probe was immobilized on the electrode using the glutaraldehyde cross-linking (PEI-Glu) method. The device successfully detected the concentration range of 0.02–0.14 μg/mL of Hepatitis B virus [106]. Another study proposed the piezoelectric quartz crystal biosensor immobilized with oligonucleotide probes to detect the Hepatitis C virus [107].

(c) HIV: To detect HIV-1 and HIV-2, a prototype piezoelectric biosensor has been described recently. Silicon dioxide layers and interdigital transducers were used as biosensor chips. These chips were further functionalized with monoclonal antibodies against HIV-1 recombinant glycoprotein 24 and HIV-2 recombinant glycoprotein 39. When reacted with infected human sera, it was observed that the LOD was 12 and 87 50% tissue culture infectious dose for HIV-1 and HIV-2, respectively [108]. Determination of HIV using a specific monoclonal antibody against glycoprotein 120 coated on a gold electrode was attempted in a separate study where quartz served as the biosensor. Using clinical samples, it was found that LOD was 6.5×10^4 viruses/mL [109].

(d) SARS-CoV-2: For detecting the SARS-CoV-2 antigen, many researchers proposed a polyvinylidene fluoride piezoelectric microcantilever-based biosensor. A specific antibody was coated on the microcantilever, and when it interacted with the SARS-CoV-2 antigen, there was a mass change and generated floating voltage [110].

4. ***Magnetic biosensors***: Magnetic biosensors that use magnetic fields by certain magnetic particles after binding to analytes are called magnets. Superparamagnetic particles and magnetic nanoparticles are extensively used for biomedical purposes due to their easy functionalization, biocompatibility, and stability [111]. The principle of magnetic biosensors relies on the changes observed through resistance and coil inductance. Various magnetic biosensors have been used to detect viruses, such as magnetometers, ferromagnetic, magnetoresistive, magneto-optical, and inductive [112] (Fig. 4).

   Virus Detection Examples

   (a) Dengue: A novel automated magnetic biomarker device has been previously proposed to detect Dengue NS1 protein in patient serum. In this device, specific monoclonal antibodies were coated on magnetic nanoparticles, and the reaction between antigen–antibody resulted in agglutination of the magnetic nanoparticle. These magnetic nanoclusters were correlated with the concentration of target NS1 protein and quantified using the magnetic method. The LOD of the device was found to be 25 ng/mL [113].

   (b) Hepatitis: For detecting Hepatitis B surface antigen, carboxylated magnetic nanoparticles were used as carriers for a magnetic biosensor device. Specific DNA aptamers were selected to develop a chemiluminescence aptasensor using magnetic separation. The LOD of the device was observed as 0.1 ng/mL [114].

   (c) HIV: A recent study developed a point-of-care device to detect HIV by employing the giant magnetoresistive effect. The magnetic nanosensor chips were functionalized with a probe specific for HIV transmembrane protein gp41, and the detection was done using a sandwich immunoassay technique with magnetic nanoparticles. The device achieved an 80% accuracy of HIV detection in saliva [115].

   (d) SARS-CoV-2: Using a giant magnetoresistance sensing technique and super magnetic nanoparticles, a device was proposed to detect the presence of

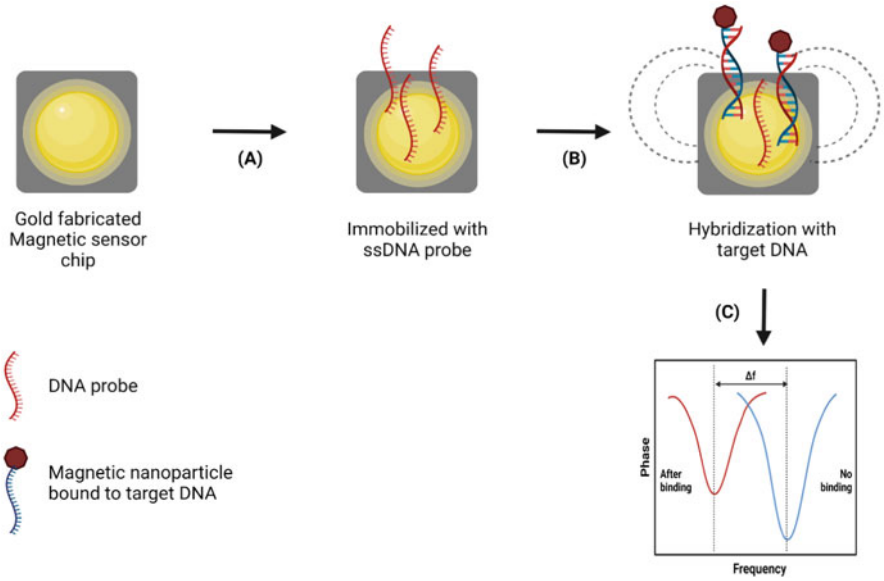

Fig. 4 Magnetic Biosensor: Schematic diagram of magnetic biosensor with gold fabricated sensor chip. (**a**) Immobilization of specific single-stranded DNA on the magnetic sensor. (**b**) Hybridization of the complementary target DNA bound to magnetic nanoparticle. (**c**) Measurement of changes in the resistance due to generated magnetic field. Created with biorender.com

SARS-CoV-2 antibodies. The study described lateral flow immunoassay for quantitative detection of anti-SARS-CoV-2 IgM and IgG antibodies, and the LOD was observed to be 10 ng/mL and 5 ng/mL, respectively [116].

5.1 Micromechanical Biosensors

The sensors that use mechanical structures and cantilevers to generate surface stress and acoustic waves to detect analytes in air, liquid, or vacuum are called micromechanical biosensors. Thus, micromechanical biosensors depend on small transducers to detect resonations resulting from molecular interactions of bioreceptor and analytes [117]. Therefore, with the development of biosensors, advances have been made in detecting viruses using micromechanical biosensors (Fig. 5).

Virus Detection Examples:

(a) Dengue: Researchers have recently proposed biosensors using Micro/Nano Electro-Mechanical systems (MEMS/NEMS) to detect dengue virus-specific antibodies. The biosensor structure comprised an array of polysilicon cantilevers coated with functionalized anti-Dengue antibodies. Upon exposure to Dengue antigen, the cantilever produced a resonance frequency of 0.89×10^{6} and an output voltage of 2.23×10^{-4} [118].

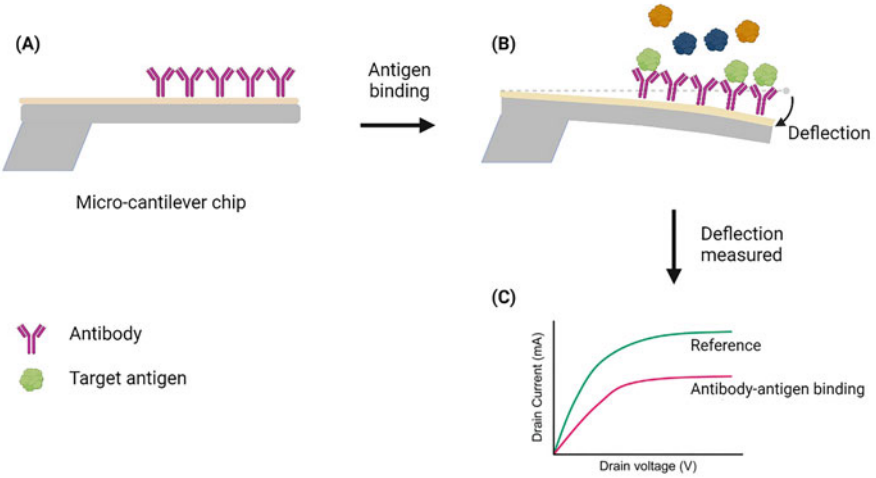

Fig. 5 Micromechanical biosensor: Schematic representation of a microcantilever-based biosensor (**a**) Microcantilever chip functionalized with specific antibodies. (**b**) The resultant deflection in the microcantilever after binding of a target antigen to the antibody. (**c**) Variation in drain current upon antibody–antigen binding and resultant deflection of microcantilever. Created with biorender.com

(b) Hepatitis: Resonant microcantilever arrays have been proposed for label-free detection of Hepatitis A and C. Anti-Hepatitis A/C were functionalized on nickel-coated MEMS cantilever. The frequency counter and a control circuit then monitored the microcantilever's resonant frequency. For both viruses, LOD was observed to be 0.1 ng/mL [119].

(c) HIV: In recent times, QCM has emerged as the new label-free and robust micromechanical biosensor platform [120]. A diagnostic device for HIV-1 was designed by scientists using Quartz crystal microbalance (QCM). In this study, gold nanoparticles were also used to augment the signals and were coated with streptavidin. Subsequently, biotinylated anti-HIV-1 polyclonal antibodies were immobilized on the surface. Clinical serum samples with as low as 1 ng/mL of antigen were detectable through this device [121].

(d) SARS-CoV-2: A recent study proposed a susceptible and rapid diagnostic device based on micromechanical technology to detect the SARS-CoV-2 antigen. They used gold-coated microcantilevers grafted with specific antibodies. To enhance the antigen–antibody interaction, the microcantilever was functionalized with EDC-NHS chemistry. The group reported high selectivity and sensitive detection of clinical nasopharyngeal swab samples with the proposed device within 5 min. The LOD was found to be 100 copies/mL [122].

6 Current Challenges and Prospects

The current diagnostic ecosystem has three prime challenges, acting as a hurdle in simplifying the global scenario [123]. First is the synchronization gap in testing guidelines, as subtle differences exist in testing requirements, procedures, time of testing, and method to follow. These discrepancies are a barrier to developing a universally accepted strategy for worldwide use. Second is the lack of validation of analytical procedures and comparability with existing methods required to demonstrate that the system is suitable for its intended use. The unavailability of a curated and reliable reference database related to the detection limit, specificity, and scope of detection makes it challenging to introduce a new method for public use. Third is technical issues related to the procedure, as some approaches come with specific problems. Detection of infectious adventitious agents in clinical laboratories relies on animal health, the commencement of symptoms, and animals' innate or acquired immunity [124].

The rapid identification methods available for most viruses can only be achieved if the system is readily available globally, even in resource-limited regions, and people are well trained to use them. To put an early break on future outbreaks and endemics, we need to analyze the situation by quickly detecting the etiologic agent with associated risks and spreading patterns. Certain factors, including viral epidemiology and molecular mechanisms, need to be carefully studied to link the data to solve the problem ultimately [125].

7 Conclusion

Considering that testing is only one component of viral safety and risk assessment combined with quality by design principles and viral clearance, newer or improved technologies for pathogen detection can significantly improve safety. There are numerous unmet needs in the biomedical point-of-care diagnostic and patient self-testing devices. As opposed to traditional diagnostic techniques, biosensors show a promising platform due to their simplicity, rapidity, sensitivity, and specificity. With the advent of nanotechnology and biotechnology, biosensors are now moving further from proof of concept and being commercially developed into devices for detecting biological analytes like blood glucose biosensors. However, while designing and using biosensors, certain caveats need careful consideration, like (i) Contamination of the device with previous samples, (ii) Stability of immobilized biomaterial due to environmental conditions [75].

Nevertheless, these methods offer great scope and opportunities with good sensitivity and broad specificity provided by a single test. Lastly, to be prepared for potential viruses in the future, we must develop the best possible diagnostic option to tackle an outbreak and prevent it from becoming an epidemic, thus saving humankind.

References

1. Wille, M., Geoghegan, J. L., & Holmes, E. C. (2021). How accurately can we assess zoonotic risk? *PLoS Biology, 19*(4), e3001135.
2. Woolhouse, M., Scott, F., Hudson, Z., Howey, R., & Chase-Topping, M. (2012). Human viruses: Discovery and emergence. *Philosophical Transactions of the Royal Society of London. Series B, Biological Sciences, 367*(1604), 2864–2871.
3. Carroll, D., Daszak, P., Wolfe, N. D., Gao, G. F., Morel, C. M., Morzaria, S., et al. (2018). The global virome project. *Science, 359*(6378), 872–874.
4. Geoghegan, J. L., & Holmes, E. C. (2017). Predicting virus emergence amid evolutionary noise. *Open Biology, 7*(10).
5. Binder, S., Levitt, A. M., Sacks, J. J., & Hughes, J. M. (1999). Emerging infectious diseases: Public health issues for the 21st century. *Science, 284*(5418), 1311–1313.
6. Simon, V., Ho, D. D., & Abdool, K. Q. (2006). HIV/AIDS epidemiology, pathogenesis, prevention, and treatment. *Lancet, 368*(9534), 489–504.
7. Peteranderl, C., Herold, S., & Schmoldt, C. (2016). Human influenza virus infections. *Seminars in Respiratory and Critical Care Medicine, 37*(4), 487–500.
8. Rabaan, A. A., Al-Ahmed, S. H., Haque, S., Sah, R., Tiwari, R., Malik, Y. S., et al. (2020). SARS-CoV-2, SARS-CoV, and MERS-COV: A comparative overview. *Le Infezioni in Medicina, 28*(2), 174–184.
9. Nicastri, E., Kobinger, G., Vairo, F., Montaldo, C., Mboera, L. E. G., Ansunama, R., et al. (2019). Ebola virus disease: Epidemiology, clinical features, management, and prevention. *Infectious Disease Clinics of North America, 33*(4), 953–976.
10. Banerjee, G., Shokeen, K., Chakraborty, N., Agarwal, S., Mitra, A., Kumar, S., et al. (2021). Modulation of immune response in Ebola virus disease. *Current Opinion in Pharmacology, 60*, 158–167.
11. Song, B. H., Yun, S. I., Woolley, M., & Lee, Y. M. (2017). Zika virus: History, epidemiology, transmission, and clinical presentation. *Journal of Neuroimmunology, 308*, 50–64.
12. Holmes, E. C., Goldstein, S. A., Rasmussen, A. L., Robertson, D. L., Crits-Christoph, A., Wertheim, J. O., et al. (2021). The origins of SARS-CoV-2: A critical review. *Cell, 184*(19), 4848–4856.
13. Jones, K. E., Patel, N. G., Levy, M. A., Storeygard, A., Balk, D., Gittleman, J. L., et al. (2008). Global trends in emerging infectious diseases. *Nature, 451*(7181), 990–993.
14. Pardee, K., Green, A. A., Takahashi, M. K., Braff, D., Lambert, G., Lee, J. W., et al. (2016). Rapid, low-cost detection of Zika virus using programmable biomolecular components. *Cell, 165*(5), 1255–1266.
15. Tang, Y. W., Procop, G. W., & Persing, D. H. (1997). Molecular diagnostics of infectious diseases. *Clinical Chemistry, 43*(11), 2021–2038.
16. Hsiung, G. D. (1984). Diagnostic virology: From animals to automation. *The Yale Journal of Biology and Medicine, 57*(5), 727–733.
17. Hematian, A., Sadeghifard, N., Mohebi, R., Taherikalani, M., Nasrolahi, A., Amraei, M., et al. (2016). Traditional and modern cell culture in virus diagnosis. *Osong Public Health and Research Perspectives, 7*(2), 77–82.
18. Leland, D. S., & Ginocchio, C. C. (2007). Role of cell culture for virus detection in the age of technology. *Clinical Microbiology Reviews, 20*(1), 49–78.
19. Fredricks, D. N., & Relman, D. A. (1999). Application of polymerase chain reaction to the diagnosis of infectious diseases. *Clinical Infectious Diseases, 29*(3), 475–486. quiz 87-8.
20. Smolinski, M. S., Hamburg, M. A., & Lederberg, J. (Eds.). (2003). *Microbial threats to health: emergence, detection, and response*. National Academies Press.
21. Mollentze, N., Babayan, S. A., & Streicker, D. G. (2021). Identifying and prioritizing potential human-infecting viruses from their genome sequences. *PLoS Biology, 19*(9).
22. Mullis, K. B. (1990). The unusual origin of the polymerase chain reaction. *Scientific American, 262*(4), 56–61. 4–5.

23. Barreda-Garcia, S., Miranda-Castro, R., de-Los-Santos-Alvarez, N., Miranda-Ordieres, A. J., & Lobo-Castanon, M. J. (2018). Helicase-dependent isothermal amplification: A novel tool in the development of molecular-based analytical systems for rapid pathogen detection. *Analytical and Bioanalytical Chemistry, 410*(3), 679–693.
24. Bharucha, T., Sengvilaipaseuth, O., Vongsouvath, M., Vongsouvath, M., Davong, V., Panyanouvong, P., et al. (2018). Development of an improved RT-qPCR assay for detection of Japanese encephalitis virus (JEV) RNA including a systematic review and comprehensive comparison with published methods. *PLoS One, 13*(3), e0194412.
25. Kojabad, A. A., Farzanehpour, M., Galeh, H. E. G., Dorostkar, R., Jafarpour, A., Bolandian, M., et al. (2021). Droplet digital PCR of viral DNA/RNA, current progress, challenges, and future perspectives. *Journal of Medical Virology, 93*(7), 4182–4197.
26. Ben Shabat, M., Meir, R., Haddas, R., Lapin, E., Shkoda, I., Raibstein, I., et al. (2010). Development of a real-time TaqMan RT-PCR assay for the detection of H9N2 avian influenza viruses. *Journal of Virological Methods, 168*(1–2), 72–77.
27. Sue, M. J., Yeap, S. K., Omar, A. R., & Tan, S. W. (2014). Application of PCR-ELISA in molecular diagnosis. *BioMed Research International, 2014*, 653014.
28. Cave, H., Acquaviva, C., Bieche, I., Brault, D., de Fraipont, F., & Fina, F., et al. (2003). [RT-PCR in clinical diagnosis]. Annales de Biologie Clinique (Paris), *61*(6), 635–644.
29. Gu, W., Miller, S., & Chiu, C. Y. (2019). Clinical metagenomic next-generation sequencing for pathogen detection. *Annual Review of Pathology, 14*, 319–338.
30. Bustin, S. A. (2000). Absolute quantification of mRNA using real-time reverse transcription polymerase chain reaction assays. *Journal of Molecular Endocrinology, 25*(2), 169–193.
31. Batten, C. A., Banyard, A. C., King, D. P., Henstock, M. R., Edwards, L., Sanders, A., et al. (2011). A real time RT-PCR assay for the specific detection of Peste des petits ruminants virus. *Journal of Virological Methods, 171*(2), 401–404.
32. van de Pol, A. C., Wolfs, T. F., van Loon, A. M., Tacke, C. E., Viveen, M. C., Jansen, N. J., et al. (2010). Molecular quantification of respiratory syncytial virus in respiratory samples: Reliable detection during the initial phase of infection. *Journal of Clinical Microbiology, 48*(10), 3569–3574.
33. Templeton, K. E., Scheltinga, S. A., Beersma, M. F., Kroes, A. C., & Claas, E. C. (2004). Rapid and sensitive method using multiplex real-time PCR for diagnosis of infections by influenza a and influenza B viruses, respiratory syncytial virus, and parainfluenza viruses 1, 2, 3, and 4. *Journal of Clinical Microbiology, 42*(4), 1564–1569.
34. Muller, D. A., Depelsenaire, A. C., & Young, P. R. (2017). Clinical and laboratory diagnosis of dengue virus infection. *The Journal of Infectious Diseases, 215*(suppl_2), S89–S95.
35. Roberts, A., & Gandhi, S. (2020). Japanese encephalitis virus: A review on emerging diagnostic techniques. *Frontiers in Bioscience (Landmark Ed)., 25*(10), 1875–1893.
36. Yuce, M., Filiztekin, E., & Ozkaya, K. G. (2021). COVID-19 diagnosis -a review of current methods. *Biosensors & Bioelectronics, 172*, 112752.
37. Wang, T., & Brown, M. J. (1999). mRNA quantification by real time TaqMan polymerase chain reaction: Validation and comparison with RNase protection. *Analytical Biochemistry, 269*(1), 198–201.
38. Borson, N. D., Salo, W. L., & Drewes, L. R. (1992). A lock-docking oligo(dT) primer for 5′ and 3' RACE PCR. *PCR Methods and Applications, 2*(2), 144–148.
39. Tahamtan, A., & Ardebili, A. (2020). Real-time RT-PCR in COVID-19 detection: Issues affecting the results. *Expert Review of Molecular Diagnostics, 20*(5), 453–454.
40. Londone-Bailon, P., & Sanchez-Robinet, C. (2018). Efficiency evaluation of the process control virus "Mengovirus" in real time RT-PCR viral detection in the bivalve *Mollusc donax* sp. *Journal of Virological Methods, 262*, 20–25.
41. Golender, N., Bumbarov, V. Y., Erster, O., Beer, M., Khinich, Y., & Wernike, K. (2018). Development and validation of a universal S-segment-based real-time RT-PCR assay for the detection of Simbu serogroup viruses. *Journal of Virological Methods, 261*, 80–85.

42. Craw, P., & Balachandran, W. (2012). Isothermal nucleic acid amplification technologies for point-of-care diagnostics: A critical review. *Lab on a Chip, 12*(14), 2469–2486.
43. Notomi, T., Okayama, H., Masubuchi, H., Yonekawa, T., Watanabe, K., Amino, N., et al. (2000). Loop-mediated isothermal amplification of DNA. *Nucleic Acids Research, 28*(12), E63.
44. Sahoo, P. R., Sethy, K., Mohapatra, S., & Panda, D. (2016). Loop mediated isothermal amplification: An innovative gene amplification technique for animal diseases. *Veterinay World., 9*(5), 465–469.
45. Butt, A. M., Siddique, S., An, X., & Tong, Y. J. M. (2020). Development of a dual-gene loop-mediated isothermal amplification (LAMP) detection assay for SARS-CoV-2: A preliminary study.
46. Selvam, K., Najib, M. A., Khalid, M. F., Mohamad, S., Palaz, F., Ozsoz, M., et al. (2021). RT-LAMP CRISPR-Cas12/13-based SARS-CoV-2 detection methods. *Diagnostics (Basel)., 11*(9).
47. Anderson, E. M., & Maldarelli, F. (2018). Quantification of HIV DNA using droplet digital PCR techniques. *Current Protocols in Microbiology, 51*(1), e62.
48. Vasudevan, H. N., Xu, P., Servellita, V., Miller, S., Liu, L., Gopez, A., et al. (2021). Digital droplet PCR accurately quantifies SARS-CoV-2 viral load from crude lysate without nucleic acid purification. *Scientific Reports, 11*(1), 1–9.
49. Vellucci, A., Leibovitch, E. C., & Jacobson, S. (2018). *Using droplet digital PCR to detect coinfection of human herpesviruses 6A and 6B (HHV-6A and HHV-6B) in clinical samples. Digital PCR* (pp. 99–109). Springer.
50. Mardis, E. R. (2011). A decade's perspective on DNA sequencing technology. *Nature, 470*(7333), 198–203.
51. Xue, Y., Ankala, A., Wilcox, W. R., & Hegde, M. R. (2015). Solving the molecular diagnostic testing conundrum for Mendelian disorders in the era of next-generation sequencing: Single-gene, gene panel, or exome/genome sequencing. *Genetics in Medicine, 17*(6), 444–451.
52. Pettersson, E., Lundeberg, J., & Ahmadian, A. (2009). Generations of sequencing technologies. *Genomics, 93*(2), 105–111.
53. Meera Krishna, B., Khan, M. A., & Khan, S. T. (2019). Next-generation sequencing (NGS) platforms: An exciting era of genome sequence analysis. In V. Tripathi, P. Kumar, P. Tripathi, A. Kishore, & M. Kamle (Eds.), *Microbial genomics in sustainable agroecosystems* (Vol. 2, pp. 89–109). Springer.
54. Crits-Christoph, A., Kantor, R. S., Olm, M. R., Whitney, O. N., Al-Shayeb, B., Lou, Y. C., et al. (2021). Genome sequencing of sewage detects regionally prevalent SARS-CoV-2 variants. *MBio, 12*(1).
55. Kannan, S. R., Spratt, A. N., Cohen, A. R., Naqvi, S. H., Chand, H. S., Quinn, T. P., et al. (2021). Evolutionary analysis of the Delta and Delta plus variants of the SARS-CoV-2 viruses. *Journal of Autoimmunity, 124*, 102715.
56. Garneau, J. E., Dupuis, M. E., Villion, M., Romero, D. A., Barrangou, R., Boyaval, P., et al. (2010). The CRISPR/Cas bacterial immune system cleaves bacteriophage and plasmid DNA. *Nature, 468*(7320), 67–71.
57. Yin, L., Man, S., Ye, S., Liu, G., & Ma, L. J. B. (2021). CRISPR-Cas based virus detection: recent advances and perspectives. *Biosensors and Bioelectronics, 193*, 113541.
58. Gootenberg, J. S., Abudayyeh, O. O., Lee, J. W., Essletzbichler, P., Dy, A. J., Joung, J., et al. (2017). Nucleic acid detection with CRISPR-Cas13a/C2c2. *Science, 356*(6336), 438–442.
59. Rowe, T., Abernathy, R. A., Hu-Primmer, J., Thompson, W. W., Lu, X., Lim, W., et al. (1999). Detection of antibody to avian influenza a (H5N1) virus in human serum by using a combination of serologic assays. *Journal of Clinical Microbiology, 37*(4), 937–943.
60. Atmar, R. L. (2014). *Immunological detection and characterization. Viral Infections of Humans* (pp. 47–62). Springer.
61. Killian, M. L. (2014). Hemagglutination assay for influenza virus. *Methods in Molecular Biology, 1161*, 3–9.

62. Spackman, E., & Sitaras, I. (2020). *Hemagglutination inhibition assay. Animal influenza virus* (pp. 11–28). Springer.
63. Olaleye, O. D., Omilabu, S. A., Ilomechina, E. N., & Fagbami, A. H. (1990). A survey for haemagglutination-inhibiting antibody to West Nile virus in human and animal sera in Nigeria. *Comparative Immunology, Microbiology and Infectious Diseases, 13*(1), 35–39.
64. Julkunen, I. (1984). Serological diagnosis of parainfluenza virus infections by enzyme immunoassay with special emphasis on purity of viral antigens. *Journal of Medical Virology, 14*(2), 177–187.
65. Kobayashi, Y., Ichiki, T., Kusaba, T., Tachibana, N., & Nagai, K. (1971) [Hemagglutination inhibition antibody against Japanese encephalitis virus and the effects of vaccination on inhabitants of Fukuoka City and its environs]. Kansenshōgaku Zasshi, *45*(11), 490–493.
66. Gauger, P. C., & Vincent, A. L. (2020). Serum virus neutralization assay for detection and quantitation of serum neutralizing antibodies to influenza a virus in swine. *Methods in Molecular Biology, 2123*, 321–333.
67. Thomas, S. J., Nisalak, A., Anderson, K. B., Libraty, D. H., Kalayanarooj, S., Vaughn, D. W., et al. (2009). Dengue plaque reduction neutralization test (PRNT) in primary and secondary dengue virus infections: How alterations in assay conditions impact performance. *The American Journal of Tropical Medicine and Hygiene, 81*(5), 825–833.
68. Nie, J., Li, Q., Wu, J., Zhao, C., Hao, H., Liu, H., et al. (2020). Quantification of SARS-CoV-2 neutralizing antibody by a pseudotyped virus-based assay. *Nature Protocols, 15*(11), 3699–3715.
69. O'Farrell, B. (2009). *Evolution in lateral flow–based immunoassay systems* (pp. 1–33). Springer.
70. Peto, T., Affron, D., Afrough, B., Agasu, A., Ainsworth, M., Allanson, A., et al. (2021). COVID-19: Rapid antigen detection for SARS-CoV-2 by lateral flow assay: A national systematic evaluation of sensitivity and specificity for mass-testing. *eClinicalMedicine., 36*, 100924.
71. Bosch, I., de Puig, H., Hiley, M., Carre-Camps, M., Perdomo-Celis, F., Narvaez, C. F., et al. (2017). Rapid antigen tests for dengue virus serotypes and Zika virus in patient serum. *Science Translational Medicine, 9*(409).
72. Le, T. T., Chang, P., Benton, D. J., McCauley, J. W., Iqbal, M., & Cass, A. E. G. (2017). Dual recognition element lateral flow assay toward multiplex strain specific influenza virus detection. *Analytical Chemistry, 89*(12), 6781–6786.
73. Goode, J., Rushworth, J., & Millner, P. J. L. (2015). Biosensor regeneration: a review of common techniques and outcomes. *Langmuir, 31*(23), 6267–6276.
74. Castillo-Henríquez, L., Brenes-Acuña, M., Castro-Rojas, A., Cordero-Salmerón, R., Lopretti-Correa, M., & Vega-Baudrit, J. R. J. S. (2020). Biosensors for the detection of bacterial and viral clinical pathogens. *Sensors (Basel), 20*(23), 6926.
75. Koyun, A., Ahlatcolu, E., & Koca, Y. (2012). Milestones. In S. Kara (Ed.), *Biosensors and their principles* (pp. 117–142). InTech Open.
76. Saylan, Y., Yilmaz, F., Ozgur, E., Derazshamshir, A., Yavuz, H., & Denizli, A. (2017). Molecular imprinting of macromolecules for sensor applications. *Sensors (Basel)., 17*(4).
77. Cho, K. H., Shin, D. H., Oh, J., An, J. H., Lee, J. S., Jang, J., et al. (2018). Multidimensional conductive nanofilm-based flexible aptasensor for ultrasensitive and selective HBsAg detection. *ACS Applied Materials & Interfaces., 10*(34), 28412–28419.
78. La Spada, L., & Vegni, L. J. M. (2018). Electromagnetic nanoparticles for sensing and medical diagnostic applications. *Materials., 11*(4), 603.
79. Pang, Y., Jian, J., Tu, T., Yang, Z., Ling, J., Li, Y., et al. (2018). Wearable humidity sensor based on porous graphene network for respiration monitoring. *Biosensors and Bioelectronics, 116*, 123–129.
80. Thevenot, D. R., Toth, K., Durst, R. A., & Wilson, G. S. J. P. (1999). Electrochemical biosensors: recommended definitions and classification. *Biosensors and Bioelectronics, 71*(12), 2333–2348.

81. Saylan, Y., Erdem, O., Unal, S., & Denizli, A. (2019). An alternative medical diagnosis method: Biosensors for virus detection. *Biosensors (Basel)., 9*(2).
82. Sharma, A., Mishra, R. K., Goud, K. Y., Mohamed, M. A., Kummari, S., Tiwari, S., et al. (2021). Optical biosensors for diagnostics of infectious viral disease: A recent update. *Diagnostics (Basel)., 11*(11).
83. Mustapha Kamil, Y., Al-Rekabi, S. H., Yaacob, M. H., Syahir, A., Chee, H. Y., Mahdi, M. A., et al. (2019). Detection of dengue using PAMAM dendrimer integrated tapered optical fiber sensor. *Scientific Reports, 9*(1), 13483.
84. Omar, N. A. S., Fen, Y. W., Abdullah, J., Chik, C. E. N. C. E., & Mahdi, M. A. (2018). Development of an optical sensor based on surface plasmon resonance phenomenon for diagnosis of dengue virus E-protein. *Sensing and Bio-Sensing Research, 20*, 16–21.
85. Chung, J., Kim, S., Bernhardt, R., Pyun, J. C. J. S., & Chemical, A. B. (2005). Application of SPR biosensor for medical diagnostics of human hepatitis B virus (hHBV). *Sensors and Actuators B: Chemical, 111*, 416–422.
86. Zengin, A., Tamer, U., & Caykara, T. J. (2017). SERS detection of hepatitis B virus DNA in a temperature-responsive sandwich-hybridization assay. *Journal of Raman Spectroscopy, 48*(5), 668–672.
87. Shafiee, H., Lidstone, E. A., Jahangir, M., Inci, F., Hanhauser, E., Henrich, T. J., et al. (2014). Nanostructured optical photonic crystal biosensor for HIV viral load measurement. *Scientific Reports, 4*(1), 1–7.
88. Inci, F., Tokel, O., Wang, S., Gurkan, U. A., Tasoglu, S., Kuritzkes, D. R., et al. (2013). Nanoplasmonic quantitative detection of intact viruses from unprocessed whole blood. *ACS Nano, 7*(6), 4733–4745.
89. Inci, F., Filippini, C., Baday, M., Ozen, M. O., Calamak, S., Durmus, N. G., et al. (2015). Multitarget, quantitative nanoplasmonic electrical field-enhanced resonating device (NE2RD) for diagnostics. *Proceedings of the National Academy of Sciences of the United States of America, 112*(32), E4354–E4363.
90. Hadi, M. U., & Khurshid, M. J. S. (2022). SARS-CoV-2 detection using optical fiber based sensor method. *Sensors (Basel), 22*(3), 751.
91. Moznuzzaman, M., Khan, I., & Islam, M. R. (2021). Nano-layered surface plasmon resonance-based highly sensitive biosensor for virus detection: A theoretical approach to detect SARS-CoV-2. *AIP Advances., 11*(6), 065023.
92. Thevenot, D. R., Toth, K., Durst, R. A., & Wilson, G. S. (2001). Electrochemical biosensors: Recommended definitions and classification. *Biosensors & Bioelectronics, 16*(1–2), 121–131.
93. Anusha, J., Kim, B. C., Yu, K.-H., & Raj, C. J. (2019). Electrochemical biosensing of mosquito-borne viral disease, dengue: A review. *Biosensors and Bioelectronics, 142*, 111511.
94. Palomar, Q., Xu, X., Gondran, C., Holzinger, M., Cosnier, S., & Zhang, Z. J. M. A. (2020). Voltammetric sensing of recombinant viral dengue virus 2 NS1 based on Au nanoparticle–decorated multiwalled carbon nanotube composites. *Microchimica Acta, 187*(6), 1–10.
95. Kim, J. H., Cho, C. H., Ryu, M. Y., Kim, J.-G., Lee, S.-J., Park, T. J., et al. (2019). Development of peptide biosensor for the detection of dengue fever biomarker, nonstructural 1. *PLoS One., 14*(9), e0222144.
96. Antipchik, M., Korzhikova-Vlakh, E., Polyakov, D., Tarasenko, I., Reut, J., Öpik, A., et al. (2021). An electrochemical biosensor for direct detection of hepatitis C virus. *Analytical Biochemistry, 624*, 114196.
97. Chowdhury, A. D., Takemura, K., Li, T.-C., Suzuki, T., & Park, E. Y. (2019). Electrical pulse-induced electrochemical biosensor for hepatitis E virus detection. *Nature Communications, 10*(1), 1–12.
98. Gong, Q., Han, H., Yang, H., Zhang, M., Sun, X., Liang, Y., et al. (2019). Sensitive electrochemical DNA sensor for the detection of HIV based on a polyaniline/graphene nanocomposite. *Journal of Materiomics, 5*(2), 313–319.
99. Zhang, D., Peng, Y., Qi, H., Gao, Q., & Zhang, C. (2010). Label-free electrochemical DNA biosensor array for simultaneous detection of the HIV-1 and HIV-2 oligonucleotides

incorporating different hairpin-DNA probes and redox indicator. *Biosensors & Bioelectronics, 25*(5), 1088–1094.
100. Chaibun, T., Puenpa, J., Ngamdee, T., Boonapatcharoen, N., Athamanolap, P., O'Mullane, A. P., et al. (2021). Rapid electrochemical detection of coronavirus SARS-CoV-2. *Nature Communications, 12*(1), 1–10.
101. Seo, G., Lee, G., Kim, M. J., Baek, S. H., Choi, M., Ku, K. B., et al. (2020). Rapid detection of COVID-19 causative virus (SARS-CoV-2) in human nasopharyngeal swab specimens using field-effect transistor-based biosensor. *ACS Nano, 14*(4), 5135–5142.
102. Berlincourt, D. (1971). *Piezoelectric crystals and ceramics. Ultrasonic transducer materials* (pp. 63–124). Springer.
103. Chen, Y., Qian, C., Liu, C., Shen, H., Wang, Z., Ping, J., et al. (2020). Nucleic acid amplification free biosensors for pathogen detection. *Biosensors & Bioelectronics, 153*, 112049.
104. Wu, T. Z., Su, C. C., Chen, L. K., Yang, H. H., Tai, D. F., & Peng, K. C. (2005). Piezoelectric immunochip for the detection of dengue fever in viremia phase. *Biosensors & Bioelectronics, 21*(5), 689–695.
105. Pirich, C. L., de Freitas, R. A., Torresi, R. M., Picheth, G. F., & Sierakowski, M. R. J. B. (2017). Piezoelectric immunochip coated with thin films of bacterial cellulose nanocrystals for dengue detection. *Biosensors and Bioelectronics, 92*, 47–53.
106. Zhou, X., Liu, L., Hu, M., Wang, L., & Hu, J. (2002). Detection of hepatitis B virus by piezoelectric biosensor. *Journal of Pharmaceutical and Biomedical Analysis, 27*(1–2), 341–345.
107. Skladal, P., dos Santos, R. C., Yamanaka, H., & da Costa, P. I. (2004). Piezoelectric biosensors for real-time monitoring of hybridization and detection of hepatitis C virus. *Journal of Virological Methods, 117*(2), 145–151.
108. Bisoffi, M., Severns, V., Branch, D. W., Edwards, T. L., & Larson, R. S. (2013). Rapid detection of human immunodeficiency virus types 1 and 2 by use of an improved piezoelectric biosensor. *Journal of Clinical Microbiology, 51*(6), 1685–1691.
109. Rozmyslowicz, T., deSa, J., Lec, R., & Gaulton, G. N. (2015). A novel point-of-care BioNanoSensor for rapid HIV detection and treatment monitoring. J AIDS. *Clinical Research, 6*(5).
110. Kabir, H., Merati, M., & Abdekhodaie, M. J. (2021). Design of an effective piezoelectric microcantilever biosensor for rapid detection of COVID-19. *Journal of Medical Engineering & Technology, 45*(6), 423–433.
111. Wang, T., Zhou, Y., Lei, C., Luo, J., Xie, S., Pu, H. J. B., et al. (2017). Magnetic impedance biosensor: A review. *Biosensors & Bioelectronics, 90*, 418–435.
112. Qureshi, T., Faisal, M., Qureshi, S., & Memon, N. (2021). Magnetic biosensors for virus detection. *Biosensors for Virus Detection*, 7–1.
113. Antunes, P., Watterson, D., Parmvi, M., Burger, R., Boisen, A., Young, P., et al. (2015). Quantification of NS1 dengue biomarker in serum via optomagnetic nanocluster detection. *Scientific Reports, 5*(1), 1–10.
114. Xi, Z., Huang, R., Li, Z., He, N., Wang, T., Su, E., et al. (2015). Selection of HBsAg-specific DNA aptamers based on Carboxylated magnetic nanoparticles and their application in the rapid and simple detection of hepatitis B virus infection. *ACS Applied Materials & Interfaces, 7*(21), 11215–11223.
115. Ng, E., Yao, C., Shultz, T. O., Ross-Howe, S., & Wang, S. X. (2019). Magneto-nanosensor smartphone platform for the detection of HIV and leukocytosis at point-of-care. *Nanomedicine, 16*, 10–19.
116. Bayin, Q., Huang, L., Ren, C., Fu, Y., Ma, X., & Guo, J. (2021). Anti-SARS-CoV-2 IgG and IgM detection with a GMR based LFIA system. *Talanta, 227*, 122207.
117. Sagdic, K., Erdem, Ö., Derin, E., Shirejini, S. Z., Aslan, Y., Celik, S., et al. (2021). Micromechanical biosensors for virus detection. *Biosensors for Virus Detection*, 8–1.

118. Katta, M., Sandanalakshmi, R. J. S., & Research, B.-S. (2021). Simultaneous tropical disease identification with PZT-5H piezoelectric material including molecular mass biosensor microcantilever collection. *Sensing and Bio-Sensing Research., 32*, 100413.
119. Timurdogan, E., Alaca, B. E., Kavakli, I. H., & Urey, H. (2011). MEMS biosensor for detection of hepatitis a and C viruses in serum. *Biosensors & Bioelectronics, 28*(1), 189–194.
120. Lim, H. J., Saha, T., Tey, B. T., Tan, W. S., & Ooi, C. W. (2020). Quartz crystal microbalance-based biosensors as rapid diagnostic devices for infectious diseases. *Biosensors & Bioelectronics, 168*, 112513.
121. Ly, T. N., Park, S., Park, S. J. J. S., & Chemical, A. B. (2016). Detection of HIV-1 antigen by quartz crystal microbalance using gold nanoparticles. *Sensors and Actuators B: Chemical, 237*, 452–458.
122. Agarwal, D. K., Nandwana, V., Henrich, S. E., Josyula, V., Thaxton, C. S., Qi, C., et al. (2022). Highly sensitive and ultra-rapid antigen-based detection of SARS-CoV-2 using nanomechanical sensor platform. *Biosensors & Bioelectronics, 195*, 113647.
123. Mallet, L., & Gisonni-Lex, L. (2014). Need for new technologies for detection of adventitious agents in vaccines and other biological products. *PDA Journal of Pharmaceutical Science and Technology, 68*(6), 556–562.
124. Roush, D. J. (2018). Integrated viral clearance strategies-reflecting on the present, projecting to the future. *Current Opinion in Biotechnology, 53*, 137–143.
125. Holmes, E. C., Rambaut, A., & Andersen, K. G. (2018). Pandemics: Spend on surveillance, not prediction. *Nature, 558*(7709), 180–182.
126. Cai, H., Parks, J. W., Wall, T. A., Stott, M. A., Stambaugh, A., Alfson, K., et al. (2015). Optofluidic analysis system for amplification-free, direct detection of Ebola infection. *Scientific Reports, 5*, 14494.
127. Song, J., Mauk, M. G., Hackett, B. A., Cherry, S., Bau, H. H., & Liu, C. (2016). Instrument-free point-of-care molecular detection of Zika virus. *Anal Chem, 88*(14), 7289–7294.
128. Bai, H., Wang, R., Hargis, B., Lu, H., & Li, Y. (2012). A SPR aptasensor for detection of avian influenza virus H5N1. *Sensors (Basel)., 12*(9), 12506–12518.
129. Ashiba, H., Sugiyama, Y., Wang, X., Shirato, H., Higo-Moriguchi, K., Taniguchi, K., et al. (2017). Detection of norovirus virus-like particles using a surface plasmon resonance-assisted fluoroimmunosensor optimized for quantum dot fluorescent labels. *Biosensors and Bioelectronics, 93*, 260–266.
130. Jin, C. E., Lee, T. Y., Koo, B., Sung, H., Kim, S.-H., Shin, Y. J. S., et al. (2018). Rapid virus diagnostic system using bio-optical sensor and microfluidic sample processing. *Sensors and Actuators B: Chemical, 255*, 2399–2406.
131. Ilkhani, H., & Farhad, S. (2018). A novel electrochemical DNA biosensor for Ebola virus detection. *Analytical Biochemistry, 557*, 151–155.
132. Faria, H. A. M., & Zucolotto, V. (2019). Label-free electrochemical DNA biosensor for zika virus identification. *Biosensors & Bioelectronics, 131*, 149–155.
133. Lee, T., Park, S. Y., Jang, H., Kim, G.-H., Lee, Y., Park, C., et al. (2019). Fabrication of electrochemical biosensor consisted of multi-functional DNA structure/porous au nanoparticle for avian influenza virus (H5N1) in chicken serum. *Materials Science and Engineering: C, 99*, 511–519.
134. Hwang, H. J., Ryu, M. Y., Park, C. Y., Ahn, J., Park, H. G., Choi, C., et al. (2017). High sensitive and selective electrochemical biosensor: Label-free detection of human norovirus using affinity peptide as molecular binder. *Biosensors & Bioelectronics, 87*, 164–170.
135. Lin, D., Tang, T., Harrison, D. J., Lee, W. E., & Jemere, A. B. (2015). A regenerating ultrasensitive electrochemical impedance immunosensor for the detection of adenovirus. *Biosensors and Bioelectronics, 68*, 129–134.
136. Baca, J. T., Severns, V., Lovato, D., Branch, D. W., & Larson, R. S. (2015). Rapid detection of Ebola virus with a reagent-free, point-of-care biosensor. *Sensors (Basel)., 15*(4), 8605–8614.
137. Dell'Atti, D., Zavaglia, M., Tombelli, S., Bertacca, G., Cavazzana, A. O., Bevilacqua, G., et al. (2007). Development of combined DNA-based piezoelectric biosensors for the simultaneous

detection and genotyping of high risk human papilloma virus strains. *Clinica Chimica Acta, 383*(1–2), 140–146.
138. Jenik, M., Schirhagl, R., Schirk, C., Hayden, O., Lieberzeit, P., Blaas, D., et al. (2009). Sensing picornaviruses using molecular imprinting techniques on a quartz crystal microbalance. *Analytical Chemistry, 81*(13), 5320–5326.
139. Carinelli, S., Kuhnemund, M., Nilsson, M., & Pividori, M. I. (2017). Yoctomole electrochemical genosensing of Ebola virus cDNA by rolling circle and circle to circle amplification. *Biosensors & Bioelectronics, 93*, 65–71.
140. Stern, M., Cohen, M., & Danielli, A. (2019). Configuration and design of electromagnets for rapid and precise manipulation of magnetic beads in biosensing applications. *Micromachines (Basel)., 10*(11).
141. Chen, H. W., Fang, Z. S., Chen, Y. T., Chen, Y. I., Yao, B. Y., Cheng, J. Y., et al. (2017). Targeting and enrichment of viral pathogen by cell membrane cloaked magnetic nanoparticles for enhanced detection. *ACS Applied Materials & Interfaces, 9*(46), 39953–39961.
142. Lee, J., Takemura, K., Kato, C. N., Suzuki, T., & Park, E. Y. (2017). Binary nanoparticle graphene hybrid structure-based highly sensitive biosensing platform for norovirus-like particle detection. *ACS Applied Materials & Interfaces, 9*(32), 27298–27304.
143. Chen, Y., Ren, R., Pu, H., Guo, X., Chang, J., Zhou, G., et al. (2017). Field-effect transistor biosensor for rapid detection of Ebola antigen. *Scientific Reports, 7*(1), 10974.
144. Dolai, S., & Tabib-Azar, M. (2019). 433 MHz Lithium Niobate microbalance aptamer-coated whole Zika virus sensor with 370 Hz/ng sensitivity. *EEE Sensors Journal, 20*(8), 4269–4274.
145. Peduru Hewa, T. M., Tannock, G. A., Mainwaring, D. E., Harrison, S., & Fecondo, J. V. (2009). The detection of influenza a and B viruses in clinical specimens using a quartz crystal microbalance. *Journal of Virological Methods, 162*(1–2), 14–21.
146. Chand, R., & Neethirajan, S. (2017). Microfluidic platform integrated with graphene-gold nano-composite aptasensor for one-step detection of norovirus. *Biosensors and Bioelectronics, 98*, 47–53.

Nanobiosensors for COVID-19

Karthik. N. and Avijit Kumar Das

Abstract

Coronavirus Disease (COVID-19) is an internationally recognized public health emergency. The disease, which has an incredibly high propagation rate, was discovered at the end of December 2019 in Wuhan, Hubei Province, China. The virus that causes COVID-19 is referred to as severe acute respiratory illness. Real-time reverse transcriptase (RT)-PCR assay is the primary diagnostic practice as a reference method for accurate diagnosis of this disease. There is a need for strong technology to detect and monitor public health. Early notification on signs and symptoms of the disorder is important and may be managed up to a few extents. To analyze the early signs and side effects of COVID-19 explicit techniques were applied. Sensors have been used as one of the methods for detection. These sensors are cost effective. These sensors will combine with a systematic device. It is utilized to detect the chemical compound and combined with a biological component. It is detected through physiochemical detector. Nanomaterials represent a robust tool against COVID-19 since they will be designed to act directly toward the infection, increase the effectiveness of standard antiviral drugs, or maybe to trigger the response of the patient. In this paper, we investigate how nanotechnology has been used in the improvement of nanosensor and the latest things of these nanosensors for different infections.

Keywords

COVID-19 · Detector · Nanotechnology · Biosensors

K. N. · A. K. Das (✉)
Department of Chemistry, CHRIST (Deemed to be University), Hosur Road, Bengaluru, Karnataka, India
e-mail: avijitkumar.das@christuniversity.in

G. Dutta (ed.), *Next-Generation Nanobiosensor Devices for Point-Of-Care Diagnostics*, https://doi.org/10.1007/978-981-19-7130-3_2

1 Introduction

By making quick decisions based on speedy diagnoses, smart data analysis, and informatics analysis, improved health care and higher standards of health care administration can be achieved [1]. Smart treatments, analytical tools, and diagnostic systems are needed in order to promote health and well-being [2]. Effective disease progression management and monitoring evaluation are crucial for epidemic comprehension and disease management if treatment optimization is to be achieved. It is therefore imperative to develop new and improved smart diagnostic technologies for personalized health care. Rapid and precise detection of analytes at the point of care for patients is made possible by the use of point-of-care testing [3]. In addition, because diseases may be detected early on, timely medical decisions can be made, improving the health of patients by allowing them to begin treatment sooner. In the last several years, a slew of new point-of-care devices have been developed, laying the groundwork for the next generation of diagnostic testing. Since they are directly responsible for the essay's bioanalytical performance, biosensors, analytical devices that translate or transduce a biological reaction into a quantifiable signal, are an essential part of point-of-care devices [4, 5]. Optical, electrochemical, piezoelectric, or thermal signals can all be used to quantify the process. Due to their high sensitivity accuracy, low detection limits, and significant potential for real-sample analysis, electrochemical biosensors have recently received much attention.

Through the discovery of new and diverse materials that combine unique features like optical, electrical, magnetic, or catalytic qualities, nanotechnology has had a huge impact on science and technology [6]. It is widely accepted that smart materials are a family of nanomaterials that respond to stimuli in a certain way (such as color, form, stiffness, opacity, or porosity) [7]. Using biosensor platforms and smart materials in combination, it is possible to improve sensitivity while also increasing specificity and eliminating the need for labels. From a viral diagnostic standpoint, there has been a range of methodologies utilizing different bio-elements (CRISPR-Cas9, nucleic acids, aptamers, and materials/transducers, such as microfluidics) and integrative platforms such as CRISPR-Cas9 [8]. When the pandemic hits, these tools will be a lifesaver, since they will allow for quick action, dependable results, ease of use, and portability [9]. As a part of this book chapter, we present a complete literature review on smart materials (such as graphene, light-sensitive, electrically sensitive, and wearable intelligent materials) and their biosensor integrations with examples of virus detection, such as SARS-CoV2 infected individuals.

2 Smart Materials for Sensor Technologies

Smart materials are characterized by their ability to sense and respond to one or more stimuli [10]. Their previous states are restored once the stimuli are removed [11]. There are a variety of external and internal stimuli that can be used, such as environmental, chemical (pH, ionic strength), electrical, and light. In addition to sensor technologies, smart materials are employed in a wide range of applications,

including actuators and robotics, artificial muscles, controlled drug delivery systems, and tissue engineering. Materials science, chemistry and physics, engineering, and nanotechnology all have a role in creating smart materials [12]. These include ionic and magnetic materials responding to ions and magnets, materials responsive to light and electricity, enzymes, temperature, pH, and materials sensitive to enzymatic reactions and all of these variables [13]. The flexibility, lightweight, mass producibility, and transparency of polymeric substances make them ideal for utilization in biological systems. In spite of this, they have a poor level of mechanical strength and stability. There are advantages to carbon-based nanomaterials that include mechanical strength and flexibility, electrical and thermal conductivity, biocompatibility, and antiviral properties [14].

In terms of electroanalytical performance and recognition element immobilization, current biosensor platforms primarily incorporate diverse nanomaterials derived from carbonaceous materials (e.g., carbon nanotubes, graphene, and carbon nanoparticles), inorganic materials (e.g., magnetic and metal nanoparticles), organic nanoparticles (e.g., dendrimers), conductive and insulating polymers (e.g., nanosized and nanostructured polymers or mo (e.g., hydrogel). The integration of these materials with biosensors aims for high selectivity, high sensitivity, rapid reaction time, ease of use, and cost-effective qualities. Cantilevers, nanotubes, ferromagnetic particles, conducting films and gels, dendrimers, microspheres, and nanoparticles are only a few examples [15].

3 Structure of SARS-CoV-2

Spherically encapsulated, the SARSCoV2 virus has a positive-strand RNA [(+) ssRNA] and measures 60–140 nm in diameter. It belongs to the Coronaviridae family, which includes both animal and human-infecting viruses. CoV. MERSCoV, SARSCoV, and SARSCoV2 are the four genera that make up the family. This is why MERSCoV, SARSCoV, and SARSCoV2 are all examples of human CoV [16]. The genome of SARSCoV2 showed structural proteins that were comparable to those reported in other CoVs. Researchers have gained a better knowledge of COVID-19 virus activity and function by identifying the virus spike, envelope, membrane, and nucleocapsid proteins (Fig. 1). Angiotensin converting enzyme 2 (ACE2) receptors on host target cells are endogenous membrane components and their binding and entrance mechanisms are tightly related with S protein binding to it. This protein is essential for the cleavage of angiotensin I and II in the plasma membrane of human epithelial cells [17].

The helical nucleocapsid produced by the interaction of N proteins with (+) ssRNA (30 kb in length) aids viral replication in the host cell. They are usually found in the area of the endoplasmic Golgi reticulum. The three transmembrane domains of the M protein play a key role in the form, size, and assembly of viruses. Viral replication and pathogenicity of the virus SARSCoV2 are dependent on the production of protein E, which is synthesized in the infected vesicles' trafficking organelles. The S-packet anchor protein is a class I trimeric fusion protein when

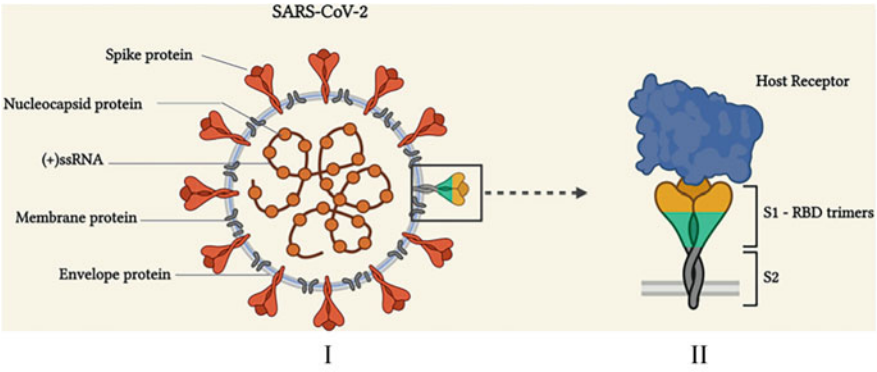

Fig. 1 Schematic representation of the SARS-CoV-2 structure and spike-receptor binding mechanism (figure created with BioRender.com which is reproduced with permission from Ref. [7])

viewed under an electron microscope and it displays a peak-like structure. They regulate viral infection and facilitate viral entry into the host cell through the N and S proteins. The S protein is made up of two distinct subunits that perform different functions (S1 and S2). The identification and binding of cellular receptors are carried out by the globular subunit S1, which has a greater RBD. Virus–cell fusion is made possible by the S2 subunit. To some extent, the host range of a virus is determined by the RBD region's interaction with receptors on host cells. Protease priming at the S1/S2 site occurs after SARS-CoV-2 interacts with human cells via the ACE2 receptor, resulting in virus entry and pathogenesis in the host cell.

4 Infection Mechanism of SARS-CoV-2

The infectious agent's S macromolecule (RBD region) interacts with the ACE2 receptors on the host cell to gain access into the cell. In order to facilitate fusion membrane and virology through intracellular processes, two amino acids transmembrane proteinases (TMPRSS2) chemically cleave S1 at the S1/S2 border, facilitating S1 dissociation and modifying S2 shape. Finally, a large polyprotein (pp1a and pp1ab polyprotein) is generated by attaching camouflage (+) ssRNA to the ribosome in the host cell, resulting in the translation of two smaller fragments. Additionally, fresh virions are gathered together. PL expert (a papain-like protease), 3CLstar (3CLstar), and RNA-dependent RNA polymerase (RD-RNA polymerase) are three of the enzymes involved in protein cleavage, as are replication and the creation of new virions (RdRp) [18].

SARSCoV2 is able to persist and spread because of these chemicals, which are currently being studied as potential treatment targets. Different cells can be infected by new infections that have been formed (cycle of development) and transferred to the cell surface in vesicles. Figure 2 depicts the SARSCoV2-related systems that connect, sever, and replicate the virus. Endocytosis allows SARSCoV2's viral S

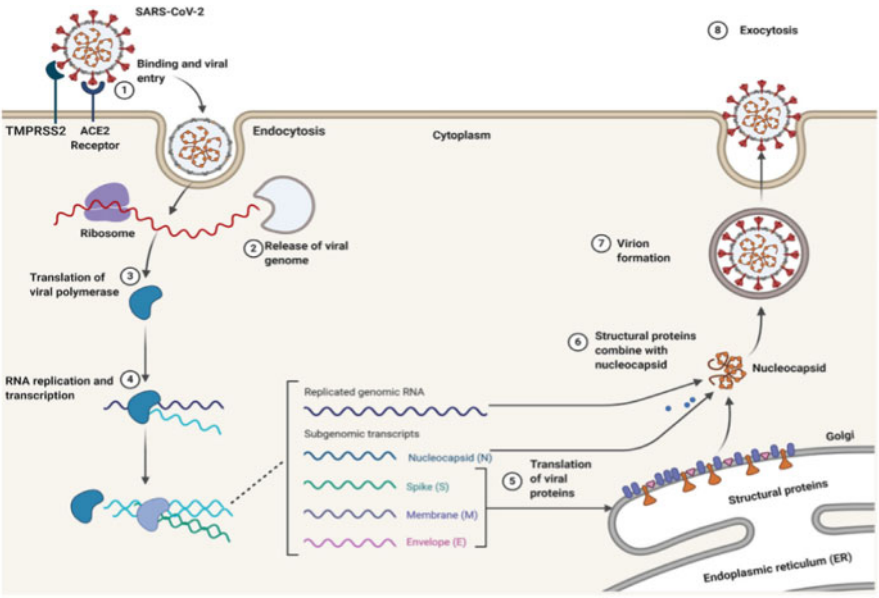

Fig. 2 Infection mechanism and life cycle of SARS-CoV-2 in the host cells (figure created with BioRender.com which is reproduced with permission from Ref. [7])

protein to enter target cells after binding to the ACE2 receptor under the direction of the TMPRSS2 gene (1). A transcript of genome RNA (sense) is then produced following the fusing of the cell membrane and appearance of virus (+) small sequence RNA in the cell (2). The viral protein polymerase is then decoded (3), (4). Interpretation is facilitated by the reconstruction of genomic and auxiliary transcripts. Exocytosis, the process by which newly formed virions are ejected from the host cell, is aided by the S, E, and M proteins' interaction with the nucleocapsid [18].

5 Nanotechnologies in the Diagnosis of COVID-19

Several nanomaterials have been utilized in POC devices because of their useful qualities for detection, including chemical stability, excellent electrical conductivity, and localized surface plasmon resonance (LSPR) [19]. Increased sensitivity and specificity can be achieved by incorporating nanomaterials into analytical equipment, such as colorimetry, electrochemistry, and plasmonics. It is common practice to utilize AuNPs to label target molecules in lateral flow assays (LFAs) since they can be read by the naked eye. The concentration of the target can be determined from a taken image using qualitative results or smartphone analysis [17]. For the detection of antibodies and proteins in complex samples like urine, blood, and saliva, LFAs are frequently utilized in POC analysis. They are cheap, quick (5–30 min) and do not

alter biomolecule function while stored at room temperature, as demonstrated by Koczula & Gallotta in 2016. However, a number of studies have shown that AuNPs boost the biosensor signal and sensitivity, allowing the detection of analytes at lower concentrations [20]. Hepatitis, influenza, and the Zika virus have all been diagnosed using this method.

LFA biosensors for diagnosing COVID-19 have recently been reported by Udugamaetal et al. and provided to health systems for decentralized testing [21]. SARSCoV2 protein-specific IgG and IgM antibodies were discovered by these LFAs, which indicated that the patient had been infected, as demonstrated by Morales Narváez and Dincer in 2020 [22]. They are useful for population screening, however, they are not as sensitive as RT-PCR testing. When these nanomaterials are functionalized with biomolecules, the most frequent detection approach is to change the color of the AuNPs when they bond to their target molecules. A colorimetric test for the identification of SARSCoV2 was published based on the following technique Two distinct sections of the SARSCoV2 N protein gene were the targets of four antisense oligonucleotides (AOs). A thiol group was added to the 3′ or 5′ end of the AOs and conjugated with AuNPs. A redshift of around 40 nm in the LSPR band is caused by the target sequence and the AO-cleaved AuNPs, and the color of the solution changes from violet to blue when they are combined. MERSCoV sequences were used to test the detection system's sensitivity and specificity. Colorimetric testing based on AuNPs' optical characteristics can provide a substantial contribution to COVID-19 care by allowing for a rapid and straightforward diagnosis. AuNPs can also be employed in electrochemical biosensors to enhance the active electrode surface and electron and signal transmission rates. Using an AuNPs-modified carbon electrode, Layqah and Eissa et al. developed an electrochemical immunosensor for the detection of MERSCoV [23]. Using a competitive technique, the biosensor immobilizes MERSCoV S proteins in an electrode by mixing a nasal sample with antibodies against the virus's S protein. A square wave potential measurement was done after the electrode had been incubated for a period of time. The current lower as the antibodies bind to the immobilized proteins on the electrodes. When antibodies are linked to MERSCoV, the pathogenicity is diminished. Deposition of AuNPs on the electrodes is responsible for the biosensor's superior analytical performance and low detection limit. AuNPs can likewise be used to detect COVID-19 using this method.

For signal amplification, analyte concentration and magnetic separation, magnetic NPs (MNPs) have been employed in biological detection devices [24]. In complex samples like blood or urine, it is difficult to detect analytes directly because of signal interference from other biomolecules or low quantities of analytes can considerably affect the analysis's accuracy. To circumvent these constraints, researchers have employed MNPs, functionalized with bioreceptors in numerous experiments. For H9N2 AIV detection, an electroluminescent biosensor using MNPs modified with mAbs to capture the virus was reported. Magnetic separation reduces interference from complex materials and allows for the detection of the virus at a limit of detection (LOD) of 14 fg/mL, according to the authors [25]. A digital microfluidic chip for the detection of the H1N1 virus was developed by Lu et al.

using functionalized magnetic NPs. The NPs capture the virus and are electromagnetically entrained toward the channels, passing through the points where they are fluorescently labelled and the probes are detected. A possible approach for the diagnosis of COVID-19 is based on magnetic NP-based biosensors [26].

6 Nanotechnologies in the Treatment of COVID-19

When it comes to COVID19 therapy, nanotechnology has a wide range of applications and can be used at various stages of disease. It has been shown to activate intracellular mechanisms that cause irreversible damage to the virus, as well as to inhibit virus–cell interactions and membrane fusion [27]. The properties of nanoparticles (NPs) (both organic and inorganic) have drawn a lot of interest with some of the characteristics of luminescence, adjustable shape and composition, huge surface-to-volume ratio, and capacity to represent numerous comparable sites [28]. Neutral silica NPs, iron oxide NPs, and metallic NPs are the most prevalent forms of inorganic NPs (gold, silver). Biodegradability, biocompatibility, non-toxicity, and site-specific medication targeting are all advantages of organic NPs. Polymeric and lipid NPs, dendrimers, extracellular vesicles (or exosomes), and liposomes are the most commonly employed organic NPs [29].

7 Inorganic Nanoparticles

The optical features of INPs distinguish them from other types of particles. As contrast agents and in photothermal therapy, these materials have been employed in the medical field [30]. Regulated stability, increased permeability, high functionalization potential, and controlled release activation are some of the key qualities that will lead to biological applications of INPs. This is based on other qualities such as luminescence as well as their capacity to be altered in size, shape, composition, and their high surface area to volume ratio. Several studies have examined the ability of these INPs to display multiple binding sites on the surface. It is still unclear whether or not inorganic NPs have any harmful characteristics in therapeutic settings. NPs can cause reactive oxygen species, genotoxicity, cell morphology, and abnormalities in osteoblasts when they are in healthy tissue [31]. Polymer or biological conjugation of NPs may minimize some of these issues, but intracellular concentration and localization may still have an impact. After iron surface degradation, the acidic pH of phagolysosomes (pH 4–5), for example, generates free ions in the cytoplasm. Large particles are deposited in tissues with low blood flow and are easily caught by macrophages, but nanostructures with a smaller size can enter cells and bind to decompensated nucleic acid fluxes. The enzymatic breakdown of NP residues (such as iron and gold) in the blood allows it to be utilized for physiological metabolism, while in the lung tissue, microparticles and nanoparticles are maintained in the bronchi and the alveoli are therefore tough to remove. As revealed by De Matteis, 2017, they exit the body before the

intracellularity of healthy cells. These nanoparticles are examined in this area to see if they can be used as antiviral medicines, along with other nanoparticles such as silver (AgNPs), iron oxide (IONPs), and neutral silica Surface functionalization of NPs offers great potential for the development of novel therapeutic treatments against COVID-19 [32] because of the interaction between the nanocomposite with viral capsid structure. The features of AuNP gold nanoparticles (previously mentioned in the section Nanotechnology in the diagnosis of COVID-19) that allow them to be employed for diagnosis and treatment have sparked attention in various scientific fields. The strong binding between gold and thiol ligands makes it easy to functionalize gold, which is a relevant property to note. Sulfonate ligands, which replicate the position of heparan sulfate proteoglycans (HSPGs) on the cell surface, are the most commonly employed functionalization molecules for metal NPs. Antiviral activity is prevented because the virus is trapped on its surface and cannot infect cells. In vitro and in vivo experiments with respiratory syncytial virus and other viruses, AuNPs with lengthy MES and MUS links caused irreversible deformation, according to a recent study. We believe that AuNPs working with MUS demonstrate multiple-valent binding to the virus, leading to capsid structural disruption. It is therefore possible that COVID-19 treatment would benefit from this multivalent binding. AuNPs capable of binding to sugars containing several sulfonate groups, such as glucose and lactose, were found to have low effective concentrations against dengue virus in another study [33]. Experimental evidence shows that the optimal molecule length for integration into the OG pocket in substratemounted tests, which suggests the role of AuNPs. The molecule's length is a crucial factor in viral infection. Large surface area of porous AuNPs led to greater suppression of influenza virus growth compared to nonporous AuNPs and AgNPs. Because AuNPs are hollow, disulfide bonds in hemagglutinin are prevented, impeding intracellular uptake [34] (Fig. 3).

8 Nanobiosensors for the Detection of Human Coronavirus (2019-nCoV, SARS/MERSCoV) and Influenza Viruses

SARS and other pandemic-causing infections can be detected with nanobiosensors, which are crucial instruments. When it comes to detecting viruses, nanosensors can be divided into various categories based on their detection mechanism (electrical, chemical, or electrochemical), as well as their measurable qualities (heat, magnetism, and biology) [35]. Brief summaries of nanobiosensor detection procedures for epidemic/pandemic respiratory viruses, such as avian influenza virus subtype H5N1 from the 2004 outbreak and H7N9 (the 2013 epidemic), are provided in the following sections. Accordingly, swine flu (2009 pandemic), seasonal H3N2 influenza, MERS (2012) and COVID 19 (2019-nCoV) and their properties are also presented [36].

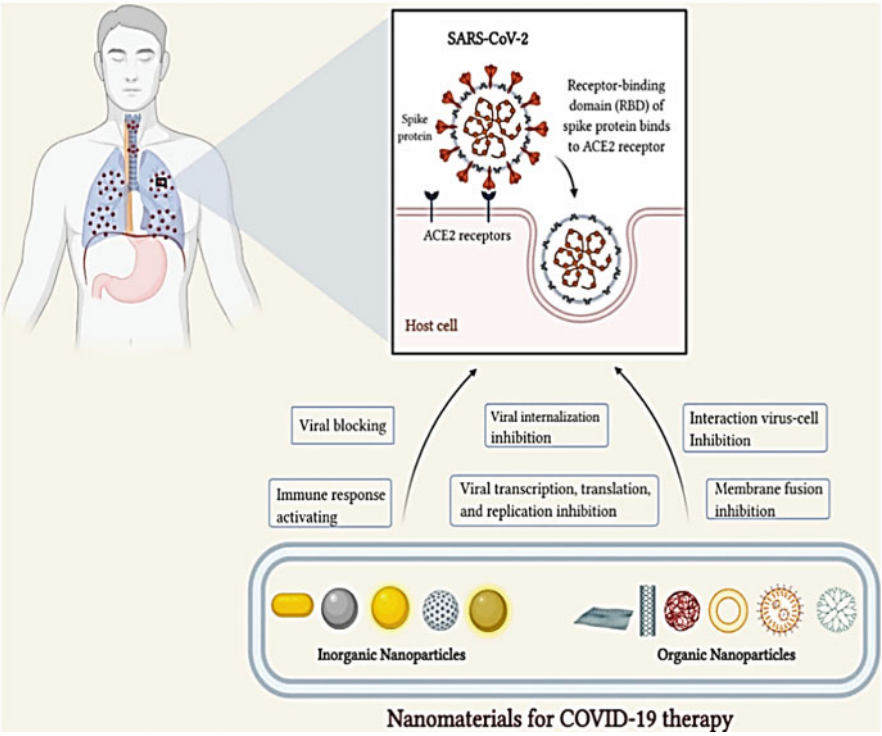

Fig. 3 Types of nanoparticles to application in COVID-19 therapy (figure created with BioRender.com which is reproduced with permission from Ref. [7])

9 Electrochemical Nanobiosensors

There are numerous applications for electrochemical nanobiosensors. To generate an electrical signal, an electrochemical nanobiosensor combines a biorecognition event with an electrode probe [37]. Electrical nanosensors have electrodes with semiconductor, dielectric, and charge distribution properties that are all essential considerations. For a given detecting surface, surface modification of nanostructures or nanomaterials is required in order to alter the functional class [38]. Many experiments have been done to boost the volume/surface ratio and selectivity of nanobiosensors by integrating nanomaterials into the surface. Applications for biodetection benefit greatly from the usage of nanomaterials. A resistance, potential, or impedance probe is employed in most nanobiosensors for the detection of infections and viruses. Electrochemical conductivity or resistance changes occur as the target material adheres to the electrode surface, which is how nanobiosensors work. An electrochemical signal is generated when electrons are consumed or produced in a biological reaction on the electrode surface. As a result, selectivity can be used to assess a single chemical in a large sample in real time with excellent

sensitivity. Chemisorption of molecules that alter conductivity as a result of chemical sensitization is the primary detecting mechanism. Any virus in the target sample must be detected using a probe that has biological receptors [39]. The majority of researchers employed electrochemical detection methods, such as field-effect transistors (FETs), bioelectrical identification tests (BERA), EIS, amperometric, cyclic voltmeter, or conductivity testing, to identify distinct forms of coronavirus. Enveloped RNA (RNA) viruses, which include Orthomyxoviridae, are the cause of influenza, an acute infectious disease [40]. Influenza consists of four distinct subtypes based on the virus's structure (ion channels, substrates, and membrane proteins), each of which is distinct from the others. It is possible to distinguish between influenza virus subtypes based on individual differences. HA and neuraminidase, two proteins found on the surface of influenza A viruses, are used to classify different strains of the virus (NA). A/H1N1, which produced the 2009 grape flu pandemic and the 1918 influenza pandemic, is one of the most studied influenza A viral subtypes. Many countries are still concerned about the threat of this disease, which has claimed the lives of millions [41].

There has been a great deal of research into the influenza A virus subtypes H5N1, H7N7, and H7N9, which are all avian influenza viruses (AIVs). With the use of nanostructures and various nanomaterials, such as magnetic iron oxide nanoparticles, the bioreactor can be transported directly to the detector. The coronavirus, which comprises SARSCoV, MERSCoV, and the novel coronavirus 2019nCoV, is the second respiratory virus to produce an epidemic or pandemic. The respiratory coronavirus that causes the disease COVID-19 has been examined extensively by researchers using electrochemical methods and biosensors that are designed to detect COVID-19. Electrochemical detection methods for influenza viruses, human coronaviruses (including COVID-19), and parameters of these viruses are summarized in Table 1. For specific proteins or DNA strains, the impedance biosensor is ideal, while optical or mass-sensitive biosensors are less sensitive than the impedance biosensor. Electrochemical impedance spectroscopy (EIS) is less destructive for measuring interactions between biological samples than other electrochemical methods, such as Differential Voltage (DPV) and Cyclic Voltage (CV) Measurement).

10 FET-Based Electrochemical Nanobiosensor

In comparison to other biosensors, field-effect transistors (FETs) biosensors have a number of advantages and features. These biosensors can detect bioanalytes at extremely low concentrations and offer results in milliseconds. Biosensors based on FETs can be employed in a variety of settings, including health care, point of service, and diagnostic applications. Carbon atoms are arranged in a two-dimensional layer to form graphene, a cutting-edge nanomaterial (Scheme 1). An active detecting surface may be created using this material's good conductivity, high mobility of the carriers, ease of usage, and vast surface area. As a result, integrating graphene-based materials into FET biosensors may be the best option

Table 1 Summarization of electrochemical detection methods for influenza viruses, human coronaviruses (including COVID-19), and various parameters of the viruses

Biological samples	Nanomaterials	Detection methods	Target	Limit of detection (l.o.d) Linear range	References
Biological substances Such as DNA and proteins	Graphene (single-layer hexagonal carbon networks)	Field-Effect Transistor (FET)	Lectin	LOD: 130 pM	[42]
Oligonucleotide sequences derived from an H5N1 avian influenza	rGO reduced graphene oxide	Field-Effect Transistor (FET	Gene (H5N1)	LOD: 50 pM	[19]
Saliva	Nanocrystalline boron-doped diamond	Electrochemical impedance (EIS)	Influenzavirus M1 protein	LOD: 5×10^{-14} g/mL	[43]
Egg sample	Graphene gold hybrid Nanocomposite	Electrochemical impedance (EIS)	Influenza A virus	LOD: 10^{-8} U/mL LR: 10^{-8}–10^{-10} U/Ml	[44]
Fetal bovine serum, extraneous bovine serum albumin (BSA)	Gold electrode	Electrochemical impedance spectroscopy (EIS)	Human influenza virus type A (H3N2)	LOD: 8 ng/mL	[45]
Saliva buffer	Diamond biosensor (nano-scale boron-doped diamond surface sensor)	Electrochemical impedance spectroscopy (EIS)	M1 protein of influenza A virus	LOD: 1 fg/mL LR:1–100 fg/mL	[46]
Viral sample of inactivated, but intact influenza viruses H3N2	Gold electrode	Electrochemical impedance spectroscopy (EIS)	Human influenza A virus (H3N2)	LOD: 1.3×10^4 viruses/mL	[47]
Isolated AIV H5N1 sample incubated for 45 min at 37 °C	Magnetic iron oxide (Fe_3O_4) nanobeads	Electrochemical impedance spectroscopy (EIS)	Avian influenza virus (AIV) (H5N1)	LOD: 0.0128 HA unit/50 µL	[48]
Biological samples with avian influenza virus	Magnetic streptavidin-coated 30 nm nanobeads	Electrochemical impedance spectroscopy (EIS)	Avian influenza virus (AIV) (H5N1)	LOD:103 EID 50/mL	[49]

(continued)

Table 1 (continued)

Biological samples	Nanomaterials	Detection methods	Target	Limit of detection (l.o.d) Linear range	References
Inactivated avian influenza virus H5N1 sample	Concanavalin A-glucose oxidase-Au nanoparticles (ConA-GOx-AuNPs)	Electrochemical impedance spectroscopy (EIS)	Avian influenza virus (AIV) (H5N1)	LOD: 0.04 HAU/mL LR:	[50]
Commercial sample Spike saliva	Gold paper electrode	Electrochemical Impedance spectroscopy (EIS)	H1N1 antigen	LOD: 4.70 PFU/mL	[51]
Influenza viral particles in infected swine nasal samples	Reduced graphene oxide nanosheets (RGO)	Chronoamperometry (CA)	Human influenza A virus (H1N1)	LOD: 0.5 PFU/mL LR: 1–104 PFU/mL	[52]
Virus culture in embryonated chicken egg	Gold nanoparticles (AuNPs)	Chronoamperoy (CA)	Influenza virus (H9N2)	LOD: 16 HAU	[53]
Virus samples in chicken embryo cultures	Conducting polymer of PEDOT-poly (3,4-ethylene-dioxythiophene) PSS film	Amperometry	Human influenza A virus (H1N1)	LOD: 0.025 HAU	[54]

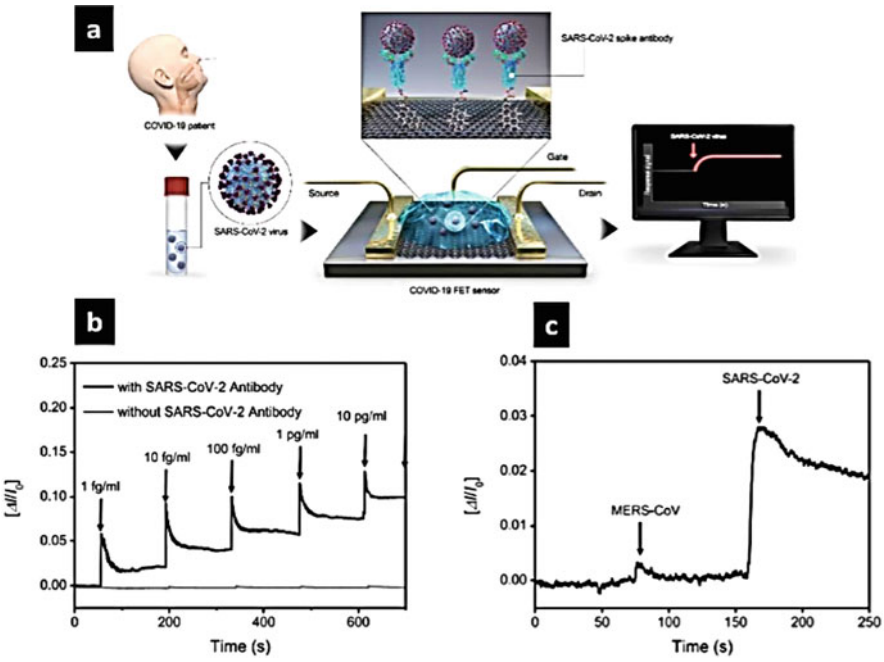

Scheme 1 (**a**) Schematic illustration of graphene-based field-effect transistor (FET) biosensor mechanism and detection, where SARS-CoV-2 (spheres) binds to antibodies (Y-shapes). (**b**) Real-time response of COVID-19 FET toward SARS-CoV-2 spike protein. (**c**) Bionanosensor selectivity response toward two different proteins: SARS-CoV-2 and MERSCoV (Scheme 1 is reproduced with the permission from Ref. 55 of the American Chemical Society)

for improving detection sensitivity [22]. Graphene is a two-dimensional nanomaterial composed of carbon atoms [56]. Because of its strong electrical conductivity, high carrier mobility, simplified surface function, and vast surface area, this material can be employed as an active detecting surface. FET biosensors may benefit from the incorporation of graphene-based materials in order to increase detection sensitivity [42].

In order to avoid a pandemic of influenza, it is required to identify viruses with pandemic potential by measuring their affinity for sialoglycan with high accuracy, speed, and sensitivity. Additionally, the graphene-based field-effect transistor approach (GFET) was utilized to detect extremely sensitive biological molecules, such as DNA and proteins (such lectins). The bioFET approach and the H5N1 influenza virus gene offer a promising platform for markerless detection using a strategy flow comb for quick detection. The bioFET method was employed to determine limit of detection (LOD) for influenza virus in the picomolar range, 130 pM and 50 pM, respectively, demonstrating high sensitivity [57]. Using a reduced graphene oxide (rGO) coating on a Si/SiO_2 substrate, increased the sensitivity of the BioFET sensor to detect the H5N1 influenza virus gene in a liquid media for influenza detection (FET graphene) [58].

11 Cell-Based Electrochemical Nanobiosensor

In contemporary COVID-19 disease treatment, estimating the number of infected patients in real time has been a key difficulty. The detection limit of 1 fg/mL of SARSCoV2 S1 spike protein may be detected using a new biosensor in 3 min and a supersensitive surface [59]. Electrochemically inserted S1 antibodies were employed to improve the binding of a protein to cellular components generated via membrane engineering, a cell assay idea for biomolecule identification. The electrical measurements of changed cell membranes were affected by biomolecules attached to the released antibodies, according to the findings. As illustrated in Fig. 4, the results demonstrate significant variations in electrical behavior characteristics. The established biosensors have several advantages for clinical testing, monitoring, and virus management. SARSCoV2 surface antigens can be detected using this biosensor's portable, easy-to-handle reader [60].

12 Piezoelectric Nanobiosensors

Because of its straightforward design, direct identification, and real-time output, the piezoelectric quartz crystal balanced microbial sensor has drawn substantial interest in biological and chemical applications. Mass wave (BW) and surface acoustic wave (SAW) are two types of piezoelectric sensors (SAW). An electrical output is provided by these biosensors, which can detect biological entities and transform mechanical power into electrical power. The mechanical resonance of a crystal vibrating at its inherent frequency is produced by piezoelectric materials (Fig. 5).

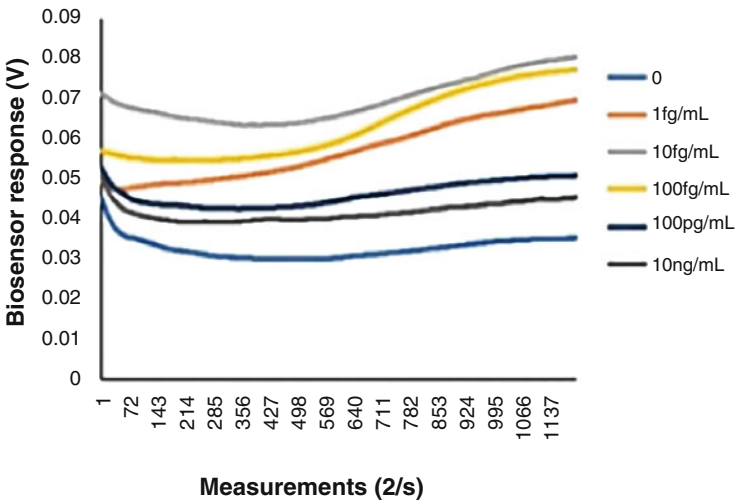

Fig. 4 Biosensor response was given by the variation of voltage in time for different concentrations of biomolecules (Figure is reproduced with permission from Ref. [23])

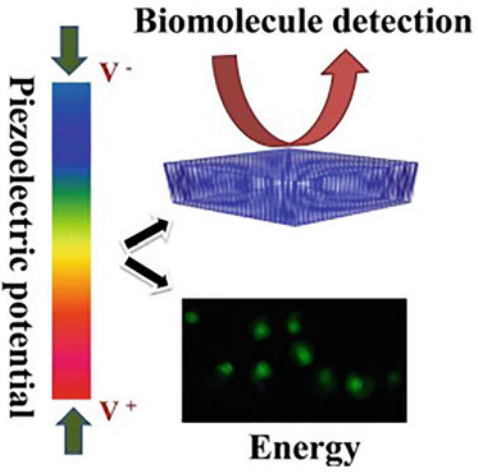

Fig. 5 Unconventional active biosensor made of piezoelectric nanoparticles for biomolecule detection

External electrical signals can alter this frequency [61]. Eventually, a reaction happens when the analyte of a person comes into touch with the detecting material, leading to a shift in frequency resulted also a shift in electrical measurements. Therefore, micro- or nano-sized sensors can be used for detection [62].

The quartz crystal resonator is tuned and the frequency of the probe is plotted to determine the change in mass and viscosity at the surface [63]. The advantage of this technique is its ability to detect molecules without labelling. The detecting process is complicated, and the measurements are not as precise [55]. These biosensors have been utilized in a wide variety of biological applications, such as determining the presence of hormones, bacteria, and cells fabricated an optical quartz crystal microbalance sensor using a three-dimensional (3D) nanocell on gold (Au) for the detection of H5N1 bird flu virus. For example, the sensor's LOD is between 2 and 4 HAU/50 L and the detection time is 10 min, making it faster than previous approaches (30 min). For mass detection, piezoelectric immunosensors have been created to detect SARS-associated coronavirus [64].

13 Nucleic Acid Biosensor

Detection of SARSCoV2 nucleic acid has been made possible by the development of a plasmonic biosensor. Plasmon photothermal effect (PPT) and locally surface plasmon resonance detection transduction are used in tandem with this biosensor. Gold nanoisoles (AuNIs) embedded on a two-dimensional chip have been immobilized by thiol bonds to a cDNA receptor for RdRp, ORF1ab, or the E gene. The detection of SARSCoV2 nucleic acids using this method uses the principle of nucleic acid hybridization with a LOD of 0.22 μM. Due to the increased local capacity of AuNI plasmonic chip PPT heat generation, the hybridization kinetics of

the complementary filaments have improved, increasing the sensitivity of the device. Clinical trials are still needed to evaluate the effectiveness of this biosensor [50].

14 Conclusion

In this book chapter, we have shown the pathway of utilizing smart materials in biosensor systems to detect COVID-19. Worldwide efforts were made throughout this epidemic to establish the best method of biological detection. Electroactive and sensitive materials platforms, microfluidic platforms, LFAs, and wearable materials are only a few examples of instances in this field of study. For example, biosensors can be used in place of more time-consuming methods, single-use to avoid contamination or infection reducing the need for specialists, and centralized laboratories equipped with expensive tolls. Biosensors have many advantages and their future will be able to perform a wide range of tasks having smart materials integration systems. The ultimate goal is to build new nanosensors for point-of-care diagnostics of various diseases, despite the fact that this subject is gaining speed and a lot of researchers have spent time developing new nanosensors. Continuous patient monitoring that is reliable for the long haul has yet to be accomplished.

References

1. Aanouz, I., Belhassan, A., El-Khatabi, K., Lakhlifi, T., El-ldrissi, M., & Bouachrine, M. (2020). Moroccan medicinal plants as inhibitors against SARSCoV-2 main protease: computational investigations. *Journal of Biomolecular Structure & Dynamics, 6*, 2971–2979.
2. Bennet, L. (1996). The common cold. *Journal of General Internal Medicine, 11*, 229–236.
3. Palese, P. (2004). Influenza: old and new threats. *Nature Medicine, 10*, S82–S87.
4. Henderson, D. A. (1999). Clinical and epidemiologic characteristics of smallpox. *Emerging Infectious Diseases, 5*, 537–539.
5. Bhardwaj, V., & Kaushik, A. (2017). Biomedical applications of nanotechnology and nanomaterials. *Micromachines, 10*, 298.
6. Kaushik, A., Yndart, A., & Kumar, S. (2018). A sensitive electrochemical immunosensor for label-free detection of Zikavirus protein. *Scientific Reports, 8*, 9700.
7. de Oliveira Cardoso, V. M., Moreira, B. J., Comparetti, E. J., Sampaio, I., Ferreira, L. M. B., Lins, P. M. P., & Zucolotto, V. (2020). Is nanotechnology helping in the fight against COVID-19? *Frontiers in Nanotechnology, 2*, 588915.
8. Vashist, S. (2017). Point-of-care diagnostics: recent advances and trends. *Biosensors, 7*, 62.
9. Vashist, S. K., Luppa, P. B., Yeo, L. Y., Ozcan, A., & Luong, J. H. T. (2015). Emerging technologies for next-generation point-of-care testing. *Trends in Biotechnology, 33*, 692–705.
10. Boopathi, S., Poma, A. B., & Kolandaivel, P. (2020). Novel 2019 coronavirus structure, mechanism of action, antiviral drug promises and rule out against its treatment. *Journal of Biomolecular Structure and Dynamics., 30*, 1–10. https://doi.org/10.1080/07391102.2020.1758788
11. Graham, R. L., Donaldson, E. F., & Baric, R. S. (2013). A decade after SARS: Strategies for controlling emerging coronaviruses. *Nature Reviews. Microbiology, 11*, 836–848.
12. Syedmoradi, L., Daneshpour, M., Alvandipour, M., Gomez, F. A., Hajghassem, H., & Omidfar, K. (2017). Point of care testing: The impact of nanotechnology. *Biosensors & Bioelectronics, 87*, 373–387.

13. Brazaca, L. C., Moreto, J. R., Martín, A., Tehrani, F., Wang, J., & Zucolotto, V. (2019). Colorimetric paper-based immunosensor for simultaneous determination of fetuin band cluster into ward early Alzheimer's diagnosis. *ACS Nano, 13*, 13325–13332.
14. Rodríguez, M. O., Covián, L. B., García, A. C., & Blanco-López, M. C. (2016). Silver and gold enhancement methods for lateral flow immunoassays. *Talanta, 148*, 272–278.
15. Luo, F., Long, C., Wu, Z., Xiong, H., Chen, M., & Zhang, X. (2020). Functional silica nanospheres for sensitive detection of H9N2 avian influenza virus based on immunomagnetic separation. *Sensors and Actuators B: Chemical, 310*, 127831.
16. Luo, P., Liu, Y., Qiu, L., Liu, X., Liu, D., & Li, J. (2020). Tocilizumab treatment in COVID-19: a single center experience. *Journal of Medical Virology, 92*, 814–818.
17. Soenen, S. J., Rivera-Gil, P., Montenegro, J.-M., Parak, W. J., De Smedt, S. C., & Braeckmans, K. (2011). Cellular toxicity of inorganic nanoparticles: Common aspects and guidelines for improved nanotoxicity evaluation. *Nano Today., 6*(5), 446–465.
18. Ishikawa, F. N., Chang, H.-K., Curreli, M., Liao, H.-I., Olson, C. A., Chen, P.-C., et al. (2009). Label-free, electrical detection of the SARS virus N-protein with nanowire biosensors utilizing antibody mimics as capture probes. *ACS Nano, 3*, 1219–1224.
19. Chan, C., Shi, J., Fan, Y., & Yang, M. (2017). A microfluidic flow-through chip integrated with reduced graphene oxide transistor for influenza virus gene detection. *Sensors & Actuators, B: Chemical, 251*, 927–933.
20. Qiu, G., Gai, Z., Tao, Y., Schmitt, J., Kullak-Ublick, G. A., & Wang, J. (2020). Dual-functional plasmonic photothermal biosensors for highly accurate severe acute respiratory syndrome coronavirus 2 detection. *ACS Nano, 14*, 5268–5277.
21. Bhalla, N., Pan, Y., Yang, Z., & Payam, A. F. (2020). Opportunities and challenges for biosensors and nanoscale analytical tools for pandemics: Covid-19. *ACS Nano, 14*, 7783–7807.
22. Morales-Narváez, E., & Dincer, C. (2020). The impact of biosensing in a pandemic outbreak: COVID-19. *Biosensors & Bioelectronics, 163*, 112274. https://doi.org/10.1016/j.bios.2020.112274
23. Mavrikou, S., Moschopoulou, G., Tsekouras, V., & Kintzios, S. (2020). Development of a portable, ultra-rapid and ultra-sensitive cell-based biosensor for the direct detection of the SARS-CoV-2 S1 spike protein antigen. *Sensors, 20*, 3121.
24. Palomar, Q., Xu, X., Gondran, C., Holzinger, M., Cosnier, S., & Zhang, Z. (2020). Voltammetric sensing of recombinant viral dengue virus 2 ns1 based on au nanoparticle–decorated multiwalled carbon nanotube composites. *Microchimica Acta, 187*, 1–10.
25. Ribeiro, B. V., Cordeiro, T. A. R., e Freitas, G. R. O., Ferreira, L. F., & Franco, D. L. (2020). Biosensors for the detection of respiratory viruses: A review. *Talanta Open, 2*, 100007.
26. Sun, Z., Ren, K., Zhang, X., Chen, J., Jiang, Z., Jiang, J., Ji, F., Ouyang, X., & Li, L. (2021). Mass spectrometry analysis of newly emerging coronavirus HCoV-19 spike S protein and human ACE2 reveals camouflaging glycans and unique post-translational modifications. *Engineering, 7*(10), 1441–1451.
27. Roh, C., & Jo, S. K. (2011). Quantitative and sensitive detection of SARS coronavirus nucleocapsid protein using quantum dots-conjugated RNA aptamer on chip. *Journal of Chemical Technology and Biotechnology, 86*, 1475–1479.
28. Hsu, Y.-R., Lee, G.-Y., Chyi, J.-I., Chang, C.-K., Huang, C.-C., Hsu, C.-P., Huang, T.-H., Ren, F., & Wang, Y.-L. (2013). Detection of severe acute respiratory syndrome (SARS) coronavirus nucleocapsid protein using AlGaN/GaN high electron mobility transistors. *ECS Transactions, 50*, 239–243.
29. Kilianski, A., Mielech, A. M., Deng, X., & Baker, S. C. (2013). Assessing activity and inhibition of middle east respiratory syndrome coronavirus papain-like and 3C-like proteases using luciferase-based biosensors. *Journal of Virology, 87*, 11955–11962.
30. Teklemariam, A. D., Samaddar, M., Alharbi, M. G., Al Hindi, R. R., & Bhunia, A. K. (2020). Biosensor and molecular-based methods for the detection of human coronaviruses: A review. *Molecular and Cellular Probes, 54*, 101662.

31. Zuo, B., Li, S., Guo, Z., Zhang, J., & Chen, C. (2004). Piezoelectric immunosensor for SARS-associated coronavirus in sputum. *Analytical Chemistry, 76*, 3536–3540.
32. Xie, B. (2000). Mini/micro thermal biosensors and other related devices for biochemical/clinical analysis and monitoring. *TrAC Trends in Analytical Chemistry, 19*, 340–349.
33. Sinnarasa, I., Thimont, Y., Presmanes, L., Barnabé, A., & Tailhades, P. (2017). Thermoelectric and transport properties of delafossite $CuCrO_2$:Mg thin films prepared by rf magnetron sputtering. *Nanomaterials, 7*, 157.
34. Kizek, R., Krejcova, L., Michalek, P., Rodrigo, M. M., Heger, Z., Krizkova, S., Vaculovicova, M., Hynek, D., & Adam, V. (2015). Nanoscale virus biosensors: State of the art. *Nanobiosensors in Disease Diagnosis, 4*, 47–66.
35. Srivastava, A. K., Dev, A., & Karmakar, S. (2018). Nanosensors and nanobiosensors in food and agriculture. *Environmental Chemistry Letters, 16*, 161–182.
36. Kaya, S. I., Karadurmus, L., Ozcelikay, G., Bakirhan, N. K., & Ozkan, S. A. (2020). Chapter 18—Electrochemical virus detections with nanobiosensors. In B. Han, V. K. Tomer, T. A. Nguyen, A. Farmani, & P. Kumar Singh (Eds.), *Nanosensors for smart cities* (pp. 303–326). Elsevier.
37. Abdel-Karim, R., Reda, Y., & Abdel-Fattah, A. (2020). Review—nanostructured materials-based nanosensors. *Journal of the Electrochemical Society, 167*, 03755.
38. Szunerits, S., Saada, T. N., Meziane, D., & Boukherroub, R. (2020). Magneto-optical nanostructures for viral sensing. *Nanomaterials, 10*, 1271.
39. Alhalaili, B., Popescu, I. N., Kamoun, O., Alzubi, F., Alawadhia, S., & Vidu, R. (2020). Nanobiosensors for the detection of novel coronavirus 2019-nCoV and other pandemic/epidemic respiratory viruses. *Sensors (Basel)., 20*(22), 6591.
40. Belhassan, A., El-Khatabi, K., Lakhlifi, T., El-ldrissi, M., & Bouachrine, M. (2020). Moroccan medicinal plants as inhibitors against SARSCoV-2 main protease: computational investigations. *Journal of Biomolecular Structure & Dynamics, 6*, 1–9.
41. Oshaghi, E., Mirzaei, F., Farahani, F., Khodadadi, I., & Tayebinia, H. (2020). Diagnosis and treatment of coronavirus disease 2019 (COVID-19): Laboratory, PCR, and chest CT imaging findings. *International Journal of Surgery, 79*, 143–153.
42. Ono, T., Oe, T., Kanai, Y., Ikuta, T., Ohno, Y., Maehashi, K., et al. (2017). Glycan-functionalized graphene-FETs toward selective detection of human-infectious avian influenza virus. *Japanese Journal of Applied Physics, 56*, 030302.
43. Siuzdak, K., Niedziałkowski, P., Sobaszek, M., Łęga, T., Sawczak, M., Czaczyk, E., Dziąbowska, K., Ossowski, T., Nidzworski, D., & Bogdanowicz, R. (2019). Biomolecular influenza virus detection based on the electrochemical impedance spectroscopy using the nanocrystalline boron-doped diamond electrodes with covalently bound antibodies. *Sensors & Actuators, B: Chemical, 280*, 263–271.
44. Anik, Ü., Tepeli, Y., Sayhi, M., Nsiri, J., & Diouani, M. F. (2018). Towards the electrochemical diagnostic of influenza virus: Development of a graphene–Au hybrid nanocomposite modified influenza virus biosensor based on neuraminidase activity. *Analyst, 143*, 150–156.
45. Hassen, W. M., Duplan, V., Frost, E., & Dubowski, J. J. (2011). Quantitation of influenza A virus in the presence of extraneous protein using electrochemical impedance spectroscopy. *Electrochimica Acta, 56*, 8325–8328.
46. Nidzworski, D., Siuzdak, K., Niedziałkowski, P., Bogdanowicz, R., Sobaszek, M., Ryl, J., et al. (2017). A rapid-response ultrasensitive biosensor for influenza virus detection using antibody modified boron-doped diamond. *Scientific Reports, 7*, 1–10.
47. Wicklein, B., Del Burgo, M., Ángeles, M., Yuste, M., Carregal-Romero, E., Llobera, A., et al. (2013). Biomimetic architectures for the impedimetric discrimination of influenza virus phenotypes. *Advanced Functional Materials, 23*, 254–262.
48. Hushegyi, A., Pihíková, D., Bertok, T., Adam, V., Kizek, R., & Tkac, J. (2016). Ultrasensitive detection of influenza viruses with a glycan-based impedimetric biosensor. *Biosensors & Bioelectronics, 79*, 644–649.

49. Lum, J., Wang, R., Lassiter, K., Srinivasan, B., Abi-Ghanem, D., Berghman, L., Hargis, B., Tung, S., Lu, H., & Li, Y. (2012). Rapid detection of avian influenza H5N1 virus using impedance measurement of immuno-reaction coupled with RBC amplification. *Biosensors & Bioelectronics, 38*, 67–73.
50. Wang, R., Li, Y., Mao, X., Huang, T., & Lu, H. (2010). Magnetic bio-nanobeads and nanoelectrode based impedance biosensor for detection of avian influenza virus. In *Proceedings of the IEEE International Conference on Nano/Molecular Medicine and Engineering (NANOMED)*, Hong Kong, China, 5–9 December (pp. 214–217).
51. Bhardwaj, J., Sharma, A., & Jang, J. (2019). Vertical flow-based paper immunosensor for rapid electrochemical and colorimetric detection of influenza virus using a different pore size sample pad. *Biosensors & Bioelectronics, 126*, 36–43.
52. Singh, R., Hong, S., & Jang, J. (2017). Label-free detection of influenza viruses using a reduced graphene oxide-based electrochemical immunosensor integrated with a microfluidic platform. *Scientific Reports, 7*, 42771.
53. Sayhi, M., Ouerghi, O., Belgacem, K., Arbi, M., Tepeli, Y., Ghram, A., Anik, Ü., Österlund, L., Laouini, D., & Diouani, M. F. (2018). Electrochemical detection of influenza virus h9n2 based on both immunomagnetic extraction and gold catalysis using an immobilization-free screen printed carbon microelectrode. *Biosensors & Bioelectronics, 107*, 170–177.
54. Hai, W., Goda, T., Takeuchi, H., Yamaoka, S., Horiguchi, Y., Matsumoto, A., & Miyahara, Y. (2018). Human influenza virus detection using sialyllactose-functionalized organic electrochemical transistors. *Sensors & Actuators, B: Chemical, 260*, 635–641.
55. Seo, G., Lee, G., Kim, M. J., Baek, S.-H., Choi, M., Ku, K. B., et al. (2020). Rapid detection of COVID-19 causative virus (SARS-CoV-2) in human nasopharyngeal swab specimens using field-effect transistor-based biosensor. *ACS Nano, 14*, 5135–5142.
56. Tharmarajah, K., Freitas, J. R., Mostafavi, H., Mahalingam, S., & Zaid, A. Liposomal delivery of the RNA genome of a live-attenuated chikungunya virus vaccine candidate provides local, but not systemic protection after one dose. *Frontiers in Immunology, 11*, 304. https://doi.org/10.3389/fimmu.2020.00304
57. Meng, S., Wu, Y.-J., Mao, Y.-P., Ye, R.-X., & Wang, Q.-Z. Epidemiology, causes, clinical manifestation and diagnosis, prevention and control of coronavirus disease (COVID-19) during the early outbreak period: a scoping review. *Infectious Diseases of Poverty, 9*, 1–12. https://doi.org/10.1186/s40249-020-00646-x
58. Fatima, F., Anwer, K., Alshahrani, S. M., Alalaiwe, A., & Katakam, P. (2019). Biosynthesis, characterization and anti-microbial activity of silver nanoparticle based gel hand wash. *Green Processing and Synthesis, 8*(2019), 577–583.
59. Troiani, E., & Corrao, S. (2020). COVID-19: hemoglobin, iron, and hypoxia beyond inflammation. A narrative review. *Clinical Practice, 10*, 1271. https://doi.org/10.4081/cp.2020.1271
60. Raghav, P. K., & Mohanty, S. (2020). Are graphene and graphene-derived products capable of preventing COVID-19 Infection? *Medical Hypotheses, 144*, 110031.
61. Tancharoen, C., Sukjee, W., Thepparit, C., Jaimipuk, T., Auewarakul, P., Thitithanyanont, A., & Sangma, C. (2019). Electrochemical biosensor based on surface imprinting for Zika virus detection in serum. *ACS Sensors., 4*, 69–75.
62. Lidorikis, E. (2007). Effective medium properties and photonic crystal superstructures of metallic nanoparticle arrays. *Journal of Applied Physics, 101*, 054304.
63. Erdem, Ö., Derin, E., Sagdic, K., Gulsen, Y. E., & Inci, F. (2021). Smart materials-integrated sensor technologies for COVID 19diagnosis. *Emergent Materials., 4*, 169–185.
64. Tectales Smart ring detects COVID-19 early. https://tectales.com/wearables-sensors/smart-ring-detects-covid-19early.html. Accessed on 18 Sep 2020.

Electrochemical Detection of Cancer Fingerprint: A Systematic Review on Recent Progress in Extracellular Vesicle Research from Lab to Market

Brateen Datta, Nirmita Dutta, Amlan Ashish, Mukti Mandal, Jai Shukla, Raghavv Suresh, Priyanka Choudhury, Koel Chaudhury, and Gorachand Dutta

Abstract

Cancer is a major global health burden and accounts for the second-highest mortality rate around the world. Despite significant advances in cancer research, minimal/noninvasive diagnostic strategies for early detection remain elusive, leading to delays in therapeutic intervention and affecting the overall survival chances. Most cancers exhibit no specific symptoms in the early stages. However, upon metastasis to nearby organs, certain symptoms become prominent and detectable. Conventional tissue biopsy performed in these cancers is not only invasive but is also limited in its diagnostic efficacy by the presence of tumor heterogeneity. In this regard, liquid biopsy has brought a revolution in early cancer diagnosis. Extracellular vesicles are among some of the reliable biomarkers for liquid biopsy. Recent advancements in technology have laid a strong foundation in understanding the role of extracellular vesicles in cancer progression. In this review, we briefly present the multifarious roles of extracellular vesicles toward an accurate cancer diagnosis. Moreover, the recent progress in extracellular vesicle liquid biopsy biosensors is also discussed, with a focus on electrochemical biosensors. Lastly, the requisite measures to be taken to improve the performance of the existing biosensors, with an aim of bringing them to the commercial point-of-care (POC) market, are concisely summarized.

B. Datta · N. Dutta · A. Ashish · M. Mandal · J. Shukla · R. Suresh · P. Choudhury · K. Chaudhury · G. Dutta (✉)
School of Medical Science and Technology (SMST), Indian Institute of Technology Kharagpur, Kharagpur, India
e-mail: g.dutta@smst.iitkgp.ac.in

G. Dutta (ed.), *Next-Generation Nanobiosensor Devices for Point-Of-Care Diagnostics*, https://doi.org/10.1007/978-981-19-7130-3_3

Keywords

Cancer liquid biopsy · Proteogenomic profile of extracellular vesicle · Electrochemical biosensor · Signal amplification · Tumor on a chip · Point-of-care diagnosis

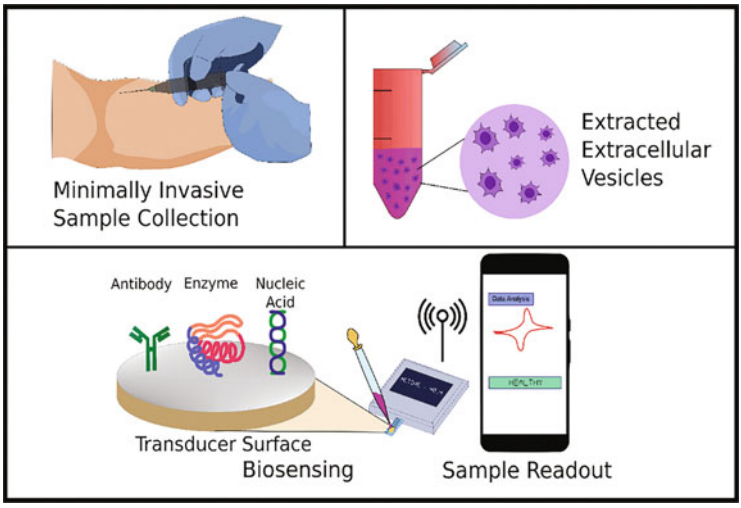

1 Introduction

Cancer is the second major cause of death worldwide [1]. Tumor heterogeneity, chemotherapeutic resistance, and delay in accurate diagnosis are some principal challenges associated with cancer [2]. Though the conventional tissue biopsy-based cancer diagnosis has advanced significantly, high turnaround time, the invasive procedure makes it very difficult for routine cancer diagnosis. Due to those technical and biological complications with tissue scientists are giving more emphasis to liquid biopsy for many years. The advancement of liquid biopsy opens an excellent outlook for future clinical diagnosis. In comparison with tissue biopsy, liquid biopsies are less risky and can capture the complete tumor heterogeneity of a patient [3]. In the case of liquid biopsy, the proteogenomic alternation of cancer can be detected from tumor-shredded components in different human bioliquids such as blood and urine [3]. Recently, extracellular vesicles (EV) have appeared as an excellent alternative biomarker for liquid biopsy. Howbeit, earlier EVs were considered cellular debris, but are currently acknowledged as one of the main factors in intercellular communication [4]. EV-incorporated biomacromolecules play a key role in mimicking the pathophysiological microenvironment of the parent cell [4]. Thusly, EVs can modulate cancer development and offers great promise as a

diagnostic element. Despite the diagnostic advances, the lack of standardization in EV separation and detection brings a great challenge in actual clinical translation.

Various conventional techniques such as ELISA, blotting, microarray, and RT-PCR are generally used to characterize cell-derived EVs [5]. Nevertheless, such conventional techniques require a substantial amount of sample which is unsuitable for repeated clinical diagnosis. Moreover, the requirement of complex instrumentation, high turnaround time, and sample pre-treatment with conventional techniques limit the utility of EVs in clinical settings. Electrochemical biosensors are a type of bioanalytical device that can convert biochemical interactions into a measurable electrical signal. These biosensors contain solid electrode surfaces to immobilize the biorecognition elements like antibodies, proteins, aptamer, and enzymes, and upon specific biochemical interactions with a target of interest electrical signals are generated which are measured in terms of the analyte concentration [6]. These electrochemistry-based biosensing platforms can be immobilized easily for onsite target detection. Considering the recent progress and difficulties in EV research with conventional techniques, electrochemical nano biosensor shows enhanced performance and accurate detection. An accurate point-of-care (POC) medical device can solve these purposes. An ideal POC device must meet all world health organization (WHO) recommended ASSURED criteria (affordable, sensitive, specific, user friendly, rapid and robust, equipment-free, and deliverable) [7].

Herein, we present the biogenesis and role of EV in cancer progression. We also discuss the role of EV as a promising biomarker in liquid biopsy. We highlight a comprehensive review of different electrochemical signal detection platforms and focus on the advantages of conventional EV sensing techniques. Further, we highlight the different applications of electrochemical biosensors in cancer-specific EV detection. Finally, we discuss the direction of future research that promises to ravel a new horizon in cancer diagnosis with electrochemical liquid biopsy sensors. We believe that with the progress of science and technology and newborn applications in different electrochemical biosensors, it is possible to facilitate personalized diagnosis in near future.

2 Early Detection Is the Best Answer for Cancer

Early diagnosis of cancer is of paramount importance for enabling successful treatment. The complex eukaryotic cellular machinery regulates cellular function in the human body. Aberrations in molecules associated with signal transduction often underlie the initiation and progression of cancer. If any of these signals get dysregulated, healthy cells might start to multiply rapidly to form a tumor [8]. Uncontrolled division of cancer cells can invade nearby tissues to form a new tumor. According to reports over 19.3 million cases of cancer are diagnosed in 2020, worldwide. In line with the Indian cancer registry program reported over 1,392,179 cancer cases in India for the year 2020 [9]. Cancers are often exhibited no clinical symptoms and hence treatment is overlooked. For that reason, most of the

patients are negligent and ignore proper diagnosis processes. Besides, healthcare literacy is very low in low-middle income countries like India. Furthermore, complex diagnosis processes and associated costs increase the anxiety level of patients. Early detection of cancer can decrease morbidity and can increase the survival rate. The majority of cancer-related deaths comes from metastasizing malignant cell [8]. Once a malignant cell starts metastasizing, then it is only treatable not curable. The delay in the specific and timely detection limits the access to treat cancer. Before becoming symptomatic, if it is detected then the tumor can be surgically removed or systematic treatment can be prescribed. Reports indicated that in 53% of cases when lung cancer patients are diagnosed at stage I, patients survive more than 5 years [10]. The extent of systematic treatment depends upon the metastasized potential and tumor size at the time of detection [8].

Although scientists put their effort to recognize early cancer symptoms but most of the time those symptoms are highly non-specific. Hence, to avoid conventional tissue biopsy complications, and to capture the whole proteogenomic profile for particular cancer, it is very important to recognize cancer-associated biological markers with minimally invasive procedures [3]. Clinical diagnosis of cancer with a minimally invasive procedure is termed a liquid biopsy [3]. Liquid biopsy studies mainly focus on circulating DNA (ct DNA), circulating RNA (ct RNA), circulating tumor cell (CTC), and extracellular vesicles (EV) that are released by tumor cells in different biological fluids like blood, urine, saliva, and cerebrospinal fluid [11]. The elevated level of these biomarkers might contribute as a predictive signature for the early detection of cancer (Fig. 1).

3 EV, a Promising Youngster in Liquid Biopsy

Recent progress in cancer research has immensely advanced early cancer diagnosis with the development of new and sophisticated approaches. Currently, tissue biopsy is regarded as the gold standard for cancer diagnosis [4]. During tissue biopsy, doctors collect a small part of tissue to examine if it is cancerous. Though tissue biopsy access doctors to determine cancer's grade and give clues to a specific treatment strategy, nevertheless this surgical strategy is invasive, and sometimes tumor organ is inaccessible for biopsy [13]. In addition, a repeat biopsy is not possible for continuous monitoring. Furthermore, high tumor heterogeneity presents a serious challenge to understanding the complete molecular profile of particular cancer by analyzing a small section of cancerous tissue [13]. In addition to that, high turnaround time, high cost, post-clinical complications, and invasive surgical procedure imposes substantial inadequacy on solid (tissue) biopsy [13]. In view of these shortcomings, researchers are increasingly shifting their research focus from solid biopsy to liquid biopsy. Liquid biopsy represents noninvasive diagnostic techniques from non-solid tumor tissue, mostly from easily isolated bioliquids [3]. As the primary tumor grows it releases certain biomarkers into the circulation that can be collected from human bioliquids like blood, urine, saliva, and cerebrospinal fluid. Liquid biopsy biomarkers generally exhibit dynamic changes associated with

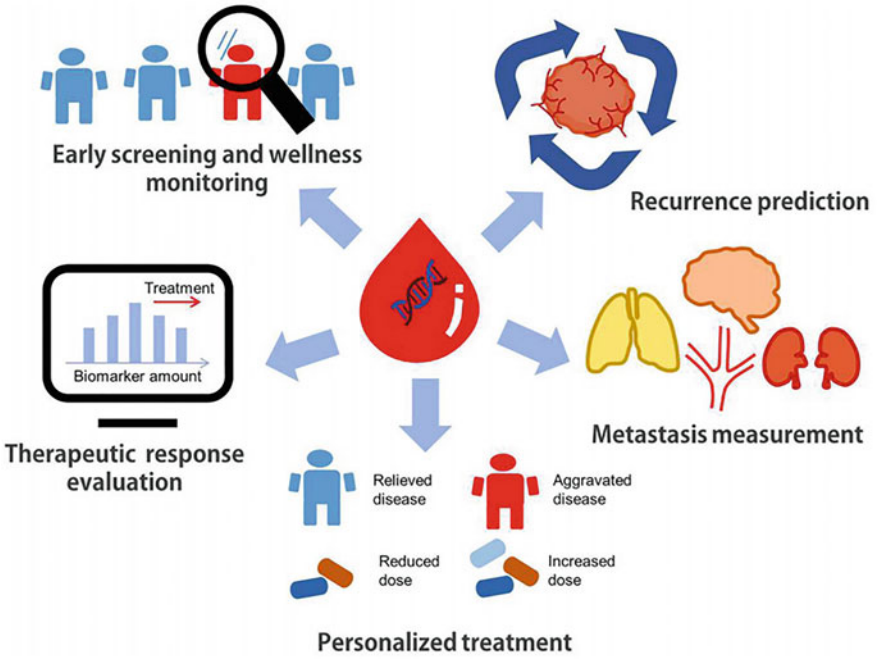

Fig. 1 Liquid biopsy explores different biological markers present in human bioliquids. Liquid biopsy could be an excellent alternative tissue biopsy to analyze the metastatic potential of tumors at a very early stage to predict the diagnosis and prognosis of cancer. Reprinted from [12] Copyright 2021, with permission from Elsevier

cancer, emerging as a promising diagnosing tool for both early and metastatic cancer (Fig. 2).

In light of that, as the genetic makeup of cancer cells evolves, liquid biopsy is very significant for repeated monitoring [13]. Based on bioliquid-derived components, liquid biopsy biomarkers can be divided into circulating tumor DNA (ctDNA), circulating tumor RNA (ctRNA), circulating tumor cell (CTC), and extracellular vesicles (EV) [11]. Recent studies indicate that malignant cells secreted EVs convey oncogenic factors between healthy cells. The intake of cancer cell-derived EVs may induce a malignant transformation in recipient cells [4]. Among other EV-incorporated cargoes oncogenic proteins and tumor-suppressive micro RNAs (miRNA) present superior diagnostic potential in early cancer diagnosis.

EVs extends substantial advantages over the other liquid biopsy biomarkers in various aspect. Lipid double-layer contained tumor-specific cargoes are free from enzymatic degradation in the case of EVs. EVs often manifest pathological stages of particular cancer by expressing certain surface proteins that can be easily used for isolation of EV subpopulation and disease monitoring. By and large, in terms of the incorporation of biological information and diagnosis sensitivity, EVs offer higher accuracy than others [4]. The concept of early cancer detection with EVs is still

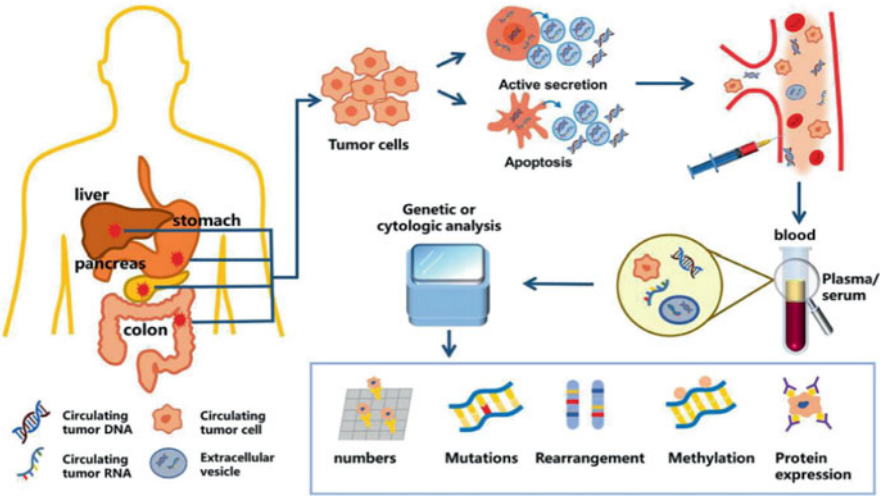

Fig. 2 Verities of biomarkers present in the circulation—circulating tumor cells, circulating tumor nucleic acids, tumor platelets, and extracellular vesicles are detected in liquid biopsy. Dysregulated proteogenomic alternations associated with those biomarkers can be used in early cancer diagnosis. Reprinted from [12] Copyright 2021, with permission from Elsevier

young and numerous clinical studies are in process to convene the complete cancer diagnostic potential of EVs.

4 Conventional EV Detection Techniques

For diagnosis, the isolated EV has to be pure. EV isolation techniques are generally categorized based on charge, size, and immunoaffinity. Currently, ultracentrifugation, immunoaffinity chromatography, and size exclusion chromatography are considered the gold standard for EV isolation [14] (Fig. 3). However, most of the current methods are labor and time-intensive process. On top of that, isolated vesicle quality is far from pure [5]. Scientists generally perform a combination of techniques to attain high purity. Furthermore, the biomechanical properties of EVs highly depend on the isolation technique. Thence, pre-analytical variables are considered to select a suitable technique [14]. Besides, conventional techniques, many new approaches are emerging. For instance, dielectrophoresis, field flow fractionation, hydrophobic interaction chromatography, field-free viscoelastic flow, etc. [5]. MISEV has listed different EV isolation, characterization, and detection techniques to recommend as per the need of the research. With the advancement of new techniques in this particular field, MISEV has revised its recommendation over the years. The standardization of an accurate EV characterization and detection technique is so compelling to understanding the physicochemical properties of an EV subpopulation [5].

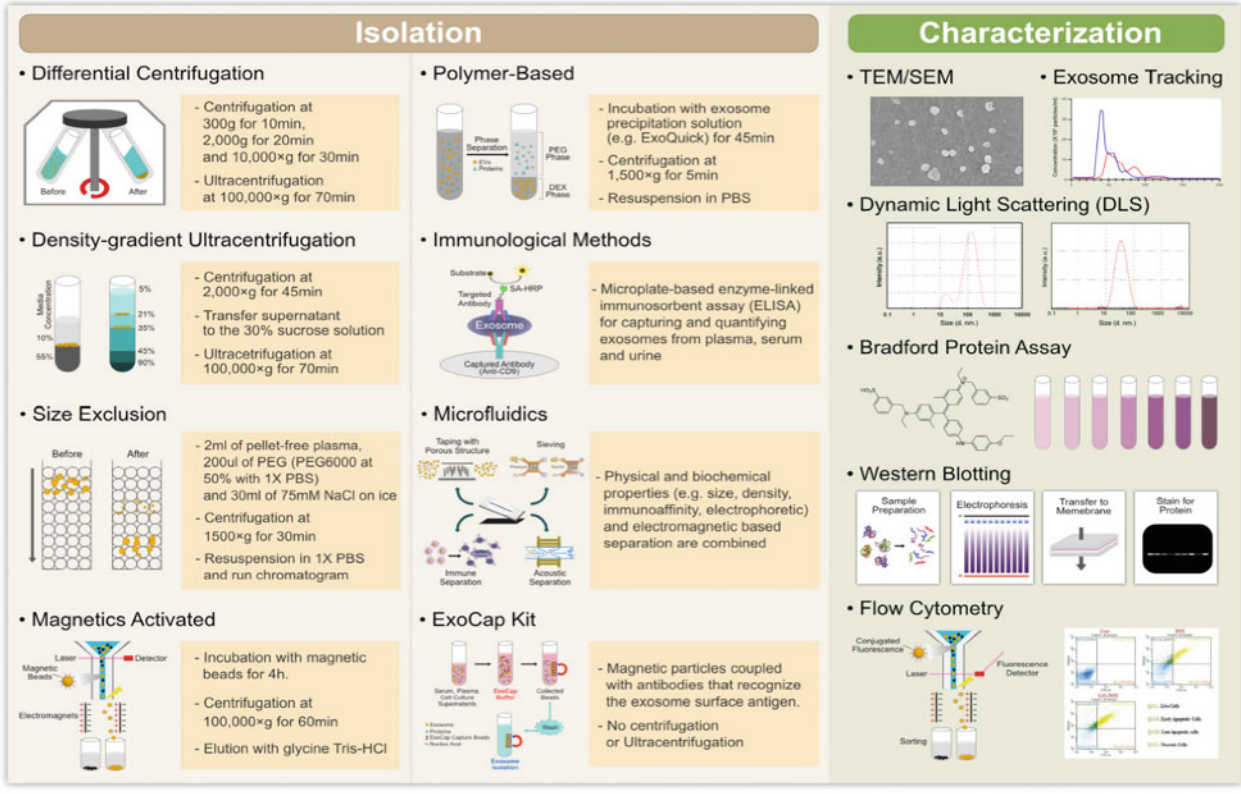

Fig. 3 The conventional techniques to isolate and characterize extracellular vesicles. Reproduced from the open-access article [14] under the terms of Creative Commons CC BY

Table 1 Conventional techniques for EV characterization

S. no.	EV characterization techniques	Advantages	Disadvantages	
1	Atomic Force Microscopy (AFM)	• Highly sensitive • Works in physiological condition • High Resolution	• Background noise can hamper reproducibility	[15]
2	Dynamic light scattering (DLS)	• Independent of sample turbidity • Simple experimental set-up • Accurate	• Highly sensitive toward mechanical noise	[16]
3	Flow cytometry	• High throughput absolute counting • Accurate • Low cost	• Expensive • Difficult to maintain physiological environment	[17]
4	Nanoparticle tracking assay (NTA)	• Accurate • Reliable	• Parameter optimization is very significant	[18]
5	Surface plasmon resonance (SPR)	• Sensitive • Label-free • No need for statistical calibration	• Instrument size is very big • Low selectivity	[19]
6	Microfluidics	• Small sample volume is required • Rapid • Low cost	• Adsorption of air bubbles in small channels • Lack of high reproducibility	[20]
7	ELISA	• Rapid • Highly specific	• The enzyme might lose the functional activity • Low sensitivity • High cost	[21–23]
8	Western blot	• A widely accepted standardized protocol is available • EVs can be visualized directly	• Complex • An experienced technician is required • Expensive	[24, 25]
9	RT-PCR	• High sensitivity • The detection range is high • No post PCR process is required	• Technically demanding • Expensive • Time consuming	[26–28]

For the quantitative and qualitative validation of EV-associated biomarkers variety of techniques are generally performed (Table 1). Most common physical methods such as nanoparticle tracking analysis (NTA), Microscopy (EM, AFM) are used to characterize the extracellular vesicles, whereas Western Blot, ELISA, and RT-PCR are used to determine the protein or nucleic acid content of EVs.

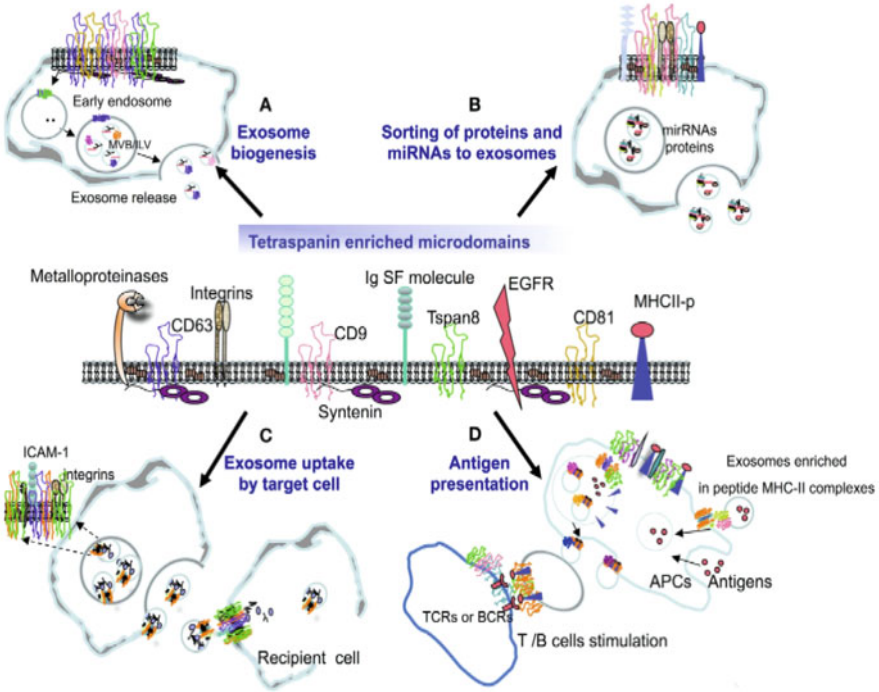

Fig. 4 Tetraspanin proteins abundantly cover the EV membrane surface. These highly glycosylated transmembrane proteins are associated with different biological processes like EV biogenesis, protein sorting inside the vesicle, and immunogenic response. Besides, conserved residues of tetraspanins signify characteristic features of the EV subpopulation. Reproduced from open-access article [29] under the terms of Creative Commons CC BY

EV-incorporated cargoes are a very important and promising tool from a diagnostic and prognostic point of view [4]. The most regularly used biochemical methods include immune assay, blotting assay, and PCR analytic methods to determine the protein or nucleic acid content of EV.

Currently, various conventional methods are used for the isolation and characterization of EVs (Fig. 4). Apart from the above-mentioned methods, different molecular detection strategies such as Raman spectroscopy, FTIR, surface plasmon resonance, and circular dichroism are regularly used for EV analysis [30–32]. Despite that fact, there is no standardized method is available now for EV detection and characterization. The application of EV research is very crucial in early disease diagnosis. Unfortunately, most of the conventional strategies demand a benchtop set up for diagnosis. Furthermore, a large amount of bioliquid is required which is not suitable for repeated analysis. In a situation like this, advancement in

point-of-care diagnosis is preferable. In the following section, we will explore the insights of the electrochemical biosensor concerning point-of-care EV research.

5 Electrochemical Detection of EVs

EV membrane-enriched tetraspanins constitute a major class of transmembrane proteins that enrich the EV membrane surface by forming a cluster of "transmembrane enriched microdomains" [29]. Out of the five critical microdomains, a highly variable extracellular loop is mainly involved in EV-mediated intercellular communication (Fig. 4).

Due to the capacity of highly specific biochemical interactions, the extracellular domain is functionally very crucial [33]. Not only, EV surface proteins but the nucleic acid composition inside EV was found to alter the biological activities of cells that take them up. A detailed multi-omic study suggested the presence of a high concentration of different micro RNAs (miRNA) in EV [34]. The double membrane boundary of EV provides stability to incorporated RNAs from cytoplasmic nucleases [4]. Not only miRNAs but noncoding (nc) RNA, genomic, and mitochondrial DNAs are also transported from one cell to another through EV [4]. The computational correlation of EV-incorporated nucleic acid cargoes displays the pathophysiological insights of secreted cells. Boriachek et al. developed a label-free, amplification-free electrochemical biosensor for the detection of EV-incorporated miR-21 from breast cancer cell lines [35] (Fig. 5).

With a very simple yet accurate detection platform, they succeed to achieve a LOD of 1 pM with a dynamic range of 0.2–20 pM [35]. Such nucleic acid base sequence information in EV exhibited the differential expression pattern between healthy controls and cancer patients, promising the potential to be used in early diagnosis.

The large repertoire of antibodies (immunoglobins) with different antigen-binding specificity makes them an excellent biorecognition molecule. Kilic et al. designed a label-free electrochemical biosensor to recognize vesicle-expressed CD81 tetraspanins (Fig. 6). They functionalized biotin-labeled CD81 antibodies on the gold-screen printed electrode with streptavidin-biotin conjugation chemistry [36]. Based on the modified sensor surface and vesicle tetraspanin interaction, with increasing sample concentration, there was a formation of a kinetic barrier for the redox probe. The measurement of charge transfer resistance exhibited a linear range with an accurate detection limit of 77 copies/mL [36].

However, a low concentration of EVs in biological fluid limits its use in clinical early diagnosis. To overcome such difficulties different types of signal amplification strategies have been advanced. Signal amplification techniques are mainly optimized to remove the background signal and amplify the lower limit of biomarker detection. Signal amplification strategies are employed in biosensing to facilitate a proportionate or ratiometric increase in the detection signal generation in response to an analyte recognition reaction. In electrochemical sensors, ultrasensitive detection of the analyte is brought forth by coupling the recognition reaction with a chemical,

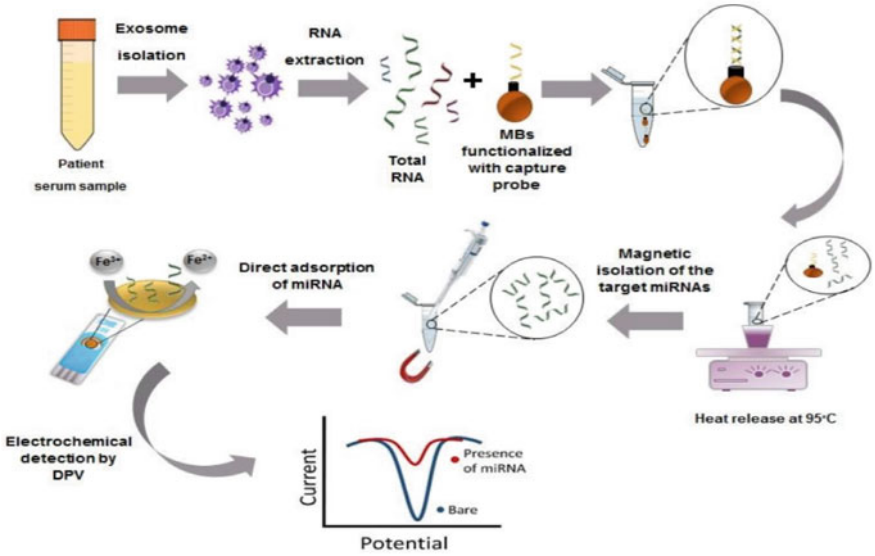

Fig. 5 Schematic representation of steps for the development of an amplification-free electrochemical biosensor to detect EV-incorporated miR-21. Reproduced from [35] with permission from the Royal Society of Chemistry

catalytic or electrocatalytic reaction and rapid electron transfer [37] (Table 2). For EV detection, surface proteins or nucleic acids (such as miRNAs) may be targeted for recognition, and the amplification can be carried out with DNA-based, enzyme-based, or enzyme-free strategies.

5.1 Enzyme-Based Amplification

Enzymes are biological catalysts that enhance the rate of reaction of a substrate to a product. The product formed can be further utilized in an electrocatalytic reaction to produce a detectable electrical signal, or the product can give a direct readout (e.g., colorimetric product formation) [66]. By maintaining optimal conditions for enzyme activity, the reaction rate, and subsequently the detectable signal can be greatly enhanced or amplified. However, the use of enzymes is limited by factors such as surface stability and optimal pH and temperature requirements [67].

Enzyme-mediated amplification for biosensing is a well-established approach, and there have been several reports on enzyme-based biosensors for EV detection. For instance, an enzyme-based multiplexed microfluidic immunosensor was reported by Vaidyanathan and the group for the specific capture of human epidermal growth factor receptor 2 (HER2) and prostate-specific antigen (PSA), expressed on the surface of EVs secreted by breast cancer cell lines [39]. After capturing the protein biomarkers in a sandwich immunocomplex, the signal was generated by the

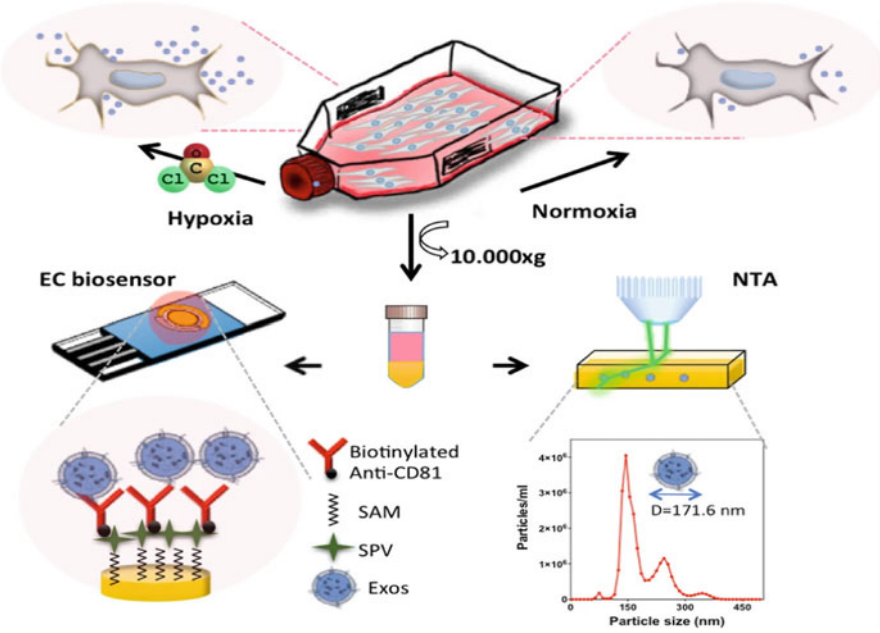

Fig. 6 Indicates the experimental steps of breast cancer cell-derived EV detection. EVs were isolated gold standard ultracentrifugation technique and followed by characterization using NTA. For the electrochemical detection, screen-printed gold electrodes were fabricated with 11 mercaptoundodecanoic acid and neutravidin to capture biotinylated CD81 antibodies. The electrochemical signal of the redox probe was decreased in presence of CD81-positive EVs. The change in the signal was correlated with EV concentration. Reproduced from the open-access article [36] under the terms of Creative Commons CC BY

signal antibody-conjugated horseradish peroxidase (HRP) enzymes with the catalytic oxidation of 3,3′,5,5′-tetramethylbenzidine (TMB), giving a colorimetric readout [39].

5.2 Hybridization-Based Amplification

The complementary base pairing property of nucleic acids to form intricate DNA/RNA structures, as well as replication-based amplification by polymerases, form the basis of amplification strategies in hybridization-based detection platforms [68]. Such structures have found application in many signal amplification strategies in biosensing devices.

Rolling Circle Amplification

Rolling cycle amplification (RCA) is one such technique. RCA is an isothermal amplification technique that uses a ligation primer against a linear DNA sequence, such that the ligation primer terminates on either side in regions complementary to

Table 2 Electrochemical detection of cancer cell-derived EVs

S. no.	Cancer type	EV target	Receptor	Detection platform	Signal label	Detection range	Detection limit	
1	Breast cancer	CD9	αCD9 antibody	Triple pulse amperometry	Horseradish peroxide	2×10^{2}–1×10^{6} copies/μL	1×10^{3} copies/μL	[38]
2	Breast cancer	CD81	Cd81 antibody	EIS DPV	$K_3[Fe(CN)_6]^{3-/4-}$	10^{2}–10^{9} copies/mL	77 copies/mL	[36]
3	Breast cancer	HER2, PSA	HER2 antibody, PSA antibody	Tunable alternating current electrodynamic	HRP	4.15×10^{4}–2.76×10^{3} copies/μL	2760 copies/μL	[39]
4	Breast cancer	CD9, HER2	CD9 antibody, HER2 antibody	DPV	$K_3[Fe(CN)_6]^{3-/4-}$		4.7×10^{5} copies/μL	[40]
5	Lung cancer	Multiplex detection	CD9, CD63, HER2, PDL-1, IGF1R antibody	Change in current				
6	Kidney cancer	CD81, Syntenin	CD81, Syntenin antibody	EIS	$K_3[Fe(CN)_6]^{3-/4-}$	50 pM – 200 nM	1.9×10^{5} copies/mL	[41]
7	Uterus cancer	CD63	PALP antibody, CD63 antibody	Current density	Au-NPFe2O3nanocrystal	10^{3}–10^{7} copies/mL	10^{3} copies/mL	[42]
8		EpCAM	EpCAM antibody	CV	Alkaline phosphatase	10–10^{6} copies/μL	5 copies/μL	[43]
9	Ovarian cancer	CD63	CD63 antibody	Amperometry	HRP	10^{4}–10^{8} copies/mL	3×10^{4} copies/mL	[44]
10	Colon cancer	CD9, CD63, CD81	Antibody	Amperometry	HRP	10^{4}–10^{9} copies/mL	10^{4} copies/mL	[45]
11	Prostate cancer	EpCAM	EpCAM antibody	LSV	CuNP		50 copies/mL	[46]

(continued)

Table 2 (continued)

S. no.	Cancer type	EV target	Receptor	Detection platform	Signal label	Detection range	Detection limit	
12	Liver cancer	CD63	CD63 aptamer	SWV	Methylene blue tagged probe	10^6–10^8 copies/mL	10^6 copies/mL	[47]
13	Cervical cancer	PTK	PTK aptamer	DPV	$Ru(NH3)_6^{3+}$		6.607×10^5 copies/mL	[48]
14	Breast cancer	EpCAM	EpCAM aptamer	Amperometry	HRP	5×10^2–1×10^5 copies/μL	285 copies/μL	[49]
15	Breast cancer	CD63	CD63 aptamer	amperometry	HRP	1.12×10^2–1.12×10^8 copies/μL	96 copies/μL	[50]
16	Liver cancer	CD63	CD63 aptamer	DPV	Hemin	7.61×10^4–7.61×10^8 copies/mL	4.39×10^3 copies/mL	[51]
17	Liver cancer	HePG2	HePG2-specific nanotetrahedron aptamer	SWV	Fe $[(CN)6]^{3-/4-}$	10^5–10^{12} copies/mL	2.09×10^4 copies/mL	[52]
18	Gastric cancer	CD63	CD63 aptamer	CV, DPV	HRP mimicking DNA zyme	4.8×10^3–4.8×10^6 copies/mL	9.54×10^2 copies/mL	[53]
19	Breast cancer	CD63, EpCAM	CD63 aptamer	EIS,DPV,CV	Ferrocene modified DNA, Fe $[(CN)6]^{3-/4-}$	10^5–10^{10} copies/mL	1.3×10^4 copies/mL	[54]
20	Breast cancer	CD63	CD63 aptamer	DPV	Doxorubicin	3.4×10^4 to 3.4×10^8 copies/mL	1.2×10^4 copies/mL	[55]
21	Prostate cancer	Prostate-specific membrane antigen	PSMA aptamer	DPV	$Ru(NH3)_6^{3+}$	1000–120,000 copies/μL	70 copies/μL	[56]

22	Liver cancer	CD63	CD63 aptamer	SWV	Fe $[(CN)6]^{3-/4-}$	1×10^5–5×10^7 copies/mL	1.72×10^4 copies/mL	[57]
23	Hepatocarcinoma, Breast cancer	miR-122	miR-122 complementary hairpin DNA	DPV	$Ru(NH3)_6^{3+}$	0.1 fM to 0.1 μM	53 aM	[58]
24	Cervical cancer, Breast cancer	miR-21	Complementary DNA probes	SWV	$[Fe(CN)6]^{3-/4-}$	10 aM to 100 fM	7.3 aM	[59]
25	Breast cancer	miR-21	miR-21 complementary DNA	SWV	Methylene blue	10 aM to 10^7 aM	3.04 aM	[60]
26	Coronary heart disease	miR-181	Oligonucleotide hairpin probe	EIS, CV, SWV	$[Fe(CN)6]^{3-/4-}$	10 fM-100 nM	7.94 fM	[61]
27	Breast cancer	miR-1246, miR-221, miR-375, and miR-21	Complementary DNA tetrahedron probes	EIS, CV, SWV	$[Fe(CN)6]^{3-/4-}$	10 fM t-100 pM	7.2 aM	[62]
28	Breast cancer	miR-21	miR-21 LNA probe	EIS, DPV	Methylene blue	10–70 fM	2.3 fM	[63]
29	Breast cancer	miR-21	miR-21 LNA capture probe	DPV	$[Fe(CN)6]^{3-/4-}$		67 aM	[64]
30	Prostatic cancer	miR-21	miR-21 DNA hairpin probe	EIS, SWV	$[Fe(CN)6]^{3-/4-}$	1 fM to 200 pM	0.4 fM	[65]
31	Breast, colon, oral cancer	miR-21	miR-21 biotinylated capture probe	DPV	$[Fe(CN)6]^{3-/4-}$	0.2–20 pM	1 pM	[35]

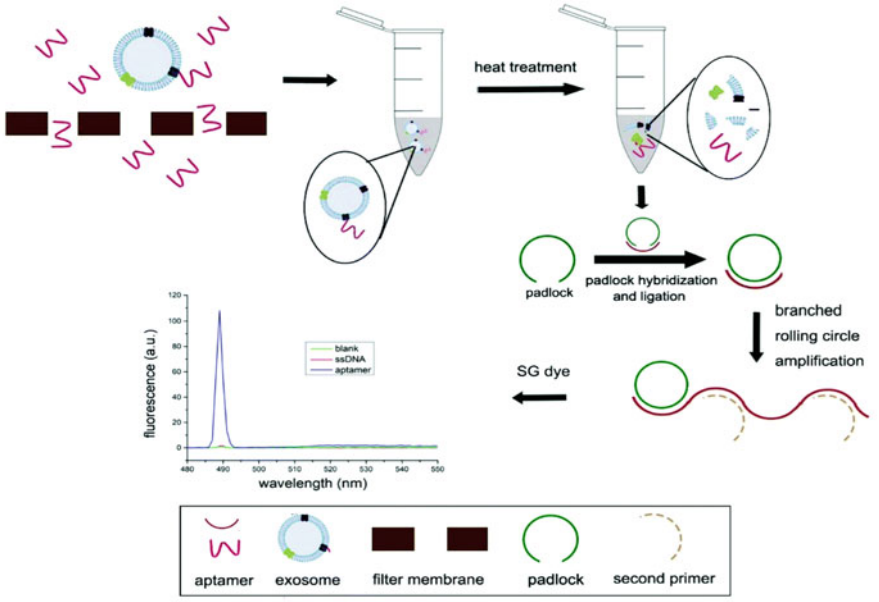

Fig. 7 Schematic illustration of branched rolling cycle amplification for gastric cancer exosome detection. Aptamer-bound exosomes are filtered and separated. Padlock DNA, ligase, polymerase, and primers are added for ligation and branched amplification steps. Reprinted from [70] with permission from The Royal Society of Chemistry

the linear DNA [69]. Annealing to the primer leads to the clipping of the two ends, which are then ligated with a ligase enzyme. This step is followed by the replication of the obtained circular DNA, yielding a continuous stretch of tandem repeats of a sequence complementary to the circular DNA [69]. In this process of signal amplification, there is an output signal increase of around 100–1000 fold, which is very important for the ultrasensitive detection of moieties in a complex biological system. Huang and the group developed a modified branched RCA method to amplify aptamers specific to gastric cancer cell-derived exosomal glycoprotein Mucin 1 (MUC1) [70]. The aptamers bound to isolated exosomes were separated with heat treatment and acted as a ligation primer against a linear 'padlock' DNA. For branched amplification, secondary primers were added and annealed to regions of the primary RCA product, followed by polymerization (Fig. 7) [70].

Proximity ligation assay (PLA) has improved traditional immunoassay technology that involves the simultaneous identification of different antigens (closely associated) on the same target [71]. The antigen targeting probes are conjugated with short specific oligonucleotide sequences. If the two probes reside in proximity, the complementary oligonucleotide strands hybridize and participate in rolling circle amplification, consequently taking part in target recognition [48]. Zhang et al. exploited similar technology to electrochemically detect human cervical cancer cell-derived EVs. They immobilized capture oligonucleotide fragments on the gold

working electrode. In order to capture protein tyrosine kinase (PTK) expressing EVs, PTK-specific S1 and S2 aptamer sequences were used. In the presence of target EVs, S1 and S2 form a duplex complex with a capture oligonucleotide sequence, which increased the electronegativity on the working surface and affected the increased detection signal [48]. This PLA-based electrochemical aptasensor specifically detected cancer-derived EVs with a detection limit of 6.607×10^5 [48]. Nevertheless, in such an amplification process, always there is a high chance of non-specific interaction between complementary RCA products.

Strand Displacement Reaction Amplification

Strand displacement reaction (SDR) amplification is another innovative strategy employing the kinetic characteristics of base complementarity for directing the displacement of a strand from a double helix, by a third strand with stronger binding kinetics [72]. One toehold-mediated SDR-based exosomal miRNA sensor was reported by Miao and Tang. The non-enzymatic strategy employed six DNA oligonucleotide sequences: probes A, B, C, D, E, and F [73]. The longer probe A partially hybridized with the shorter probe B and C to form a nicked duplex. Upon addition of miR-21 (target), miR-21 hybridized to the 5′-overhang (toehold) of probe A and replaced probe C in subsequent entropy-favored steps. The single-stranded region was then hybridized with probe D, which further displaced miR-21 and probe B [73]. The thus released miR-21 could further react with new probes A-B-C structures for many more cycles, so long as probe D was exhausted [73]. The cycles led to the release of a large number of probe B strands. Probe B then participated in downstream SDR by opening a methylene blue-labeled hairpin probe E, on a gold electrode. In the final step, hairpin probe F hybridized partially to the opened probe E and displaced probe B [73]. The distance acquired between the electroactive methylene blue and the electrode because of the hybridization could be monitored by a reduction in voltammetric signal, due to the decreased oxidation rate of methylene blue [73]. Liu and the group developed a biosensor with localized toehold-mediated SDR strategy and DNA nanosheets (DNS) as labels for miR-21 detection [74]. Nine DNA strands: S1, S2, S3, S4, S5, S6, S7, S8, and S9 were designed to self-assemble into a nanosheet [74]. The annealing process was based on shared partial sequence complementarity between multiple strands, forming a DNA network. Double-stranded DNA redox intercalator methylene blue was loaded onto the DNS in high concentration [74]. The localized SDR setup also involved the formation of a polymeric T substrate (T_s) by chain hybridization, with L_1, L_2, P, and R strands forming a quadruple-stranded monomeric unit. L_1 had two terminal regions: I_1 and I_2, and L_2 had two terminal regions: I_1* and I_2* complementary to I_1 and I_2 respectively [74]). Lateral hybridization led to a bridge-like structure, while an R strand was bound to the mid-region of L_2, and a P strand to that of L_1. L_1 also had a mid-region sequence complementarity with the target miR-21, and the latter was capable of displacing and releasing the P strand in the reaction buffer [74]. Next, an F strand with a greater number of base pairings with L_1 and L_2 simultaneously was added which led to the release of both miR-21 and R strands. The released miR-21 could initiate further rounds of similar annealing and displacement reactions,

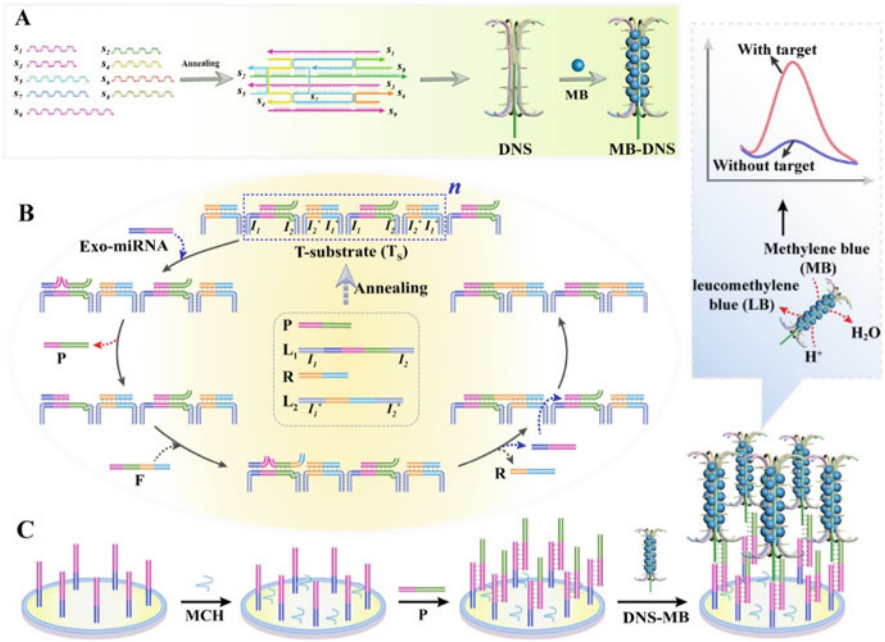

Fig. 8 Schematic illustration of the electrochemical biosensor for ultrasensitive detection of Exo-miRNA (miR-21); (**a**) assembly procedure of the methylene blue-loaded DNA nanosheet (DNS-MB); (**b**) the operation steps of the localized toehold-mediated strand displacement reaction; (**c**) binding of the methylene blue-loaded DNA nanosheets with the capture probes on the electrode via P strands. Reprinted from [74] with permission from the American Chemical Society

releasing a large number of P strands into the buffer [74]. The P strands were collected and hybridized into the immobilized capture probes on a gold electrode. In the final step, methylene blue-loaded DNS were hybridized to the single-stranded sticky end of the P strands, via the protruding end of the S_8 strand. Methylene blue was oxidized to leucomethylene blue to obtain the detection signal (Fig. 8) [74].

Shi and the group prepared an enzyme-based SDR strategy for miRNA detection. The target miRNA was 3′-end hybridized with a primer (primer 1) terminating in a nicking enzyme (Nt. AlwI) recognition site overhang [75]. Next, the Klenow fragment polymerase extended the 3′-ends of both primer 1 and miRNA. This was followed by Nt. AlwI nicking at the recognition site, and strand displacement by another intact primer 1, which could proceed for the next round of polymerization, nicking, and strand displacement steps [75]. The complementary miRNA strands released after nicking and strand displacement steps were hybridized with another primer (primer 2), with a similar nicking site overhang [75]. Subsequent polymerization, nicking, and strand displacement steps were undergone in a cyclic fashion. This dual cyclic process led to the exponential synthesis of miRNA target and complementary target sequences isothermally, from a very small starting amount of the miRNA [75].

Catalytic Hairpin Assembly

A modified form of SDR is the catalytic hairpin assembly (CHA), wherein kinetically stable hairpin structures are sequentially unwound via a triggered SDR with an added linear strand, to form an assembled structure [76]. Zhang and the group prepared a CHA-based biosensor specific for exosomal miR-181. Three hairpins (H1, H2, and H3) with partially complementary sequences were designed. Of these, H1 and H3 were biotin-labeled [61, 62]. SDR was sequentially triggered by miR-181, wherein it first unwound H1. The mid-section of H1 partially hybridized and opened H2, and the mid-section of H2 further hybridized with H3. H3 finally displaced miR-181, and the latter could initiate the next round of CHA. H1, H2, and H3 formed a T-shaped triple-stranded junction, which could associate with other similar hairpin junction structures via hybridization between 3'-H3 and 5'-H1 overhangs, to form long concatemers [61, 62]. In the detection step, the concatemers were captured via the 3'-H2 overhangs annealed to complementary probes on a gold electrode. Alkaline phosphatase (ALP) conjugated to streptavidin was captured with biotin labels and utilized for the conversion of α-naphthyl phosphate to the electroactive product α-naphthol [61, 62].

Compared with other isothermal amplification strategies, this technique comes out to be a suitable alternative to low concentration target detection. Although multiple step-based signal amplification increases the sensitivity significantly, it takes a huge time. In addition to that, stability is a big issue in such a sensor. To overcome those problems, ye zhang et al. designed DNA tetrahedrons assisted catalytic hairpin assembly (MDTs-CHA) based electrochemical biosensor for the specific detection of four breast cancer cell-derived EV-incorporated miRNAs (miR-1246, miR-221, miR-375, and miR-21) [62] (Fig. 9).

Howbeit, this kind of highly sensitive strategy requires multiple probes and a very complex signal amplification process, which limits their use in a practical scenario.

Hybridization Chain Reaction

Hybridization chain reaction (HCR) is another modified form of SDR, similar to CHA, comprising sequential partial hybridization of amplification probes to form ladder-like multistranded structures (concatemers). The detection signal is greatly amplified by labeling individual probes with a signaling tag [68]. For instance, Choi, Beck, and Pierce designed an HCR strategy for the detection of mRNA targets within whole-mount, intact zebrafish embryos with complementary DNA initiator probe sets and amplification hairpin pairs [77]. The hairpins coexisted stably until an initiator strand destabilized and opened the hairpins sequentially via toehold-mediated displacement [77]. A specific DNA initiator, say I1, contained a mid-region complementary to a region of the target mRNA and generated a 3′- and 5′- overhang/sticky end each upon hybridization. The 5′- sticky end was hybridized with H1 via its toehold, opening it [77]. The sticky end of H1 was further hybridized with H2, such that the sticky end of H2 was rendered identical to that of I1[77]. Thus, a chain reaction could be initiated indefinitely, till H1 and H2 were

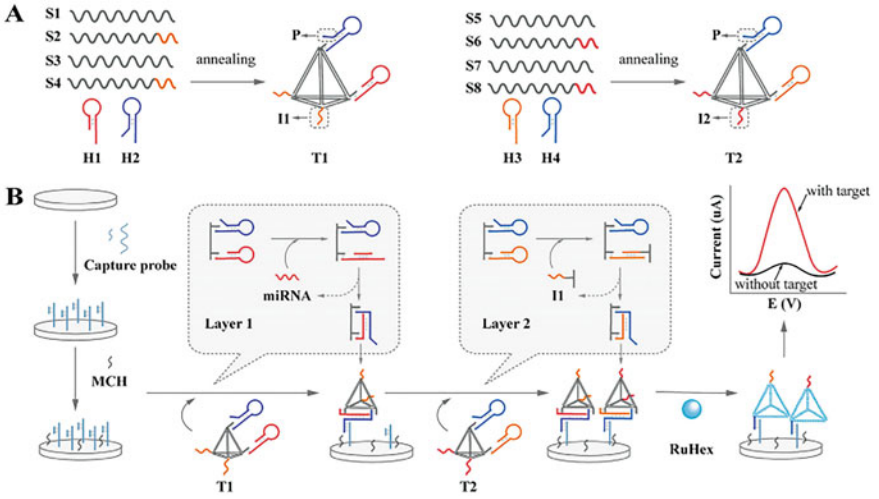

Fig. 9 Schematic illustration of electrochemical approach for the detection of breast cancer cell-derived exosome extracted micro RNAs. (**a**) Strand displacement assembly reaction was performed to synthesize T1 with S1-S4, H1, H2, and T2 with S5-S8, H3, H4 (**b**) Catalytic hairpin assembly based electrochemical biosensing steps on the surface of the gold working electrode. Reprinted from [62] Copyright (2021), with permission from Elsevier

exhausted. The authors of this study fluorescent-labeled the hairpins to amplify manifold the fluorescent signal (Fig. 10) [77].

In comparison with enzyme-based signal amplification, HCR show promises in terms of simplicity, stability, and efficiency in isothermal amplification. In recent times, HCR is highly popular in miRNA detection. Guo et al. fabricated miR-122 complementary hairpin DNA on the gold working electrode surface. In presence of HepG2 and MCF7 cell-derived EV extracted miR-122, the hairpin probe opened up to form a single straight hybrid [58]. Then helper DNA 1 and helper DNA 2 were used to initiate the HCR process (Fig. 11). Electroactive intercalation of the signal molecule $[Ru(NH_3)_6]^{3+}$ (RuHex) in the long-chain hybrid generated signal for sensitive detection [58].

Though HCR is a potential alternative to enzyme-based signal amplification it is restricted to dsDNA amplification only [60]. A recent novel isothermal nucleic acid amplification strategy has captured research attention that can amplify any arbitrary ssDNA in just one step with the help of a primer exchange reaction. Wang et al. designed a highly sensitive sensor using the concept of primer exchange DNA amplification reaction (PEDAR) and target-mediated cyclic strand displacement reaction (TMCSDR) [60]. As indicated in Fig. 12, the gold working electrode was modified with a primer probe that initiated the first round of signal amplification in presence of breast cancer cell-derived EV extracted miR-21 [60]. After a few cycles of TMCSDR, it generated many single-stranded primers. Then template probe was hybridized with the generated primer to start the second round of PEDAR signal amplification. Finally, the redox molecule methylene blue (MB) is bound

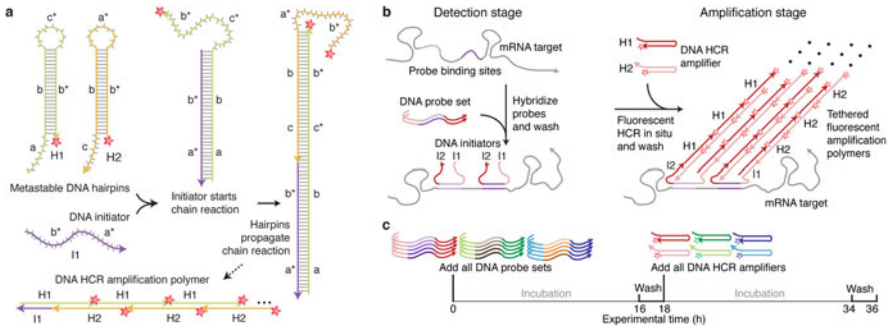

Fig. 10 Schematic illustration of in situ amplification via hybridization chain reaction (HCR). (**a**) HCR mechanism. Metastable fluorescent hairpins self-assemble into fluorescent amplification polymers upon detection of a cognate initiator. Initiator I1 nucleates with hairpin H1 via base-pairing to single-stranded toehold "a", mediating a branch migration that opens the hairpin to form complex I1-H1 containing single-stranded segment "c*-b*". This complex nucleates with hairpin H2 by means of base-pairing to toehold "c", mediating a branch migration that opens the hairpin to form complex I1-H1-H2 containing single-stranded segment "b*-a*". Thus, the initiator sequence is regenerated, providing the basis for a chain reaction of alternating H1 and H2 polymerization steps. Red stars denote fluorophores. (**b**) In situ hybridization protocol. Detection stage: probe sets are hybridized to mRNA targets, and unused probes are washed from the sample. Amplification stage: initiators trigger self-assembly of tethered fluorescent amplification polymers, and unused hairpins are washed from the sample. (**c**) Experimental timeline. The same two-stage protocol is used independently of the number of target mRNAs. For multiplexed experiments (three-color example depicted), probe sets for different target mRNAs (five probes depicted per set) carry orthogonal initiators that trigger orthogonal HCR amplification cascades labeled by spectrally distinct fluorophores. Reprinted from [77] with permission from the American Chemical Society

electrostatically with the amplified product to generate the electrochemical signal. In this label-free dual amplification process, they achieved a LOD of 3.04 aM that accurately discriminated even single-base mismatch. Such highly selective biosensors exhibited the significant potential to be used in point-of-care diagnosis [60] (Fig. 12).

DNA Nanomachines

Recently, several DNA nanomachines have been synthesized and designed to perform triggered motion, signaling, and conformation switching tasks. The nanomachines are categorized as DNA switches, walkers, motors, etc. [78]. A sensing platform reported by Zhao and the group utilized a DNA walker for the ratiometric release of signal probes from a small population of captured target EVs [54]. The designed DNA walker was composed of exosomal CD63-specific aptamers, immobilized on magnetic beads (MBs) via biotin-streptavidin linkage [54]. To discriminate MCF cell-secreted EVs from normal cellular EVs, dual recognition was conducted with exosomal EpCAM aptamers alongside CD63 aptamers. EpCAM aptamers were captured to the MBs only in the presence of target EVs, forming a sandwich complex with CD63- and EpCAM- aptamers. The EpCAM aptamer was extended to a swing arm and an Mg^{2+}-dependent DNAzyme,

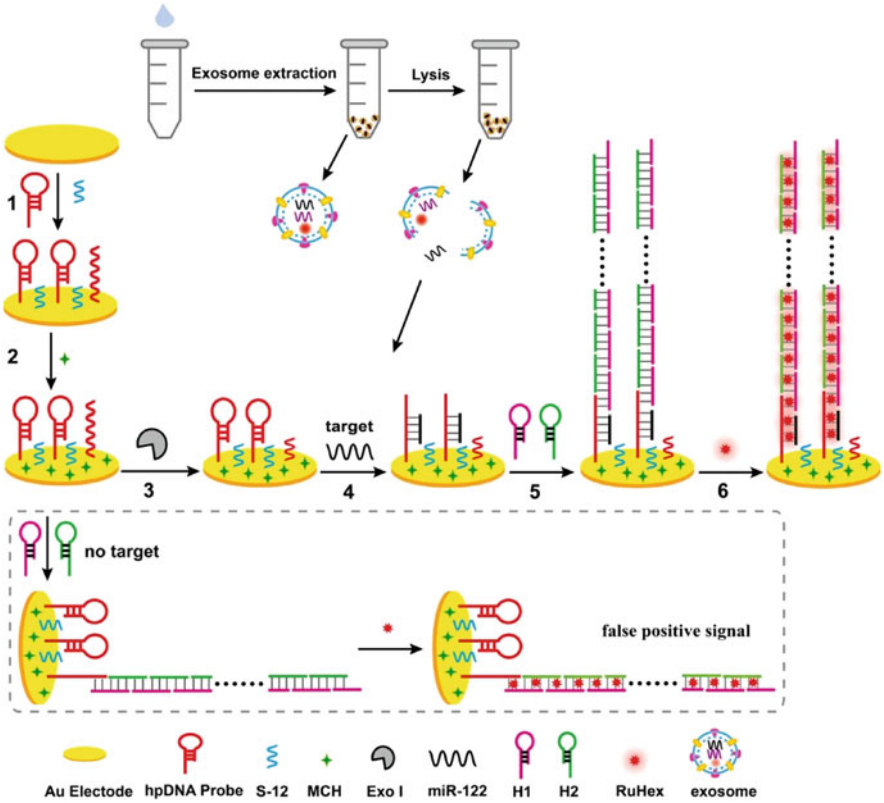

Fig. 11 Schematic representation of HCR-based electrochemical biosensor for the detection of breast cancer EV-derived miR-122. In the absence of target miR-122, H1 had the potential to trigger HCR reaction with single-stranded hpDNA which resulted in the false-positive signal. So as to reduce the false-positive signal, exonuclease 1 was used just before the incubation of miR-122. Exonuclease 1 hydrolyzed the single-stranded hpDNA in order to prevent any background signal from the sensor. Reprinted with permission from [58] Copyright (2021), American Chemical Society

flanked by A1 and A2 sequences [54]. The MBs were also functionalized with DNAzyme substrate sequences comprised of a ribonucleobase (rA) cleavage point and flanking P1 and P2 sequences. P2 and P1 hybridized to A1 and A2, respectively, when brought into proximity in the presence of EVs [54]. The DNAzyme then mediated a cleavage at rA and released P1 strands. This step destabilized and caused the melting of the hybridized structure. The cleavage and melting events propelled the free EpCAM aptamer-DNAzyme strands to hybridize into another DNAzyme substrate [54]. The released P1 strands were then used to unwind methylene blue-conjugated hairpin DNAs on a gold electrode. The exposed 3′-ends of the unwound hairpins were digested with a 3′-5′ exonuclease (Exo III), and P1 strands were further released for initiating multiple steps of hybridization and exonuclease

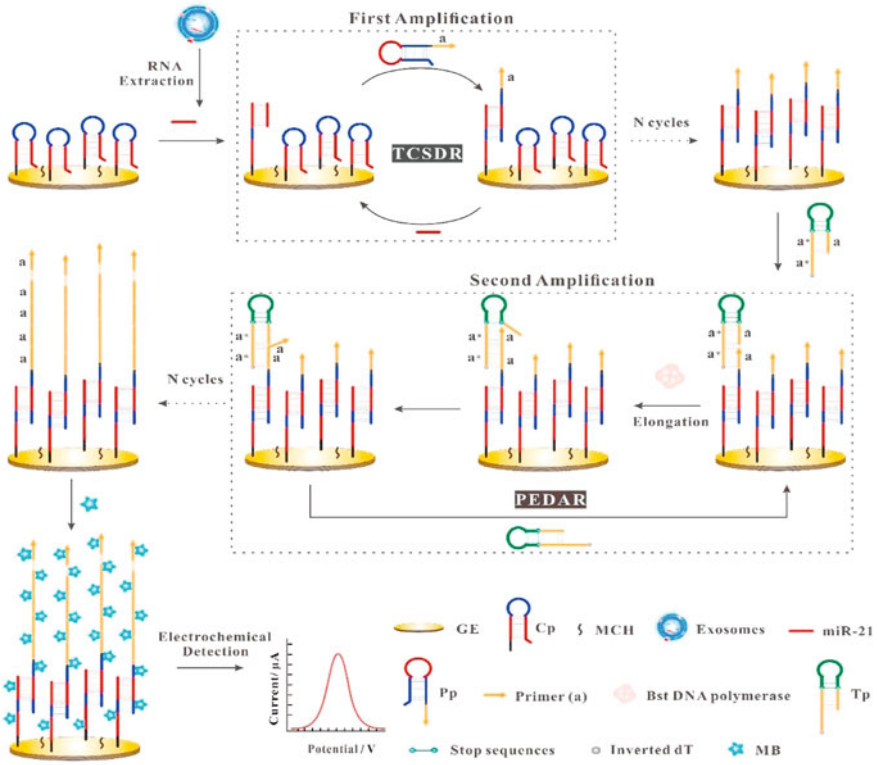

Fig. 12 Schematic representation of dual amplification electrochemical biosensor for the detection of breast cancer EV-derived miR-21. Reprinted from [60] Copyright (2021), with permission from Elsevier

activity. In the final signal generation step, several 5′-ferrocene (Fc) labeled DNA strands were hybridized into the partially digested hairpin DNAs on the gold electrode [54]. The ratiometric biosensing signal was obtained from the oxidation currents of both the electroactive labels: methylene blue and ferrocene (Fig. 13) [54].

6 Challenges and Future Directions

The inadequacies of conventional invasive diagnostic techniques coupled with recent advancements in molecular profiling of biofluids have led to the popularization of liquid biopsy as a tool for cancer diagnosis. EVs as novel analytes in liquid biopsies have triggered interest among researchers and exhibit potential as excellent biomarkers. Electrochemical sensing, associated with good selectivity and high sensitivity and the added features of low cost, rapid detection, minimum sample requirement, and simplicity, is an attractive alternative to conventional methods of

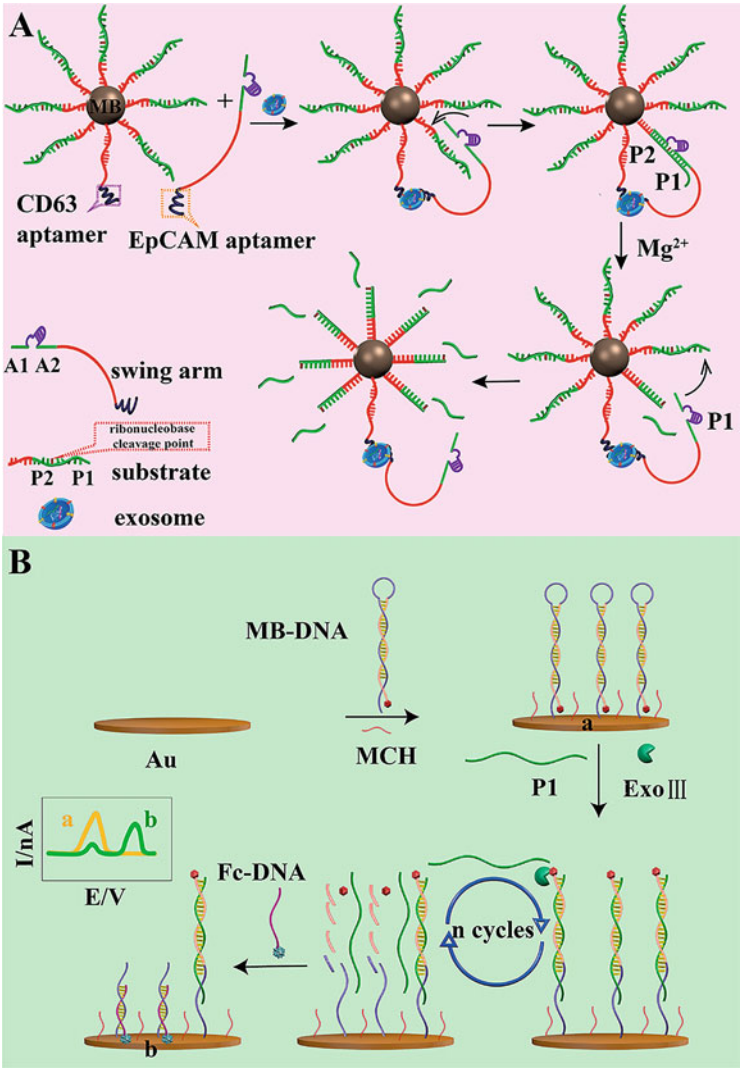

Fig. 13 Schematic illustration for the detection of exosomes through (**a**) 3D DNA walker amplification and (**b**) Exo III-assisted electrochemical ratiometric assay. Reprinted from [54] with permission from the American Chemical Society

EV detection and characterization. However, several bottlenecks could arise and need attention for facilitating the use of these techniques in the clinical setup.

Clinical samples are prone to biological variability; variations are often introduced during the collection and handling of biospecimens. Furthermore, detection of low abundant biomarkers is often challenging due to the inherent complexity of biological matrices and requires the use of appropriate sample extraction or

pre-treatment steps. The development of sensors based on a single marker while clinically appealing due to simplicity and low cost, may not capture the variability of disease through the population, which again lowers accuracy, sensitivity, and specificity. It is well accepted that even a small deviation in the sensor fabrication process including but not limited to electrode surface modification, sample pre-treatment, etc. may lead to inconsistencies in detection. Another challenge is the low signal-to-noise ratio and the presence of false positives which pose a serious threat to achieving high specificity. A number of excellent clinically useful sensors have been developed so far; however, reports on clinical trials conducted globally for validation of these fabricated sensing devices are lacking, thereby raising the question of reproducibility.

EV research has emerged as an attractive noninvasive diagnostic option for cancer in the last decade. Not only in diagnosis but these natural stable vesicles show promise in drug delivery, regenerative, and personalized medicine. Rose Johnstone first used the word "exosome" in 1983 [79]. Initially, these small vesicles were reviewed as "garbage bags," just to remove the waste products from cells. It took almost four decades to understand the pathological and structural aspects of EVs in cellular communication. In 2013, Dr. Rothman, Dr. **Schekman, and Dr. Südhof were honored with the Nobel prize for reporting the vesicular transporting machinery in the human system** [80]**.** Since then there is an unexpected growth in EV research. According to journal citation reports published in 2016, a total of 51, 913 times the keyword "exosome research" was used in correlation with any analytical disorders [81]. The "PLOS ONE," "JOURNAL OF BIOLOGICAL CHEMISTRY," and "SCIENTIFIC REPORTS" were the highest holding journals for EV research according to the report published in 2016 [81]. Initiation of a few dedicated societies for EV research such as the *Journal of Extracellular Vesicle* (JEV), *International Society of Extracellular Vesicles* (ISEV), and *European Journal of extracellular vesicle* (ESEV) appeared to motivate newborn ideas in this field. There are a large number of databases for instance "Vesiclepedia" (www.microvesicles.org), ExoCarta (www.exocarta.org), EV-TRACK (www.evtrack.org), exRNA Atlas (www.exrna-atlas.org), etc. were started to encourage to store and access the EV related information. According to the UTSPO database in 2016 in total 524 US patents were granted involving EV [81]. Various clinical and pre-clinical trials are ongoing in this particular field and most of them are associated with a cancer diagnosis. Many governments and nongovernment agencies have been involved in granting funding for EV research. Understanding the impact of EV research numerous companies have started to commit to this area. Companies include Aethlon Medical, Inc., Exopharm Ltd., Lineage Cell Therapeutics, Exosome Diagnostics Inc., Clara Biotech, Sphere Fluidics, ThermoFisher Scientific Inc., etc. The global EV market is expected to reach $2.28 billion at a CAGR of 18.8% by 2030 [82]. Although many new perspectives have emerged related to EVs for clinical translation, still standardization of qualitative and quantitative EV research is still a challenging job. According to MISEV, the clinical application of EV depends on various pre-clinical factors such as coagulation agent, storage time,

and isolation steps [5]. Several biochemical and biophysical variables have been found to alter the pathophysiological profile of EVs.

Recent progress in the sensitive sensing of EVs by electrochemical biosensors has promised to bridge the challenges. The real-time accurate point-of-care (POC) diagnosis of the target analyte is very important especially in highly populated countries like India to reduce the massive burden on the healthcare sector [83]. Various electrochemical biosensors have achieved a very low detection limit by manipulating sensing parameters. With the recent integration of microfluidics and nanotechnology, it is envisioned that the issues associated with sample pre-treatment and signal amplification can be addressed significantly. The extensive use of nanomaterials has improved the sensitivity of the platforms to a considerable extent. Multiplexed detection is another prominent feature that can influence the development of electrochemical sensors.

7 Conclusion

EVs have amassed an ample amount of research recognition in the recent era due to their capacity to carry disease-specific biomarkers from one cell to another. An elevated number of tumor-specific EVs emerged as an excellent circulating liquid biopsy biomarker for cancer. To explore these aspects, standardized EV analysis techniques are essential. Many interesting biochemical, and biophysical techniques are unable to quantify tumor-derived EVs with high sensitivity. Scientists are constantly trying to advance the science, technology, and innovation (STI) sector for the development of accurate POC medical devices. With the immense pressure that has stretched in the healthcare sector after the COVID-19 pandemic, it is relevant to develop low-cost, rapid, sensitive POC medical devices for high prevalence diseases. The performance of an effective biosensor not only relies on the stability of the biorecognition molecule aptamer or antibody but also on a sensitive signal detection method to quantify cancer-derived EVs at very low concentrations. Herein, we presented the advantage of electrochemical biosensors and their potential implications in EV sensing. Further, the newborn ideas and signal detection strategies with electrochemical biosensors were discussed in this review. The majority of electrochemical proof-of-concept studies for cancer-derived EV quantification are listed in Table 2. Despite the considerable advances in these fields, most of the sensors require traditional strategies like ultracentrifugation and chromatography for the isolation of EVs from human bioliquids. Moreover, it is well reported that the biochemical properties of EVs get affected by different isolation strategies. For that reason, it is very important to standardize the EV isolation method, before detection. On top of that, the vague knowledge of EV storage conditions, and stability faces difficulty to translate individual research insights into the clinical market. We believe that more research and recommendations will enable us to design an electrochemical ‘extracellular vesicle on chip’ POC medical device in near future.

Acknowledgments Authors gratefully acknowledge the Start-Up Research Grant (SRG) funded by the Science & Engineering Research Board (SERB) (SRG/2020/000712), Department of Science and Technology (DST) (Government of India, Ministry of Science and Technology, (Technology Development and Transfer, TDP/BDTD/12/2021/General), Indo-German Science & Technology Center (IGSTC) (IGSTC/Call 2019/NOMIS/22/2020–21/164), and Institute Scheme for Innovative Research and Development (ISIRD) (IIT/SRIC/ISIRD/2019–2020/17), Indian Institute of Technology Kharagpur (IIT Kharagpur), India for the financial support.

Conflicts of Interest The authors declare no conflict of interest.

References

1. Cancer. (2021). Retrieved September 29, 2021, from https://www.who.int/news-room/fact-sheets/detail/cancer.
2. Al-Azri, M. H. (2016). Delay in cancer diagnosis: causes and possible solutions. *Oman Medical Journal, 31*(5), 325–326.
3. Palmirotta, R., Lovero, D., Cafforio, P., Felici, C., Mannavola, F., Pellè, E., et al. (2018). Liquid biopsy of cancer: A multimodal diagnostic tool in clinical oncology. *Therapeutic Advances in Medical Oncology, 10*, 1–24. https://doi.org/10.1177/1758835918794630
4. Kalluri, R., & LeBleu, V. S. (2020). The biology, function, and biomedical applications of exosomes. *Science, 367*(6478), 1–17.
5. Théry, C., Witwer, K. W., Aikawa, E., Alcaraz, M. J., Anderson, J. D., Andriantsitohaina, R., et al. (2018). Minimal information for studies of extracellular vesicles 2018 (MISEV2018): A position statement of the International Society for Extracellular Vesicles and update of the MISEV2014 guidelines. *Journal of Extracellular Vesicles, 7*(1), 1–47. https://doi.org/10.1080/20013078.2018.1535750
6. Vigneshvar, S., Sudhakumari, C. C., Senthilkumaran, B., & Prakash, H. (2016). Recent advances in biosensor technology for potential applications – an overview. *Frontiers in Bioengineering and Biotechnology, 4*, 1–11.
7. Drain, P. K., Hyle, E. P., Noubary, F., Freedberg, K. A., Wilson, D., Bishai, W., et al. (2014). Evaluating diagnostic point-of-care tests in resource-limited settings. *The Lancet Infectious Diseases, 14*(3), 239–249.
8. Dominiak, A., Chełstowska, B., Olejarz, W., & Nowicka, G. (2020). Communication in the cancer microenvironment as a target for therapeutic interventions. *Cancers, 12*(5), 1–24.
9. Mathur, P., Sathishkumar, K., Chaturvedi, M., Das, P., Sudarshan, K. L., Santhappan, S., et al. (2020). Cancer statistics, 2020: Report From National Cancer Registry Programme, India. *JCO Global Oncology, 6*, 1063–1075.
10. Nesbitt, J. C., Putnam, J. B., Walsh, G. L., Roth, J. A., & Mountain, C. F. (1995). Survival in early-stage non-small cell lung cancer. *The Annals of Thoracic Surgery., 1*, 1–7.
11. Marrugo-Ramírez, J., Mir, M., & Samitier, J. (2018). Blood-based cancer biomarkers in liquid biopsy: a promising non-invasive alternative to tissue biopsy. *International Journal of Molecular Sciences, 19*(10), 1–21. https://doi.org/10.3390/ijms19102877
12. Wu, C., Zhang, J., Li, H., Xu, W., & Zhang, X. (2020). The potential of liquid biopsies in gastrointestinal cancer. *Clinical Biochemistry, 84*, 1–12.
13. Ilié, M., & Hofman, P. (2016). Pros: Can tissue biopsy be replaced by liquid biopsy? *Translational Lung Cancer Research, 5*(4), 420–423. https://doi.org/10.21037/tlcr.2016.08.06
14. Gurunathan, S., Kang, M.-H., Jeyaraj, M., Qasim, M., & Kim, J.-H. (2019). Review of the isolation, characterization, biological function, and multifarious therapeutic approaches of exosomes. *Cell, 8*(4), 1–36.

15. Sharma, S., Rasool, H. I., Palanisamy, V., Mathisen, C., Schmidt, M., Wong, D. T., et al. (2010). Structural-mechanical characterization of nanoparticle exosomes in human saliva, using correlative AFM, FESEM, and force spectroscopy. *ACS Nano, 4*(4), 1921–1926.
16. Szatanek, R., Baj-Krzyworzeka, M., Zimoch, J., Lekka, M., Siedlar, M., & Baran, J. (2017). The methods of choice for extracellular vesicles (EVs) characterization. *International Journal of Molecular Sciences, 18*(6), 1–18.
17. van der Pol, E., van Gemert, M. J. C., Sturk, A., Nieuwland, R., & van Leeuwen, T. G. (2012). Single vs. Swarm detection of microparticles and exosomes by flow cytometry. *Journal of Thrombosis and Haemostasis, 10*(5), 919–930.
18. Gardiner, C., Ferreira, Y. J., Dragovic, R. A., Redman, C. W. G., & Sargent, I. L. (2013). Extracellular vesicle sizing and enumeration by nanoparticle tracking analysis. *Journal of Extracellular Vesicles, 2*, 1–11.
19. Im, H., Shao, H., Park, Y. I., Peterson, V. M., Castro, C. M., Weissleder, R., & Lee, H. (2014). Label-free detection and molecular profiling of exosomes with a nano-plasmonic sensor. *Nature Biotechnology, 32*(5), 490–495.
20. Grabarek, A. D., Weinbuch, D., Jiskoot, W., & Hawe, A. (2019). Critical evaluation of microfluidic resistive pulse sensing for quantification and sizing of nanometer- and micrometer-sized particles in biopharmaceutical products. *Journal of Pharmaceutical Sciences, 108*(1), 563–573.
21. Duijvesz, D., Versluis, C. Y. L., van der Fels, C. A. M., Vredenbregt-van den Berg, M. S., Leivo, J., Peltola, M. T., et al. (2015). Immuno-based detection of extracellular vesicles in urine as diagnostic marker for prostate cancer. *International Journal of Cancer, 137*(12), 2869–2878.
22. Musante, L., Tataruch-Weinert, D., Kerjaschki, D., Henry, M., Meleady, P., & Holthofer, H. (2016). Residual urinary extracellular vesicles in ultracentrifugation supernatants after hydrostatic filtration dialysis enrichment. *Journal of Extracellular Vesicles, 6*(1), 1–17.
23. Zarovni, N., Corrado, A., Guazzi, P., Zocco, D., Lari, E., Radano, G., et al. (2015). Integrated isolation and quantitative analysis of exosome shuttled proteins and nucleic acids using immunocapture approaches. *Methods (San Diego, Calif.), 87*, 46–58.
24. Böing, A. N., van der Pol, E., Grootemaat, A. E., Coumans, F. A. W., Sturk, A., & Nieuwland, R. (2014). Single-step isolation of extracellular vesicles by size-exclusion chromatography. *Journal of Extracellular Vesicles, 3*, 1–13.
25. Harshman, S. W., Canella, A., Ciarlariello, P. D., Agarwal, K., Branson, O. E., Rocci, A., et al. (2016). Proteomic characterization of circulating extracellular vesicles identifies novel serum myeloma associated markers. *Journal of Proteomics, 136*, 89–98.
26. Bai, Y., Qu, Y., Wu, Z., Ren, Y., Cheng, Z., Lu, Y., et al. (2019). Absolute quantification and analysis of extracellular vesicle lncRNAs from the peripheral blood of patients with lung cancer based on multi-colour fluorescence chip-based digital PCR. *Biosensors & Bioelectronics, 142*, 1–8.
27. Chen, W. W., Balaj, L., Liau, L. M., Samuels, M. L., Kotsopoulos, S. K., Maguire, C. A., et al. (2013). BEAMing and droplet digital pcr analysis of mutant IDH1 mRNA in glioma patient serum and cerebrospinal fluid extracellular vesicles. *Molecular Therapy – Nucleic Acids, 2*, 1–10.
28. Xiao, D., Ohlendorf, J., Chen, Y., Taylor, D. D., Rai, S. N., Waigel, S., et al. (2012). Identifying mRNA, microRNA and protein profiles of melanoma exosomes. *PLoS One, 7*(10), 1–10.
29. Andreu, Z., & Yáñez-Mó, M. (2014). Tetraspanins in extracellular vesicle formation and function. *Frontiers in Immunology, 5*, 1–13.
30. Liu, C., Zeng, X., An, Z., Yang, Y., Eisenbaum, M., Gu, X., et al. (2018). Sensitive detection of exosomal proteins via a compact surface plasmon resonance biosensor for cancer diagnosis. *ACS Sensors, 3*(8), 1471–1479.
31. Murakami, K., Zhao, J., Yamasaki, K., & Miyagishi, M. (2017). Biochemical and structural features of extracellular vesicle-binding RNA aptamers. *Biomedical Reports, 6*(6), 615–626.

32. Soares Martins, T., Magalhães, S., Rosa, I. M., Vogelgsang, J., Wiltfang, J., Delgadillo, I., et al. (2020). Potential of FTIR spectroscopy applied to exosomes for Alzheimer's disease discrimination: a pilot study. *Journal of Alzheimer's Disease, 74*(1), 391–405.
33. Kovalenko, O. V., Metcalf, D. G., DeGrado, W. F., & Hemler, M. E. (2005). Structural organization and interactions of transmembrane domains in tetraspanin proteins. *BMC Structural Biology, 5*(1), 1–20.
34. Dong, L., Lin, W., Qi, P., Xu, M., Wu, X., Ni, S., et al. (2016). Circulating long RNAs in serum extracellular vesicles: their characterization and potential application as biomarkers for diagnosis of colorectal cancer. *Cancer Epidemiology Biomarkers & Prevention, 25*(7), 1158–1166.
35. Boriachek, K., Umer, M., Islam, M. N., Gopalan, V., Lam, A. K., Nguyen, N.-T., et al. (2018). An amplification-free electrochemical detection of exosomal miRNA-21 in serum samples. *The Analyst, 1*(1), 1–28.
36. Kilic, T., Valinhas, A. T. D. S., Wall, I., Renaud, P., & Carrara, S. (2018). Label-free detection of hypoxia-induced extracellular vesicle secretion from MCF-7 cells. *Scientific Reports, 8*(1), 1–9.
37. Cho, I.-H., Lee, J., Kim, J., Kang, M., Paik, J. K., Ku, S., et al. (2018). Current technologies of electrochemical immunosensors: perspective on signal amplification. *Sensors, 18*(1), 1–18.
38. Doldán, X., Fagúndez, P., Cayota, A., Laíz, J., & Tosar, J. P. (2016). Electrochemical sandwich immunosensor for determination of exosomes based on surface marker-mediated signal amplification. *Analytical Chemistry, 88*(21), 10466–10473.
39. Vaidyanathan, R., Naghibosadat, M., Rauf, S., Korbie, D., Carrascosa, L. G., Shiddiky, M. J. A., et al. (2014). Detecting exosomes specifically: A multiplexed device based on alternating current electrohydrodynamic induced nanoshearing. *Analytical Chemistry, 86*(22), 11125–11132.
40. Yadav, S., Boriachek, K., Islam, M. N., Lobb, R., Möller, A., Hill, M. M., et al. (2017). An electrochemical method for the detection of disease-specific exosomes. *ChemElectroChem, 4*(4), 967–971.
41. Li, Q., Tofaris, G. K., & Davis, J. J. (2017). Concentration-normalized electroanalytical assaying of exosomal markers. *Analytical Chemistry, 89*(5), 3184–3190.
42. Boriachek, K., Masud, M. K., Palma, C., Phan, H.-P., Yamauchi, Y., Hossain, M. S. A., Nguyen, N.-T., et al. (2019). Avoiding pre-isolation step in exosome analysis: direct isolation and sensitive detection of exosomes using gold-loaded nanoporous ferric oxide nanozymes. *Analytical Chemistry, 91*(6), 3827–3834.
43. Mathew, D. G., Beekman, P., Lemay, S. G., Zuilhof, H., Le Gac, S., & van der Wiel, W. G. (2020). Electrochemical detection of tumor-derived extracellular vesicles on nanointerdigitated electrodes. *Nano Letters, 20*(2), 820–828.
44. Jeong, S., Park, J., Pathania, D., Castro, C. M., Weissleder, R., & Lee, H. (2016). Integrated magneto–electrochemical sensor for exosome analysis. *ACS Nano, 10*(2), 1802–1809.
45. Park, J., Park, J. S., Huang, C.-H., Jo, A., Cook, K., Wang, R., et al. (2021). An integrated magneto-electrochemical device for the rapid profiling of tumour extracellular vesicles from blood plasma. *Nature Biomedical Engineering, 5*(7), 678–689.
46. Zhou, Y.-G., Mohamadi, R. M., Poudineh, M., Kermanshah, L., Ahmed, S., Safaei, T. S., Stojcic, J., et al. (2016). Interrogating circulating microsomes and exosomes using metal nanoparticles. *Small (Weinheim an Der Bergstrasse, Germany), 12*(6), 727–732.
47. Zhou, Q., Rahimian, A., Son, K., Shin, D.-S., Patel, T., & Revzin, A. (2016). Development of an aptasensor for electrochemical detection of exosomes. *Methods, 97*, 88–93.
48. Zhang, H., Qiao, B., Guo, Q., Jiang, J., Cai, C., & Shen, J. (2020). A facile and label-free electrochemical aptasensor for tumour-derived extracellular vesicle detection based on the target-induced proximity hybridization of split aptamers. *The Analyst, 145*(10), 3557–3563.
49. Wang, L. (2021). Electrochemical aptasensor based on multidirectional hybridization chain reaction for detection of tumorous exosomes. *Sensors and Actuators, 332*, 1–9.

50. An, Y., Jin, T., Zhu, Y., Zhang, F., & He, P. (2019). An ultrasensitive electrochemical aptasensor for the determination of tumor exosomes based on click chemistry. *Biosensors and Bioelectronics, 142*, 1–7.
51. Xu, H., Liao, C., Zuo, P., Liu, Z., & Ye, B.-C. (2018). Magnetic-based microfluidic device for on-chip isolation and detection of tumor-derived exosomes. *Analytical Chemistry, 90*(22), 13451–13458.
52. Wang, S., Zhang, L., Wan, S., Cansiz, S., Cui, C., Liu, Y., et al. (2017). Aptasensor with expanded nucleotide using DNA nanotetrahedra for electrochemical detection of cancerous exosomes. *ACS Nano, 11*(4), 3943–3949.
53. Huang, R., He, L., Xia, Y., Xu, H., Liu, C., Xie, H., et al. (2019). A sensitive aptasensor based on a hemin/g-quadruplex-assisted signal amplification strategy for electrochemical detection of gastric cancer exosomes. *Small, 15*(19), 1–7.
54. Zhao, L., Sun, R., He, P., & Zhang, X. (2019). Ultrasensitive detection of exosomes by target-triggered three-dimensional DNA walking machine and exonuclease III-assisted electrochemical ratiometric biosensing. *Analytical Chemistry, 91*(22), 14773–14779.
55. Yin, X., Hou, T., Huang, B., Yang, L., & Li, F. (2019). Aptamer recognition-trigged label-free homogeneous electrochemical strategy for an ultrasensitive cancer-derived exosome assay. *Chemical Communications, 55*(91), 13705–13708.
56. Dong, H., Chen, H., Jiang, J., Zhang, H., Cai, C., & Shen, Q. (2018). Highly sensitive electrochemical detection of tumor exosomes based on aptamer recognition-induced multi-dna release and cyclic enzymatic amplification. *Analytical Chemistry, 90*(7), 4507–4513.
57. Cao, Y., Li, L., Han, B., Wang, Y., Dai, Y., & Zhao, J. (2019). A catalytic molecule machine-driven biosensing method for amplified electrochemical detection of exosomes. *Biosensors and Bioelectronics, 141*, 1–6.
58. Guo, Q., Yu, Y., Zhang, H., Cai, C., & Shen, Q. (2020). Electrochemical sensing of exosomal microRNA based on hybridization chain reaction signal amplification with reduced false-positive signals. *Analytical Chemistry, 92*(7), 5302–5310.
59. Miao, P., & Tang, Y. (2020). Dumbbell hybridization chain reaction based electrochemical biosensor for ultrasensitive detection of exosomal miRNA. *Analytical Chemistry, 92*(17), 12026–12032.
60. Wang, L.-L., Chen, W.-Q., Wang, Y.-R., Zeng, L.-P., Chen, T.-T., Chen, G.-Y., & Chen, J.-H. (2020). Numerous long single-stranded DNAs produced by dual amplification reactions for electrochemical detection of exosomal microRNAs. *Biosensors and Bioelectronics, 169*, 1–10.
61. Zhang, R. Y., Luo, S. H., Lin, X. M., Hu, X. M., Zhang, Y., Zhang, X. H., et al. (2021). A novel electrochemical biosensor for exosomal microRNA-181 detection based on a catalytic hairpin assembly circuit. *Analytica Chimica Acta, 1157*, 1–9.
62. Zhang, Y., Zhang, X., Situ, B., Wu, Y., Luo, S., Zheng, L., et al. (2021). Rapid electrochemical biosensor for sensitive profiling of exosomal microRNA based on multifunctional DNA tetrahedron assisted catalytic hairpin assembly. *Biosensors and Bioelectronics, 183*, 1–9.
63. Luo, L., Wang, L., Zeng, L., Wang, Y., Weng, Y., Liao, Y., et al. (2020). A ratiometric electrochemical DNA biosensor for detection of exosomal MicroRNA. *Talanta, 207*, 1–8.
64. Zhang, J., Wang, L.-L., Hou, M.-F., Xia, Y.-K., He, W.-H., Yan, A., et al. (2018). A ratiometric electrochemical biosensor for the exosomal microRNAs detection based on bipedal DNA walkers propelled by locked nucleic acid modified toehold mediate strand displacement reaction. *Biosensors and Bioelectronics, 102*, 33–40.
65. Cheng, W. (2020). Enzyme-free electrochemical biosensor based on double signal amplification strategy for the ultra-sensitive detection of exosomal microRNAs in biological samples. *Talanta, 219*, 1–6.
66. Su, J., Zhang, H., Jiang, B., Zheng, H., Chai, Y., Yuan, R., et al. (2011). Dual signal amplification for highly sensitive electrochemical detection of uropathogens via enzyme-based catalytic target recycling. *Biosensors & Bioelectronics, 29*(1), 184–188.

67. Rocchitta, G., Spanu, A., Babudieri, S., Latte, G., Madeddu, G., Galleri, G., et al. (2016). Enzyme biosensors for biomedical applications: strategies for safeguarding analytical performances in biological fluids. *Sensors (Basel, Switzerland), 16*(6), 1–21.
68. Bi, S., Yue, S., & Zhang, S. (2017). Hybridization chain reaction: A versatile molecular tool for biosensing, bioimaging, and biomedicine. *Chemical Society Reviews, 46*(14), 4281–4298.
69. Xu, L., Duan, J., Chen, J., Ding, S., & Cheng, W. (2021). Recent advances in rolling circle amplification-based biosensing strategies-A review. *Analytica Chimica Acta, 1148*, 1–16.
70. Huang, R., He, L., Li, S., Liu, H., Jin, L., Chen, Z., et al. (2020). A simple fluorescence aptasensor for gastric cancer exosome detection based on branched rolling circle amplification. *Nanoscale, 12*(4), 2445–2451.
71. Jalili, R., Horecka, J., Swartz, J. R., Davis, R. W., & Persson, H. H. J. (2018). Streamlined circular proximity ligation assay provides high stringency and compatibility with low-affinity antibodies. *Proceedings of the National Academy of Sciences, 115*(5), 925–933.
72. Walker, G. T., Fraiser, M. S., Schram, J. L., Little, M. C., Nadeau, J. G., & Malinowski, D. P. (1992). Strand displacement amplification—An isothermal, in vitro DNA amplification technique. *Nucleic Acids Research, 20*(7), 1691–1696.
73. Miao, P., & Tang, Y. (2021). Cascade toehold-mediated strand displacement reaction for ultrasensitive detection of exosomal MicroRNA. *CCS Chemistry, 3*(7), 2331–2339.
74. Liu, P., Qian, X., Li, X., Fan, L., Li, X., Cui, D., & Yan, Y. (2020). Enzyme-free electrochemical biosensor based on localized DNA cascade displacement reaction and versatile DNA nanosheets for ultrasensitive detection of exosomal MicroRNA. *ACS Applied Materials & Interfaces, 12*(40), 45648–45656.
75. Shi, C., Liu, Q., Ma, C., & Zhong, W. (2014). Exponential strand-displacement amplification for detection of MicroRNAs. *Analytical Chemistry, 86*(1), 336–339.
76. Cui, L., Zhou, J., Yang, X.-Y., Dong, J., Wang, X., & Zhang, C. (2020). Catalytic hairpin assembly-based electrochemical biosensor with tandem signal amplification for sensitive microRNA assay. *Chemical Communications, 56*(70), 10191–10194.
77. Choi, H. M. T., Beck, V. A., & Pierce, N. A. (2014). Next-generation in situ hybridization chain reaction: higher gain, lower cost, greater durability. *ACS Nano, 8*, 4284–4294.
78. Bath, J., & Turberfield, A. J. (2007). DNA nanomachines. *Nature Nanotechnology, 2*(5), 275–284.
79. Harding, C. V., Heuser, J. E., & Stahl, P. D. (2013). Exosomes: Looking back three decades and into the future. *The Journal of Cell Biology, 200*(4), 367–371.
80. Ray, K. (2014). From fission to fusion: A perspective on the research that won the Nobel Prize in Physiology or Medicine, 2013. *Journal of Biosciences, 39*(1), 3–12.
81. Roy, S., Hochberg, F. H., & Jones, P. S. (2018). Extracellular vesicles: The growth as diagnostics and therapeutics; a survey. *Journal of Extracellular Vesicles, 7*(1), 1–11.
82. Inc, G. V. R. (n.d.). Exosomes Market Size to Reach $2.28 Billion by 2030 | CAGR: 18.8%: Grand View Research, Inc. Retrieved October 2, 2021, from https://www.prnewswire.com/news-releases/exosomes-market-size-to-reach-228-billion-by-2030%2D%2Dcagr-188-grand-view-research-inc-673089403.html.
83. Price, C. P. (2001). Regular review: Point of care testing. *BMJ, 322*(7297), 1285–1288.

Nano-biosensors for Diagnosing Infectious and Lifestyle-Related Disease of Human: An Update

Somrita Padma, Pritha Chakraborty, and Suprabhat Mukherjee

Abstract

At present time, a variety of infectious and lifestyle diseases are becoming life-threatening day by day. Development in technology and immergence of nanoscience helped to provide a better health care system. Based on the working mechanism nano-biosensors are of majorly two types: electrochemical nano-biosensor and optical nano-biosensor. Nanomaterials used in the nano-biosensor increased their efficacy, sensitivity, and selectivity of the device. Different diseases have different biomarkers to get detected such as, absorption of cholesterol oxidase detect cholesterol, glaucoma in a diabetes patient is detected by cytokine Interleukin 12 in tear, C-reactive protein is detected for liver inflammation, the SARS virus is detected by N-protein and miRNA is a potential biomarker of cancers, especially colorectal cancer. Hitherto, identification of a biomarker for a specific disease is the major work. The accuracy of nano-biosensor in diagnosing diseases put them in demand in the biomedical field. But the major drawback comes with the cost-effectiveness and use of nanomaterial in health sectors focussing on any toxicological impact of the nano-biosensor on health in long run. In this chapter, we present an overview

Authors Somrita Padma and Pritha Chakraborty contributed equally to this work.

S. Padma · P. Chakraborty
Integrative Biochemistry and Immunology Laboratory, Department of Animal Science, Kazi Nazrul University, Asansol, India

S. Mukherjee (✉)
Integrative Biochemistry and Immunology Laboratory, Department of Animal Science, Kazi Nazrul University, Asansol, India

Department of Animal Science, Kazi Nazrul University, Asansol, India
e-mail: suprabhat.mukherjee@knu.ac.in

G. Dutta (ed.), *Next-Generation Nanobiosensor Devices for Point-Of-Care Diagnostics*, https://doi.org/10.1007/978-981-19-7130-3_4

of the working mechanism of different nano-biosensors in diagnosing different infectious and lifestyle diseases.

Keywords

Infectious disease · Lifestyle-related disease · Nano-biosensor · Biomarker · Electrochemical nano-biosensor · Optical nano-biosensor

Abbreviations

AD	Alzheimer's Disease
ADP3	Alzheimer's disease peptoids
AMP	Antibody-Mimic Proteins
Apo	Apolipoprotein
Aβ	Amyloidβ
ChOx	Cholesterol oxidase
CMOS	Complementary Metal Oxide
CNTs	Carbon nanotubes
CRC	Colorectal Cancer
CSF	Cerebrospinal fluid
Cu-CD	Cu-Carbon Dot
SARS	Severe Acute Respiratory Syndrome
DP	Dopamine
EDC	N-ethyl-N-(3-dimethylaminopropyl) carbodiimide hydrochloride
EIS	Impedance Spectroscopy
ELISA	Enzyme-Linked Immunoassay
FET	Field-Effect Transistor
Fn	Fibronectin-based protein
HCFA	Hypoxia-activatable and cytoplasmic protein-powered fluorescence cascade amplifier
HE4	Human Epididymis Protein 4
IBD	Irritable Bowel Disease
IBS	Irritable Bowel Syndrome
IL-12p70	Cytokine Interleukin 12
MERS	Middle East Respiratory Syndrome
MONp	Metal oxide nanoparticles
MRI	Magnetic Resonance Imaging
MUA	11-Mercaptoundecanoic acid
NFT	Neurofibrillary Tangles
NHS	N-Hydroxysulfosuccinimide
NIR	Near-infrared
NP	Nanoparticle
N-protein	Nucleocapsid protein
OPD	Optical Path Difference

ORR	Optical Ring Resonators
PD	Parkinson's Disease
PfHRP-2	*Plasmodium falciparum* histidine-rich protein-2
POC	Point of Care
QD	Quantum Dot
RA	Rheumatoid arthritis
RIA	Radioimmunoassay
SERS	Surface-Enhanced Raman Spectroscopy
SiNW	Silicon Nanowire
SN	Substantia Nigra
SPR	Surface Plasmon Resonance
SPRi	Surface Plasmon Resonance Imaging
SPs	Surface Plasmons
LRET	Luminescence Resonance Energy Transfer
TIRF	Total Internal Reflection Fluorescence
UCL	Ulcerative Colitis
ZnS	Zinc sulfide

1 Introduction

The biological world has dynamic environmental developments and alteration in homeostasis. However, these changes need to be detected hence, the biotechnological industry comes into play. Nanotechnology has opened the horizon for the development of nano-biosensors consisting of biological recognition molecules to detect different classes of diseases. But this nanoscience-based technology is not a newborn, it was developed with the discovery of atom, but the concept of nanotechnology was first introduced by Nobel laureate Richard Feynman in 1959. He made a hypothesis, "Why can't we write the entire 24 volumes of the Encyclopedia Britannica on the head of a pin?" and gave an idea to develop smaller machine work at the molecular level [1]. After the hypothesis got proved, Japanese scientist Norio Taniguchi, coined the term "Nanotechnology" in 1974. It defines an analytical instrument combining a suitable physical converter with a bioactive element to generate a quantifiable signal directly proportional to the number of analytes present in any kind of biological sample using nanomaterial. Nanoscaled biosensors are developed with exceptional sensitivity and adaptability [2]. The unique physical, chemical, mechanical, magnetic, and optical features of nanomaterials increase their efficacy as compared to biosensors. Biosensors are combined with nanomaterials including carbon nanotubes (CNTs), gold nanoparticles, quantum dots, and magnetic nanoparticles to provide a larger surface area for the analytes to complete a reaction [3].

Due to the collective oscillations of metal conduction band electrons in strong resonance with visible-light wavelength, gold nanoparticles exhibit a significant absorption band in the visible range, which is known as surface plasmon resonance [3]. The benign, plentiful, low cost, low toxicity, and strong bioactivity of C-dots are advantageous for applications in bioimaging, biosensors, and drug administration due to their outstanding features such as low toxicity and strong bioactivity [4]. Carbon Nanotubes can attain excellent electrical conductivity and mechanical characteristics, opening up the tantalizing prospect of building ultrasensitive, electrochemical biosensors [5, 6]. The special magnetic properties of magnetic nanoparticles are broadly used in applications like magnetic resonance imaging (MRI) contrast agent, hyperthermia, tissue repair, immunoassay, cell separation, and GMR-sensor [7–9]. The overall purpose of nano-biosensors is to identify any physicochemical and biological signal linked to a specific disorder at the single-cell or molecular level. These nanostructures of nanomaterial used in nano-biosensor, have the ability to recognize a wide range of chemicals via biorecognition processes. It has proved to be a useful tool for the quick and sensitive assessment of infections, abnormalities, drug screening, genetic disorders, and other in vitro screening applications [10]. As a result, the utilization of nanomaterials in biosensors with various compositions, combinations, and nanostructures allowed for rapid diagnosis with greater accuracy [10].

In recent times, a busy schedule results in an unhealthy life with a high incidence of various infectious and inflammatory diseases hindering human longevity. Nanoscience came as a blessing to modern medical science in the form of nano-biosensor. By employing nanomaterials to develop new signal transduction technologies, it has opened a wide field to researchers [11, 12]. Nano-biosensors could be divided into different types as an electrochemical biosensor in which a gold nanoparticle is employed to detect glucose levels in the blood as well as a graphene-based biosensor, which is used in different sensing devices [13]. Nano-biosensors are also specific in detecting diseases based on biomarkers. There is a large variety of biomarkers present for different diseases. The selection of a proper biomarker for the diagnosis of diseases is posing a greater challenge to the researchers.

Several applications of nanotechnology include disease diagnosis, monitoring, treatment, and drug designing [14, 15]. Nano-biosensor is also used in delivering drugs in the human system, also referred to as “nanomedicine” [16]. Utilization of nanometer-scaled particles in tissue implant engineering increased the surface area which helps in better responses and effective tissue-implantation mechanism [17]. Their uses include microbe identification in diverse samples, metabolite tracking in bodily fluids, and diagnosis of tissue diseases such as cancer. Besides the biomedical application, nano-biosensors are used broadly in the field of food packaging, tracking, and safety as well as environmental analysis [18]. Nano-biosensor is tremendously efficient in working with a minimum concentration of analytes. In this book chapter, we are discussing about the mode of working of different nano-biosensors and their application in the biomedical field as depicted in Fig. 1.

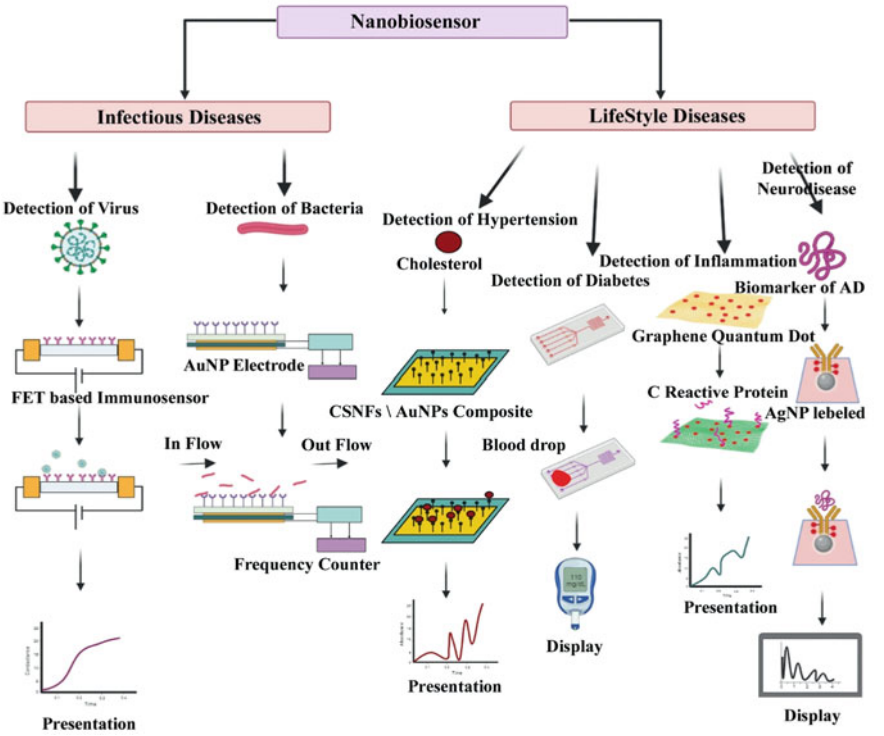

Fig. 1 Different types of Nano-biosensor applied in the biomedical field. Nano-biosensors are used in the diagnosis of infectious and lifestyle diseases. FET-based Immunosensor is used to detect virus pathogens as well as bacterial pathogens could be detected by AuNP-based piezoelectric biosensor. Nano-biosensor is also used in the diagnosis of lifestyle diseases like diabetes, hypertension, inflammatory diseases, and neurological disorders. CSNFS/AuNP composite network is used to detect cholesterol levels in blood-related to hypertension and an electrochemical chip sensor is used to detect glucose levels from a drop of blood. Graphene Quantum Dot is used to identify C-reactive protein, a biomarker of inflammatory diseases. Different types of specific biomarker are present for different neurological disorders. They could be diagnosed by biomarker-specific AgNP labeled antibody electrochemical biosensor

2 Design of Nano-biosensors

Diseases-associated biomolecules including, proteins, pathogens, nucleic acids, disease-specific metabolites, and circulating tumor antigens need to be detected for the diagnosis of diseases in the clinical setting as well as for biomedical research resulting in drug discovery and development. Nanotechnology has powered the nano-biosensors with high-affinity recognition probes of biological components and a transducer to rapidly improve the biodiagnostic capacity [19]. Nano-biosensors are used in the identification of different types of biochemical and molecular parameters in a biological system by converting the biochemical,

chemical, or biological signal into an electrical or optical signal that could be displayed easily.

Human health needs to be monitored for early detection of ailing conditions or disorders to maintain a healthy life. Hence, different biomolecules within the human system also known as biomarkers are detected for interventions. Nano-biosensors provide rapid analysis, active monitoring, data generation, processing, and data manipulation. A nano-biosensor consists of three parts: a bioreceptor for receiving a signal; a transducer that converts the signal into optical, electrochemical, piezoelectric, electronic, or gravitimetric; and an electronic unit that would amplify, process, and display the converted signals [20]. Depending on different technologies, nano-biosensors are categorized into different groups: electrochemical, acoustic wave, nanowire, and nanotube-based sensors [12]. In an acoustic wave nanosensor, a wave is generated in several anisotropic materials that have the potential to convert electric signals into mechanical motion [21]. The difference in the charge density causes variations in the electric field at the nanowire's external surface, based on this principle nanowire-based biosensors could sense different biological parameters [22]. Nanotubes in a biosensor serve as scaffolds for immobilization of biomolecules, and their properties, allow for signal transduction, and aided in the recognition of disease biomarkers and analytes. The working mechanism of the nano-biosensor divides it into two categories of electrochemical and optical nano-biosensor [20, 23]. Nanomaterials are also used in developing nanoelectrode. Graphene, graphene oxide, carbon nanotubes, diamond, carbon nanofibers, ZnO nanofibers, conductive polymers such as polythiophene nanofibers, Pt–Au nanoparticle-decorated titania nanotube array, boron-doped diamond nanorods, and gold nanofiber electrodes are some of the biosensing materials used in biosensor [21]. Gold nanoparticle-modified electrodes also demonstrated a considerably broader pH adaptable range and bigger reaction currents in detecting H_2O_2 level, which is a biomarker of oxidative stress in the human body [3].

Nanotechnology is merged with biosensors to lay the foundation for developing nano-biosensors. Particular kind of nanomaterials used in the development of biosensor depends on biosensing applications. Nano-biosensors can be classified based on the nature of nanomaterials incorporated in the application of biosensing. However, the classification can be done either on the basis of signal transduction or on the basis of the type of material to be analyzed. The fabrication of nano-biosensor is categorized into two parts depending on speed, quality, and cost which are top-down approach and bottom-up approach. The breaking of bulk material into nanomaterial is known as top-down approach. During the production process, precision engineering technology played a major role and the performance could be improved by the use of nanosized-based diamond or cubic boron nitrate and sensors for controlling size, numerical number, etc. [4]. The bottom-up approach is known to build nanomaterial by assembling atom–atom or molecular–molecular by physical and chemical methods that are in the nano range (1–100 nm) [4, 24–26].

Biosensor technology advancements have primarily focused on meeting analytic requirements in the treatment of various diseases, as well as other applications such as environmental protection. An electrochemical nano-biosensor helps to determine

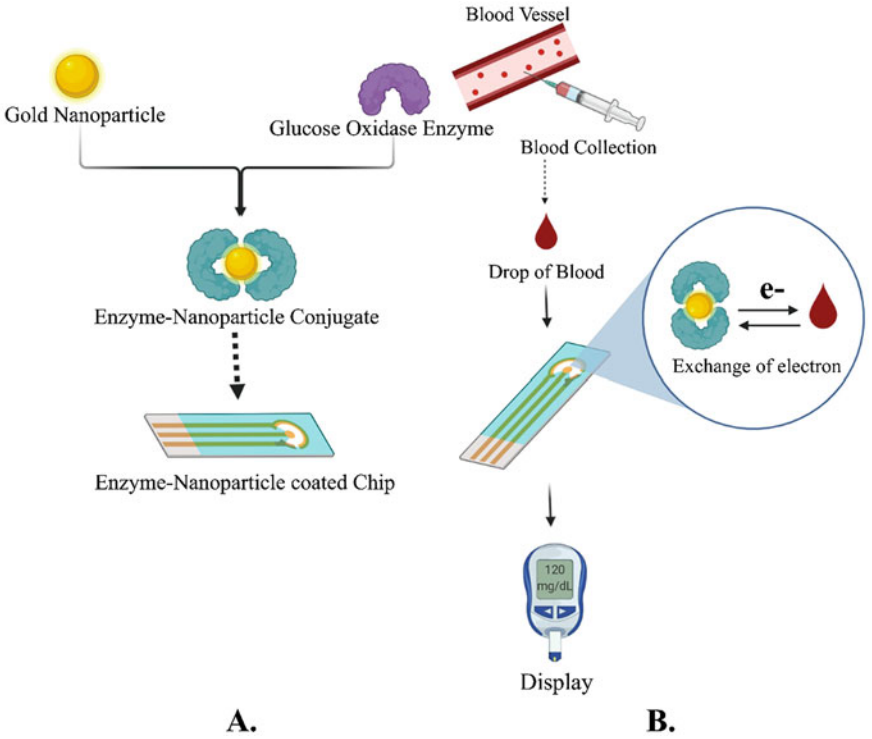

Fig. 2 Working mechanism of electrochemical nano-biosensor. (**a**) Gold NP is conjugated with glucose oxidase enzyme and an electric chip is coated with the enzyme–NP conjugate. (**b**) Exchange of electron occur between the blood, collected from the blood vessel and the enzyme–NP conjugate coated on the electric chip through a chemical reaction

the degree of a patient's condition or to monitor the patient's behavior in post-therapy and intervention. The first step is based on the interaction of a bioreceptor and an analyte. Any biological entity, generally live-derived such as proteins as antibodies, glycans, and nucleic acids coupled to an electrode conjugated with a nanosized substance or nanomaterial. Whenever the analyte is detected, physiological or chemical alterations occurred on the transducer's sensing surface, which is processed as a quantifiable signal in a concentration-dependent way [27]. Electrochemical biosensors are able to assess changes that occurred in the electrochemical characteristics of transducers, such as electron transfer and charge deposition. In this nano-biosensor, nanomaterials such as nanoparticles, graphene, carbon dots, and carbon nanotube are used in coating the working electrode, where the receptor–analyte interaction occurs [28, 29]. The electrochemical signal produced from an enzyme-catalyzed oxidoreductive reaction is displayed as shown in Fig. 2 and based on this principle the widely used, glucose oxidase-based nano-biosensor is

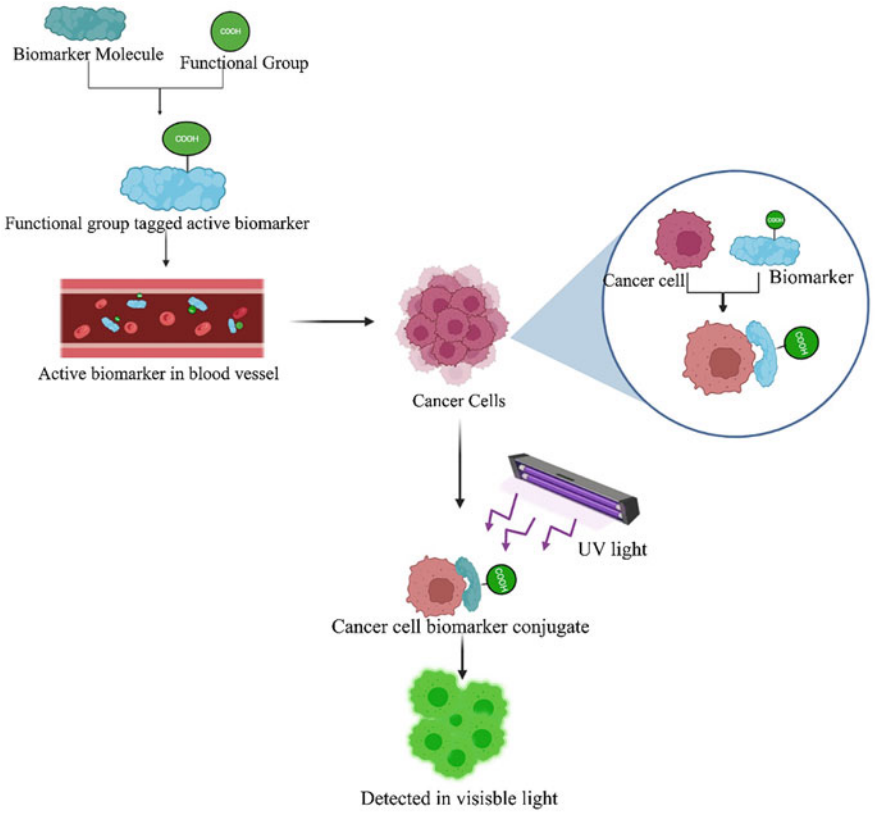

Fig. 3 Working mechanism of optical nano-biosensor. A functional group is tagged with the biomarker molecule and activated it. The activated biomarker is released in the bloodstream and gets attached to the cancer cell. This attachment causes some conformational change in biomarker and after absorbing UV light the whole conjugate gets visible

developed [30]. Later some other enzymes such as polyphenol oxidase is also used in some nano-biosensor for detecting the enzymatic reaction [31–33].

Optical nano-biosensors sense analytes ranging from tiny to big molecules, including proteins, using both labeled and label-free signal transduction technologies [34]. Fluorophores, nanoparticles, quantum dots, and carbon nanotubes are all used and as labeling technology or label-free technology to detect refraction [35]. Based on the optical and luminescent characteristics of nanomaterials, as well as surface plasmons (SPs) and luminescence resonance energy transfer (LRET) effects, optical nano-biosensors are designed as described in Fig. 3 [36]. LRET is a technique by which energy is transmitted from the donor to the receiver via resonance interaction, which leads to a decline in the luminescence intensity of the donor, and the luminescence intensity of the receiver get increased [36]. LRET-based nano-biosensor detect the analytes by manipulation of spectrum overlap and proximity between donor and acceptor [37]. The earliest optical sensor was the total

internal reflection fluorescence (TIRF), later some other optical sensors like, photonic crystals, surface plasmon resonance (SPR), and optical ring resonators (ORR) are developed. [20]. The detection technique of SPR is associated with the change in the local refractive index generated by adsorbed analytes, which alters the resonance conditions of surface plasmon waves [36].

The modification of the hybrid structure's optical and electrical properties by inserting suitable functional groups or equivalents is highly interesting for rapid and simple disease diagnosis [38]. Some of the nano-biosensors work in both working principles, as they are capable to use both electrochemical and optical properties, such as Cu-Carbon Dot (Cu-CD). Thiol is a very important component in a biological system, depending on that Thiol Nanosensor is developed using the properties of Cu-CD as both an optical and an electrochemical detection device. Thiols specifically, systematically, and intensely inhibited the electrochemical peak of Cu-CDs because of strong electrostatic contact and covalent bonding between the NH_2 functional groups of the Cu-CDs and the -SH groups of thiols [39]. Whereas the blue photoluminescence emission of Cu-CDs rose significantly due to the separation of Cu ions from the margins of Cu-CDs in the presence of thiols. The emission could be visible in a transmission electron microscope, photoluminescence, and X-ray photoelectron spectroscopy scanning [39].

3 Clinical Application of Nano-biosensors

With the advancement in our research, some limitations also raise concerns regarding good quality of living. Herein prevention of a diseases outbreak, whether communicable or non-communicable, is the most appropriate means for survival. Applications of nano-biosensors have been highly versatile, endless, multifactorial, and involved in managing and monitoring different infectious and inflammatory diseases.

3.1 Application of Nano-biosensors for the Diagnosis of Infectious Diseases

Pathogens like bacteria, fungus, parasites, and viruses have been reigning the living organisms for over a hundred years resulting in the death of both humans and animals globally. Around, one-third of the infectious deaths are caused by *Escherichia coli* (*E. coli*) and *Staphylococcus aureus* (*S. aureus*) bacteria. Viruses like Severe Acute Respiratory Syndrome (SARS), Middle East Respiratory Syndrome (MERS), and Zika virus have impacted the population severely leading to the high mortality rate in the past years [40]. Among all the pathogens, viruses are the intracellular parasites that can create havoc in the population. As we know, SARS-CoV-2 has created a high surge in infection as well as death waves with an urgent need for detection methods to control the spreading of the diseases. Traditional methods of detection are efficient but time consuming and are limited due to the

varying sizes of the pathogen. Thus, the need of the hour is cost-effective, efficient, and time-saving nano-biosensors for effective management of disease progression, and evaluation of epidemic or pandemic situations focusing on detection of bacterial, fungal, parasitic, and viral pathogens to prevent the coercion of epidemic and pandemics [40].

Healthcare management solely relies on providing better healthcare which can be achieved by optimum standards of medical facilities, timely decisions, and rapid diagnosis with smart and informatics data analysis [41]. To achieve better results, smart therapeutic tools and diagnosing systems can enhance the wellness of healthcare. Biosensing technology has become an integral part of detection and diagnosis in which nanotechnology holds the potential to detect and treat different infectious diseases rapidly with ease, utmost accuracy, and inexpensively [42].

Detection of Viral Pathogens

Viral pathogens, like SARS-CoV-2, are identified based on their antigenic determinants, using a FET-based immunosensor. The antigen–antibody interaction generates a conductance based on the concentration of the viral pathogen by using antigen nucleocapsid protein (N-protein) [43]. Fibronectin-based protein (Fn) is engineered in vitro as antibody-mimic proteins (AMP) act as bioreceptors that capture the antigen of the viral pathogen. FET-based immunosensor is modified with In_2O_3 nanowires on a Si/SiO_2 substrate which improves the signal transducing and immobilized the AMP. Higher sensitivity and selectivity are achieved by the synergic effect of the In_2O_3 nanowires/Fn protein, which detects the SARS biomarker N-protein [44]. Also, another nano-immunosensor detects MERS-CoV amperometrically. It is based on indirect competition between the free virus and immobilized MERS-CoV recombinant spike protein S1. AuNPs are added to carbon electrodes to enhance the electrochemical properties resulting in a faster electron transfer rate with higher surface area and improved detection capacity. By using the drop-casting procedure, viral antigens are immobilized onto AuNPs followed by incubation. Results showed linear responses with high sensitivity as compared to ELISA. HIV subtypes are captured on the biosensing surface by modifying antibody layers. Polystyrene surfaces conjugated with AuNP were modified by poly-L-Lysine to generate amino groups. Coupling was performed by NeutrAvidin, 11-mercaptoundecanoic acid (MUA), biotinylated anti-gp120 polyclonal antibody, N-ethyl-N-(3-dimethylaminopropyl) carbodiimide hydrochloride (EDC), and N-hydroxysulfosuccinimide (NHS). After the HIV capture, spectral analysis was performed to analyze the point of care (POC) [45].

Detection of Bacterial Pathogens

Low-cost nano-biosensor for the detection of *Mycobacterium tuberculosis* has been a challenge so far in the healthcare industry, but still, piezoelectric sensor based on AuNPs is combined with aptamer technology to detect MTB. Though it has a limitation in detecting more than 100 CFU/ml [46]. Also, silicon nanowire-based nano-biosensor (SiNW) with field-effect transistor (FET) is conjugated with antigen 85 (Ag85B) to detect MTB and tuberculosis following antigen–antibody immune

reaction [47]. To enhance the detection of MTB Ag85 protein, noninvasively, sputum collected containing water and solids from peripheral airways and alveolar chambers. It is subjected to SiNW-FET combined with traditional complementary metal oxide (CMOS) to detect MTB in an actual environment.

Detection of Other Pathogens

Nanoscience and nanotechnology have led to the development of nanomaterials of which *Plasmodium falciparum* histidine-rich protein-2 (PfHRP-2) antigen can be detected with the presence of very low as 0.01 ng/ml using carbon nanofibers attached to glass microballoons [48]. Metal oxide nanoparticles (MONp) are deposited on the gold electrodes for the detection of β-Hematin biomarker and *Salmonella typhi* antiserum VI found in clinical samples of malaria and typhoid. β-Hematin and antiserum VI is electrocatalyzed on Au-electrode modified with CuONp providing high electrochemical stability in the analytes and better signal separation during detection between malaria and typhoid biomarkers [49]. Different nano-biosensors have been currently in use for the detection of different pathogens as mentioned in Table 1.

3.2 Nano-biosensors Used in Lifestyle Diseases

Globalization advancements with economic developments are increasing the prevalence of lifestyle diseases. It has been a major public health problem affecting a larger population since it is primarily attributed to a person's daily life. It increases the risk of different diseases related to our regular lifestyle such as hypertension, diabetes, and gut-related inflammatory disorders.

Detection of Diabetes and Hypertension

Diabetes is also known as the "silent killer" which can be a serious health issue of this century. Our regular busy life is drowning in stress, irregular food habit, and consumption of packaged food making us a patient suffering from diabetes and hypertension. Severe consequences are followed by increasing levels of blood sugar including blindness, heart disease, and neurological disorders that can be life threatening. Hence, detection, as well as diagnosis, is very important. This can be achieved using a drop of blood onto an electrochemical biosensor with disposable screen-printed electrodes [20, 70]. An enzyme namely, Glucose Oxidase converts glucose into glucuronic acid through an electrochemical reaction. Clark et al. [71] first developed a biosensor using this catalytic affinity property to detect diabetes. Recent studies proposed the concept of nanorobots in the bloodstream for monitoring the sugar level in diabetic patients. The nanorobot detects the biochemical changes in patient blood by using proteomics-based information [72]. However, noninvasive monitoring techniques such as microcalorimetry, enzyme-fabricated electrodes, sonophoresis, and near-infrared (NIR) spectroscopy have been known to be successful in detecting even a little amount of glucose in body fluids [73, 74]. Also, diabetes could be monitored by the presence of glucose in the tear of a

Table 1 Nano-biosensors as a detection tool for different infectious diseases

Sl. no.	Diseases category	Pathogen	Diseases	Nano-biosensor	Biomarker and source	References
1.	Viral	SARS-CoV-2	COVID-19	Graphene FET-based immunosensor	Antigen spike protein S1, SARS-CoV-2 nucleic acid, Nasopharyngeal swab, blood	[44]
2.	Viral	HIV	AIDS	Nanostructured Optical Photonic Crystal Biosensor	sTNFR-1, sTNFR-2, hsCRP, D-dimer, sCD27, IP-10, sCD14, and hyaluronan, Plasma	[45]
3.	Viral	MERS-Cov	Middle East respiratory syndrome	Amperometric Immunosensor	Virus spike protein S1	[50]
4.	Viral	Rotavirus	Diarrheal disease	Graphene oxide-based electrochemical nano-biosensor	CRP, citrulline, kynurenine, tryptophan ratio, soluble CD14, neopterin and myeloperoxidase, plasma, stool	[51]
5.	Viral	*Dengue* virus	Dengue fever	Carbon nanotube-based electrochemical biosensor	*Dengue nonstructural protein 1 (NS1)*	[52]
6.	Viral	Zika virus	Zika virus disease	IDE-Au-based electrochemical immunosensor	Elevated levels of pro-inflammatory cytokines IL-1β, IL-6, TNF-α, IFN-g, and IL-17, chemokine CXCL8, CCL11, CCL3, CCL4, CCL2, CCL5, CXCL10, and growth factors FGF-basic, PDGF, VEGF, G-CSF, and GM-CSF, serum	[53, 54]
7.	Bacterial	*Mycobacterium tuberculosis*	Tuberculosis	Silicon nanowire field-effect transistor (SiNW-FET) biosensor	MTB, DNA, lipoarabinomannan, blood, urine	[47]
8.	Bacterial	*Mycobacterium simae*	Pulmonary disease	DNA-based label-free electrochemical biosensor	*M. simiae* ITS sequence	[55]
9.	Bacterial	*Salmonella typhi*	Typhoid	Metal oxide nanoparticles (MONp) deposited on Au-electrode	*Salmonella typhi* antiserum VI	[49]
10.	Bacterial	*Vibrio cholerae*	Cholera			[56, 57]

				Golden-graphene nanoparticles-based electrochemical biosensor	Myeloperoxidase, alpha-anti-trypsin, endotoxin core antibody, intestinal fatty acid binding protein, stool, plasma	
11.	Protozoa	*Plasmodium falciparum*	Malaria	Metal oxide nanoparticles (MONp) deposited on Au-electrode	β-Hematin biomarker	[49]
12.	Protozoa	*Plasmodium falciparum*	Malaria	Carbon nanofibers attached to glass microballoons	*Plasmodium falciparum* histidine-rich protein-2 (PfHRP-2) antigen	[48]
13.	Fungal	*Candida albicans*	Candidiasis	Localized surface plasmon resonance optical sensor	*Candida albicans* germ tube antibody, mannan antigen, anti-mannan antibodies, blood	[58, 59]
14.	Fungal	*Cryptococcus neoformans*	Cryptococcal meningitis	Immunosensor	Cryptococcal capsular antigen	[60]
15.	Parasitic	*Plasmodium vivax*	Malaria	Metal oxide (MO) nanoparticles-based electrochemical biosensor	β-hematin, *Plasmodium* 18S rRNA, blood	[61, 62]
16.	Parasitic	*Wuchereria bancrofti*	Lymphatic filariasis	Silver nanoparticle-based electrochemical biosensor	Raised levels of IL-6 and IL-8, serum	[62, 63]
17.	Parasitic	*Leishmania donovani*	Leishmaniasis	Gold nanoparticle-based electrochemical immunosensor	EGF/TFGbta1 ratio	[64, 65]
18.	Parasitic	*Ascaris lumbricoides*	Ascariasis		2-methyl pentanoyl carnitine, urine	[66]
19.	Parasitic	*Giardia* lamblia	Giardiasis	Gold nanoparticle-based label-free plasmonic DNA biosensors	Acetic acid, 1,4-dimethoxy-2,3-butanediol and 1,3-dimethoxy-2-propanol	[67, 68]
20.	Parasitic	*Entamoeba histolytica*	Amebiasis		Jacob2	[69]

glaucoma patient [75]. One putative biomarker is the cytokine Interleukin-12 (IL-12p70) since current findings indicated that the average content of IL-12p70 in tear film was considerably lower in patients with primary open-angle glaucoma than in a normal person [76]. A soft contact lens-based sensor is used to monitor the glucose level by detecting the IL-12p70 biomarker in a glaucoma patient. The optically reflected signal from the nanopore thin-film sensor integrated into the contact lens is used to measure IL-12p70 [77, 78]. The attachment of the biomarker to the sensor's nanoporous surface causes a change in the Optical Path Difference (OPD) [75]. Diabetes can also affect arteries and causes a condition known as atherosclerosis, which is one of the prime reasons for hypertension like comorbidity.

Moreover, diagnosis of cholesterol in serum samples at early stage could prevent a wide number of clinical disorders including hypertension. An amperometric cholesterol nano-biosensor could detect cholesterol on basis of the absorption of cholesterol oxidase (ChOx) onto the chitosan nanofibers–gold nanoparticles, designated as CSNFs/AuNPs composite network [79]. Hypertension could be detected by a decrease in the fluidity of plasma membrane of the erythrocyte and a decrease in mobility of membrane-bound heme. Silver nanoparticle-based biosensor Surface-Enhanced Raman spectroscopy (SERS) can detect the change in erythrocyte and act as a biomarker of hypertension in the blood. A study has shown that hypertension could also lead to dysbiosis in the gut by increasing lactic acid-producing bacteria and decreasing acetate and butyrate-producing bacteria [79]. Some environmental, genetic, and dietary factors are common in both hypertension and diabetes that aid dysbiosis in the gut.

Detection of Inflammatory Disease

Our busy schedule, workload, physical and mental stress, and intake of fast and processed food, increases the bad or pathogenic microbes in our gut, known as gut dysbiosis. This type of disturbance in the colony of gut microbes leads to life-threatening diseases like, irritable bowel syndrome (IBS), irritable bowel disease (IBD), and Ulcerative Colitis (UC), which may end up in Colorectal cancer (CRC) [80]. Karban et al. [81] proposed a chemical nano-biosensor based on programmable molecularly modified gold nanoparticle for the detection and separation of IBS and IBD. Headspace gas chromatography in conjunction with a chemiresistive metal oxide gas sensor was used to construct a stool analysis technique [82]. A hypothesis proposed that 5-aminosalicylic acid-SiO_2 NPs had a targeted drug dissolution strategy that targets the inflammatory colon and UC characteristics, and that they might considerably increase the efficacy of treatment in UC [83]. Early detection of inflammatory bowel disease with great sensitivity can prevent CRC progression, minimizing the risk of metastasis. Gold nanoparticle, silver nanoparticle, quantum dot, etc. based biosensors are used in detecting miRNA biomarkers of different cancers, especially CRC [84].

Besides gut inflammation, some other inflammatory diseases are also becoming life threatening. It is necessary to diagnose those diseases to get time to apply some therapeutics. C-reactive protein is a biomarker of liver inflammation thus, Lv et al. [85] have developed a new quantum dot-labeled immunosorbent technique for fast

C-reactive protein detection. Cytokine or chemokines are well-established indicators for lung inflammation that could be detected by an iron/iron oxide nanoparticles-based optical biosensor [86].

Detection of Cancer

Cancer is one of the most recorded causes of death in today's world, among which breast, colorectal, ovarian, lung, and prostate cancers are at the top of the list [87]. Cancer is triggered by genetic factors as well as environmental factors like pollution, usage of chemical compounds, radiation, and smoking [87]. As suggested by different reports, gut dysbiosis can be a causative factor in some life-threatening diseases like CRC and cervical cancer. Therefore, the diagnosis of cancer plays a crucial role at an early stage to expand the life span. Nanosized (around 1–100 nm) particles or nanoparticles (NP) that are used as a biomarker in a biosensor have microlevel sensitivity. Grimm et al. [88] developed a nano-biosensor using magnetic NP, which could detect elevated telomerase activity which is known to play a crucial role in tumorigenesis and malignancies. This NP changed the magnetic state of the telomeric repeats synthesized by telomerase, which could be detected easily by the magnetic readers. In photodynamic therapy, cytochrome *c* is used as a biomarker to detect human breast cancer MCF-7 cell lines. After activation of photodynamic therapy by He-Ne laser beam, cytochrome c start releasing in the cytoplasm of the cancer cell line, which could be monitored using an optical nano-biosensor [89]. Nano-biosensor conjugate with different immunoassay such as RIA (radioimmunoassay) and ELISA (enzyme-linked immunoassay) to increases the limit of sensitivity to detect cancer from both inside and outside of the cell because of enzymatic amplification [89]. Studies on nano-biosensor emphasized several genomic modified technologies that could be utilized in rapid detection, therapeutic, and monitoring of any kind of cancer in the human body [90, 91]. Williams et al.[92] addressed the development and testing of a carbon nanotube-based optical sensor for the ovarian cancer protein biomarker human epididymis protein 4 (HE4). They observed that the sensor can detect HE4 in patients' serum samples at meaningful biomarker quantities in the case of an ovarian cancer patient [92]. Overexpression of HE2 in a breast cancer cell is detected in a patient by an electrochemical nano-biosensor directly in blood fluid [93]. The sensor of the nano-biosensor was made by immobilizing anti-HER2 onto a nanoconducting surface, and the signal was acquired using a unique bioconjugate of hydrazine-gold nanoparticle aptamer, where the hydrazine operated as an electrocatalyst and the aptamer as a sensor molecule [87]. In these methods, even ultrasensitive cancer cells can also be detected by the nano-biosensor device.

Detection of Neurological Disorders

Protein misfolding disorders or neurological disorders including Parkinson's disease (PD), Alzheimer's disease (AD), brain stroke, epilepsy, and encephalitis can be detected using nano-biosensors [94]. From the past evidence, apolipoprotein (apo) plays a critical role in AD. Whereas, apoE4, a polymeric lipid-binding protein variant act as a biomarker in AD. Amyloidβ (Aβ) is an amphipathic peptide of

42 residues long and is a known biomarker of AD. Insoluble fibrillar Aβ42 accumulated on neurons has the potential to destroy neural circuits. Surface Plasmon Resonance Imaging (SPRi) is used to quantitatively measure Aβ42 levels in the blood by gold-coated glass chips created on Alzheimer's disease peptoids (ADP3) [95]. ADP3 is able to identify Aβ42 present in a high concentration as well as in a low concentration [94]. The transmitted signal that is displayed could be increased by using Quantum Dot (QD) nanomaterial at the place of the gold nanoparticle [96]. AD could be detected through an electrochemical nano-biosensor also, by a biomarker, Tau protein, which is the key component of the pathological infection of AD. Excessive or aberrant phosphorylation of tau in CSF(Cerebrospinal fluid) converts the healthy neurofilaments into coupled helical filament-tau and neurofibrillary tangles (NFT), which are considered toxic to neurons [97, 98]. This Tau protein has an affinity to a gold nanoparticle. Depending on these characteristics a nano-biosensor is developed, which monitors the binding reaction of the Tau by Electrochemical Impedance Spectroscopy (EIS) [99]. PD is a chronic neurodegenerative illness defined by the loss of dopaminergic neurons in the Substantia Nigra (SN) area of the brain, resulting in pathological changes like tremors, stiffness, and postural instability [100]. Clinical characteristics of PD include 50–70% neurodegeneration in the SN area, the neuronal aggregates consisting of α-synuclein protein, which is found in Lewy bodies and neurite, combinedly known as "Lewyneurites"[101]. Studies revealed that in presence of metallic ions changes in the morphology of α-synuclein occur, due to defective regulation and misfolding patterns, which causes neuronal toxicity [102]. A single gene mutation in the α-synuclein gene, dopamine (DP), Tau gene is the potential cause of pathogenesis of PD [103]. The accumulation of the protein α-synuclein may be identified in a precise, label-free manner by employing MEMS cantilevers [75]. QD is used to detect DP, which is a potential biomarker of PD. Zinc sulfide (ZnS) coated with QD participates in a coupling reaction in presence of ascorbic acid, in which QD is replaced with L-cysteine. DP is detected by the emitted fluorescence by cysteine-capped ZnS-QD [104].

Detection of Other Diseases

Odontogenic ameloblast-associated protein is a potential biomarker for periodontitis disease [20]. Loosing of teeth in periodontitis is associated with oral cancer. Detection and treatment of periodontitis in early stage, by aptamer-based biosensor, could inhibit future cancer. Rheumatoid arthritis (RA) patients could be identified by a graphene-based nano-immunosensor and a zinc oxide nanorod-based sensor with an immobilized biomarker, anti-cyclic citrullinated peptide [20]. Monitoring of hypoxia and differentiating its various cellular levels could be possible by hypoxia-activatable and cytoplasmic protein-powered fluorescence cascade amplifier (HCFA) fluorescence imaging [20]. All these types of diseases are detected by different biomarkers listed in Table 2.

Table 2 List of biomarkers and nano-biosensors to detect lifestyle diseases

Sl. no.	Disease	Nano-biosensor	Biomarker	References
1.	Diabetes and glaucoma	Disposable screen printed electrodes, nanorobot, microcalorimetry, enzyme-fabricated electrodes, sonophoresis, and NIR spectroscopy	Glucose oxidase, IL-12p70	[20, 70, 73, 74]
2.	Hypertension	Chitosan nanofibers-gold nanoparticles composite network, Silver nanoparticle-based biosensor Surface-Enhanced Raman spectroscopy	Cholesterol oxidase, fluidity of plasma membrane of the erythrocyte	[8, 12, 15, 37]
3.	Liver inflammation	quantum dot-labeled immunosorbent	C-reactive protein	[85]
4.	Lung inflammation	Iron/iron oxide nanoparticles-based optical biosensor	Cytokines and chemokines	[86]
5.	Gut inflammation	chemical nano-biosensor based on the programmable molecularly modified gold nanoparticle, 5-aminosalicylic acid-SiO_2 NPs	C-reactive protein	[81, 83]
6.	Cancer	Magnetic Np-based biosensor, optical nano-biosensor, carbon nanotube-based optical sensor	miRNA, telomerase, cytochrome C, HE4, HE2	[88, 89, 92, 93]
7.	Alzheimer's disease	Gold-coated glass chips on ADP3, electrochemical nano-biosensor, electrochemical impedance spectroscopy	Aβ42, apoE4, Tau protein	[94, 95, 97, 99]
8.	Parkinson's disease	Cysteine-capped ZnS-QD fluorescence	α-Synuclein, dopamine	[104]
9.	Rheumatoid arthritis	Graphene-based nano-immunosensor and Zinc oxide nanorod-based sensor	Anti-cyclic citrullinated peptide	[20]
10.	Periodontitis	Aptamer-based biosensor	Odontogenic ameloblast-associated protein	[20]

4 Advantages and Disadvantages

Better quality of healthcare can be achieved with fast and efficient technologies for clinical diagnosis hence, the development of nano-biosensors is the need of the hour for point-of-care diagnostics. In recent years, biosensors conjugated with nanomaterials have risen different practical issues regarding potential applicability to solve real problems. Though there have been many nano-biosensors detecting

different infectious and inflammatory diseases but still not all diseases can be diagnosed. Also, already developed strategies remain complicated due to non-feasible approaches [105]. However, the application of nano-biosensors to different outskirts and rural areas has been also a drawback due to cost and accessibility [106]. Research in nano-biosensors can be considered a thrust area since there is always a scope for developing more better sensors, to monitor, detect, and prevent diseases. Several small start-ups are coming up with various disease detection technologies powered by nano-biosensors but before moving onto a global platform, it is necessary to maintain uniformity and control synthesis to omit device-to-device variability [107]. Upcoming years will have the trends in the miniaturization of biosensors to the nanoscale range to develop more precise detection tools in the healthcare industry. With the use of novel nanomaterials, limitations posed by traditional biosensors can be overcome. Next-generation nano-biosensors have the potential to use new classes of different nanomaterials for sensing purposes and revolutionize the ubiquitous healthcare system.

5 Conclusion and Future Direction

Modern therapeutic tactics necessitate precise diagnosis. With the increasing population, it is very much essential to detect the different ailing conditions and prevent mortality. Several infectious diseases and inflammatory diseases such as diabetes, IBS, and IBD among others are severely affecting our immune system posing a serious threat to human survival every day. In this aspect, the use of an effective nano-biosensor can be an alternative to a healthy life. The utilization of diverse nanomaterial properties in biosensors is evolving as a strengthening technique for long-term sustainability. The selection of an appropriate biomarker and the development of a perfect strategy is the most important criteria for developing a nano-biosensing device. Although a lot of nano-biosensor are working efficiently in the healthcare sector for diagnosing and treatment of many diseases, some lethal diseases are not detectable at their first stage. It is very much important to detect disease at its preliminary stage to provide proper treatment. Nano-biosensor not only aided in diagnosing but also showed their efficacy in therapeutics. Some disease-specific sensors are in high demand. Transcriptional factor-based sensors are still in the embryonic stages of development, although they have shown potential in identifying disease-specific metabolism. In this chapter, a thorough review of the working principle and many applications of nano-biosensor in the medical field for human and animal wellbeing is given. Furthermore, the current research on nano-biosensor can be expanded to produce an effective intervention approach against the continuing COVID-19 outbreak.

Acknowledgments SM acknowledges University Grants Commission (UGC) (Ref no. F.2-12/2019 (STRIDE) and KNU-UGC STRIDE (Ref no. KNU/R/STRIDE/1077/21) and Department of Science and Technology-Science & Engineering Research Board (DST-SERB) (Ref no.-SRG/2021/002605) for supporting his research activities and laboratory through awarding research grants. PC thanks DST, Govt. of India for the award of the DST-INSPIRE fellowship.

References

1. Feynman, R. P. (1960). There's plenty of room at the bottom. *Engineering and Science, 23*, 22–36.
2. Reshetilov, A., Iliasov, P., Reshetilova, T., & Rai, M. (2011). Nanobiosensors and their applications. In *Metal nanoparticles in microbiology*. Springer. https://doi.org/10.1007/978-3-642-18312-6_12
3. Zhang, X., Guo, Q., & Cui, D. (2009). Recent advances in nanotechnology applied to biosensors. *Sensors., 9*(2), 1033–1053. https://doi.org/10.3390/s90201033
4. Bayda, S., Adeel, M., Tuccinardi, T., Cordani, M., & Rizzolio, F. (2020). The history of nanoscience and nanotechnology: From chemical-physical applications to nanomedicine. *Molecules., 25*(1). https://doi.org/10.3390/molecules25010112. MDPI AG.
5. Cui, D. (2007). Advances and prospects on biomolecules functionalized carbon nanotubes. *Journal of Nanoscience and Nanotechnology, 7*, 1298–1314.
6. Cui, D., Tian, F., Kong, Y., Titushikin, I., & Gao, H. (2004). Effects of single-walled carbon nanotubes on the polymerase chain reaction. *Nanotechnology, 15*, 154–157.
7. Ito, A., Ino, K., Kobayashi, T., & Honda, H. (2005). The effect of RGD peptide-conjugated magnetite cationic liposomes on cell growth and cell sheet harvesting. *Biomaterials, 26*, 6185–6193.
8. Kim, D. H., Lee, S. H., Kim, K. N., Kim, K. M., Shim, I. B., & Lee, Y. K. (2005). Cytotoxicity of ferrite particles by MTT and agar diffusion methods for hyperthermic application. *Journal of Magnetism and Magnetic Materials, 293*, 287–292.
9. Lee, H., Lee, E., Kim, D. K., Jang, N. K., Jeong, Y. Y., & Jon, S. (2006). Antibiofouling polymer-coated superparamagnetic iron oxide nanoparticles as potential magnetic resonance contrast agents for in vivo cancer imaging. *Journal of the American Chemical Society, 128*, 7383–7389.
10. Vernet-Crua, A., Medina-Cruz, D., Mostafavi, E., Benko, A., Cholula-Diaz, J. L., Saravanan, M., et al. (2021). *Nanobiosensors for theranostic applications, nanobiomaterials for therapeutics and diagnostic applications* (pp. 511–543). Elsevier. https://doi.org/10.1016/B978-0-12-821013-0.00005-2
11. Bharti, A., Rana, S., & Prabhakar, N. (2019). Electrochemical nanobiosensors for cancer diagnosis. *Materials Research Foundations, 47*, 157–210.
12. Singh, A. K., Das, A., & Kumar, P. (2021). Nanobiosensors and their applications. In *Nanotechnology* (pp. 249–288). Jenny Stanford Publishing.
13. Kang, M., & Lee, S. (2022). Graphene for nanobiosensors and nanobiochips. *Advances in Experimental Medicine and Biology, 1351*, 203–232. https://doi.org/10.1007/978-981-16-4923-3_10. PMID: 35175618.
14. Bharathala, S., & Sharma, P. (2019). Biomedical applications of nanoparticles. In *Nanotechnology in modern animal biotechnology: concepts and applications* (pp. 113–132). Elsevier. https://doi.org/10.1016/B978-0-12-818823-1.00008-9
15. Das, N. C., Roy, B., Patra, R., Choudhury, A., Ghosh, M., & Mukherjee, S. (2021). Surface-modified noble metal nanoparticles as antimicrobial agents: biochemical, molecular and therapeutic perspectives. In *Nanotechnology for advances in medical microbiology. environmental and microbial biotechnology*. Springer.
16. Moghimi, S. M., Hunter, A. C., & Murray, J. C. (2005). Nanomedicine: current status and future prospects. *The FASEB Journal, 19*, 311–330.
17. Saji, V. S., Choe, H. C., & Yeung, K. W. K. (2010). Nanotechnology in biomedical applications: A review. *International Journal of Nano and Biomaterials, 3*(2), 119–139. https://doi.org/10.1504/IJNBM.2010.037801
18. Saylan, Y., Yılmaz, F., & Denizli, A. (2021). Nanobiosensors for biomedical applications. In N. Saglam, F. Korkusuz, & R. Prasad (Eds.), *Nanotechnology applications in health and environmental sciences. Nanotechnology in the life sciences*. Springer. https://doi.org/10.1007/978-3-030-64410-9_8

19. Marks, R., & Robert, S. (2007). *Handbook of biosensors and biochips*. John Wiley.
20. Mukherjee, S., & Mukherjee, N. (2021). Current developments in diagnostic biosensor technology: relevance to therapeutic intervention of infectious and inflammatory diseases of human. In G. Dutta, A. Biswas, & A. Chakrabarti (Eds.), *Modern techniques in biosensors* (Studies in systems, decision and control) (Vol. 327). Springer. https://doi.org/10.1007/978-981-15-9612-4_1
21. Huang, Y., Das, P. K., & Bhethanabotla, V. R. (2021). Surface acoustic waves in biosensing applications. *Sensors and Actuators Reports, 3*. https://doi.org/10.1016/j.snr.2021.100041
22. Namdari, P., Daraee, H., & Eatemadi, A. (2016). Recent advances in silicon nanowire biosensors: synthesis methods, properties, and applications. *Nanoscale Research Letters., 11*(1). https://doi.org/10.1186/s11671-016-1618-z. Springer New York LLC.
23. Dey, B., Mukherjee, S., Mukherjee, N., Mondal, R. K., Satpati, B., Senapati, D., & Babu, S. P. S. (2016). Green silver nanoparticles for drug transport, bioactivities and a bacterium (Bacillus subtilis)-mediated comparative nano-patterning feature. *RSC Adv., 6*, 46573–46581.
24. Mohammadniaei, M., Park, C., Min, J., Sohn, H., & Lee, T. (2018). Fabrication of electrochemical-based bioelectronic device and biosensor composed of biomaterial-nanomaterial hybrid. *Advances in Experimental Medicine and Biology., 1064*, 263–296. https://doi.org/10.1007/978-981-13-0445-3_17. Springer New York LLC.
25. Tamer, U., Seçkin, A. İ., Temur, E., & Torul, H. (2011). Fabrication of biosensor based on polyaniline/gold nanorod composite. *International Journal of Electrochemistry, 2011*, 1–7. https://doi.org/10.4061/2011/869742
26. Yüce, M., & Kurt, H. (2017). How to make nanobiosensors: Surface modification and characterisation of nanomaterials for biosensing applications. *RSC Advances., 7*(78), 49386–49403. https://doi.org/10.1039/c7ra10479k. Royal Society of Chemistry.
27. Thévenot, D. R., Toth, K., Durst, R. A., & Wilson, G. S. (2001). Electrochemical biosensors: Recommended definitions and classification. *Biosensors and Bioelectrontronic., 6*(1–2), 121–131.
28. Mondal, M. K., Mukherjee, S., Saha, S. K., Chowdhury, P., & Babu, S. P. S. (2017). Design and synthesis of reduced graphene oxide based supramolecular scaffold: a benign microbial resistant network for enzyme immobilization and cell growth. *Materials Science and Engineering, 75*, 1168–1177.
29. Pérez, D. J., Patiño, E. B., & Orozco, J. (2022). Electrochemical nanobiosensors as point-of-care testing solution to cytokines measurement limitations. *Electroanalysis., 34*(2), 184–211. https://doi.org/10.1002/elan.202100237
30. Gruhl, F. J., Rapp, B. E., & Länge, K. (2011). Biosensors for diagnostic applications. In *Molecular diagnostics* (pp. 115–148). Springer.
31. Dey, B., Mondal, R. K., Mukherjee, S., Satpati, B., Mukherjee, N., Mandal, A., et al. (2015). A supramolecular hydrogel for generation of a benign DNA-hydrogel. *RSC Adv., 5*, 105961–105968.
32. Dey, B., Mukherjee, S., Mukherjee, N., Mondal, R. K., Satpati, B., & Babu, S. P. S. (2018). Polyphenoloxidase-based luminescent enzyme hydrogel: an efficient redox active immobilized scaffold. *Bulletin of Materials Science., 41*, 14. https://doi.org/10.1007/s12034-017-1529-3
33. Mukherjee, S., Basak, B., Bhunia, B., Dey, A., & Mondal, B. (2013). Potential use of polyphenol oxidases (PPO) in the bioremediation of phenolic contaminants containing industrial waste water. *Reviews in Environmental Science and Bio/Technology., 12*, 61–73.
34. Patel, S., Nanda, R., Sahoo, S., & Mohapatra, E. (2016). Biosensors in health care: the milestones achieved in their development towards lab-on-chip-analysis. *Biochemistry Research International.* https://doi.org/10.1155/2016/3130469
35. Gouvea, C. (2011). Biosensors for health applications. In *Biosensors for health, environment and biosecurity*. InTech Open. https://doi.org/10.5772/16983
36. Song, M., Yang, M., & Hao, J. (2021). Pathogenic virus detection by optical nanobiosensors. *Cell Reports Physical Science., 1*(2). https://doi.org/10.1016/j.xcrp.2020.100288. Cell Press.

37. Gu, B., & Zhang, Q. (2018). Recent advances on functionalized upconversion nanoparticles for detection of small molecules and ions in biosystems. *Advanced Science., 5*, 1700609.
38. Fahmy, H. M., Serea, E. S. A., Salah-Eldin, E. R., Al-Hafiry, S. A., Ali, M. K. Shalan, A. E., et al.(2022). Recent progress in graphene- and related carbon-nanomaterial-based electrochemical biosensors for early disease detection. The Sciences and Engineering 964–1000. doi: https://doi.org/10.1021/acsbiomaterials.1c00710
39. Behboodi, H., Pourmadadi, M., Omidi, M., Rahmandoust, M., Siadat, S. O. R., & Shayeh, J. S. (2022). Cu-CDs as dual optical and electrochemical nanosensor for βME detection. *Surfaces and Interfaces, 29*. https://doi.org/10.1016/j.surfin.2021.101710
40. Vidic, J., Manzano, M., Chang, C. M., & Jaffrezic-Renault, N. (2017). Advanced biosensors for detection of pathogens related to livestock and poultry. *Veterinary Research, 48*(1), 1–22. https://doi.org/10.1186/S13567-017-0418-5
41. Kaushik, A., & Mujawar, M. A. (2018). Point of care sensing devices: Better care for everyone. *Sensors (Switzerland), 18*(12). https://doi.org/10.3390/S18124303
42. Vashist, S. K. (2017). Point-of-care diagnostics: recent advances and trends. *Biosensors., 7*(4), 62. https://doi.org/10.3390/BIOS7040062
43. Antiochia, R. (2020). Nanobiosensors as new diagnostic tools for SARS, MERS and COVID-19: from past to perspectives. *Microchimica Acta, 187*(12), 1–13. https://doi.org/10.1007/S00604-020-04615-X/FIGURES/6
44. Ishikawa, F. N., Chang, H. K., Curreli, M., Liao, H. I., Olson, C. A., Chen, P. C., et al. (2009). Label-free, electrical detection of the SARS virus N-protein with nanowire biosensors utilizing antibody mimics as capture probes. *ACS Nano, 3*(5), 1219. https://doi.org/10.1021/NN900086C
45. Inci, F., Tokel, O., Wang, S., Gurkan, U. A., Tasoglu, S., Kuritzkes, D. R., et al. (2013). Nanoplasmonic quantitative detection of intact viruses from unprocessed whole blood. *ACS Nano, 7*(6), 4733–4745. https://doi.org/10.1021/NN3036232/SUPPL_FILE/NN3036232_SI_001.PDF
46. Zhang, X., Feng, Y., Duan, S., Su, L., Zhang, J., & He, F. (2019). Mycobacterium tuberculosis strain H37Rv electrochemical sensor mediated by aptamer and AuNPs-DNA. *ACS Sensors, 4*(4), 849–855. https://doi.org/10.1021/ACSSENSORS.8B01230/SUPPL_FILE/SE8B01230_SI_001.PDF
47. Ma, J., Du, M., Wang, C., Xie, X., Wang, H., Li, T., et al. (2021). Rapid and sensitive detection of mycobacterium tuberculosis by an enhanced nanobiosensor. *ACS Sensors.* https://doi.org/10.1021/ACSSENSORS.1C01227/SUPPL_FILE/SE1C01227_SI_001.PDF
48. Brince, K. P., Kumar, S., Tripathy, S., Vanjari, S. R. K., Singh, V., & Singh, S. G. (2016). A highly sensitive self assembled monolayer modified copper doped zinc oxide nanofiber interface for detection of Plasmodium falciparum histidine-rich protein-2: Targeted towards rapid, early diagnosis of malaria. *Biosensors and Bioelectronics, 80*, 39–46. https://doi.org/10.1016/J.BIOS.2016.01.036
49. Obisesan, O. R., Adekunle, A. S., Oyekunle, J. A. O., Sabu, T., Nkambule, T. T. I., & Mamba, B. B. (2019). Development of electrochemical nanosensor for the detection of malaria parasite in clinical samples. *Frontiers in Chemistry, 7*(FEB), 89. https://doi.org/10.3389/FCHEM.2019.00089/BIBTEX
50. Layqah, L. A., & Eissa, S. (2019). An electrochemical immunosensor for the corona virus associated with the Middle East respiratory syndrome using an array of gold nanoparticle-modified carbon electrodes. *Mikrochimica Acta, 186*(4). https://doi.org/10.1007/S00604-019-3345-5
51. Mokhtarzadeh, A., Eivazzadeh-Keihan, R., Pashazadeh, P., Hejazi, M., Gharaatifar, N., Hasanzadeh, M., et al. (2017). Nanomaterial-based biosensors for detection of pathogenic virus. *TrAC Trends in Analytical Chemistry, 97*, 445–457. https://doi.org/10.1016/J.TRAC.2017.10.005
52. Wasik, D., Mulchandani, A., & Yates, M. V. (2018). Point-of-use nanobiosensor for detection of dengue virus NS1 antigen in adult aedes aegypti: A potential tool for improved dengue

surveillance. *Analytical Chemistry, 90*(1), 679–684. https://doi.org/10.1021/ACS.ANALCHEM.7B03407/SUPPL_FILE/AC7B03407_SI_001.PDF
53. Kaushik, A., Yndart, A., Kumar, S., Jayant, R. D., Vashist, A., Brown, A. N., et al. (2018). A sensitive electrochemical immunosensor for label-free detection of Zika-virus protein. *Scientific Reports, 8*(1), 1–5. https://doi.org/10.1038/s41598-018-28035-3
54. Naveca, F. G., Pontes, G. S., Chang, A. Y. H., da Silva, G. A. V., do Nascimento, V. A., da Monteiro, D. C. S., da Silva, M. S., et al. (2018). Analysis of the immunological biomarker profile during acute Zika virus infection reveals the overexpression of CXCL10, a chemokine linked to neuronal damage. *Memorias Do Instituto Oswaldo Cruz, 113*(6). https://doi.org/10.1590/0074-02760170542
55. Zare, H., Meshkat, Z., Hatamluyi, B., Rezayi, M., Ghazvini, K., Derakhshan, M., et al. (2022). The first diagnostic test for specific detection of Mycobacterium simiae using an electrochemical label-free DNA nanobiosensor. *Talanta, 238*(Pt 2). https://doi.org/10.1016/J.TALANTA.2021.123049
56. Al-Abodi, H. R., Jawad, Z. N., Al-Yasiri, M. H., Al-Saadi, A. G. M., Memariani, H., Sabokrouh, A., et al. (2020). Novel gold nanobiosensor platforms for rapid and inexpensive detection of Vibrio cholerae. *Reviews in Medical Microbiology, 31*(2), 70–74. https://doi.org/10.1097/MRM.0000000000000197
57. Uddin, M. I., Islam, S., Nishat, N. S., Hossain, M., Rafique, T. A., Rashu, R., et al. (2016). Biomarkers of environmental enteropathy are positively associated with immune responses to an oral cholera vaccine in Bangladeshi children. *PLoS Neglected Tropical Diseases, 10*(11). https://doi.org/10.1371/JOURNAL.PNTD.0005039
58. Farooq, S., Neves, W. W., Pandoli, O., del Rosso, T., de Lima, L. M., Dutra, R. F., et al. (2018). Engineering a plasmonic sensing platform for Candida albicans antigen identification. *Journal of Nanophotonics., 12*(3), 033003. https://doi.org/10.1117/1.JNP.12.033003
59. León, C., Ruiz-Santana, S., Saavedra, P., Castro, C., Loza, A., Zakariya, I., et al. (2016). Contribution of Candida biomarkers and DNA detection for the diagnosis of invasive candidiasis in ICU patients with severe abdominal conditions. *Critical Care (London, England), 20*(1). https://doi.org/10.1186/S13054-016-1324-3
60. Hussain, K. K., Malavia, D., Johnson, E. M., Littlechild, J., Winlove, C. P., Vollmer, F., et al. (2020). Biosensors and diagnostics for fungal detection. *Journal of Fungi (Basel, Switzerland), 6*(4), 1–26. https://doi.org/10.3390/JOF6040349
61. Murphy, S. C., Ishizuka, A. S., Billman, Z. P., Olsen, T. M., Seilie, A. M., Chang, M., et al. (2018). Plasmodium 18S rRNA of intravenously administered sporozoites does not persist in peripheral blood. *Malaria Journal, 17*(1), 1–7. https://doi.org/10.1186/S12936-018-2422-2/FIGURES/2
62. Kon, K., & Rai, M. (2015). Silver nanoparticles for the control of vector-borne infections. In *Nanotechnology in diagnosis, treatment and prophylaxis of infectious diseases* (pp. 39–49). Elsevier. https://doi.org/10.1016/B978-0-12-801317-5.00003-7
63. Satapathy, A. K., Sartono, E., Sahoo, P. K., Dentener, M. A., Michael, E., Yazdanbakhsh, M., et al. (2006). Human bancroftian filariasis: immunological markers of morbidity and infection. *Microbes and Infection, 8*(9–10), 2414–2423. https://doi.org/10.1016/J.MICINF.2006.05.003
64. Carrillo, E., & Moreno, J. (2019). Editorial: biomarkers in leishmaniasis. *Frontiers in Cellular and Infection Microbiology, 9*, 388. https://doi.org/10.3389/FCIMB.2019.00388/BIBTEX
65. Martins, B. R., Barbosa, Y. O., Andrade, C. M. R., Pereira, L. Q., Simão, G. F., de Oliveira, C. J., et al. (2020). Development of an electrochemical immunosensor for specific detection of visceral leishmaniasis using gold-modified screen-printed carbon electrodes. *Biosensors., 10*(8), 81. https://doi.org/10.3390/BIOS10080081
66. Lagatie, O., Verheyen, A., van Asten, S., Odiere, M. R., Djuardi, Y., Levecke, B., et al. (2020). 2-Methyl-pentanoyl-carnitine (2-MPC): a urine biomarker for patent Ascaris lumbricoides infection. *Scientific Reports, 10*(1), 1–13. https://doi.org/10.1038/s41598-020-72804-y
67. Lednický, T., & Bonyár, A. (2020). Large scale fabrication of ordered gold nanoparticle-epoxy surface nanocomposites and their application as label-free plasmonic DNA biosensors. *ACS*

Applied Materials and Interfaces, 12(4), 4804–4814. https://doi.org/10.1021/ACSAMI.9B20907/SUPPL_FILE/AM9B20907_SI_001.PDF

68. Ubeda, C., Lepe-Balsalobre, E., Ariza-Astolfi, C., & Ubeda-Ontiveros, J. M. (2019). Identification of volatile biomarkers of Giardia duodenalis infection in children with persistent diarrhoea. *Parasitology Research, 118*(11), 3139–3147. https://doi.org/10.1007/S00436-019-06433-4/FIGURES/2
69. Spadafora, L. J., Kearney, M. R., Siddique, A., Ali, I. K., Gilchrist, C. A., Arju, T., et al. (2016). Species-specific immunodetection of an entamoeba histolytica cyst wall protein. *PLoS Neglected Tropical Diseases, 10*(5), e0004697. https://doi.org/10.1371/JOURNAL.PNTD.0004697
70. Chu, M. X., Miyajima, K., Takahashi, D., Arakawa, T., Sano, K., Sawada, S.-i., Kudo, H., Iwasaki, Y., Akiyoshi, K., Mochizuki, M., & Mitsubayashi, K. (2011). Soft contact lens biosensor for in situ monitoring of tear glucose as non-invasive blood sugar assessment. *Talanta, 83*(3), 960–965. S0039914010008519. https://doi.org/10.1016/j.talanta.2010.10.055
71. Clark, L. C., Jr. (1962). Electrode systems for continuous monitoring in cardiovascular surgery. *Annals of New York of Academy Science., 102*, 29–45.
72. Cavalcanti, A., Shirinzadeh, B., Zhang, M., & Kretly, L. C. (2008). Nanorobot hardware architecture for medical defense. *Sensors (Basel, Switzerland), 8*(5), 2932–2958. https://doi.org/10.3390/s8052932
73. Beauharnois, M. E., Neelamegham, S., & Matta, K. L. (2006). Quantitative measurement of selectin-ligand interactions. In *Glycobiology protocols* (pp. 343–358). Springer.
74. Koschwanez, H. E., & Reichert, W. M. (2007). In vitro, in vivo and post explantation testing of glucose-detecting biosensors: current methods and recommendations. *Biomaterials, 28*, 3687–3703.
75. Song, C., Que, S., Heimer, L., & Que, L. (2020). On-chip detection of the biomarkers for neurodegenerative diseases: Technologies and prospects. *Micromachines., 11*(7). https://doi.org/10.3390/MI11070629. MDPI AG.
76. Ding, X., Song, C., & Que, L. (2019). Fabrication of Contact Lens Device with Integrated Microtubes for in Situ ExtendedDrug Delivery for Ocular Disease Treatment. In *Proceedings of the 2019 20th International Conference on Solid-State Sensors, Actuators and Microsystems & Eurosensors XXXIII (TRANSDUCERS & EUROSENSORSXXXIII)*, Berlin, Germany. https://doi.org/10.21741/9781644900130-5.
77. Park, J., Kim, J., Kim, S. Y., Cheong, W. H., Jang, J., Park, Y. G., et al. (2018). Soft, smart contact lenses with integrations of wireless circuits, glucose sensors, and displays. *Science Advances., 4*, 9841.
78. Song, C., Ben-Shlomo, G., & Que, L. A. (2019). Multifunctional smart soft contact lens device enabled by nanopore thin film for glaucoma diagnostics and in situ drug delivery. *Journal of Microelectromechanical Systems, 28*, 810–816.
79. Yang, T., Santisteban, M. M., Rodriguez, V., Li, E., Ahmari, N., Carvajal, J. M., et al. (2015). Gut dysbiosis is linked to hypertension. *Hypertension, 65*(6), 1331–1340. https://doi.org/10.1161/HYPERTENSIONAHA.115.05315
80. Barani, M., Rahdar, A., Sargazi, S., Amiri, M. S., Sharma, P. K., & Bhalla, N. (2021). Nanotechnology for inflammatory bowel disease management: Detection, imaging and treatment. In *Sensing and bio-sensing research* (Vol. 32). Elsevier. https://doi.org/10.1016/j.sbsr.2021.100417
81. Karban, A., Nakhleh, M. K., Cancilla, J. C., Vishinkin, R., Rainis, T., Koifman, E., et al. (2016). Programmed nanoparticles for tailoring the detection of inflammatory bowel diseases and irritable bowel syndrome disease via breathprint. *Advanced Healthcare Materials., 5*(18), 2339–2344.
82. Shepherd, S., McGuire, N. D., de Lacy Costello, B., Ewen, R., Jayasena, D., Vaughan, K., et al. (2014). The use of a gas chromatograph coupled to a metal oxide sensor for rapid assessment of stool samples from irritable bowel syndrome and inflammatory bowel disease patients. *Journal of Breath Research., 8*(2), 026001.

83. Tang, H., Xiang, D., Wang, F., Mao, J., Tan, X., & Wang, Y. (2017). 5-ASA-loaded SiO2 nanoparticles-a novel drug delivery system targeting therapy on ulcerative colitis in mice, Molecular Medicine Reports. *Pp., 15*(3), 1117–1122.
84. Girigoswami, K., & Girigoswami, A. (2021). A review on the role of nanosensors in detecting cellular miRNA expression in colorectal cancer. *Endocrine, Metabolic & Immune Disorders Drug Targets, 21*(1), 12–26. https://doi.org/10.2174/1871530320666200515115723
85. Lv, Y., Wu, R., Feng, K., Li, J., Mao, Q., Yuan, H., et al. (2017). Highly sensitive and accurate detection of C-reactive protein by CdSe/ZnS quantum dot- based fluorescence-linked immunosorbent assay. *Journal of Nanobiotechnology., 15*(1), 35.
86. Covarrubias-Zambrano, O., Motamedi, M., Ameredes, B. T., Tian, B., Calhoun, W. J., Zhao, Y., et al. (2022). Optical biosensing of markers of mucosal inflammation. *Nanomedicine: Nanotechnology, Biology and Medicine, 40*, 102476. https://doi.org/10.1016/J.NANO.2021.102476
87. Chandra, P. (2015). Electrochemical nanobiosensors for cancer diagnosis. *Journal of Analytical and Bioanalytical Techniques., 6*(2), 1000–1119. https://doi.org/10.4172/2155-9872
88. Grimm, J., Perez, M., Josephson, L., & Weissleder, R. (2004). Novel nanosensor for raid analysis of telomerase activity. *Cancer Research., 64*, 639.
89. Rai, M., Gade, A., Gaikwad, S., Marcato, P. D., & Durán, N. (2012). Biomedical applications of nanobiosensors: the state-of-the-art. *Journal of the Brazilian Chemical Society, 23*(1), 14–24.
90. Pathak, P., Katiyar, V. K., & Giri, S. (2007). Cancer research-nanoparticles, nanobiosensors and their use in cancer research. *Journal of Nanotechnology, 3*, 1–4.
91. Prasad, M., Lambe, U. P., Brar, B., Shah, I., Manimegalai, J., Ranjan, K., & Iqbal, H. M. (2018). Nanotherapeutics: an insight into healthcare and multi-dimensional applications in medical sector of the modern world. *Biomedicine & Pharmacotherapy, 97*, 1521–1537.
92. Williams, R. M., Lee, C., Galassi, T. V, Harvey, J. D., Leicher, R., Sirenko, M., et al. (2018). C A N C E R Noninvasive ovarian cancer biomarker detection via an optical nanosensor implant. https://www.science.org
93. Zhu, Y., Chandra, P., & Shim, Y. B. (2013). Ultrasensitive and selective electrochemical diagnosis of breast cancer based on a hydrazine-Au nanoparticle-aptamer bioconjugate. *Analytical Chemistry, 85*, 1058–1064.
94. Ganesh, H. V. S., Chow, A. M., & Kerman, K. (2016). Recent advances in biosensors for neurodegenerative disease detection. Trends in Analytical Chemistry. 79: 363–370). doi: https://doi.org/10.1016/j.trac.2016.02.012.Elsevier
95. Zhao, Z., Zhu, L., Bu, X., Ma, H., Yang, S., Yang, Y., et al. (2015). Label-free detection of Alzheimer's disease through the ADP3 peptoid recognizing the serum amyloid-beta42 peptide. *Chemical Communications (Camb), 51*, 718–721.
96. Morales-Narvaez, E., Monton, H., Fomicheva, A., & Merkoci, A. (2012). Signal enhancement in 505antibody microarrays using quantum dots nanocrystals: application to potential Alzheimer's 506disease biomarker screening. *Analytical Chemistry, 84*, 6821–6827.
97. Bateman, R. J., Xiong, C., Benzinger, T. L., Fagan, A. M., Goate, A., Fox, N. C., et al. (2012). Clinical and biomarker changes in dominantly inherited Alzheimer's disease. *The New England Journal of Medicine, 367*, 795–804.
98. Preische, O., Schultz, S. A., Apel, A., Kuhle, J., Kaeser, S. A., Barro, C., et al. (2019). Serum neurofilament dynamics predicts neurodegeneration and clinical progression in presymptomatic Alzheimer's disease. *Nature Medicine., 25*, 277–283.
99. Iqbal, K., Alonso-Adel, C., Chen, S., Chohan, M. O., El-Akkad, E., Gong, C. X., et al. (2005). Tau pathology in Alzheimer's disease and other tauopathies. *Biochimica et Biophysica Acta, 1739*, 198–210.
100. Jankovic, J. (2008). Parkinson's disease: clinical features and diagnosis. *Journal of Neurology and Neurosurgery Psychiatry., 79*(4), 368–376.
101. Dickson, D. W. (2012). Parkinson's disease and parkinsonism: Neuropathology. *Cold Spring Harbour in Perspective Medicine, 2*, 445.

102. Lundvig, D., Lindersson, E., & Jensen, P. H. (2005). Pathogenic effects of alpha-synuclein aggregation. *Brain Research. Molecular Brain Research, 134*, 3–17.
103. Shulman, M., De Jager, P. L., & Feany, M. B. (2011). Parkinson's disease: genetics and pathogenesis. *Annual Review of Pathology, 6*, 193–222.
104. Ankireddy, S. R., & Kim, J. (2015). Selective detection of dopamine in the presence of ascorbic acid via 511fluorescence quenching of InP/ZnS quantum dots. *International Journal of Nanomedicine, 10*, 113–119.
105. Chamorro-Garcia, A., & Merkoçi, A. (2016). Nanobiosensors in diagnostics. *Nanobiomedicine, 3*, 1849543516663574. https://doi.org/10.1177/1849543516663574
106. Wang, S., Li, K., Chen, Y., Chen, H., Ma, M., Feng, J., et al. (2015). Biocompatible PEGylated MoS2 nanosheets: Controllable bottom-up synthesis and highly efficient photothermal regression of tumor. *Biomaterials, 39*, 206–217. https://doi.org/10.1016/J.BIOMATERIALS.2014.11.009
107. Aqra, M. W., & Ramanathan, A. A. (2021). Review of the recent advances in nano-biosensors and technologies for healthcare applications. *Chemistry Proceedings., 5*(1), 76. https://doi.org/10.3390/CSAC2021-10473

Design and Analysis of One-Dimensional Photonic Crystal Biosensor Device for Identification of Cancerous Cells

Abinash Panda and Puspa Devi Pukhrambam

Abstract

The present chapter highlights one-dimensional photonic crystal (1D PhC) and its vital applications. The remarkable scientific progress in PhC has been able to draw the attention of researchers to novel bio-sensing applications. With the advancement in technology, different defect-based PhCs have been successfully fabricated with extensive analysis of propagation characteristics, and tested for various sensing applications like blood, gas, salinity, DNA, alcohol, liquid, food, hormones, enzymes, cells, urine, glucose, and chemicals. The transfer matrix method is the most suitable method to study the spectral characteristics of 1D PhC structure. The sensing principle is based on the study of alteration in the resonant mode wavelength according to the modification in the analyte refractive index. This chapter deals with the study of a defect-based 1D PhC cancer cells sensor, where TMM is employed to detect basal, cervical, and breast cancer cells. In order to enhance the sensitivity, a thin graphene layer is deposited at the side wall of the defect layer. Complete optimization of geometrical parameters has been performed to envisage high performance. The 3D colormap plot is studied to clearly show the variation in the properties of the defect mode with a change in the incident angle. Moreover, signal-to-noise ratio, Q-factor, resolution, and figure of merit of the sensor are measured meticulously. The noteworthy sensing performance can open an avenue to effectively detect cancer cells in the early stage.

A. Panda (✉) · P. D. Pukhrambam
Department of Electronics and Communication Engineering, National Institute of Technology, Silchar, India

G. Dutta (ed.), *Next-Generation Nanobiosensor Devices for Point-Of-Care Diagnostics*, https://doi.org/10.1007/978-981-19-7130-3_5

Keywords

Photonic crystal · Transfer matrix method · Graphene · Transmittance spectrum · Sensitivity

1 Introduction

Most technological innovations have been brought up by deeply perceiving nature. There are numerous examples that validates the existence of periodic nature of variations in nature. For example, the wings of butterflies, opal of the bracelet, feathers of birds, and barbules of colorful birds contain systematic periodic arrangements, which resemble the property of photonic crystals [1–3]. The color changes with respect to the angle of observation, which is primarily owing to the interaction between the light and the above-mentioned material's natural design. Figure 1 demonstrates some nature-based multilayer effects.

The study on periodic multilayer structures by E. Yablonvitch and S. John in early 1987 is considered the flagship research on photonics, which ignited the minds of the researchers to explore different applications using the photonics principle [4, 5]. In their work, the authors revealed the effect of periodicity in two and three dimensions. As far as research on photonic crystals is concerned, it can be realized in 1D, 2D, and 3D forms. Among these, 3D PhCs are facing fabrication feasibility issues, and still research is going on to find an effective fabrication technique to produce low-loss 3D PhCs [6, 7]. On the other hand, 2D PhCs can be successfully fabricated by etching technique resulting in triangular, square, and honeycomb

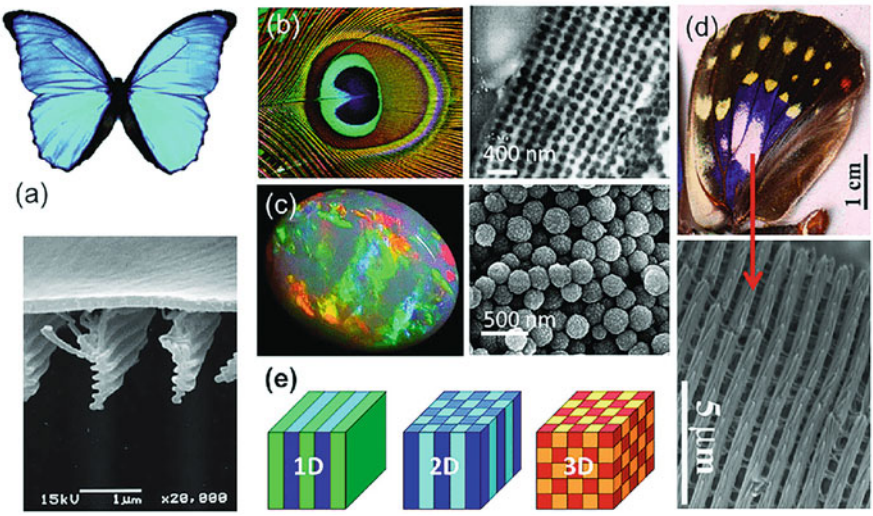

Fig. 1 Natural photonic crystals (**a**) Morpho butterfly, (**b**) multi-colored peacock feather, (**c**) opal gemstone, (**d**) wing of Sasakia Charonda with their microscopic images, and (**e**) 1D/2D/3D PhCs

structures. 2D PhCs can be designed in the form of a slab, which can be organized in two ways: arrangement of dielectric materials with air as the background, and the arrangement of holes on a dielectric slab [8–10]. Defect-based PhCs have brought a revolution in the photonics research community. The defects can be created by omitting a series of air holes or by altering the properties of air holes along a particular shape in the PhC, which makes it behaves as a photonic crystal waveguide (PCW) [11–13]. The light signals that fall within the PBG can be effectively guided and trapped in PCW, which enables the manipulation of electromagnetic waves in the nanostructure. Nonetheless, several efforts have been given by scientists and researchers to mimic 2D and 3D PhCs, but 1D PhCs are the utmost explored structures and investigated from theoretical to experimental aspects due to their fabrication feasibility, high compatibility, and broad application domain [14–16]. 1D PhCs are blessed with an elegant characteristic called photonic band gap (PBG), which appears owing to the periodical arrangement of different dielectric materials along the stacking direction [17]. The PBG reflects that wavelength band which is restricted to propagating along the multilayer structure. The PBG characteristic of the 1D PhC has a significant effect in envision many novel applications such as laser applications, sensing applications, filters, optical mirrors, polarizers, communication applications, and biomedical applications [18–20]. PhC must be structurally altered to produce a resonant mode in the spectral characteristics in order to be used as a biosensor. The finest technique to create such a resonant mode is to insert a defect in the design [21]. If the input wavelength and the defect mode wavelength match each other, a discrete spike is formed in the spectral characteristics. The light (photons) is strongly localized near the defect layer [22]. A slight change in the surrounding refractive index leads to a significant modification in the location of the defect mode. Till now, 1D PhCs are widely used for a variety of purposes [23–26]. Moreover, 1D PhCs are highly reliable pertaining to temperature fluctuations, offer fast operation, and possess a higher lifetime compared to the high dimensional PhCs.

In the last decade, researchers have explored numerous novel 2D materials, which be integrated with photonic devices to improve performance. Graphene has come up as a promising material for the design of various optical devices, and therefore evolved as a center of attraction for researchers worldwide [27, 28]. Geim and Novoselov first introduced graphene as a 2D material, for which they received the prestigious Nobel Prize in the year 2010 [29, 30]. Graphene possesses a unique lattice configuration and is considered a novel material due to its outstanding electronic properties. Graphene has a hexagonally arranged lattice structure of sp2 hybridization having noteworthy electronic properties. Most importantly, graphene has a higher conductivity of 10^6 s/m and a very low resistivity of 10^{-6} Ω cm, which makes it convenient to work in a broad applications domain compared to conventional materials [31]. Moreover, graphene demonstrates zero bandgap properties and excellent carrier mobility. Even though the approximate thickness of graphene is only 0.34 nm, but still it shows a remarkable absorption property [32]. It has been experimentally observed that a monolayer of graphene can absorb 2.3% of light in a wide wavelength band. Owing to its high absorption property, graphene shows

distinguished reflectance for TE and TM modes under total internal reflection, which is very sensitive toward a small deviation in the RI of the contacting surface [33]. Due to the aforementioned properties, graphene has successfully entered the photonics industry to realize different electromagnetics applications. The properties like flexibility, durability, robustness, high conductivity, and excellent mobility make graphene a right candidate for the design of photonic devices [34–36]. Notably, the conductivity of graphene can be adjusted by controlling the chemical potential across the graphene sheet. So, by suitably controlling the chemical potential across the graphene sheet, the optical properties of the integrated graphene photonic devices can be varied according to the user's requirement. From the energy band transition point of view, two types of interactions are noticed between graphene and light signal, namely inter-band transition and in-band transition. The inter-band transition is mainly seen in the visible to NIR wavelength range, whereas the in-band transition is observed in the far-infrared wavelength regime. In the case of in-band transition, graphene behaves as a free electron that is capable of exciting the surface. Nevertheless, a monolayer of graphene bestows high light absorption, but it shows a poor absorption of only 2.3% as material, which demands more deep research to boost the interaction between graphene and electromagnetic signal.

For the last two decades, 1D PhCs are dominating the field of designing biosensors. A 1D PhC sensor is proposed by Nouman et al. for the detection of brain lesions within the refractive index range of 1.3333–1.4833, and achieved an excellent sensitivity of 3080.8 nm.RIU^{-1} [37]. Zaky et al. reported a Tamm plasmon structure to detect various gases. Ag plays a vital role in generating the plasmonic modes at the interface between the metal and 1D PhC [38]. A thorough analysis is carried out on the characteristics of the defect modes, where it is seen that the cavity resonance tends to decrease with an escalation in the RI of the targeted gases [39]. Ahemad explored a Psi-based photonic crystal including a metal layer and investigated TPP (Tamm plasmon polariton) resonant modes for sensing liquid analytes. The authors studied the shifting nature of the defect mode by infiltrating the cavity with liquids of different refractive indices [40]. Aly manipulated TMM to examine the transmission spectrum in a defect 1D PhC for sensing the creatinine concentrations in blood [41]. Panda et al. studied the absorption spectrum and transmission spectrum in both symmetric and asymmetric 1D PhC structures to detect various viruses present in the drinking water, which find a suitable application in rural areas [42]. A hemoglobin sensor is realized by M. Abadla and his team to sense wide concentrations of hemoglobin. After optimizing numerous structure parameters, they attained a sensitivity of 167 nm per RIU [43]. A glucose sensor is designed using defect-based 1D PhC through the analysis of reflectance characteristics [44]. A steady and low-cost sensor is reported by Elsayed et al. [45], to sense various types of biodiesels. The bandgap properties of a 1D PhC comprising a single layer of graphene sandwiched between the dielectric materials are inspected by Fu et al. [46]. A graphene-based 1D PhC is investigated by Fan et al., where the authors explored the dependence of optical properties of graphene on its chemical potential [47]. By varying the chemical potential. The authors measured the change in the defect mode frequency. A novel protein sensor is

investigated on the ground of 1D PhC. Although the authors used the optimized parameters, they found a sensitivity of only 170 nm per RIU, which is not up to the mark [48].

Cancer, the leading reason of fatality worldwide, has evolved into a precarious disease. As per the information of IARC, around 19.3 million population around the globe are contrived by cancer, and nearly ten million fatalities have occurred in the year 2020 [49]. The primary reason behind the growth of cancer cells in the human body is the interaction between the genetic factors of the body with different external agents like physical carcinogens, chemical carcinogens (tobacco, aflatoxin), and biological carcinogens (bacteria, viruses) [50]. Due to this effect, the cells grow in an uncontrolled manner by absorbing relatively more protein and nutrients from the body [51]. The main point of concern is that to date there is no fully guaranteed treatment of cancer in medical science. Probably, the single approach to combat the situation is the early detection of these diseases. So, a label-free and point-of-care cancer testing device is indispensable to effectively fight cancer. In the last decade, researchers have greatly relied on photonics technologies to successfully detect different cancer cells with high accuracy and less time. A cancer cell sensor is proposed by Bijalwan et al., which is consisted of alternating layers of SiO_2 and TiO_2. The authors used the TMM technique to achieve a sensitivity of 73 nm/RIU [52]. Aly et al. optimized the geometrical parameters of a 1D PhC, and tested the spectral characteristics of the structure by filling different cancer cells in the defect layer. The authors settled with a sensitivity of 2200 nm/RIU [53]. The transmission spectrum of a defected photonic crystal is analyzed in detail by Ramanujam and his team, where a very low sensitivity of 43 nm/RIU is achieved, which is very low [54]. A point defect-based 2D photonic crystal waveguide is studied for the detection of different types of cancer cells. In their work, the authors rely on the electric field analysis in the defect region and measured the reflected wavelength, which differentiated the normal cells from the cancer cells [55]. Ayyanar et al. investigated a dual-core photonic crystal fiber to detect various cancer cells like cervical and basal cells [56]. Sani et al. studied the bandgap characteristics in a 2D photonic crystal to differentiate cancer cells from normal cells [57]. Jabin et al. attempted to integrate a metal layer in the core of the photonic crystal fiber and studied the plasmonic behavior of the device. Further, the authors tested their device to distinguish cells infected with cancer cells in a broad wavelength band visible to NIR regime [58].

2 Theoretical Formulation

This chapter explores a 1D PhC, which is realized as a regular periodic arrangement of MgF_2 and ZnSe. A cavity/defect layer is formed at the center of the arrangement. A monolayer of graphene sheet is sandwiched between the defect layer and the dielectric layer. The alignment of the whole structural arrangement is $(MgF_2/ZnSe)^N$/Graphene/Defect/Graphene/$(MgF_2/ZnSe)^N$, which is represented in Fig. 2. The thickness of the layer MgF_2, ZnSe and Graphene is represented as d_A, d_B, and d_G, respectively. The cavity is loaded with different cancer cells. A 589-nm light,

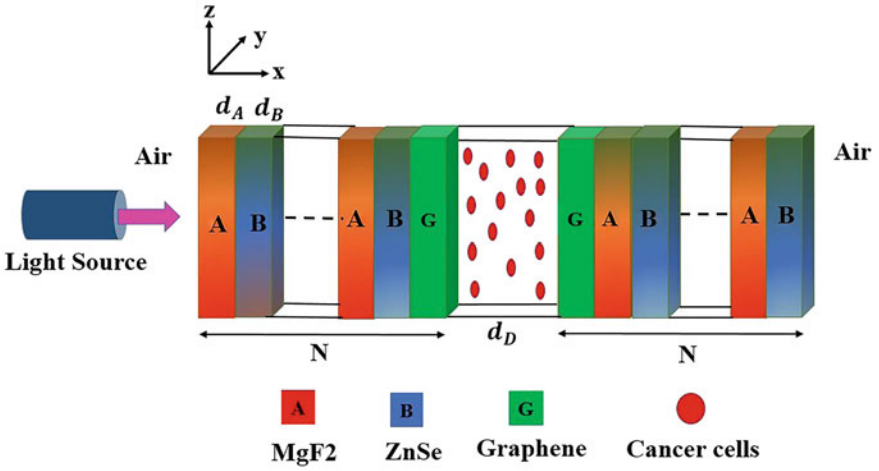

Fig. 2 Schematic of the proposed sensor

produced from a laser source, is made to strike the proposed structure normally along the *X*-*Z* plane.

The constituent material RI plays a significant part in finding the spectral response of the entire configuration. The RI of MgF_2 and ZnSe can be measured with the help of Sellemier equations [59, 60]:

$$n^2_{\mathrm{ZnSe}} = 4 + \frac{1.90\lambda^2}{\lambda^2 - 0.113} \tag{1}$$

$$n^2_{\mathrm{MgF2}} = 1 + \frac{0.48755\lambda^2}{\lambda^2 - 0.04338^2} + \frac{0.39875\lambda^2}{\lambda^2 - 0.09461^2} + \frac{2.31203\lambda^2}{\lambda^2 - 23.7936^2} \tag{2}$$

The dielectric permittivity of graphene is stated as [61]:

$$\varepsilon_G = \begin{bmatrix} \varepsilon_{Gt} & 0 & 0 \\ 0 & \varepsilon_{Gt} & 0 \\ 0 & 0 & \varepsilon_{G\downarrow} \end{bmatrix} \tag{3}$$

The terms ε_{Gt} and $\varepsilon_{G\downarrow}$ denote the normal and tangential components of permittivity, respectively. $\varepsilon_{G\downarrow} = 1$, and ε_{Gt} is expressed as below:

$$\varepsilon_{Gt} = 1 + i\frac{\sigma(\omega)}{\varepsilon_0 \omega d_G} \tag{4}$$

where, ω signifies the angular frequency, d_G denotes the graphene thickness and ε_0 is the permittivity of air. The surface conductivity (σ_ω) regulates the physical properties of graphene. The transfer matrix representation of the graphene layer

takes the form$M_G = \begin{bmatrix} 1 & 0 \\ -\sigma_G & 1 \end{bmatrix}$ for TE mode, $M_G = \begin{bmatrix} 1 & 0 \\ -\sigma_\omega & 1 \end{bmatrix}$, where σ_ω can be mathematically expressed by the Kubo formula [62] as written below:

$$\sigma_\omega = \sigma_\omega^{\text{intra}} + \sigma_\omega^{\text{inter}} \tag{5}$$

$$\sigma_\omega^{\text{intra}} = \left(\frac{ie^2}{8\pi\hbar}\right)\left[\frac{16K_BT}{\hbar\omega}\log\left(2\cosh\left(\frac{\mu_c}{2K_BT}\right)\right)\right] \tag{6}$$

$$\sigma_\omega^{\text{inter}} = \left(\frac{e^2}{4\hbar}\right)\left[H(\hbar\omega - 2\mu) - \frac{i}{2\pi}\times\left(\log\left(\frac{(\hbar\omega+2\mu)^2}{\hbar\omega - 2\mu^2 + (2K_BT)^2}\right)\right)\right] \tag{7}$$

where H denotes the Heaviside step function, K_B represents the Boltzmann constant, ω be the angular frequency, e is the electron charge, μ_c represents the chemical potential, and T is the temperature on Kelvin scale.

The field components can be written as:

$$\begin{pmatrix} E_p \\ H_p \end{pmatrix} = \begin{pmatrix} \exp\left(-iq_p y\right) & \exp\left(iq_p y\right) \\ -n_s\exp\left(-iq_p y\right) & n_s\exp\left(iq_p y\right) \end{pmatrix}\begin{pmatrix} A_p \\ B_p \end{pmatrix} \tag{8}$$

All the terms in Eq. (8) are defined in Ref. [41]. The field components between the adjacent layers of p and p+1 are stated as [42]:

$$\begin{pmatrix} E_p \\ H_p \end{pmatrix} = \frac{1}{2}\begin{pmatrix} \left[\exp\left(iq_p\alpha_p\right) + \exp\left(-iq_p\alpha_p\right)\right] & \left(-\frac{1}{\gamma_p}\right)\left[\exp\left(iq_p\alpha_p\right) - \exp\left(-iq_p\alpha_p\right)\right] \\ -\gamma_p\left[\exp\left(iq_p\alpha_p\right) - \exp\left(-iq_p\alpha_p\right)\right] & \left[\exp\left(iq_p\alpha_p\right) + \exp\left(-iq_p\alpha_p\right)\right] \end{pmatrix}\begin{pmatrix} E_{p+1} \\ H_{p+1} \end{pmatrix} \tag{9}$$

where, $\alpha_p = d_p \cos\theta_p$. Here, d_p and θ_p signify the thickness and incident angle, respectively. The widely accepted transfer matrix method (TMM) is manipulated for studying the spectral characteristics of the projected 1D PhC. The TMM describes the discrete layer p in matrix form, which can be stated as [42]:

$$M_p = \begin{bmatrix} \cos\sigma_p & \left(-\frac{i}{\varnothing_p}\right)\sin\sigma_p \\ -i\varnothing_p\sin\sigma_p & \cos\sigma_p \end{bmatrix} \tag{10}$$

For TE mode, σ_p and $\varnothing_p$ are defined as:

$$\sigma_p = \frac{2\pi}{\lambda} d_p n_p \cos\theta_p \quad \text{and} \quad \varnothing_p = n_p \cos\theta_p \tag{11}$$

The TMM of the entire structure can be calculated by multiplying the characteristics matrix of each layer and can be written as [45]:

$$M = (M_A M_B)^N M_{\text{MXene}} M_D M_{\text{MXene}} (M_A M_B)^N = \begin{bmatrix} M(1,\ 1) & M(1,\ 2) \\ M(2,\ 1) & M(2,\ 2) \end{bmatrix} \tag{12}$$

The transmission and reflection coefficients are stated as [44]:

$$t = \frac{2\gamma_0}{(M(1,\ 1) + M(1,2)\gamma_1)\gamma_0 + (M(2,\ 1) + M(2,2)\gamma_s)} \tag{13}$$

$$r = \frac{(M(1,\ 1) + M(1,2)\gamma_s)\gamma_0 - (M(2,\ 1) + M(2,\ 2)\gamma_s)}{(M(1,\ 1) + M(1,2)\gamma_s)\gamma_0 + (M(2,\ 1) + M(2,\ 2)\gamma_s)} \tag{14}$$

where, $\gamma_0 = \sqrt{\mu_0/\varepsilon_0} n_0 \cos\theta_0$ and $\gamma_s = \sqrt{\mu_0/\varepsilon_0} n_s \cos\theta_s$.

Lastly, transmittance (T) and reflectance (R) are numerically expressed as [42]:

$$T = \frac{\gamma_s}{\gamma_0} \left| t^2 \right| \quad \text{and} \quad R = |r|^2 \tag{15}$$

Absorbance can be computed as [43]:

$$A = 1 - T - R \tag{16}$$

3 Results Analysis

In this chapter, different cancer cells like breast, basal, and cervical cells are considered, which are received from different body parts in liquid form. The sensing principle relies on the contrast in index value of the normal and infected cells. The experimental refractive index (RI) data collected from references [63, 64] are enumerated in Table 1.

The geometrical parameters of the designed structure are properly optimized to accomplish a sharp and high-intensity resonant mode inside the bandgap. We consider $d_{\text{MgF2}} = 150$ nm, $d_B = 150$ nm, $d_G = 0.34$ nm, $\varepsilon_{\text{MgF2}} = 1.90$, $\varepsilon_B = 6.8$, and N=5. TMM is employed to analyze the transmission spectrum by changing the

Table 1 Cell's refractive index

Cell type	RI
Normal	1.35
Basal	1.38
Cervical	1.392
Breast	1.399

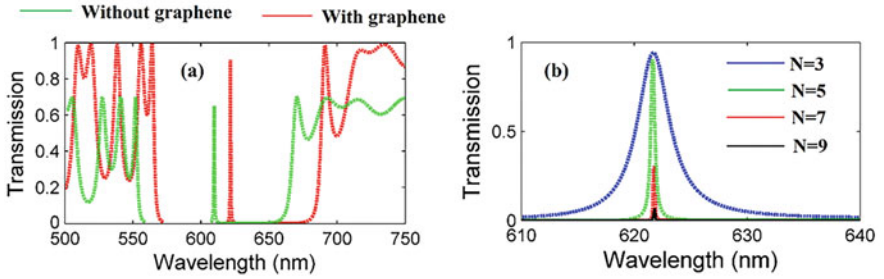

Fig. 3 (**a**) Effect of graphene layer on the transmittance spectrum (**b**) variation in the period of the crystal

width of the cavity region, angle of incidence, and chemical potential across the graphene sheet. Initially, an attempt is taken to show the effect of graphene on the transmission characteristics. As shown in Fig. 3a, by including the graphene layer, the intensity of the resonance mode increases, which is suitable for sensing purposes. With the presence of graphene, the overall transfer matrix is updated, which is the reason behind the red-shifting of defect mode wavelength. Figure 3b demonstrates the study of the defect mode characteristics with reference to different periods (N) of the photonic crystal. As, it can be seen at $N = 5$, the maximum intensity with the lowest FWHM is obtained, which is considered the most apposite result. For higher values of N, the FWHM is relatively higher and therefore not suitable from a sensor design point of view.

By setting D=500 nm, $\theta_{in} = 0^o$, $\mu_c = 0.2eV$, we simulated the proposed multilayer structure in COMSOL Multiphysics software to study the electric field propagation in the structure, which is represented in Fig. 4. Owing to the presence of graphene layer, most of the light is confined inside the defect layer thereby increasing the interaction between light and infiltrated cancer cells. An electric field intensity in the order of 10^3 V/m is observed inside the cavity layer and gradually decays to both sides of the defect layer.

For understanding the nature of variation of the defect mode, a colormap plot has been studied in Fig. 5, which shows the change in the transmission characteristics with respect to the wavelength and incident angle. In this figure, the high-intensity defect mode can be clearly seen inside the bandgap.

The transmission spectrum is examined for numerous selected cells at varied cavity layer thicknesses, which is depicted in Fig. 6. A substantial shift in the resonant mode is observed from normal to cancer-type cells. In particular, the resonant wavelength (λ_{res}) experiences a red-shift as we infiltrate the cavity layer from the normal cells to the cancerous cells. This shifting nature closely follows the standing wave condition [26]. At d_D= 500 nm, the λ_{res} is moved from 621.6 nm to 633.8 nm as the cell type is changed from normal to breast cancerous cells. At d_D= 600 nm, the λ_{res} experiences a total shift from 612.3 nm to 625.5 nm, at d_D= 700 nm, the λ_{res} undertakes a total shift from 604.8 nm to 618.8 nm. Similarly, at d_D= 800 nm, the λ_{res} experiences a total shift from 898.8 nm to 613.3 nm.

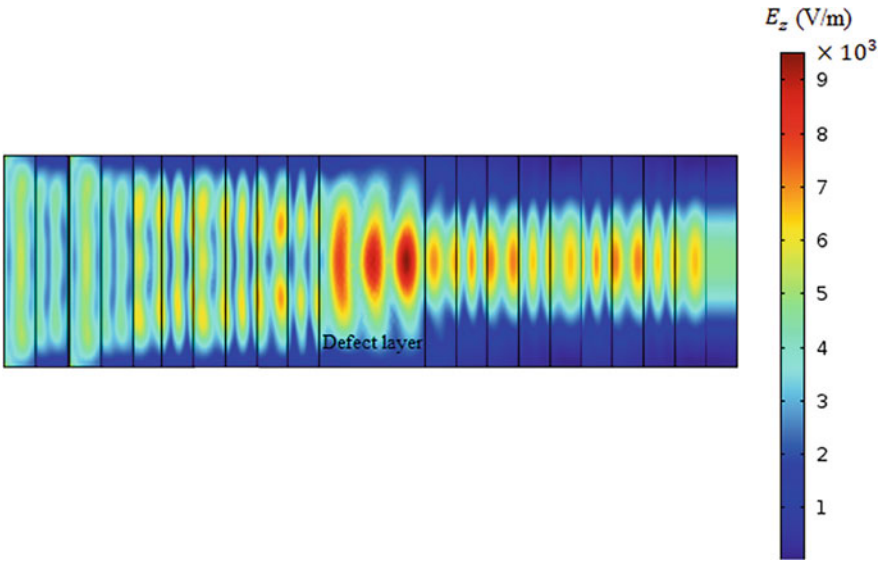

Fig. 4 The electric field distribution in the proposed structure

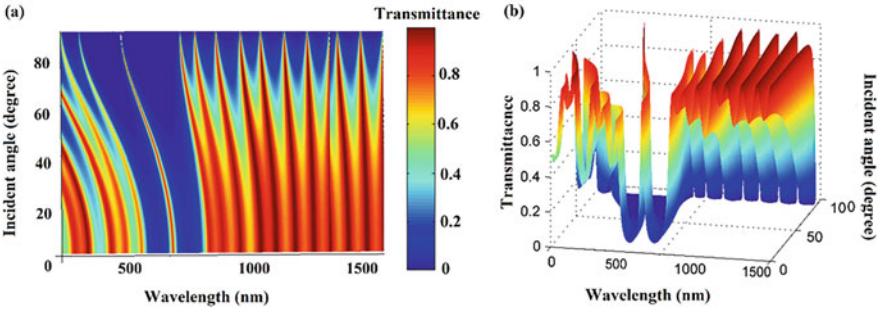

Fig. 5 Study of the colormap plot

Afterward, the incident angle is varied and the changes in the defect mode properties are studied as demonstrated in Fig. 7. By increasing the incident angle (θ_{in}) from 25° to 50°, the defect mode position experiences a blue shift. This analysis is carried out at all the considered values of d_D. The blue-shifting nature of the defect mode is in accordance with the Bragg condition [26].

A thorough analysis of transmission spectrum is performed at d_D= 500 nm and $\theta_{in} = 0^o$, by varying the number of graphene layers (L) from L = 1 to L = 4, which is illustrated in Fig. 8a. By incrementing the L value, it is perceived that λ_{res} is moved to higher wavelength. On the other hand, with an increase in L, the intensity of the resonant mode goes on decreasing. As L increases, the effective thickness of the proposed design increases, which in turn escalates the geometrical path difference. Due to this reason, the wavelength is red-shifted. Based on this analysis, we chose a

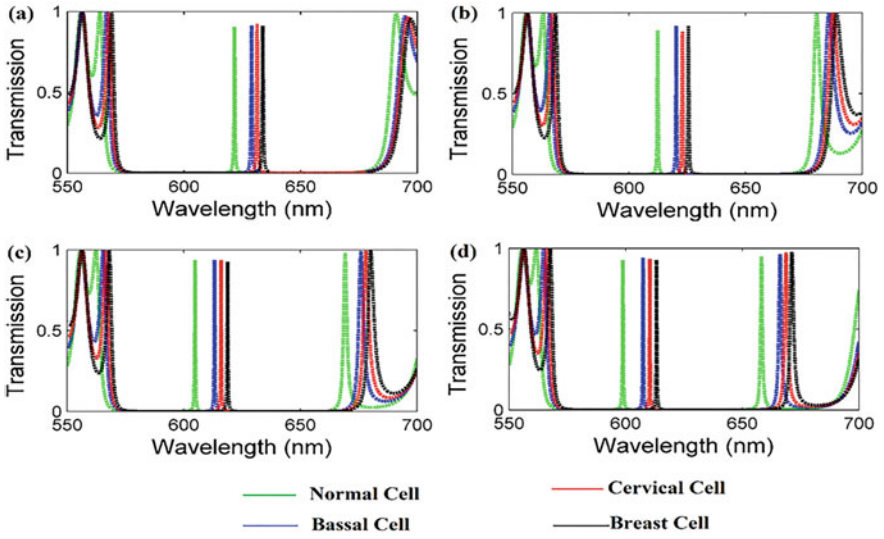

Fig. 6 Transmittance spectrum of different cells under normal incidence at (**a**) d_D= 500 nm, (**b**) d_D= 600 nm, (**c**) d_D= 700 nm, and (**d**) d_D= 800 nm

monolayer of graphene (L = 1) as the optimized condition, where the most desirable characteristics are attained. Further, the effect of chemical potential (μ_c) across the graphene sheet can have a noteworthy effect on the device performance, which is examined in Fig. 8b. Here, it is perceived that at a constant L, the λ_{res} is red-shifted with rise in the chemical potential. With a variation in the chemical potential, the permittivity of the graphene sheet is changed, hence the red-shifting nature is observed in the λ_{res}.

In Fig. 9, the solid line and the dashed line indicate the transmission characteristics at $\mu_c = 0.3\text{eV}$ and $\mu_c = 0.4\text{eV}$, respectively. From this figure, it is affirmed that by increasing the μ_c, the defect mode wavelength is moved to a higher wavelength value for the normal as well as the cancer cells, so μ_c can greatly affect the sensing performance. As the defect modes are formed within the bandgap, there is a possibility of absorption with different cells, and the same is analyzed in Fig. 10. As we change the cell type from the normal cells to the high refractive indexed cancer cells, the defect mode wavelength is red-shifted. Additionally, the absorption intensity increases for high-indexed cancer cells.

Evaluation of sensitivity is utmost important to judge the performance. It is explained as the ratio of a shift in the defect mode wavelength with respect to different cells under consideration. Sensitivity is written as [26]:

$$S(\text{nm/RIU}) = \frac{\Delta\lambda_{\text{res}}}{\Delta n} \tag{17}$$

The sensitivity analysis at different incident angles is presented in Fig. 11. It is concluded that the sensitivity shows a declining trend with a rise in the incidence

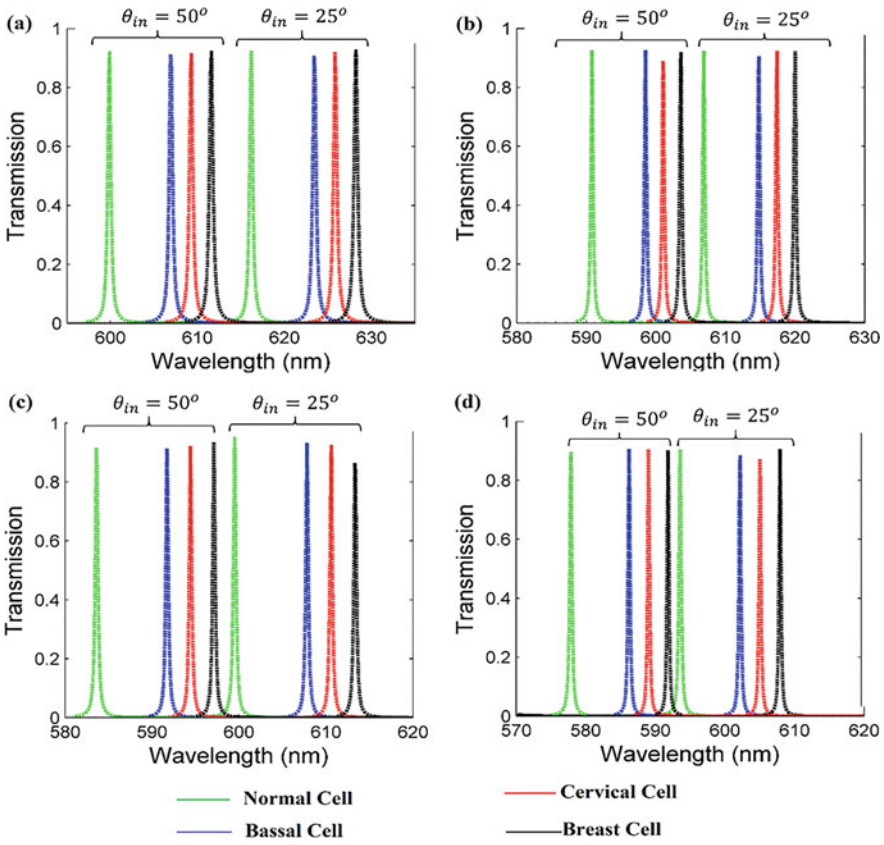

Fig. 7 Shift in the resonant modes for $\theta_{\text{in}} = 25^o$ and 50^o for (**a**) d_D= 500 nm, (**b**) d_D= 600 nm, (**c**) d_D= 700 nm, and (**d**) d_D= 800 nm

angle, and the sensitivity rises upon increasing the d_D. With the designed parameters d_D= 800 nm, and $\theta_{\text{in}} = 0^o$, the maximum sensitivity of 290 nm/RIU is accomplished.

Finally, other important performance parameters such as SNR, QF, resolution, and FoM are computed for different values of d_D at normal incidence, and summarized in Table 2.

4 Conclusions

This chapter presents a novel graphene-integrated photonic crystal configuration for the identification of numerous cancer cells. The layer thickness and incident angle can greatly control the spectral characteristics. The transmission spectrum is systematically scrutinized using TMM. The impact of chemical potential across the graphene sheet and the number of layers of graphene are studied on the sensing

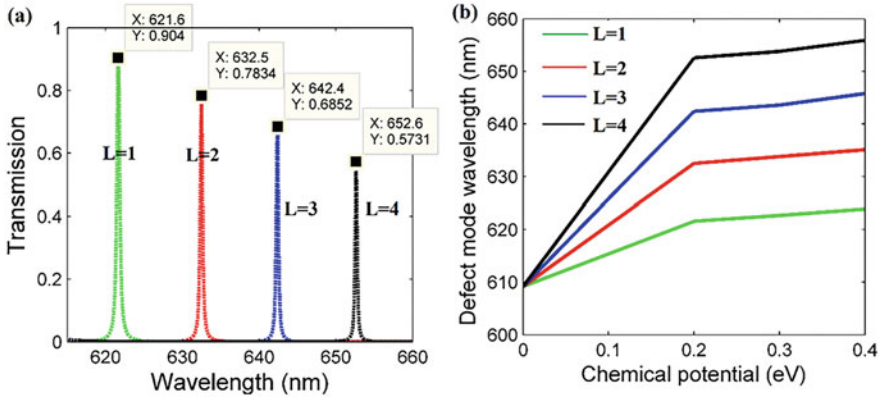

Fig. 8 (**a**) Transmittance as a function of L. (**b**) Effect of chemical potential on the defect mode position

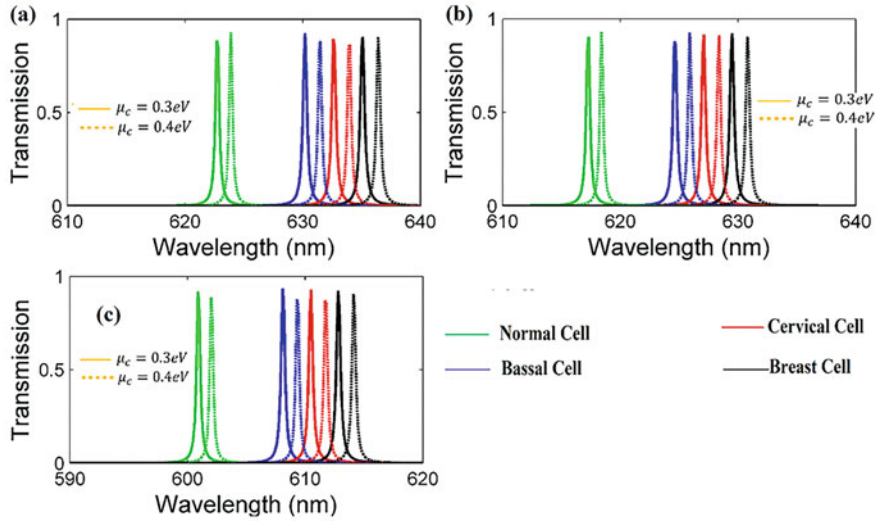

Fig. 9 Shifting the defect mode position w.r.t. μ_c at d_D= 500 nm for (**a**) $\theta_{in} = 0^{\circ}$ (**b**) $\theta_{\text{in}} = 25^{\circ}$ (c) $\theta_{\text{in}} = 50^{\circ}$

performance. The sensitivity is evaluated by assessing the defect mode wavelength shift between the normal cell and infected cancerous cells. A notable sensitivity of 290 nm/RIU, Q-factor of 2270.74, FoM of 1074.07 RIU^{-1}, SNR of 52.96, and resolution of 0.0668 has been accomplished with the designed structure. So, the authors are confident that the projected sensor can be a suitable candidate as a cancer cells sensor.

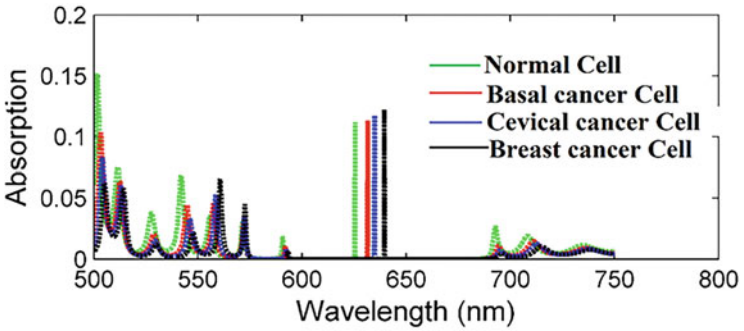

Fig. 10 Analysis of absorption spectra of different cells

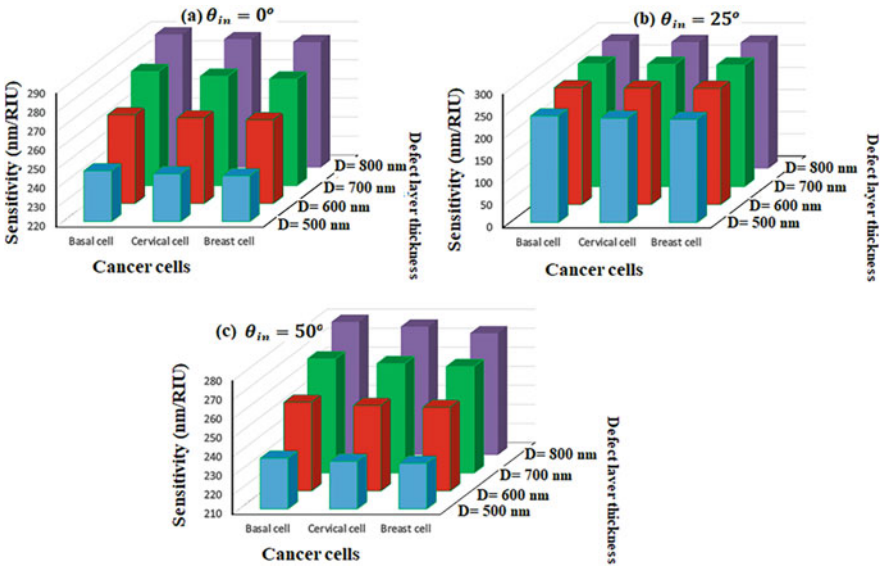

Fig. 11 Sensitivity analysis

Table 2 Measurement of sensor performance parameters

Cancerous cells	d_D (nm)	FoM (1/RIU)	QF	SNR	R (nm)
Basal	500	649.1	1640.5	19.4	0.121
Cervical		644.7	1646.3	25.7	0.113
Breast		642.1	1652.1	32.1	0.107
Basal	600	784.2	1808.2	23.5	0.103
Cervical		779.4	1815.8	31.1	0.096
Breast		776.4	1823.5	38.8	0.091
Basal	700	903.2	1960.6	27.0	0.090
Cervical		895.1	1969.6	35.8	0.084
Breast		890.3	1978.0	44.5	0.080
Basal	800	1074.0	2238.3	32.2	0.075
Cervical		1064.81	2255.7	42.5	0.070
Breast		1059.2	2270.7	52.9	0.066

References

1. Armstrong, E., & Dwyer, C. O. (2015). Artificial opal photonic crystals and inverse opal structures: Fundamentals and applications from optics to energy storage. *Journal of Material Chemistry C, 3*(24), 6109–6143.
2. Cucci, C., & Tornari, V. (2014). Photonic technologies for the safeguarding of cultural assets. In *Photonics for safety and security* (pp. 21–45). World Scientific Press.
3. Shen, H., Wang, Z., Wu, Y., & Yang, B. (2016). One-dimensional photonic crystals: fabrication, responsiveness and emerging applications in 3D construction. *RSC Advances., 6*(4505).
4. Yablonovitch, E. (1987). Inhibited spontaneous emission in solid–state physics and electronics. *Physical Review Letters, 58*, 2059–2062.
5. John, S. (1987). Strong localization of photons in certain in disordered dielectric superlattices. *Physical Review Letters, 58*, 2486–2489.
6. Ishizaki, K., Suzuki, K., & Noda, S. (2016). Fabrication of 3D photonic crystals toward arbitrary manipulation of photons in three dimensions. *Photonics., 3*(2), 36.
7. Panda, A., & Devi, P. P. (2021). Design and analysis of porous core photonic crystal fiber based ethylene glycol sensor operated at infrared wavelengths. *Journal of Computational Electronics, 20*, 943–957.
8. Pang, L., Nakagawa, W., & Fainman, Y. (2003). Fabrication of two-dimensional photonic crystals with controlled defects by use of multiple exposures and direct write. *Applied Optics., 42*(27), 5450–5456.
9. Panda, A., & Pukhrambam, P. D. (2020). Photonic crystal biosensor for refractive index based cancerous cell detection. *Optical Fiber Technology., 54*(102123).
10. Panda, A., & Pukhrambam, P. D. (2021). Analysis of GaN-based 2D photonic crystal sensor for real-time detection of alcohols. *Brazilian Journal of Physics, 51*, 481–492.
11. Baba, T., Mori, D., Inoshita, K., & Kuroki, Y. (2004). Light localizations in photonic crystal line defect waveguides. *IEEE Journal of Selected Topics in Quantum Electronics, 10*(3), 484–491.
12. Wellenzohn, M., et al. (2018). Design of a photonic crystal defect waveguide biosensor operating in aqueous solutions at 1.34 μm. *Proceedings, 2*, 1026.
13. Moghaddam, M. K., & Fleury, R. (2019). Slow light engineering in resonant photonic crystal line-defect waveguides. *Optics Express., 27*(18), 26229–26238.

14. Panda, A., & Pukhrambam, P. D. (2021). A theoretical proposal of high performance blood components biosensor based on defective 1D photonic crystal employing WS2, MoS2 and graphene. *Optical and Quantum Electronics, 53*, 357.
15. Panda, A., Pukhrambam, P. D., & Keiser, G. (2021). Realization of sucrose sensor using 1D photonic crystal structure vis-à-vis band gap analysis. *Microsystem Technologies, 27*, 833–842.
16. Panda, A., et al. (2018). Research on SAD-PRD losses in semiconductor waveguide for application in photonic integrated circuits. *Optik, 154*, 748–754.
17. Panda, A., & Pukhrambam, P. D. (2021). Investigation of defect based 1D photonic crystal structure for real-time detection of waterborne bacteria. *Physics B Condensed Matter, 607*(3), 412854.
18. Aly, A. H., et al. (2020). Theoretical study of hybrid multifunctional one-dimensional photonic crystal as a flexible blood sugar sensor. *Physica Scripta., 95*(3), 035510.
19. Goyal, A., Suthar, B., & Bhargava, A. (2021). Biosensor application of one-dimensional photonic crystal for malaria diagnosis. *Plasmonics, 16*, 59–63.
20. Sharma, S., & Kumar, A. (2021). Design of a biosensor for the detection of dengue virus using 1D photonic crystals. *Plasmonics*. https://doi.org/10.1007/s11468-021-01555-x
21. Abadla, M. M., & Elsayed, H. A. (2020). Detection and sensing of hemoglobin using one-dimensional binary photonic crystals comprising a defect layer. *Applied Optics, 59*(2), 418–424.
22. Algorri, J. F., Zografopoulos, D. C., Tapetado, A., Poudereux, D., & Sánchez-Pena, J. M. (2018). Infiltrated photonic crystal fibers for sensing applications. *Sensors., 18*(12), 4263.
23. Panda, A., & Pukhrambam, P. D. (2022). Design and analysis of 1D photonic crystal doped with magnetized cold plasma defect for application of single/multi-channel tunable narrowband filter. *Physica Scripta, 97*, 065507. https://doi.org/10.1088/1402-4896/ac6f92
24. Panda, A., Pukhrambam, P. D., Dadure, P., & Pakray, P. (2022). Application of machine learning for accurate detection of hemoglobin concentrations employing defected 1D photonic crystal. *Silicon.* https://doi.org/10.1007/s12633-022-01926-x
25. Abinash, P., Vigneswaran, D., Pukhrambam, P. D., Ayyanar, N., & T. K. (2022). Nguyen, design and performance analysis of reconfigurable 1D photonic crystal biosensor employing Ge2Sb2Te5 (GST) for detection of women reproductive hormones. *IEEE Transactions on Nanobioscience, 21*(1), 21–28.
26. Panda, A., Pukhrambam, P. D., Wu, F., & Belhadj, W. (2021). Graphene-based 1D defective photonic crystal biosensor for real-time detection of cancer cells. *European Physical Journal - Plus, 136*, 809.
27. Falkovsky, L. A., & Pershoguba, S. S. (2007). Optical far-infrared properties of a graphene mono layer and multilayer. *Physical Review B., 76*(15), 153410.
28. Mak, K. F., Shan, J., & Heinz, T. F. (2010). Electronic structure of few-layer graphene: Experimental demonstration of strong dependence on stacking sequence. *Physical Review Letters, 104*, 176404.
29. Geim, A. K. (2009). Graphene: Status and prospects. *Science, 324*, 1530–1534.
30. Novoselov, K. S. (2007). The rise of graphene. *Nature Materials, 6*, 183–191.
31. Bonaccorso, F., Sun, Z., Hasan, T., & Ferrari, A. C. (2010). Graphene photonics and optoelectronics. *Nature Photonics, 4*, 611–622.
32. Stauber, T., Peres, N. M. R., & Geim, A. K. (2008). Optical conductivity of graphene in the visible region of the spectrum. *Physical Review B., 78*(8), 085432.
33. Schedin, F., Geim, A., Morozov, S., Hill, E., Blake, P., Katsnelson, M., et al. (2007). Detection of individual gas molecules adsorbed on graphene. *Nature Materials, 6*, 652.
34. Pop, E., Varshney, V., & Roy, A. K. (2012). Thermal properties of graphene: Fundamentals and applications. *MRS Bulletin, 37*, 1273–1281.
35. Rahman, M. R., Rashid, M. M., Islam, M. M., & Akanda, M. M. (2019). Electrical and chemical properties of graphene over composite materials: A technical review. *Material Science Research India, 16*(2). https://doi.org/10.13005/msri/160208

36. Liao, G., Hu, J., Chen, Z., Zhang, R., Wang, G., & Kuang, T. (2018). Preparation, properties, and applications of graphene-based hydrogels. *Frontier in Chemistry, 6*, 450.
37. Nouman, W. M., El-Ghany, S. E. S. A., Sallam, S. M., et al. (2020). Biophotonic sensor for rapid detection of brain lesions using 1D photonic crystal. *Optical and Quantum Electronics, 52*, 287.
38. Zaky, Z. A., Ahmed, A. M., Shalaby, A. S., & Aly, A. H. (2020). Refractive index gas sensor based on the Tamm state in a one-dimensional photonic crystal: Theoretical optimisation. *Scientific Reports., 10*, 9736.
39. Shi, X., Zhao, Z. S., & Han, Z. H. (2018). Highly sensitive and selective gas sensing using the defect mode of a compact terahertz photonic crystal cavity. *Sensors and Actuators, 274*, 188–193.
40. Ahmed, A. M., & Mehaney, A. (2019). Ultra-high sensitive 1D porous silicon photonic crystal sensor based on the coupling of Tamm/Fano resonances in the mid-infrared region. *Scientific Reports, 9*, 6973.
41. Aly, A. H., et al. (2020). Biophotonic sensor for the detection of creatinine concentration in blood serum based on 1D photonic crystal. *RSC Advances., 10*, 31765–31772.
42. Panda, A., & Pukhrambam, P. D. (2021). Investigation of defect based 1D photonic crystal structure for real-time detection of waterborne bacteria. *Physica B Condensed Matter., 607*(3), 412854.
43. Abadla, M. M., & Hussein, A. E. (2020). Detection and sensing of hemoglobin using one-dimensional binary photonic crystals comprising a defect layer. *Applied Optics, 59*(2), 418–424.
44. Bouzidi, A., Bria, D., Falyouni, F., Akjouj, A., Lévêque, G., Azizi, M., et al. (2017). A biosensor based on one dimensional photonic crystal for monitoring blood glycemia. *Journal of Materials and Environmental Science, 8*(11), 3892–3896.
45. Elsayed, H. A., & Mehaney, A. (2020). Theoretical verification of photonic crystals sensor for biodiesel detection and sensing. *Physica Scripta, 95*, 085507.
46. Fu, J., Chen, W., & Lv, B. (2016). Tunable defect mode realized by graphene-based photonic crystals. *Physics Letters A, 380*, 1793–1798.
47. Fan, H. M. (2014). Tunable plasmonic band gap and defect mode in onedimensional photonic crystal covered with graphene. *Journal of Opticals., 16*, 125005.
48. Abd El-Aziz, O. A., Elsayed, H. A., & Sayed, M. I. (2019). One-dimensional defective photonic crystals for the sensing and detection of protein. *Applied Optics, 58*(30), 8309–8315.
49. Katz, R., & Edelson, M. (2009). *The cancer-fighting kitchen: nourishing, big-flavor recipes for cancer*. Ten Speed Press, Crown Publishing Group.
50. Bray, F., Ferlay, J., Soerjomataram, I., Siegel, R. L., Torre, L. A., & Jemal, A. (2018). Global cancer statistics 2018: GLOBOCAN estimates of incidence and mortality worldwide for 36 cancers in 185 countries. *CA: A Cancer Journal for Clinicians, 68*, 394–424.
51. Yaroslavsky, A. N., et al. (2012). High-contrast mapping of basal cell carcinomas. *Optics Letters., 37*(4), 644–646.
52. Bijalwan, A., Singh, B. K., & Rastogi, V. (2021). Analysis of one-dimensional photonic crystal based sensor for detection of blood plasma and cancer cells. *Optik., 226*(1), 165994.
53. Aly, A. H., & Zaky, Z. A. (2019). Ultra-sensitive photonic crystal cancer cells sensor with a high quality factor. *Cryogenics, 104*, 102991.
54. Ramanujam, N. R., Amiri, I., Taya, S. A., Olyaee, S., Udaiyakumar, R., & Pandian, A. P. (2019). Enhanced sensitivity of cancer cell using one dimensional nano composite material coated photonic crystal. *Microsystem Technologies, 25*, 189–196.
55. Panda, A., & Devi, P. P. (2020). Photonic crystal biosensor for refractive index based cancerous cell detection. *Optical Fiber Technology., 54*, 102123.
56. Ayyanar, N., Raja, G. T., Sharma, M., & Kumar, D. S. (2018). Photonic crystal fiber-based refractive index sensor for early detection of cancer. *IEEE Sensors Journal, 18*, 7093–7099.

57. Sani, M. H., & Khosroabadi, S. (2020). A novel design and analysis of high-sensitivity biosensor based on nano-cavity for detection of blood component, diabetes, cancer and glucose concentration. *IEEE Sensors Journal, 20*(13), 7161–7168.
58. Jabin, M. A., et al. (2019). Surface plasmon resonance based titanium coated biosensor for cancer cell detection. *IEEE Photonics Journal, 11*(4), 1–10.
59. https://refractiveindex.info/?shelf=main&book=ZnSe&page=Marple
60. https://refractiveindex.info/?shelf=main&book=MgF2&page=Dodge-o
61. Kumar, A., Singh, P., & Thapa, K. B. (2020). Study of super absorption properties of 1D graphene and dielectric photonic crystal for novel applications. *Optical and Quantum Electronics, 52*, 423.
62. Ghasemi, F., Entezar, S. R., & Razi, S. (2019). Terahertz tunable photonic crystal optical filter containing graphene and nonlinear electro-optic polymer. *Laser Physics, 29*, 056201.
63. Liang, X. J. AQ Liu, XM Zhang, PH Yap, TC Ayli, HS Yoon (2005). Determination of refractive index for single living cell using integrated biochip. In *Solid-State Sensors, Actuators and Microsystems, 2005. Digest of Technical Papers*. TRANSDUCERS'05. IEEE (Vol. 2, pp. 1712–1715).
64. Sharan, P., Bharadwaj, S. M., Gudagunti F.D., & Deshmukh P.. (2014). Design and modelling of photonic sensor for cancer cell detection. In *Impact of E-Technology on US (IMPETUS), IEEE International Conference on the*, (pp. 20–24).

Smart Nanobiosensing for COVID-19 Diagnosis

Sayak Roy Chowdhury and Monidipa Ghosh

Abstract

Repeated public health menace caused by the pathogenic coronaviruses, including the present COVID-19 caused by the Severe Acute Respiratory Syndrome Coronavirus-2 (SARS-CoV-2), has had devastating aftereffects, and an intense need for a promising solution has developed. Currently, reverse transcription polymerase chain reaction (RT-PCR) is being extensively utilized for detecting the virus from biological samples. However, it has certain limitations and fails to provide accurate and reliable results. Consequently, simple, portable, and point-of-care testing enabled biosensors have turned up as the most efficient and sustainable diagnostic tool. This review provides a brief introduction about the present global scenario due to the ongoing pandemic and concise information regarding the morphological details of coronaviruses. Thereafter, a summarized data is presented regarding the contemporary biosensing platforms fabricated to specifically identify fatal coronaviruses with particular emphasis towards surface plasmon resonance (SPR)-based biosensor, field-effect transistor (FET)-based biosensor, colorimetric sensors, fluorescence-based sensors, and electrochemical (EC) immunosensors. A comparative analysis of the sensors is also presented along with a few future perspectives that can aid the development of smart and futuristic sensors. This review is expected to provide details to researchers about the ongoing biosensor-related experimentations and encourage them to develop innovative detection devices to manage the current pandemic.

S. R. Chowdhury · M. Ghosh (✉)
Department of Biotechnology, National Institute of Technology Durgapur, Durgapur, India
e-mail: monidipa.ghosh@bt.nitdgp.ac.in

G. Dutta (ed.), *Next-Generation Nanobiosensor Devices for Point-Of-Care Diagnostics*, https://doi.org/10.1007/978-981-19-7130-3_6

Keywords

Biosensor · Coronavirus · Point-of-care testing · SARS-CoV-2 · COVID-19

1 Introduction

Over the last few decades, viral outbreaks have led to several life-threatening respiratory diseases, with the latest and most severe one being COVID-19. Severe Acute Respiratory Syndrome Coronavirus-2 (SARS-CoV-2) is the causative agent, and it started spreading from late 2019 following its emergence in Wuhan, a city in China. Reports show that the virus majorly transmits through respiratory droplets, aerosols, contact with the abiotic surface, etc. [1, 2]. Moreover, asymptotic infections and consequent transmission have made situations even worse [3]. A recent escalation in the frequency of viral diseases has resulted in global pandemics and severe economic loss. Repeated fatal human health hazards caused by the actively mutating coronavirus such as the Severe Acute Respiratory Syndrome (SARS) in 2002 [4], the Middle East Respiratory Syndrome (MERS) [5] in 2012, and the present COVID-19 has raised concerns regarding the development of proper and effective treatment strategies.

In order to develop potential vaccines and therapeutic methods, it is crucial to understand viral pathogenicity, contagiousness, and transmission properties, which can be possible only after obtaining specific information regarding the viral genome, associated protein structures, and corresponding host immunologic responses. Presently the most effective detection method in use is the real-time quantitative polymerase chain reaction (RT-qPCR) [6]. However, it has several drawbacks like prolonged experimentation periods (around 4 hrs.) and delayed report results (1–3 days) [7]. Moreover, it is prone to higher rates of false-positive and false-negative results, requires skilled personnel and advanced kits to execute the tests, making the process less economic. Additionally, some other techniques are also available like computed tomography (CT) scans of the chest, enzyme-linked immunosorbent assay (ELISA) based antibody detection methods, lateral flow immunochromatographic strip (LFICS), and automated chemiluminescence assay [7]. However, each has some drawbacks, like CT scan-based diagnosis is available only in well-developed city hospitals and not in rural ones. Moreover, expert radiologists must analyze the results, and the method cannot confirm if the disease is caused by SARS-CoV-2 or any other pathogen. Meanwhile, the antibody targeting assays cannot provide reliable results for asymptotic patients and cannot help efficiently for early diagnosis as it takes some time (approximately 10 days) to trigger the antibody response. Thus, there is an unprecedented need for a fast, simple, cost-effective yet sensitive and efficient detection system.

Analytical ready-to-use devices like biosensors with features like easy portability, simple instrumentation, miniaturization, high specificity, fast and accurate diagnosis [8] can be a sustainable choice to control the spreading of viral infection and pathology. Timely detection and following recognition of the pathogens with

reasonable accuracy is essential [9]. Consequently, biosensors capable of generating fast reproducible results and having properties mostly superior to conventional assaying techniques have found enormous applications in current medical diagnostic fields [10].

In this review, composite information about the recent contributions made to fabricate various potential biosensing devices is presented, along with background knowledge regarding the present global scenario owing to the viral pandemic. Currently, the development of biosensors for efficacious detection of coronavirus is a work in progress. Hence, the information summarized in this review can help researchers understand the present situation regarding biosensor-related explorations and experimentations. Thus, facilitating the formulation of new strategies to construct unique state-of-the-art devices, enabling faster recognition of the pathogens and accelerating disease diagnosis, control, and establishment of potential therapeutic remedies.

2 Coronavirus

Sudden and rapid global development and excessive anthropogenic influences have elevated the rates of pathogen transference resulting in viral pandemics. Three serious viral epidemics in recent decades have created enough fatality and raised alarms making the world and the scientific community look at the *Coronaviridae* family differently. The emergence of the unknown viral type referred to as severe acute respiratory syndrome coronavirus (SARS-CoV) in 2002 imposed a critical threat by spreading across nearly about 26 countries with higher than 8000 reported cases, including 900 plus deaths indicating a mortality rate of 11% [11]. Later again, in 2012, the middle east respiratory syndrome coronavirus (MERS-CoV) originating in bats was transmitted to humans via dromedary camel and caused significant casualties with a much higher mortality rate of about 35% with 2000 plus cases and deaths beyond 800 [12]. Lastly, the present COVID-19 global pandemic caused by the novel SARS-CoV-2 rising from Wuhan city in China. As of December 2020, the virus has spread across 216 countries with 67,780,361 confirmed cases and 1,551,214 deaths [13].

2.1 Structure and Morphology

Coronaviruses belonging to the *Coronavirinae* subfamily are highly virulent RNA viruses with single-stranded, enveloped structures and a positive sense genome. The virus can be grouped into four different genera, namely alphacoronavirus (αCoV), betacoronavirus (βCoV), gammacoronavirus (γ CoV), and deltacoronavirus (δCoV) [14]. So far, seven different pathogen strains have been discovered, including HKU1, 229E, NL63, and OC43—and the three most infectious ones viz., SARS-CoV MERS-CoV, and SARS-CoV-2. The last three belong to the novel βCoVs and have proved to be a severe threat for humans and animals alike [15, 16].

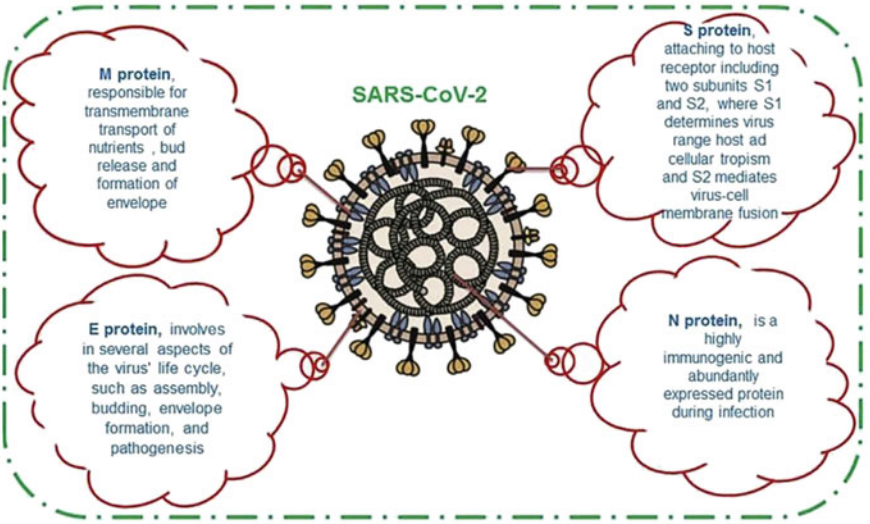

Fig. 1 Schematic illustration of SARS-CoV-2 structure and four structural proteins (Reprinted with permission from Ref. [21], Copyright 2020, Elsevier)

SARS-CoV-2, a member of the *Sarbecovirus* subgenus, likewise has a diameter ranging from 50nm to 200 nm in size and a large genome of approximately 30Kb encoding around 9860 amino acids [7, 17]. The viral surface is characterized by club-like spike projections made of structural spike (S) glycoproteins that appear like a crown under the electron microscope (crown in Latin is "coronam," hence the name "coronavirus") [18]. The S protein interacts with the Angiotensin-Converting Enzyme 2 (ACE2) receptors on the host cells, helping the virus to adhere. Subsequently, the pathogen enters the cellular system, causing the following complications [19]. Other structural proteins like the nucleocapsid (N) protein support and hold the viral genome, and the small envelope (E) and matrix (M) proteins along with the S protein help form the envelope structure. The viruses have a unique RNA structure comprising of a 5′ cap and a 3′ poly (A) tail; thus, they can mimic an mRNA facilitating its easy translation within the host cells [20]. Figure 1 schematically illustrates the SARS-CoV-2 structure along with all the four structural proteins.

2.2 Origin, Natural Reservoirs, and Intermediate Hosts of SARS-CoV-2

Initially, on discovering that the infected people had exposure to a live seafood market, it was suspected that the virus might have a zoonotic origin. Subsequently, the sequential analysis of the viral genome revealed an identity of about 88% between SARS-CoV-2 and two SARS-like CoVs in bats, namely bat-SL-

CoVZC45 and bat-SL-CoVZXC21. Moreover, 79% identity with SARS-CoV and 50% with MERS-CoV were also observed [22]. Ideas regarding the ancestral similarity between the human SARS-CoV-2 and bat CoV can also be supported by the fact that a 96.2% overall identity in genomic sequence exists between SARS-CoV-2 and Bat CoV RaTG13 [19]. Several reports prove that the virus has been transmitted to humans through animals like bats, camels, etc., considered as a natural reservoir for the virus and acting as intermediate hosts [11]. Additionally, sequential identities detected between the CoVs in pangolins and SARS-CoV-2, along with studies reporting similar ACE2 receptor residues in snakes and turtles, indicate to them as the probable alternative intermediate hosts [23].

2.3 Transmission of Novel SARS-CoV-2

The virus exhaled by the infected person remains active and airborne for an extended time and once inhaled, causes infection. Other possible modes of transference can be through contact with any infected surface and then passing it via the nasal or oral routes [4], skin to skin transmissions, improper or partial sanitizations after handling patients, etc. The pathogen remaining viable on metal surfaces can also infect individuals contacting frequently. The fecal route can also potentially transmit the disease, as the stool samples from patients, when detected, contain live and active viruses [24]. As a result of various investigations, it is observed that the virus can remain stable in stool samples for approximately 4 days [25] and in sewage water for about 3 days to 3 weeks [26], retaining its pathogenicity. So, virus-laden aerosols generated during sewage water treatment containing stool samples from infected patients can effectively spread the disease. Hence, proper monitoring and implementation of safer treatment strategies have become a need of the hour. Viral cells can also be efficiently transferred by airborne particulate matter. Fine particulate matters ladened with viral cells when inhaled can cause severe infections as it may help the cells get direct access to the deep alveolar tissue and tracheobronchial regions, mediating acute cellular damage [4]. Further investigations can help adequately understand the role of particulate matter in viral transmission, which might help develop proper techniques to control further spreading.

2.4 Viral Pathogenesis and Cellular Replication

The pathogenesis of SARS-CoV-2 is initiated by recognition and binding to specific receptors on host cells, followed by entry through membrane fusion [27]. Studies have shown that the ACE2 acts as the major cell receptor for the virus [28], and higher expression of the particular receptor protein on the alveolar epithelial cells of lungs and the enterocytes of the small intestine explains the reason for them being the primary target sites. The spike glycoprotein covering the viral surface attaches to the ACE2 receptors through the Receptor Binding Domain (RBD) and establishes the contact [18, 29, 30]. Following the binding, the cell surface-associated

transmembrane protease serine 2 (TMPRSS2) protein mediates the cleavage of the cell membrane. Then, the virion entering the host cell releases the genomic RNA into the cytoplasm and protein is generated via its translation, which helps produce new RNAs. While cellular development, a strand of the virion enters the Golgi body and helps evolve several new virions that are then released from the cell. Thus, a particular virion gives rise to several new virions which further infect new host cells. Various theories suggest that the mucosal epithelium of the upper respiratory tract, including the pharynx and the nasal cavity, serves as the primary replication site for the virus [31].

2.5 Specific Biomarkers for Diagnosing COVID-19

Laboratory-based detection of COVID-19 is majorly based on the selection of appropriate biomarkers. The biomarkers generally preferred for the identification of positive individuals are all summarized below.

Viral Genomic RNA

Conserved genes or genes with higher expression rates encoding various structural proteins of SARS-CoV-2 virus, like the genes for the spike glycoprotein (S gene), envelop protein (E genes) and nucleocapsid protein (N genes) along with the genes of the non-structural proteins like RNA-dependent RNA polymerase (RdRp) and replicase open reading frame 1a/b (ORF1a/b) genes are considered to be the favorable targets for detection involving RT-qPCR assays [6, 32]. Experimental results have confirmed that specific primers designed for these particular gene targets show high sensitivity for the novel SARS-CoV-2 and cross-reaction with similar corona viruses (MERS, OC43, and 229E) are completely prevented [33]. The sequential similarity of at least 79% between SARS-CoV-2 and SARS-CoV [22, 36] makes it mandatory to develop specific and unique primers and guide RNAs (gRNAs) to interact specifically with the novel pathogen. Out of several works already made, it is worth mentioning the work of Park et al. [34], who have designed two sets of primers targeting a specific region present exclusively within the genome of SARS-CoV-2, excluding the chances of reaction with other viruses. Moreover, Broughton and his team developed a novel gRNA specifically targeting the N protein gene of SARS-CoV-2 having no cross-reactivity for SARS-CoV [35]. Furthermore, extensive experimental analysis conducted by Kim et al. [36] pointed out that assays targeting the N gene have about 7–43 folds higher sensitivity than those targeting the RdRp gene. Thus, it is evident that at present various studies and associated research are in progress to identify more potential genome-related biomarkers and corresponding detection methodologies that can ease up the diagnosis process so that timely treatment can be initiated.

Viral Antigens

The SARS-CoV-2 virus is assumed to have approximately 28 proteins [37]. Most of them, including all the structural proteins and the entire virus itself, are considered

potential antigenic biomarkers that can help effectively diagnose COVID-19. The S and N proteins are essential biomarkers for disease diagnosis and are primarily targeted for developing various detection methods [38, 39]. Jiang and his co-workers [40], in order to examine the antibody responses of convalescent-phase patients designed a proteome microarray consisting of about 18 out of the 28 assumed viral proteins and on monitoring the assay results it revealed that a 100% response was recorded mainly for the protein N, S1, ORF9b, and NSP5. Several investigations and developmental research are already being carried on for detecting more responsive antigens, which can be rapidly detected and help accelerate the overall diagnosis process.

Host Antibodies

The onset of the COVID-19 disease triggers a substantial immunogenic response in the host system. Antibodies generated against the virus can be desirable biomarkers for efficient diagnosis. Basic concepts of immunology suggest that primarily the immunoglobulin M (IgM) defends the host cells from the pathogen, but later on the immunoglobulin G (IgG) is produced to develop a prolonged, specific and adaptive immune response with a definite memory enabling the system to fight against the virus [41]. Time series based statistical analysis carried out for positive cases by Pan and his team [42] revealed that a colloidal gold-based immunochromatographic assay had different levels of sensitivity for detecting combinations of IgM and IgG at different time phases after the onset of the disease ranging from 11.1% during the early phase (1–7 days), to 92.9% in the intermediate phase (8–14 days), and 96.8% at the late phase (after 15 days). However, it is mostly observed that the antibodies IgM and IgG are detected only after 3–6 days and 8 days from the onset [46, 47], so they cannot be considered suitable targets for examining the diseased individuals at early stages.

Predictive Algorithms for Discovering Potential Biomarkers

Discovery of novel and potential biomarkers becomes essential when the lab-based assays fail to confirm if the patients with symptoms are positive. So, to avoid slowing down the clinical diagnosis process, several Artificial Intelligence (AI) based predictive algorithms are developed that can effectively handle a considerable number of samples and provide accurate information related to specific characteristics that help assess the health conditions of the individuals. Peng et al. [43] had thoroughly monitored 174 clinical characteristics of COVID positive patients using four advanced AI algorithms and discovered 18 crucial diagnostic factors distinctly associated with COVID-19 affected cases. Some significant ones were the overall white blood cell count (WBC), eosinophil count, eosinophil ratio, 2019 new Coronavirus RNA (2019n-CoV), and serum amyloid A (SAA). An abnormal rise in the count of cytokines like interleukin-6 (IL-6), IL-10, IL-2, and interferons-γ (IFN-γ) in patients with severe conditions indicated that proinflammatory cytokine storm is related to the disease acuteness [44, 45] and confirmed cytokines to be an essential biomarker for determining coronavirus disease prognosis. Table 1 illustrates various

Table 1 Diagnostic biomarkers and indicators available for identification of COVID-19

Diagnostic biomarkers	Mechanism/ mode of action	Sample/instrument	Comments
Lung	Observation of clinical symptoms	CT scanning of the chest	Availability limited to modern urban hospitals
RNA	Viral genome	Throat/Pharyngeal/Oropharyngeal swab/Nasal swab, Deep Sputum, BALF, Feces/Rectal swab, Urine, Aerosols	High rates of false-negative results
Whole virus and antigen	Virulent viral proteins	Throat/Pharyngeal/Oropharyngeal swab/Nasal swab, Deep Sputum, BALF, Feces/Rectal swab, Urine, Aerosols	Requirement of ultrasensitive detection approaches
Host antibody	Host immunogenic responses	Human blood	Susceptible to higher false-positive results
Cytokines	A severe rise in cytokine levels	Blood samples	Helps predicting severity of COVID-19

diagnostic biomarkers and indicators available for the recognition and identification of COVID-19.

2.6 Clinical Specimens for COVID-19

Efficient collection of suitable specimens is also a critical step in determining the success of the diagnosis process. To date, specimens from the upper and lower respiratory tract including the respiratory secretions have been diagnosed [46]. Exhaustive investigations have led to the detection of the fatal virus from nasopharyngeal [47, 48], oropharyngeal [48, 49], throat [50], rectal [51, 52] and conjunctival swabs [53, 54] and also in sputum [55], and bronchoalveolar lavage fluid (BALF) [56–58]. Identification of the pathogen in stool [49, 59, 60], urine [51, 61], and saliva samples [41, 62] have helped researchers investigate other probable routes of transmission and strategize better remedial options.

For critical patients with developing clinical conditions, diagnosis of lower respiratory tract samples has been essential despite having negative results for specimens from the upper respiratory tract [63]. The reason being the primary distribution of ACE2 receptors on alveolar type II epithelial cells [23], indicating that these sites in the lower respiratory tract including sputum, tracheal aspirates, and BALF will have higher viral loads. Furthermore, collecting nasopharyngeal or throat swab specimens from the upper respiratory tract can create a sense of discomfort and induce sneezing or coughing. Consequently, the medical personnel get exposed to the aerosols, which can have serious aftereffects. Simple and safe methods like

sputum induction proven to be beneficial for diagnosing respiratory diseases can also be utilized by healthcare workers [64].

Frequent detection of SARS-CoV-2 virus in stool, urine, saliva, and conjunctival swabs has led to extensive investigation of these non-respiratory specimens. RT-PCR and associated assays confirmed the presence of SARS-CoV-2 in saliva samples of 11 out of 12 COVID-19 patients. After initiating treatment, a downward trend was observed on monitoring the viral load in saliva samples serially [41]. Moreover, studies were also carried out to detect the viral RNA in posterior oropharyngeal saliva samples. Positive results were obtained from about 87% of the patients, and it was observed that the load of the virus was at its peak in the first few days from the initiation of the disease and reduced gradually with time [62]. Hence these investigative analyses and experiments confirmed that even saliva samples are a preferable, reliable and non-invasive source for diagnosis, tracking, and regulation of COVID-19. Furthermore, reports on RT-PCR based assays have put forward certain information showing that about 2 out of 60 COVID-19 patients have SARS-CoV-2 cells present in their tear and conjunctival swab samples [54]. But, with the ratio of positive cases being very less further evaluations are still in progress.

3 Contemporary Biosensing Devices for Detection of Coronaviruses

Biosensors are portable analytical devices that transform biological reactions into quantifiable signals. Enzymes, antibodies, functional DNA/RNA probes, cellular receptors, or biomimetic compounds, etc. [65] immobilized over a transducer surface are used as the biorecognition component that recognizes and selectively interacts with the specific analyte present in the sample solution. As a result, a biochemical response is generated and converted by the transducer into an electrical signal and transmitted to a suitable signal processor. Finally, the processed, amplified, and noise filtered signal is passed onto a digital detection module, and appropriate information about the analyte concentration is retrieved [66–68].

One of the advantageous features of biosensors increasing its applicability in medical diagnostics is point-of-care testing. The device enables the execution of diagnostic tests anywhere near the patients producing rapid and accurate results. Following this quick diagnosis, infected individuals can be identified early, and the medical attention provided after that can help prohibit the aggressively progressing infection [69]. Contemporary sensing devices having advanced specificity and selectivity properties can appropriately examine the rapid variations in biological samples and accomplish a precise and real-time approximation of the analyte concentrations. Moreover, the incorporation of nanomaterials with better surface characteristics, higher conductivity, finer magnetic and catalytic properties has helped enhance biocompatibility, sensitivity, and various analytical properties like the limit of detection (LOD), reaction accuracy, fidelity, precision of immobilization, etc. [26, 27]. A simple schematic illustration of a biosensing device is presented in Fig. 2.

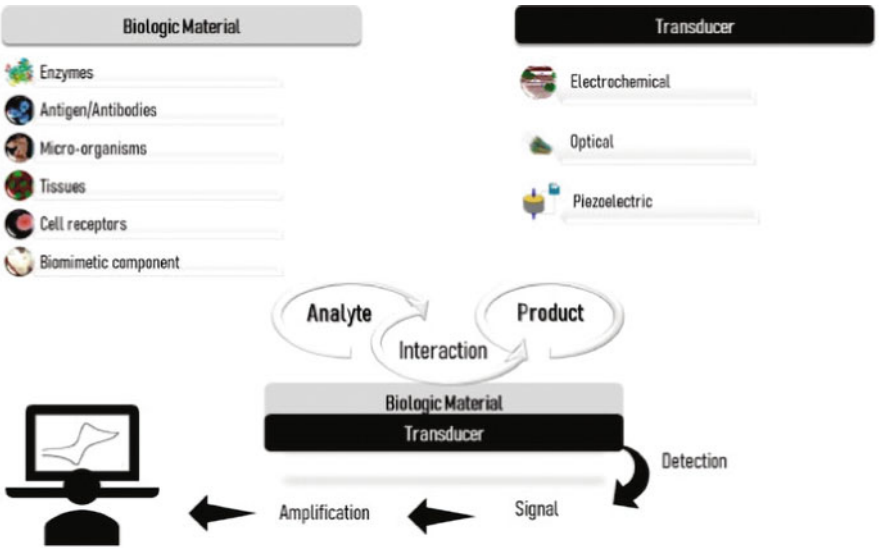

Fig. 2 Schematic illustration of a biosensor (Reprinted with permission from ref. [70], Copyright 2020, Elsevier)

Biosensors can be classified depending on the transduction system into three major types: electrochemical, optical, and piezoelectric sensors. In electrochemical biosensors, variations in transducer surface charge distribution is studied following the principles of amperometry [71, 72], potentiometry [73, 74], or impedimetry [75, 76]. For optical biosensors, a multifold detection and analysis of various optical features of the transducer surface are accomplished at a time as the analyte and the recognition component interact [77, 78]. Lastly, the piezoelectric or the acoustic biosensors mainly focus on measuring the alterations in the resonance frequency of the piezoelectric crystals due to changes in their mass caused by the adsorption of the biological material. This mass difference can be further evaluated by obtaining a corresponding change in the signal following a specific contact with the analyte [79]. In modern-day biosensors, suitable receptors are utilized, reacting distinctively with the target analyte of interest and producing signals simplifying the overall detection process. Thus, depending on these bioreception components used, the sensors can also be categorized as:

Immunosensors: These are the basic biological sensors monitoring the antigen-antibody reactions. Antibodies having high and specific binding affinity can separate the desired analyte from a sample matrix. So far, numerous studies have shown that antibodies have superior binding constants compared to most of the recognition elements, making it a reliable identification element for various conventional assaying techniques and for developing novel detection approaches [80]. The devices with convenient features like point-of-care sensing, portability, cost-effectiveness, easy operation, and high fidelity has led to its extensive

employment for detecting food contaminants [80], biomarkers [81], mycotoxin [82], pathogens [83, 84], fatal viruses [85, 86], etc.

Genosensors: Functional nucleic acid strand (probe) based biosensors with prolonged shelf life, high stability, and flexible modifications are immensely used for recognizing different infectious microorganisms. DNA or RNA strands with definite sequences can help differentiate between various pathogens and express any gene-related anomaly as a possible cause for a disease. Specific biorecognition depends on the principle of hybridization and duplex formation between the immobilized probe and its complementary target sequence. Successful binding can be determined using appropriate indicators or via tracking post-attachment alterations. With the advancement of research, quite a few potent genosensors have been exploited for sensing many pathogenic disease-causing agents [87–89].

Enzymatic sensors: Enzymes catalyzing varied chemical reactions and expressing high selectivity are used as target-specific biorecognition elements for accurately detecting distinctive substrates. Appropriate enzyme-substrate interactions generate suitable signals corresponding to relevant information regarding the sample analyte levels [90, 91]. Steady tracking on enzyme activities can also help reveal several inhibitory molecules interrupting the reactions [80]. For many such favorable applications, the particular sensors are widely used for medical diagnosis and the identification and analysis of a diverse array of analytes [92–94].

After successfully producing the first biosensor to detect the blood glucose level, investigations and explorations have exploded in this field. Along with the extensive use in healthcare facilities for routine clinical diagnosis, several devices are also being made to detect the various coronaviruses. The probability of being driven with smartphones [95] is among the several noteworthy attributes of biosensing devices that has helped it be the ideal alternative tool for diagnosis. A general schematic diagram illustrating the recent trends in diagnostic techniques and the potential biosensing platforms utilized for explicitly detecting the novel SARS-CoV-2 is represented in Fig. 3.

Presently some contemporary devices are being used for the diagnosis of COVID-19 like fluorescence-based biosensors, colorimetric sensors, plasmonic sensors, Quartz Crystal Microbalance (QCM), Field-Effect Transistor (FET)-based, and electrochemical immunosensors [97–99]. Table 2 contains summarized data regarding most of the recent sensors developed for detecting coronaviruses.

3.1 Plasmonic Biosensor

Surface plasmonic resonance (SPR) sensors have become a crucial device in modern clinical and scientific research based on their properties of accurate characterization and quantification of bioanalytical targets [116]. The surface plasmon resonance generated in the sensors via optical illumination of the metal surface enables label-free and real-time monitoring of binding events between specific target and

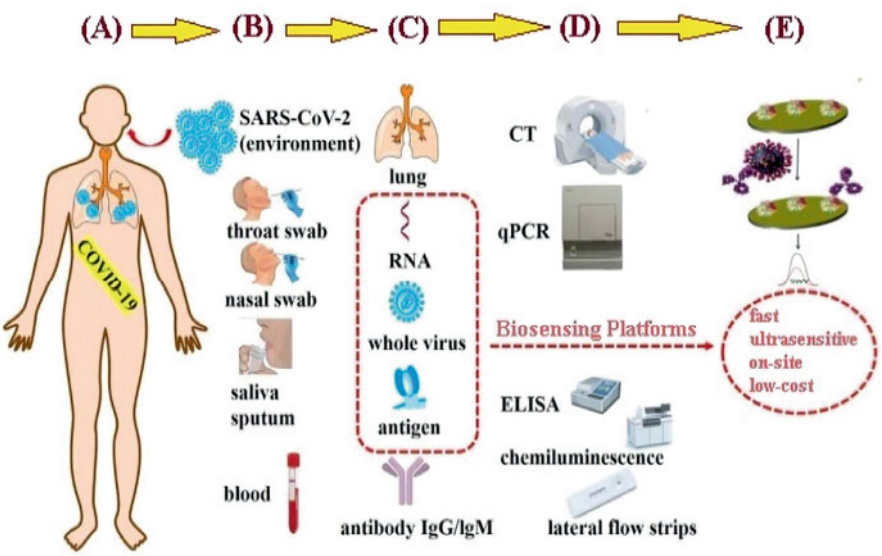

Fig. 3 Schematic illustration of the recent trends in diagnostic tools and potential biosensing platforms utilized for specific detection of the novel SARS-CoV-2 (Reprinted in a modified form with permission from ref. [96], Copyright 2020, Elsevier)

biorecognition molecules [117]. Advantages like high-throughput capabilities, sensitivity, economical, easy-to-use, simple instrumentation, etc. have led to the immense utilization of the sensor for diagnostic purposes [118].

Huang et al. [100] constructed a localized surface plasmon coupled fluorescence (LSPCF) fiber-optic biosensor coupling together the LSP technique with the principle of sandwich ELISA for sensitive detection of nucleocapsid protein (N protein) of SARS-CoV in the serum samples of positive patients. A LOD of 1 pg/mL was recorded for recombinant SARS-CoV N (GST-N) protein. The fluorescence signal was also found to have a linear correlation with the amount of GST-N protein within the working range of 0.1 pg/mL to 1 ng/mL. The system could successfully achieve a 10^4-times increase in detection limit compared to a commercial ELISA kit for antigen capture. Thereafter, Park et al. [103] designed a SPR biosensor for rapidly detecting SARS-CoV. The group created a fusion protein by genetical fusion of gold binding polypeptides (GBPs) to SARS-CoV membrane-envelope (SCVme) protein antigen. The GBPs acting as anchors helped in the assembly of fusion proteins onto the SPR gold chip. Consequently, a biosensing platform was developed, enabling the specific recognition of the target anti-SCVme antibodies. The SPR sensor chip revealed a low detection limit of 200 ng/mL and a quick response time of 10 min. Selectivity studies conducted using mouse IgG as negative controls showed very low SPR responses, proving that the proposed SPR immunosensor had no significant cross-reactivity. An illustration of the work is presented in Fig. 4. A dual-functional plasmonic biosensor coupling together the plasmonic photothermal (PPT) effect and localized surface plasmon resonance (LSPR) is fabricated by Qiu and his co-workers

Table 2 Emerging biosensing platforms for the rapid and POC diagnosis of coronaviruses

Virus target	Type of biosensor	Substrate	Immobilized recognition element	Target molecule	Working range	LOD	Sample used	References
SARS-CoV	Optical—(LSPCF) fiber-optic biosensor	(PMMA) optical fiber	Anti-SARS-CoV N protein antibodies	GST-tagged SARS-CoV nucleocapsid (N) protein (GST-N)	0.1 pg/mL to 1 ng/mL	1 pg/mL	Blood serum from a healthy human donor	Huang et al. [100]
SARS-CoV	Optical—Confocal laser scanning microscopy	Glass chip	SARS-CoV N protein	RNA aptamer conjugated to QDs	0.1–50 pg/mL	0.1 pg/mL	Synthesized RNA aptamer	Roh et al. [101]
SARS-CoV	Electrochemical-nanowire biosensors	In_2O_3 nanowire FET	Fibronectin-based AMP mimicking anti-SARS-CoV N protein antibodies	SARS-CoV N protein	0.6–10 nM	0.6 nM	Commercial N protein solution	Ishikawa et al. [102]
SARS-CoV	Optical—SPR	Gold-micropatterned chip	GBP-E-SCVme (SARS-CoV) fusion proteins	Anti-SCVme antibody	Not determined	200 ng/mL	Rabbit anti-SCVme	Park et al. [103]
SARS-CoV	Piezoelectric	PQC sensor	SARS-CoV NG-8 aptamer	SARS-CoV helicase protein	0.050–1.00 μg/mL	3.50 ng/mL	Blood serum from a healthy human donor	Albano et al. [104]
MERS-CoV	Optical—Colorimetric assay	Multiplexed paper	acpcPNA-AgNPs	(a)MERS-CoV DNA (b)MTB DNA (c)HPV DNA	(a)20.0–1.00 × 10^3 nM (b)50.0–2.5 × 10^3 nM (c)50.0–2.5 × 10^3 nM	(a)1.53 nM (b)1.27 nM (c)1.03 nM	Synthetic DNA oligonucleotides	Teengam et al. [105]

(continued)

Table 2 (continued)

Virus target	Type of biosensor	Substrate	Immobilized recognition element	Target molecule	Working range	LOD	Sample used	References
MERS-CoV	Electrochemical immunosensor—SWV	DEP microarray electrode with eight carbon working electrodes	MERS-CoV and HCoV proteins	HCoV and MERS-CoV specific antibodies	0.001–100 ng/mL (MERS-CoV) and 0.01–1 × 10^4 ng/mL (HCoV)	1.04 pg./mL (MERS-CoV) and 0.4 pg./mL (HCoV)	Artificial nasal samples spiked with MERS-CoV and HCoV proteins	Layqah et al. [106]
MERS-CoV	Optical—multiplex microfiber-based immunoassay	ESPS microfiber membrane filters	HAS and His-MERS-NP antigen protein	FITC-conjugated anti-HAS and FITC-conjugated anti-MERS NP #20 antibodies	Not determined	200 µg/mL	Commercial antigen and antibody solutions	Hoy et al. [107]
SARS-CoV-2	Electrochemical—Semiconductor based biosensor	Graphene FET	SARS-CoV-2 Anti-spike antibody	SARS-CoV-2 spike protein	1.00 fg/mL–10.0 pg./mL 16.0–1.60 × 10^4 PFU/mL 10.0–1.00 × 10^5 copies/mL	1.00 fg/mL 1.6 × 10^1 pfu/mL 2.42 × 10^2 copies/mL	PBS buffer Viral culture Nasopharyngeal swab samples from COVID positive patients	Seo et al. [108]
SARS-CoV-2	Optical—LSPR combined with PPT effect	AuNIs chip	SARS-CoV-2 thiol-cDNA oligonucleotides	SARS-CoV-2 specific RNA sequences	0.100 pM–1.00 µM	0.220 pM	Synthetic oligonucleotide	Qiu et al. [109]

SARS-CoV-2	Electrochemical immunosensor -	Eight gold screen-printed electrodes on a disposable sensor strip	Anti-S1 antibody	SARS-CoV-2 S1 spike protein	10 fg/ml–1 μg/mL	1 fg/mL	Standard SARS-CoV-2 spike protein (S1) solution or SARS-CoV-2 nucleocapsid protein	Mavrikou et al. [110]
SARS-CoV-2	Optical—LFIA	Sample pad, conjugate pad, nitrocellulose membrane, absorbent pad	AuNP-COVID-19 recombinant antigen conjugate, AuNP-rabbit-IgG conjugate, anti-human-IgM antibody, anti-human-IgG antibody, anti-rabbit-IgG antibody	Anti-SARS-CoV-2-IgM antibody, anti-SARS-CoV-2-IgG antibody	Not determined	Not determined	Whole blood, serum, and plasma from both COVID-19 and non-COVID-19 patients	Li et al. [111]
SARS-CoV-2	Electrochemical immunosensor—DPV	(a)Glass electrode coated with FTO (b)SPCE (eCovSens)	(a)Anti-SARS-CoV-2 spike antibody (b)Anti-SARS-CoV-2 spike antibodies	(a)SARS-CoV-2 spike protein antigen (b)SARS-CoV-2 spike protein antigen	(a)1 fM to 1 μM (b)1fM to 1 μM	(a)120 fM (b)90 fM	(a)Spiked saliva samples (b)Spiked saliva samples	Mahari et al. [112]
SARS-CoV-2	Optical—DNHCR-based nucleic acid assay	DNA nanoscaffolds	Self-quenching hairpin DNA probes H1	SARS-CoV-2 RNA and free H2 DNA probes	0.96 pM–100 nM	0.96 pM	Commercial RNA solution	Jiao et al. [113]

(continued)

Table 2 (continued)

Virus target	Type of biosensor	Substrate	Immobilized recognition element	Target molecule	Working range	LOD	Sample used	References
SARS-CoV-2	Optical—SPR	SPR sensor	SARS-CoV-2 recombinant N protein	SARS-CoV-2 anti-N protein antibodies	10–75 μg/mL	1 μg/mL	undiluted human serum	Djaileb et al. [114]
SARS-CoV-2	Optical—mRT-LAMP-LFB	Sample pad, conjugate pad, nitrocellulose membrane, absorbent pad	Anti-FITC antibody, Anti-Dig antibody, biotin-BSA, SA-DNPs	ORF1ab-RT-LAMP labeled with FITC and biotin, and N-RT-LAMP labeled with Dig and biotin	1.2×10^4–1.2×10^{-2} copies	12 copies (for each detection target) per reaction	Oropharynx swab samples from both COVID-19 and non-COVID-19 patients	Zhu et al. [115]

Abbreviations: *LSPCF* Localized surface plasmon coupled fluorescence, *PMMA* Polymethyl methacrylate, *AMP* Antibody mimicking protein, GBP-*E* Gold binding polypeptides-enhanced green fluorescent protein, *SCVme* SARS coronaviral surface antigen, *SPR* Surface plasmon resonance, *PQC* Piezoelectric quartz crystal, *acpcPNA* Pyrrolidinyl peptide nucleic acid, *SWV* Square wave voltammetry, *DEP* Disposable electrical printed, ESPS Electro Spun Polystyrene, *HAS* Human serum albumin, *FITC* Fluorescein isothiocyanate, *PPT* Plasmonic photothermal, *AuNIs* Gold nano islands, *LFIA* Lateral flow immunoassay, *AuNP* Gold nanoparticle. *FTO* Fluorine doped tin oxide, *DPV* Differential pulse voltammetry, *SPCE* Screen printed carbon electrode, *mRT-LAMP-LFB* Multiplex reverse transcription loop-mediated isothermal amplification coupled with a nanoparticle-based lateral flow biosensor assay, *Anti-Dig* Anti-digoxigenin, *biotin-BSA* Biotinylated bovine serum albumin, *SA-DNPs-Dye* Streptavidin coated polymer nanoparticles, *ORF1ab-RT-LAMP* Reverse transcription loop-mediated isothermal amplification amplified SARS-CoV-2 specific ORF1ab gene products, *N-RT-LAMP* Reverse transcription loop-mediated isothermal amplification amplified SARS-CoV-2 specific N gene products

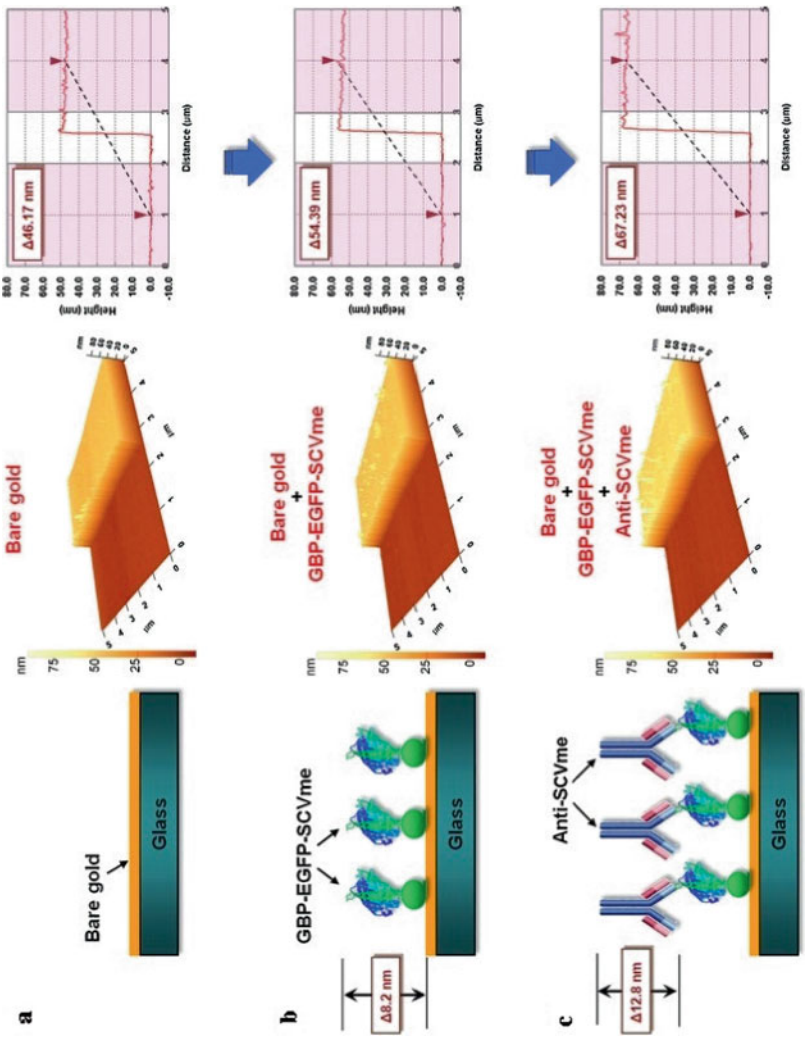

Fig. 4 AFM images of the sequential binding of GBP-E-SCVme and anti-SCVme on the gold-micropatterned surface of an SPR biosensor. (**a**) Bare gold surface, (**b**) Subsequent binding of the GBP-E-SCVme fusion proteins onto the gold surface, and (**c**) Final binding of the anti-SCVme antibodies on the GBP-E-SCVme layer. In the left are the schematic diagrams for the successive binding of GBP-E-SCVme and anti-SCVme on the gold micropatterns; three-dimensional topological images are presented in the middle; and in the right are the cross-sectional contours of samples a–c, sequentially (these are average height differences of the individual scan lines from each area) (Reprinted with permission from Ref. [103], Copyright 2009, Elsevier)

[109] which has led to the introduction of a potential alternative to faulty clinical assays for the diagnosis of COVID-19. Functionalization of the two-dimensional gold nano islands (AuNIs) using complementary DNA receptors was done to help perform a real-time and label-free detection of the selected sequences, including RNA-dependent RNA polymerase (RdRp), open reading frame 1 ab (ORF1ab), and E genes from severe SARS-CoV-2. To enhance the stability and sensitivity of the sensing platform, plasmonic resonances of PPT and LSPR transducer were combined at two different incident angles followed by excitation at two different wavelengths. The locally generated thermoplasmonic heat on the AuNIs chips helps elevate the *in situ* hybridization temperature due to illumination at their respective plasmonic resonance frequency. As a result, it helps ameliorate the kinetics of hybridization and genomic detection specificity. Excellent detection abilities have been exhibited by the sensor with LOD concentrations as low as 0.22 pM for the specific target sequence. Moreover, it also revealed accurate recognition of target gene in a multigene mixture and turning up as a simple and easy-to-implement analytical device providing rapid and POC diagnosis mitigating the pressure on PCR-based assays. A surface plasmon resonance (SPR) biosensor was also introduced by Djaileb et al. [114] for detection of specific antibodies against the novel coronavirus 2019 (SARS-CoV-2) in undiluted human serum samples. Antibodies are generated due to a natural immunogenic response against the virus and if the levels can be monitored then it might help gather useful information regarding the particular patient population who have become immunized against SARD-CoV-2. Furthermore, it can facilitate the process of a successful vaccine development. Thus, this device like all other POC testing and diagnostic tools is believed to have a significant clinical value. The sensor is decorated with a peptide monolayer which in turn is functionalized with SARS-CoV-2 nucleocapsid recombinant protein. Swift detection of specific anti-SARS-CoV-2 antibodies even with minimal concentrations of 1 μg/mL and displaying of accurate results was exhibited by the device within just 15 min. Therefore, the sensor is considered to be a potential platform paving the way to rapid antibody testing.

3.2 Field-effect Transistor Based Biosensor (BioFRT)

Smart and up-to-date sensing devices based on conventional FET systems have become potential tools for point-of-care testing and on-site diagnostics [119]. High sensitivity and instantaneous detection of target analytes in minimal volumes are some of the promising features of the sensor. A three-electrode structure comprising the drain, source, and gate is the significant component of the FET system and can precisely diagnose viral diseases and detect small molecules [117]. The binding of the target analyte to the recognition component immobilized on the highly conductive chip surface results in a minute change in the surface potential that is tracked by the sensor [120]. Rapid detection of even the slightest amounts of target analyte bound to the immobilized probe is facilitated by the use of different semiconductor materials such as graphene, molybdenum disulfide, titanium oxide, etc.

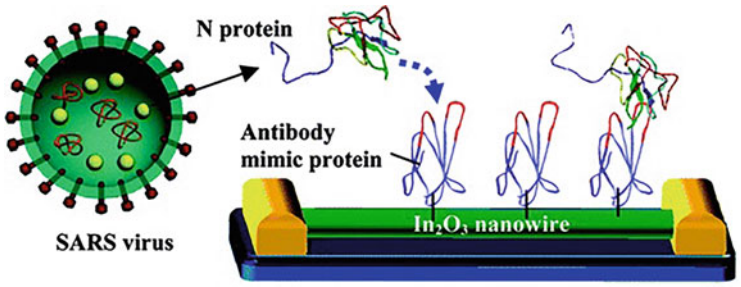

Fig. 5 Schematic illustration of the interactions in an In_2O_3 nanowire FET modified with fibronectin for the detection of SARS-CoV N protein (Reprinted with permission from Ref. [102], Copyright 2009, American Chemical Society)

[121]. Hexagonal carbon atoms exposed on the surface of graphene account for its high carrier mobility, high electronic conductivity, and specific surface area and enhances its sensitivity which leads to its excessive utilization in sensing systems. Hence, graphene-based FET biosensors sense the minute changes in the sensor surface and offer ideal sensing conditions, allowing ultrasensitive detection with low noise [122]. Consequently, these sensing platforms are considered very significant for executing sensitive immunological diagnoses [123].

Ishikawa and his group [102] developed an In_2O_3 nanowire field-effect transistor (FET) for label-free detection of SARS-CoV (N) protein. Firstly, the Si/SiO_2 substrate of the sensor was functionalized with In_2O_3 nanowires. The nanowire surface was then modified with fibronectin (Fn) based antibody mimic proteins (AMP) to detect SARS-CoV N protein selectively. Viral protein with minimal concentrations of 0.6 nM was detected in bovine serum albumin. A schematic illustration of the device is presented here in Fig. 5. Precise detection of SARS-CoV-2 antigenic spike protein in clinical samples was enabled by a graphene-based FET biosensor fabricated by Seo [108] and his group. Spike protein of the virus was utilized as the biomarker due to its diversity in sequence among different coronaviruses. The graphene sheets of the sensing platform were successfully modified with a coating of a specific antibody against the SARS-CoV-2 spike protein. Recognition sensitivity of the sensor was assessed using antigen protein, self-cultured virus, and nasopharyngeal swab samples were taken from COVID-19 infected patients. The device showed a LOD of 1 fg/mL and 100 fg/mL for the spike protein in phosphate-buffered saline and clinical transport medium. Moreover, it could also detect SARS-CoV-2 in cultured medium and swab samples even if present at minimal concentrations of 1.6×10^1 (plaque-forming units) pfu/mL and 2.42×10^2 copies/mL. Furthermore, the device had no cross-reactivity for other coronaviruses like MERS-CoV, proving to be a highly selective and specific immunological diagnostic tool providing effective results without requirements for sample pretreatment or labeling.

3.3 Quartz Crystal Microbalance Biosensors

The quartz crystal microbalance (QCM) based biosensors permit a label-free detection of biomolecules and have thus gained ample significance in studies associated with pathogen detection [124]. The device operates based on surface sensitive and real-time monitoring QCM technologies facilitating detection of any mass changes on the sensor surface [125]. Features like swift detection and enhanced sensitivity have drawn attraction towards developing novel QCM systems to diagnose various infectious diseases [126]. In a true sense, these instruments work as very small mass balances and detect the molecule-surface interactions as changes in mass. The major component of this oscillating system is a thin quartz crystal disk, with electrodes on each side serving as the sensing surfaces. Being a piezoelectric material, the crystal experiences some mechanical stress due to the application of an external electric field, and due to the imposition of an alternating voltage, the crystal is excited and oscillates in the direction perpendicular to the plate surface [127] with a resonance frequency relating to the disk thickness. So, with changes in the thickness, corresponding changes in the resonance frequency will occur simultaneously. Hence, tracking these resonance frequency changes can help detect small changes in the crystal thickness (mass).

Presently, in order to study the dissipative losses (energy loss) in crystal oscillation in addition to the changes in resonant frequency, QCM with dissipation monitoring (QCM-D) has been introduced. As biomolecules bind to the sensor surface, viscoelastic and soft films are formed, which dampen the oscillations [128]. It is seen that simultaneous monitoring of the changes in the energy loss helps the analysis and quantification of layer properties. Furthermore, it also provides additional information regarding structural changes at the crystal surface [129, 130]. A piezoelectric aptamer-PQC biosensor based on paramagnetic nanoparticle technology was first developed by Albano and his group [104] to selectively detect SCV helicase protein biomarkers at pg/mL level in high protein sera sample. Rapid and sensitive detection to a limit of 3.5 ng/mL was achieved as a result of a quick 1-min assay. Moreover, a linear correlation between a frequency shift of the aptamer-coated crystals and the amounts of SARS helicase was observed within the concentration range of 0.05–1 μg/mL. Samples spiked with SARS helicase at concentrations of 10 ng/mL and 1.0 ng/mL when analyzed with the sensor resulted in 102% and 119% recoveries, making the sensor a particular and precise diagnostic tool. Such results prove the device to be functional and dependable for recognizing various viral pathogens.

3.4 Colorimetric Biosensors

Colorimetric sensors can detect harmful pathogens via reactions mediating color changes easily visible to naked eyes [131]. Moreover, accurate quantification using portable optical detectors is also possible. Efficient calorimetric assays like loop-mediated isothermal amplification (LAMP) with rapid detection time, high efficacy,

cost-effectivity, and higher reliability [132] are being coupled with the nanoparticle-based colorimetric biosensors to develop sophisticated lab-on-a-chip devices [131]. Zhu et al. [115] introduced a potential biosensing platform based on multiplex reverse transcription loop-mediated isothermal amplification (mRT-LAMP) integrated with a nanoparticle-based lateral flow biosensor (LFB) assay (mRT-LAMP-LFB) for detecting SARS-CoV-2 ORF1ab and N genes. Fluorescein isothiocyanate (FITC)-/digoxin- and biotin-labeled primers used mRT-LAMP for simultaneous amplification of the viral genes producing several FITC-/digoxin- and biotin-attached duplex amplicons, which was then detected by the LFB through immunoreactions (via observation of the FITC/digoxin bound on the duplex and the anti-FITC/digoxin complex visible on the test line of the sensor) and biotin/streptavidin interaction (via observation of the biotin attached to the duplex and streptavidin bounded to the polymerase nanoparticle). Formation of a crimson band due to the accumulation of nanoparticles enabled a multiplex analysis of the ORF1ab and N genes. The rapid diagnostic test taking only about 1 h to complete, achieved a LOD of 12 copies (for each detection target) per reaction. Furthermore, experiments conducted using clinical samples to evaluate the analytical performance of the device revealed 100% specificity (96/96 oropharynx swab samples from non-COVID-19 patients) and 100% sensitivity (33/33 oropharynx swab samples from COVID-19 patients) properties. Hence, the COVID-19 mRT-LAMP-LFB assay can be considered to be a promising diagnostic tool for detecting SARS-CoV-2 infections. The overall working principle is illustrated in Fig. 6a.

Calorimetric sensors based on lateral flow immunoassay (LFIA) are widely used for testing the presence of antibodies in the patient's blood. These cellulose-based devices simply employ a lateral chromatographic flow for the qualitative detection of a target analyte (SARS-CoV-2 specific antibodies) in blood, serum, or plasma samples. It consists of four essential parts: a sample pad, a conjugate pad, a nitrocellulose membrane, and an absorbent pad. Minimal volumes of the sample (a mixture of blood cells, vesicles, cell debris, antibodies, small molecules, etc.) is added to the sample pad, which works like a filter and enables lateral flow. The sample flowing to the conjugate pad helps rehydrate the pre-immobilized gold-conjugated recombinant antigen (i.e., spike protein or its receptor binding domain (RBD)). The specific immunogenic interactions lead to the binding of the antibodies with their matching antigens. The sample flows under the action of the capillary force and along the nitrocellulose membrane and reaches the test line and the control line. The absorbent pad thereafter absorbs the excess sample fluid. Colorimetric visualization is usually permitted by colloidal gold nanoparticles, colored latex nanoparticles, fluorophores, etc. Li and his fellow scientists [111] utilized this strategy to construct a portable and rapid lateral flow immunosensor aiming to simultaneously recognize the IgM and IgG antibodies against the SARS-CoV-2 virus in blood samples from COVID positive individuals within 15 min. Clinical tests performed with blood samples from 397 PCR confirmed COVID-19 patients and 128 negative patients at eight different clinical sites validated the clinical efficiency of the device, and overall sensitivity of 88.66% and specificity of 90.63% was noticed. Furthermore, results from experimental investigations carried

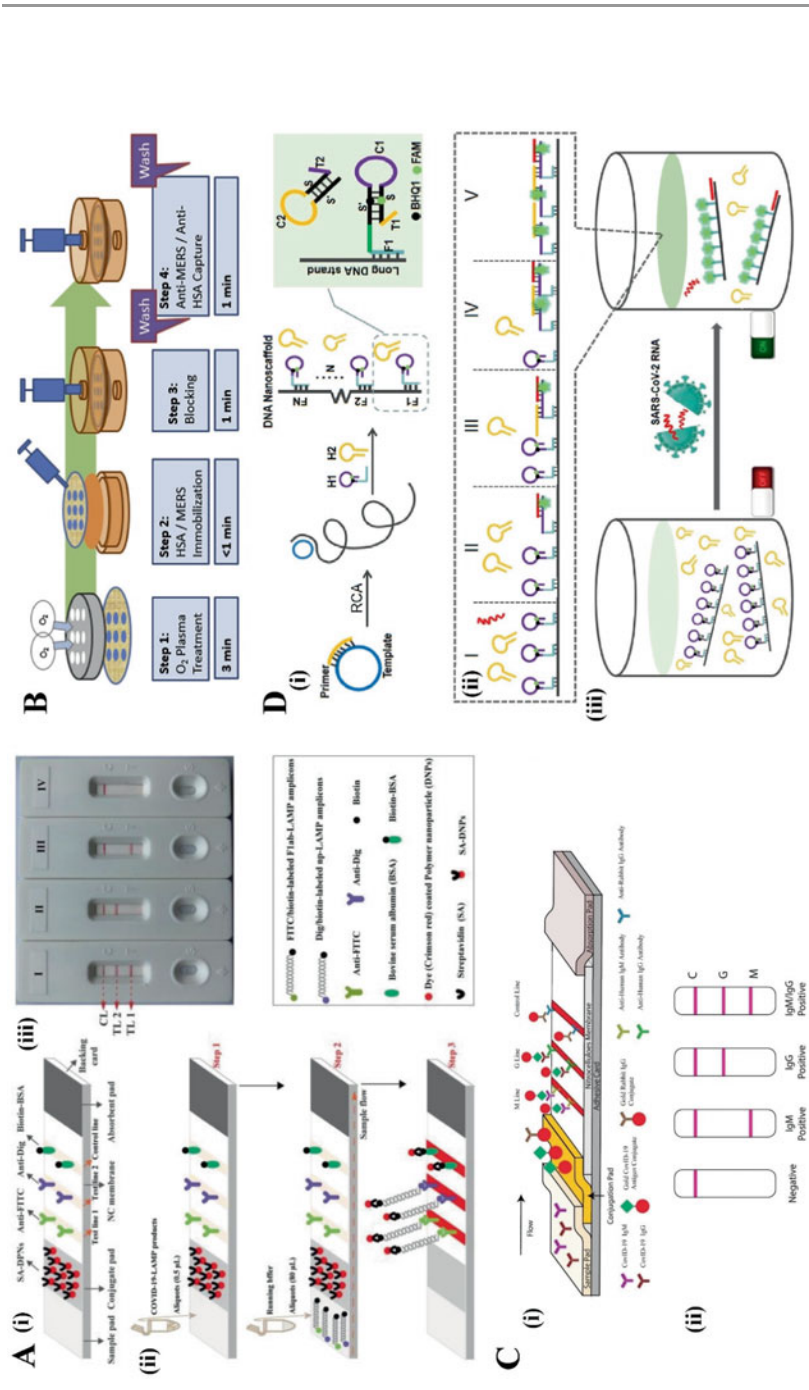

Fig. 6 Latest state-of-the-art colorimetric and fluorescence-based biosensors for selectively diagnosing coronaviruses. (**a**) Schematic diagram of the principle of LFB to visualize COVID-19 RT-LAMP products in a mRT-LAMP coupled nanoparticle-based lateral flow biosensor. (i), Parts of LFB. (ii), Major steps

involved in the principle of LFB for COVID-19 RT-LAMP products. (iii), Interpretation of assay result. (I), result positive for ORF1ab and N (appearance of Test line 1, Test line 2 and Control line on the LFB); (II), result positive for N (appearance of Test line 2 and Control line on the detection region); (III), result positive for ORF1ab (appearance of Test line 1 and Control line on the detection region); (IV), results negative (appearance of only the control line on the LFB) (Reprinted with permission from ref. [115], Copyright 2020, Elsevier). (**b**) Overview of steps involved in a rapid MERS immunoassay protocol followed in a novel and multiplex electrospun polystyrene (ESPS) microfiber-based antibody immunoassay testing platform (Reprinted in a modified form with permission from ref. [107]., Copyright 2019, Elsevier). (**c**) Principles of rapid SARS-CoV-2 IgM-IgG combined antibody test of a portable and rapid lateral flow immunosensor. (i), Schematic diagram of the sensor device for detection. (ii), Interpretation of various test results; C, means control line; G, means IgG line; M, means IgM line. IgG, immunoglobulin G; IgM, immunoglobulin M; SARS-CoV-2 (Reprinted from ref. [111]). (**d**) Overall illustration of the working mechanism of a fluorescence biosensor based on a DNA nanoscaffold hybrid chain reaction (DNHCR). (i), Overall process of hybridization of H1 probes with long DNA strands produced by RCA for synthesizing the DNA nanoscaffolds. (ii), SARS-CoV-2 RNA triggered DNHCR process. (iii), Principle of detection of target SARS-CoV-2. (Reprinted with permission from ref. [113], Copyright 2020, Elsevier)

out using various venous and fingerstick blood samples reflected appreciable detection consistency of the device for different samples. The group also concluded that IgM-IgG combined assays had shown better results compared to a single IgM or IgG test. Figure 6c elaborates the assaying strategy.

Multiplex paper-based colorimetric (MPBC) sensors are sensitive point-of-care devices extensively used to investigate clinical and environmental specimens to detect nucleic acids. The devices are based on the principles of hybridization to a complementary detection strand which is integrated with a highly sensitive reporter molecule, and the devices produce semiquantitative results even with limited resources [133, 134]. Moreover, the detection sensitivities of the sensor surface is enhanced by incorporating gold (AuNPs) and silver (AgNPs) nanoparticles helping elevate the optical signals. Teengam et al. [105] fabricated a colorimetric sensor based on pyrrolidinyl peptide nucleic acid (acpcPNA) probe-induced aggregation of silver nanoparticles allowing real-time and multiplexed detection of viral and DNA including MERS-CoV, human papillomavirus (HPV), and Mycobacterium tuberculosis (Mtb). The positive acpcPNA probes in the absence of complementary DNA sequence mediate aggregation of citrate anion-stabilized silver nanoparticles (AgNPs). Whereas, in the presence of target DNA, the formation of the anionic DNA-acpcPNA duplex results in the dispersion of the AgNPs which leads to a color change that can be easily detected. Detection limits of 1.53, 1.03, and 1.27 nM for MERS-CoV, HPV, and Mtb was observed, and the device was also found to have higher selectivity for complementary oligonucleotides in comparison to single or dual-base mismatch, and noncomplementary DNA targets

3.5 Fluorescence-Based Biosensor

In fluorescent sensors, information relating to spectral change is often used to transduce the presence of a particular biomarker [135–137]. Fluorescent components integrated with various viral molecular assays are employed to diagnose the samples and produce precise results. Quantum dots (QDs), semiconductor nanoparticles acting as fluorescent labels, give photons of a particular wavelength upon excitation and produce readable optical signals [138, 139]. Sensors fabricated using modified and functionalized fluorescent molecules help detect infectious viral agents [140–144].

Roh et al. [101] developed an optical sensor having the lowest LOD for coronaviruses detecting SARS-CoV (N) protein at low concentrations of 0.1 pg/mL. Molecular interactions were based on the specific hybridization of QD-conjugated RNA aptamers with antigenic SARS-CoV N protein immobilized on the surface of a glass chip. Finally, the fluorescence intensity of the QDs was analyzed via confocal laser scanning microscopy. A novel and multiplex antibody immunoassay testing platform comprising electrospun polystyrene (ESPS) microfiber arrays was designed by Hoy et al. [107] for multifold capturing of specific antibodies. The microfibers acting as three-dimensional membrane filters were patterned via localized oxygen plasma which helped create hydrophilic zones to

enhance fluid flows and immobilizations of antigens. HSA (human serum albumin) and MERS-CoV specific antigens were immobilized onto O_2–plasma treated spots on the microfibers and treated with FITC-conjugated anti-HSA and FITC-conjugated anti-MERS antibody solutions. Fluorescence-linked immunosorbent assay (FLISA) results revealed simultaneous detection of both the antibodies with high sensitivity and specificity for MERS-CoV specific antibodies down to 200 μg/mL. An overview of the various steps involved in the diagnosis is presented in Fig. 6b. A fluorescence biosensor based on a DNA nanoscaffold hybrid chain reaction (DNHCR) was prepared by Jiao and his group [113] to rapidly detect the SARS-CoV-2 RNA sequence (Fig. 6d). Firstly, the DNA nanoscaffolds structure was designed through self-assembly of long DNA strands with repetitive sequences attached to self-quenching probes (H1) working as the sensing component. In the presence of target RNA sequences, the free H2 DNA probes hybridized to the H1 probes along the nanoscaffold resulting in the illumination of the complete DNA nanostring and reflecting the viral concentration. The said assay working under mild conditions (15–35 °C) takes only about 10 min for target detection. Moreover, specificity studies revealed the ability of the system to discriminate between mismatched target sequences and recovery values ranging from 89% to 108.7% obtained on analyzing the performance of the system with saliva and serum samples demonstrated good repeatability and stability of the DNHCR method, indicating the remarkable propensity of the device for clinical application.

3.6 Other Prospective Electrical or Electrochemical Immunosensors for Detecting Coronaviruses

As already discussed, immunosensors are analytical devices presenting a sensitive detection platform depending on the specific affinity-based reactions between antigens and their corresponding antibodies. Two significant components of these systems are a bioreceptor and a transducer [145]. The bioreceptor molecules (either antigen or antibody) on selectively recognizing and interacting with their target analyte produce a biological signal that is converted into a desired signal by the transducers. In an electrochemical immunosensor suitable electrical signal (voltametric, potentiometric, conductometric, or impedimetric [146]) is produced on the formation of strong antigen-antibody complexes, which is then transduced via special electrochemical transducers and thereafter reliable readout systems measure the signals and display results accurately [147]. Such devices exhibiting favorable attributes like simple instrumentation, portability, sensitive and specific interaction capabilities, easily disposable and enabling in situ or automated detection have been extensively employed for detecting pathogenic viruses [148–151]. Both labeled and non-labeled detection strategies can be implemented using these devices depending upon the transduction mechanisms. Non-labeled electrochemical immunosensors rely on simple and economic techniques associated with easy sample preparation, swift detection procedures without the requirements of any secondary antibodies, unlike labeled techniques [152]. Currently, various approaches for label-free

detection of antibody-antigen complex via electrochemical immunosensors have been reported. Among them, some noteworthy works are stated in this review.

Layqah et al. [106] constructed an electrochemical immunosensor for detecting MERS-CoV spike protein S1 through electrodeposition of gold nanoparticles (AuNPs) on an array of carbon disposable electrodes (DEP). The analyzing strategy depends mainly on how the MERS-CoV spike protein immobilized on the electrode surface and unbound MERS-CoV virus spiked in the sample compete for a fixed concentration of specific antibody mixed to the sample mixture. MERS-CoV antigen was added in varying concentrations, and square wave voltammetry (SWV) was used to measure the alterations in the reduction peak currents of the ferro/ferricyanide redox couple. Antibodies attaching to the immobilized protein reduced the electron transfer efficiency of the ferro/ferricyanide probe and hence, correspondingly lowered the reduction peak. Selectivity studies were also performed by incubating the sensor with mixtures of anti-HCoV antibody or MERS-CoV antibody along with free target analytes (MERS-CoV or HCoV) used in varying concentrations revealing a low cross-reactivity. Low detection limits of 0.4 pg/mL and 1.0 pg/mL for HCoV and MERS-CoV were achieved within an assay time of 20 min, proving the device to be a reliable sensing platform. In order to estimate the exact number of asymptomatic patients, a novel electrochemical sensor was fabricated by Mavrikou et al. [110]. The sensor depends on a specific cell-based bioassay. For detecting the spike protein antigen S1 of SARS-CoV-2 virus, mammalian cell membranes were engineered to bear electro-inserted chimeric spike S1 antibody on their surface, which when interacted with antigenic S1 protein, a change in the membrane potential of the cells occurred. As a result, a potentiometric signal was generated on the eight-channel gold screen-printed electrode, proportional to the S1 antibody concentrations. Ultra-rapid detections within 3 min with low limits of 1 fg/mL were recorded within a semi-linear range of response between 10 fg and 1 μg/mL. Furthermore, no cross-reactivity was observed on performing specificity studies with SARS-CoV-2 nucleocapsid protein. The researchers also proposed integrating a smart and sensitive and potable readout device with the ready-to-use sensor that can be operated via smartphone/tablet. Hence a potential device was introduced that could help screen SARS-CoV-2 surface antigens and offer a promising solution for timely monitoring of the infected. Recently, a comparative analysis was made by Mahari et al. [112] between an in-house built biosensor device (eCovSens) and a commercial potentiostat for the sensitive diagnosis of COVID-19 spike antigen protein (COVID-19 Ag) in spiked saliva samples. The potentiostatic biosensor consisted of a fluorine-doped tin oxide electrode (FTO) whose surface was modified with gold nanoparticles (AuNPs) functionalized with COVID-19 monoclonal antibody (COVID-19 Ab) for enhancing the electrical conductivity and amplification of the electrochemical signal. Contrastingly, the eCovSens device was based on a screen-printed carbon electrode with immobilized antibodies. Variances in conductivity were recorded in both the devices upon specific antigen-antibody interactions. Both the devices displayed superb recognition efficiency within the analyte concentrations ranging from 1 fM to 1 μM. After that, LODs of 90 fM and 120 fM were showed by the eCovSens and potentiostatic device in

clinical samples. Furthermore, the in-house built biosensor showed ultrasensitive and rapid detection within 10–30 s using very less voltage of 1.3–3 V, which can even be operated with battery. Such attributes validate the fact that the said device can be a substantial point-of-care diagnostic apparatus.

4 Comparative Analysis of Biosensors on a Few Technical Parameters

In this section, a detailed comparison between different biosensors is made based on few technological parameters, including sensor selectivity, LOD, linear working range, instrumentation, portability, and processing time period.

The introduction of novel and innovative operating strategies for electrochemical sensors generating high-throughput results and focusing on detection limit, analysis time, and portability has helped enhance the large-scale market demands for economic biosensors such as the ones required for glucose and pregnancy tests based on lateral flow immune assaying technologies [153]. Detection sensitivities of these devices are enhanced using layers of polymers and nanomaterials over the transducer surface, allowing better immobilization of the biomolecules. From this perspective, it is noticed that lateral flow techniques help in the precise delivery of biosamples onto particular sites on the sensing platform leading to specific interactions and preventing the possibilities of random binding events. Modern and advanced methodologies utilizing gold or silver nanoparticles with a coating of polymers have revolutionized contact-based electrochemical sensing. These smart and up-to-date electrochemical devices, despite having superior selectivity and sensitivity attributes have certain drawbacks in terms of durability factors as the polymers, and other associated compounds get used up due to repeated operations and require timely replacements. Nevertheless, economical price values, real-time monitoring capabilities, and rapid result generation abilities make the sensors attractive and affordable yet efficient choice for the users. New and sophisticated transducers like FRET, bioluminescent resonance energy transfer, fluorescent-based, and surface plasmon resonance-based transducers have been proposed [154] for use in the sensors, which would help in multifold improvement in the single analyte detection. Features of the electrochemical sensors for multiple analyte detection are also being ameliorated by using suitable micro- or nano-cantilevers as transducers. Furthermore, successful employment of 3D bioprinting for fabricating non-contact-based sensors has produced considerable results yet, drawbacks persist in regard to the development cost and desired customizations. Presently a remarkable integration of several productive sensors with electrochemical sensing approaches and their corresponding implementation for sensitive and real-time analysis of body fluids for disease diagnosis is being observed [155].

Next in line are the optical biosensors based on fiber-optic chemistry principles and exhibiting substantial technological advancement. Hydrogel-based cross-linking technologies with capacity for high loading and appreciable hydrophilic properties allow sensitive detection of single molecules like target peptides or DNA sequences.

Effective fusion of enzyme/substrate, antibody/antigen, and nucleic acids to the sensor platform has paved the way for the development of smart and innovative optical sensing devices. Moreover, the combination of microorganisms, animal or plant cells, and tissue sections has also been made possible. With the advancement of molecular optoelectronics and optical integrative technologies, it has been made possible to integrate passive as well as active optical components on a single substrate for devising miniaturized compact sensing devices allowing a multivariate diagnosis. Furthermore, utilization of sophisticated electron and atomic force microscopy principles for analysis of alterations in surface morphology has helped improve the overall operations of the optic-based biosensors. However, devices with detection limits down to femto-levels have still not been developed due to the instrumentation-associated costs. Presently, to achieve real-time monitoring and selective analysis of target analytes, contemporary DNA chips have been fabricated using nanomechanical devices based on microcantilevers and surface resonance technology [156–158]. Briefly, it can be said that optical sensing systems provide several benefits like swift sample analysis, display of accurate results, simple and easily observable changes caused due to specific interactions, etc. However, some instrumentational difficulties prevail, like the intricacy requirements regarding immobilization of recognition compounds and need for a sterilized environment to achieve results with best accuracy.

Advancements in micro-and nano fabrication technologies lead to the development of nano-sized mechanical devices which help produce better analytical results for mass-based biosensors [159]. These structures are mainly developed using semiconductor processing procedures merging the principles of biophysics and bioengineering. Silicon and quartz materials tagged with fluorescence or gold nanoparticles are effectively used in these devices to procure best results. In spite of performing precise single molecular detection, large-scale affordable productions are not achievable [160, 161]. A great challenge for mass-based sensors is the construction of capturing agents at nanoscale and their employment for high-throughput analysis. In this context, potential applicability and appreciable contributions of semiconductor materials and quantum dot technology have to be mentioned. It is also worth mentioning the wide application of synthetic fluorescent biosensors for rigorous analysis of molecular mechanisms of biological processes [162, 163]. These devices possess tremendous sensitivity for single molecule detection and precise measurement of specific analytes, but the overall processes of functional probe preparation are difficult and require expensive instrumentation. Lastly, it can be concluded that different biosensors utilizing the electrochemical or bioelectric and optical detection principles incorporating appropriate biomolecules, polymers, and nanomaterials offer an effective sensing platform which can be efficaciously employed for highly sensitive and specific biochemical assays.

5 Future Perspectives

The current COVID-19 pandemic caused by the novel SARS-CoV-2 is the most alarming public health crisis requiring an immediate and effective solution. To control further spreading and eventually prevent occurrence of the infectious disease, early detection and following initiation of favorable treatment strategies is crucial. In order to cope up with such circumstances, a huge shift has taken place in the healthcare and disease diagnosis sector, from utilizing laboratory-based conventional detection assays to the extensive employment of smart and selective biosensing tools. Biosensors prove to be a functional diagnostic platform providing reliable, sensitive and precise results rapidly. Moreover, the easy portability options help meet the demands for a point of care testing facility. Nevertheless, in spite of such advantageous features, the development of sensors faces several challenges in current times concerning its large-scale fabrication and easy commercial availability. Both the research community and industry personnel should consider a few factors for constructing the sensors to develop a stable device producing uniform results. Firstly proper devising methodologies should be implemented to achieve appropriate surface modifications facilitating better immobilizations leading to enhanced detection sensitivities and ensuring specific interactions. Efforts from the developers have already been made to improve the sensitivity levels of the sensors by applying coatings of semiconductors or other metallic oxides on the transducers, helping enhance the conductance and associated properties. With the advancement in research and development in fabrication strategies, several portable, smart and wireless biosensors are already developed by research institutions and commercial sectors that have profound applications in the biomedical field and are also adopted for environmental monitoring processes. But similar implementations for frontline diagnosis are yet to be made. Moreover, the sensing platforms suffer from biofouling issues which limit their extensive usage for routine clinical purposes. The longevity attributes are highly diminished, leaving them non-functional just after few operations. Accumulation of biomolecules obstructs the flow of analytes to the detector modules preventing the overall detection process. After that, the use of certain biosensors for rapid disease diagnosis can be narrowed down due to some associated factors such as critical immobilization and surface assembly conditions, lowered yield rates, prolonged incubation time and strict temperature constraints, sample preparation and loading, variety of biological fluids to be used, etc. Introduction of multi-tasking enabled biosensors via all-encompassing and comprehensive knowledge research can be the only way to deal with the future disease detection stipulations. Hence, generic devices with intricate designs incorporating multiple sensors on a single chip are being synthesized, which would be capable of detecting multiple molecules (specific disease biomarkers) simultaneously and providing more desirable results along with proper data management. Inclusion of microfluidic systems can help solve the purpose of analyzing small volume samples and escalate the overall diagnosis procedure. In addition to this, existent research should be pushed in a way to transfer the overall disease detection processes from benchtop to the point-of-care with the aim to come up with lab-independent, hospital

decentralized, personalized diagnostic approaches with cheap, fast, high-throughput and portable screening. In support of this, potent biosensors should be assembled which can be conveniently used by individuals at homes to determine their health conditions. This can help them avoid visiting the hospitals reducing the risk of getting exposed to the pathogen. Smart and futuristic biosensors can also be made available which would easily connect to smartphones and tablets and once the analysis is done, proper results can be sent to servers of the healthcare center to monitor the extent of disease transmission. Various artificial intelligence and machine learning-based processes should be applied for signal processing in the sensors to procure safe and correct results. Lastly, proper investments should be made to develop a universal big data server for healthcare systems that will be extracting maximum information regarding the results generated by the sensors and thereafter forward them to the concerned authorities to help them develop epidemiological models to combat the current global pandemic. It can be concluded that the combined efforts of the worldwide scientific communities will help develop highly sensitive diagnosis platforms that will gradually help mitigate the problems associated with the viral outbreak and ensure safety from future attacks.

Acknowledgement This work was supported by the Centre of Biomedical Instrumentation and Assistive Technology, NIT Durgapur.

References

1. Ong, S. W. X., Tan, Y. K., Chia, P. Y., Lee, T. H., Ng, O. T., Wong, M. S. Y., et al. (2020). Air, surface environmental, and personal protective equipment contamination by severe acute respiratory syndrome coronavirus 2 (SARS-CoV-2) from a symptomatic patient. *JAMA*. https://doi.org/10.1001/jama.2020.3227
2. Kaushik, K., & Rawtani, D. (2022). Chapter 5 - Sensor-based techniques for detection of COVID- 19. In *COVID-19 in the Environment*. Elsevier. https://doi.org/10.1016/B978-0-323-902724.00012-9
3. Hoehl, S., Rabenau, H., Berger, A., Kortenbusch, M., Cinatl, J., Bojkova, D., et al. (2020). Evidence of SARS-CoV-2 infection in returning travelers from Wuhan, China. *The New England Journal of Medicine*. https://doi.org/10.1056/NEJMc2001899
4. Qu, G., Li, X., Hu, L., & Jiang, G. (2020). An imperative need for research on the role of environmental factors in transmission of novel coronavirus (COVID-19). *Environmental Science & Technology*. https://doi.org/10.1021/acs.est.0c01102
5. de Groot, R., Baker S., Baric, R., Enjuanes, L., Gorbalenya, A., Holmes, K., et al. (2012). Part II – The Positive Sense Single Stranded RNA Viruses Family Coronaviridae. In: Virus Taxon. Ninth Rep. Int. Comm. Taxon. Viruses. https://doi.org/10.1016/B978-0-12-384684-6.00068-9.
6. Chu, D. K. W., Pan, Y., Cheng, S. M. S., Hui, K. P. Y., Krishnan, P., Liu, Y., et al. (2020). Molecular diagnosis of a novel coronavirus (2019-nCoV) causing an outbreak of pneumonia. *Clinical Chemistry*. https://doi.org/10.1093/clinchem/hvaa029
7. Cui, F., & Zhou, H. S. (2020). Diagnostic methods and potential portable biosensors for coronavirus disease 2019. *Biosensors & Bioelectronics*. https://doi.org/10.1016/j.bios.2020.112349

8. Silvestrini, M., Fruk, L., Moretto, L. M., & Ugo, P. (2015). Detection of DNA hybridization by methylene blue electrochemistry at activated nanoelectrode ensembles. *Journal of Nanoscience and Nanotechnology*. https://doi.org/10.1166/jnn.2015.10214
9. Ricci, F., Adornetto, G., & Palleschi, G. (2012). A review of experimental aspects of electrochemical immunosensors. *Electrochimica Acta*. https://doi.org/10.1016/j.electacta.2012.06.033
10. Saylan, Y., Yilmaz, F., Özgür, E., Derazshamshir, A., Yavuz, H., & Denizli, A. (2017). Molecular imprinting of macromolecules for sensor applications. *Sensors (Switzerland)*. https://doi.org/10.3390/s17040898
11. Gong, S., & Bao, L. (2018). The battle against SARS and MERS coronaviruses: Reservoirs and animal models. *Animal Models and Experimental Medicine*. https://doi.org/10.1002/ame2.12017
12. World Health Organization, Statistics on Middle East respiratory syndrome, Who.Int/. (2019). https://www.who.int/emergencies/mers-cov/en/ (Accessed 11 Sept. 2020).
13. World Health Organization, WHO Coronavirus Disease (COVID-19) Dashboard | WHO Coronavirus Disease (COVID-19) Dashboard, Who.Int/. (2020). https://covid19.who.int/ (Accessed 10 Dec. 2020).
14. Chan, J. F., Kok, K. H., Zhu, Z., Chu, H., To, K. K., Yuan, S., et al. Genomic characterization of the 2019 novel human-pathogenic coronavirus isolated from a patient with atypical pneumonia after visiting Wuhan. *Emerging Microbes & Infections, 9*(2020), 221–236. https://doi.org/10.1080/22221751.2020.1719902
15. Woo, P. C. Y., Lau, S. K. P., Huang, Y., & Yuen, K. Y. (2009). Coronavirus diversity, phylogeny and interspecies jumping. *Experimental Biology and Medicine*. https://doi.org/10.3181/0903-MR-94
16. Zumla, A., Chan, J. F. W., Azhar, E. I., Hui, D. S. C., & Yuen, K. Y. (2016). Coronaviruses-drug discovery and therapeutic options. *Nature Reviews. Drug Discovery, 15*, 327–347. https://doi.org/10.1038/nrd.2015.37
17. Chen, L., Liu, W., Zhang, Q., Xu, K., Ye, G., Wu, W., et al. RNA based mNGS approach identifies a novel human coronavirus from two individual pneumonia cases in 2019 Wuhan outbreak, Emerg. *Microbes and Infection, 9*(2020), 313–319. https://doi.org/10.1080/22221751.2020.1725399
18. Peiris, J. S. M. (2012). Coronaviruses. In *Medicine microbiology* (18th ed., pp. 587–593). Elsevier Inc.. https://doi.org/10.1016/B978-0-7020-4089-4.00072-X
19. Zhou, P., Lou Yang, X., Wang, X. G., Hu, B., Zhang, L., Zhang, W., et al. (2020). A pneumonia outbreak associated with a new coronavirus of probable bat origin. *Nature, 579*, 270–273. https://doi.org/10.1038/s41586-020-2012-7
20. Fehr, A. R., & Perlman, S. (2015). Coronaviruses: An overview of their replication and pathogenesis. In *Coronaviruses methods protocols* (pp. 1–23). Springer. https://doi.org/10.1007/978-1-4939-2438-7_1
21. Asif, M., Ajmal, M., Ashraf, G., Muhammad, N., Aziz, A., Iftikhar, T., et al. (2020). The role of biosensors in coronavirus disease-2019 outbreak. *Current Opinion in Electrochemistry, 23*, 174–184. https://doi.org/10.1016/j.coelec.2020.08.011
22. Lu, R., Zhao, X., Li, J., Niu, P., Yang, B., Wu, H., et al. Genomic characterisation and epidemiology of 2019 novel coronavirus: Implications for virus origins and receptor binding. *Lancet, 395*(2020), 565–574. https://doi.org/10.1016/S0140-6736(20)30251-8
23. Liu, Z., Xiao, X., Wei, X., Li, J., Yang, J., Tan, H., et al. (2020). Composition and divergence of coronavirus spike proteins and host ACE2 receptors predict potential intermediate hosts of SARS-CoV-2. *Journal of Medical Virology, 92*, 595–601. https://doi.org/10.1002/jmv.25726
24. Wang, W., Xu, Y., Gao, R., Lu, R., Han, K., Wu, G., et al. (2020). Detection of SARS-CoV-2 in different types of clinical specimens. *JAMA, 323*, 1843–1844. https://doi.org/10.1001/jama.2020.3786
25. Weber, D. J., Rutala, W. A., Fischer, W. A., Kanamori, H., & Sickbert-Bennett, E. E. (2016). Emerging infectious diseases: Focus on infection control issues for novel coronaviruses

(Severe Acute Respiratory Syndrome-CoV and Middle East Respiratory Syndrome-CoV), hemorrhagic fever viruses (Lassa and Ebola), and highly pathogenic avian influenza viruses, A (H5N1) and A(H7N9). *American Journal of Infection Control, 44*, e91–e100. https://doi.org/10.1016/j.ajic.2015.11.018

26. Casanova, L., Rutala, W. A., Weber, D. J., & Sobsey, M. D. (2009). Survival of surrogate coronaviruses in water. *Water Research, 43*, 1893–1898. https://doi.org/10.1016/j.watres.2009.02.002
27. Rothan, H. A., & Byrareddy, S. N. (2020). The epidemiology and pathogenesis of coronavirus disease (COVID-19) outbreak. *Journal of Autoimmunity, 109*, 102433. https://doi.org/10.1016/j.jaut.2020.102433
28. Wan, Y., Shang, J., Graham, R., Baric, R. S., & Li, F. (2020). Receptor recognition by the novel coronavirus from Wuhan: An analysis based on decade-long structural studies of SARS coronavirus. *Journal of Virology, 94*, 127–147. https://doi.org/10.1128/jvi.00127-20
29. Tortorici, M. A., & Veesler, D. (2019). Structural insights into coronavirus entry. In *Advancesin virus research.* (pp. 93–116). Academic Press. https://doi.org/10.1016/bs.aivir.2019.08.002
30. Singhal, T. (2020). A review of coronavirus disease-2019 (COVID-19), Indian. *The Journal of Pediatrics, 87*, 281–286. https://doi.org/10.1007/s12098-020-03263-6
31. Y. Jin, H. Yang, W. Ji, W. Wu, S. Chen, W. Zhang, et al.. (n.d.). Viruses virology, epidemiology, pathogenesis, and control of COVID-19, Mdpi.Com. https://doi.org/10.3390/v12040372.
32. Corman, V. M., Landt, O., Kaiser, M., Molenkamp, R., Meijer, A., Chu, D. K. W., et al. (2020). Detection of 2019 novel coronavirus (2019-nCoV) by real-time RT-PCR. *Eurosurveillance.* https://doi.org/10.2807/1560-7917.ES.2020.25.3.2000045
33. Won, J., Lee, S., Park, M., Kim, T. Y., Park, M. G., Choi, B. Y., et al. (2020). Development of a laboratory-safe and low-cost detection protocol for SARS-CoV-2 of the Coronavirus Disease 2019 (COVID-19). *Experimental Neurobiology*. https://doi.org/10.5607/en20009
34. Park, G. S., Ku, K., Baek, S. H., Kim, S. J., Il Kim, S., Kim, B. T., et al. (2020). Development of reverse transcription loop-mediated isothermal amplification assays targeting severe acute respiratory syndrome coronavirus 2 (SARS-CoV-2). *Journal of Molecular Diagnostics.* https://doi.org/10.1016/j.jmoldx.2020.03.006
35. Broughton, J. P., Deng, X., Yu, G., Fasching, C. L., Servellita, V., Singh, J., et al. (2020). CRISPR–Cas12-based detection of SARS-CoV-2. *Nature Biotechnology, 38*, 870–874. https://doi.org/10.1038/s41587-020-0513-4
36. Kim, S., Kim, D.-M., & Lee, B. (2020). Insufficient sensitivity of RNA dependent RNA polymerase gene of SARS-CoV-2 viral genome as confirmatory test using Korean COVID-19 cases. *Preprint*, 1–4. https://doi.org/10.20944/PREPRINTS202002.0424.V1
37. Wu, A., Peng, Y., Huang, B., Ding, X., Wang, X., Niu, P., et al. (2020). Genome composition and divergence of the novel coronavirus (2019-nCoV) originating in China. *Cell Host & Microbe, 27*, 325–328. https://doi.org/10.1016/j.chom.2020.02.001
38. Woo, P. C. Y., Lau, S. K. P., Wong, B. H. L., Tsoi, H. W., Fung, A. M. Y., Kao, R. Y. T., et al. (2005). Differential sensitivities of severe acute respiratory syndrome (SARS) coronavirus spike polypeptide enzyme-linked immunosorbent assay (ELISA) and SARS coronavirus nucleocapsid protein ELISA for serodiagnosis of SARS coronavirus pneumonia. *Journal of Clinical Microbiology, 43*, 3054–3058. https://doi.org/10.1128/JCM.43.7.3054-3058.2005
39. Che, X. Y., Qiu, L. W., Pan, Y. X., Wen, K., Hao, W., Zhang, L. Y., et al. (2004). Sensitive and specific monoclonal antibody-based capture enzyme immunoassay for detection of nucleocapsid antigen in sera from patients with severe acute respiratory syndrome. *Journal of Clinical Microbiology, 42*, 2629–2635. https://doi.org/10.1128/JCM.42.6.2629-2635.2004
40. H. Jiang, Y. Li, H. Zhang, W. Wang, D. Men, X. Yang, et al., Global profiling of SARS-CoV-2 specific IgG/IgM responses of convalescents using a proteome microarray, MedRxiv. (2020) 2020.03.20.20039495. doi: https://doi.org/10.1101/2020.03.20.20039495.

41. To, K. K. W., Tsang, O. T. Y., Yip, C. C. Y., Chan, K. H., Wu, T. C., Chan, J. M. C., et al. Consistent detection of 2019 novel coronavirus in saliva. *Clinical Infectious Diseases, 71*(2020), 841–843. https://doi.org/10.1093/cid/ciaa149
42. Pan, Y., Li, X., Yang, G., Fan, J., Tang, Y., & Zhao, J. (2020). Serological immunochromatographic approach in diagnosis with SARS-CoV-2 infected COVID-19 patients. *The Journal of Infection, 81*, e28–e32. https://doi.org/10.1016/j.jinf.2020.03.051
43. Peng, M., Yang, J., Shi, Q., Ying, L., Zhu, H., Zhu, G., et al. (2020). Artificial intelligence application in COVID-19 diagnosis and prediction. *SSRN Electronic Journal*. https://doi.org/10.2139/ssrn.3541119
44. Liu, J., Li, S., Liu, J., Liang, B., Wang, X., Wang, H., et al. (2020). Longitudinal characteristics of lymphocyte responses and cytokine profiles in the peripheral blood of SARS-CoV-2 infected patients. *eBioMedicine, 55*, 102763. https://doi.org/10.1016/j.ebiom.2020.102763
45. Wang, Y., Kang, H., Liu, X., & Tong, Z. (2020). Combination of RT-qPCR testing and clinical features for diagnosis of COVID-19 facilitates management of SARS-CoV-2 outbreak. *Journal of Medical Virology, 92*, 538–539. https://doi.org/10.1002/jmv.25721
46. World Health Organization, Laboratory testing for 2019 novel coronavirus (2019-nCoV) in suspected human cases, Who.Int/. (2020). https://www.who.int/publications/i/item/laboratory-testing-for-2019-novel-coronavirus-in-suspected-human-cases-20200117 (Accessed 5 Oct. 2020).
47. Chan, J. F. W., Yuan, S., Kok, K. H., To, K. K. W., Chu, H., Yang, J., et al. (2020). A familial cluster of pneumonia associated with the 2019 novel coronavirus indicating person-to-person transmission: A study of a family cluster. *Lancet, 395*, 514–523. https://doi.org/10.1016/S0140-6736(20)30154-9
48. Kim, J. M., Chung, Y. S., Jo, H. J., Lee, N. J., Kim, M. S., Woo, S. H., et al. (2020). Identification of coronavirus isolated from a patient in Korea with covid-19. *Osong Public Health and Research Perspectives, 11*, 3–7. https://doi.org/10.24171/j.phrp.2020.11.1.02
49. Zhang, W., Du, R. H., Li, B., Zheng, X. S., Lou Yang, X., Hu, B., et al. (2020). Molecular and serological investigation of 2019-nCoV infected patients: Implication of multiple shedding routes. *Emerging Microbes Infectections., 9*, 386–389. https://doi.org/10.1080/22221751.2020.1729071
50. Yu, F., Yan, L., Wang, N., Yang, S., Wang, L., Tang, Y., et al. (2020). Quantitative detection and viral load analysis of SARS-CoV-2 in infected patients. *Clinical Infectious Diseases, 71*, 793–798. https://doi.org/10.1093/cid/ciaa345
51. Guan, W., Ni, Z., Hu, Y., Liang, W., Ou, C., He, J., et al. Clinical characteristics of coronavirus disease 2019 in China. *The New England Journal of Medicine, 382*(2020), 1708–1720. https://doi.org/10.1056/NEJMoa2002032
52. Van Tan, L., Ngoc, N. M., That, B. T. T., Uyen, L. T. T., Hong, N. T. T., Dung, N. T. P., et al. (2020). *Duration of viral detection in throat and rectum of a patient with COVID-19*. https://doi.org/10.1101/2020.03.07.20032052
53. Zhou, Y., Zeng, Y., Tong, Y., & Chen, C. (2020). Ophthalmologic evidence against the interpersonal transmission of 2019 novel coronavirus through conjunctiva, MedRxiv. 2020.02.11.20021956. https://doi.org/10.1101/2020.02.11.20021956.
54. Xia, J., Tong, J., Liu, M., Shen, Y., & Guo, D. (2020). Evaluation of coronavirus in tears and conjunctival secretions of patients with SARS-CoV-2 infection. *Journal of Medical Virology, 92*, 589–594. https://doi.org/10.1002/jmv.25725
55. Rothe, C., Schunk, M., Sothmann, P., Bretzel, G., Froeschl, G., Wallrauch, C., et al. (2020). Transmission of 2019-NCOV infection from an asymptomatic contact in Germany. *The New England Journal of Medicine, 382*, 970–971. https://doi.org/10.1056/NEJMc2001468
56. Wu, F., Zhao, S., Yu, B., Chen, Y. M., Wang, W., Song, Z. G., et al. (2020). A new coronavirus associated with human respiratory disease in China. *Nature, 579*, 265–269. https://doi.org/10.1038/s41586-020-2008-3

57. Zhu, N., Zhang, D., Wang, W., Li, X., Yang, B., Song, J., et al. (2020). A novel coronavirus from patients with pneumonia in China, 2019. *The New England Journal of Medicine, 382*, 727–733. https://doi.org/10.1056/NEJMoa2001017
58. Chen, L., Liu, W., Zhang, Q., Xu, K., Ye, G., Wu, W., et al. (2020). RNA based mNGS approach identifies a novel human coronavirus from two individual pneumonia cases in 2019 Wuhan outbreak, Emerg. *Microbes and Infection, 9*, 313–319. https://doi.org/10.1080/22221751.2020.1725399
59. Chen, W., Lan, Y., Yuan, X., Deng, X., Li, Y., Cai, X., et al. (2020). Detectable 2019-nCoV viral RNA in blood is a strong indicator for the further clinical severity. *Emerging Microbes and Infection, 9*, 469–473. https://doi.org/10.1080/22221751.2020.1732837
60. Holshue, M. L., DeBolt, C., Lindquist, S., Lofy, K. H., Wiesman, J., Bruce, H., et al. (2020). First case of 2019 novel coronavirus in the united states. *The New England Journal of Medicine, 382*, 929–936. https://doi.org/10.1056/NEJMoa2001191
61. Peng, L., Liu, J., Xu, W., Luo, Q., Chen, D., Lei, Z., et al. (2020). SARS-CoV-2 can be detected in urine, blood, anal swabs, and oropharyngeal swabs specimens. *Journal of Medical Virology, 92*, 1676–1680. https://doi.org/10.1002/jmv.25936
62. To, K. K. W., Tsang, O. T. Y., Leung, W. S., Tam, A. R., Wu, T. C., Lung, D. C., et al. (2020). Temporal profiles of viral load in posterior oropharyngeal saliva samples and serum antibody responses during infection by SARS-CoV-2: An observational cohort study. *The Lancet Infectious Diseases, 20*, 565–574. https://doi.org/10.1016/S1473-3099(20)30196-1
63. Hong, K. H., Lee, S. W., Kim, T. S., Huh, H. J., Lee, J., Kim, S. Y., et al. (2020). Guidelines for laboratory diagnosis of coronavirus disease 2019 (COVID-19) in Korea. *Annals of Laboratory Medicine, 40*, 351–360. https://doi.org/10.3343/alm.2020.40.5.351
64. Fahy, J. V. (1998). A safe, simple, standardized method should be used for sputum induction for research purposes. *Clinical and Experimental Allergy, 28*, 1047–1049. https://doi.org/10.1046/j.1365-2222.1998.00330.x
65. Krejcova, L., Huska, D., Hynek, D., Kopel, P., Adam, V., Hubalek, J., et al. (2013). Using of paramagnetic microparticles and quantum dots for isolation and electrochemical detection of influenza viruses' specific nucleic acids. *International Journal of Electrochemical Science., 8*(1), 689–702.
66. Yang, F., Ma, Y., Stanciu, S. G., & Wu, A. (2020). Transduction process-based classification of biosensors. *Nanobiosensors*. https://doi.org/10.1002/9783527345137.ch2
67. Goode, J. A., Rushworth, J. V. H., & Millner, P. A. (2015). Biosensor regeneration: A review of common techniques and outcomes. *Langmuir*. https://doi.org/10.1021/la503533g
68. Lazcka, O., Del Campo, F. J., & Muñoz, F. X. (2007). Pathogen detection: A perspective of traditional methods and biosensors. *Biosensors & Bioelectronics*. https://doi.org/10.1016/j.bios.2006.06.036
69. Baryeh, K., Takalkar, S., Lund, M., & Liu, G. (2017). Introduction to medical biosensors for point of care applications. In *Medical biosensors for point of care (POC) applications*. Woodhead Publishing. https://doi.org/10.1016/B978-0-08-100072-4.00001-0
70. Ribeiro, B. V., Cordeiro, T. A. R., e Freitas, G. R. O., Ferreira, L. F., & Franco, D. L. (2020). Biosensors for the detection of respiratory viruses: A review. *Talanta Open., 2*, 100007. https://doi.org/10.1016/j.talo.2020.100007
71. German, N., Ramanavicius, A., & Ramanaviciene, A. (2017). Amperometric glucose biosensor based on electrochemically deposited gold nanoparticles covered by polypyrrole. *Electroanalysis*. https://doi.org/10.1002/elan.201600680
72. Labban, N., Hughes, L., Wayu, M., Pollock, J., & Leopold, M. (2019). MON-182 adaptable amperometric biosensor platforms for the diagnosis of endocrine disorders. *Journal of Endocrine Society*. https://doi.org/10.1210/js.2019-mon-182
73. Saeedfar, K., Heng, L. Y., & Rezayi, M. (2017). Fabricating long shelf life potentiometric urea biosensors using modified MWCNTs on screen printed electrodes. *Sensor Letters*. https://doi.org/10.1166/sl.2017.3780

74. Ding, J., & Qin, W. (2020). Recent advances in potentiometric biosensors. *Trends in Analytical Chemistry*. https://doi.org/10.1016/j.trac.2019.115803
75. Chakraborty, A., Tibarewala, D. N., & Barui, A. (2019). Impedance-based biosensors. In *Bioelectronics and Medical Devices From Materials to Devices - Fabr. Appl. Reliab.* Apple Academy Press. https://doi.org/10.1016/B978-0-08-102420-1.00005-4
76. Cordeiro, T. A. R., Gonçalves, M. V. C., Franco, D. L., Reis, A. B., Martins, H. R., & Ferreira, L. F. (2019). Label-free electrochemical impedance immunosensor based on modified screen-printed gold electrodes for the diagnosis of canine visceral leishmaniasis. *Talanta*. https://doi.org/10.1016/j.talanta.2018.11.087
77. Soni, A., Surana, R. K., & Jha, S. K. (2018). Smartphone based optical biosensor for the detection of urea in saliva. *Sensors Actuators B Chemistry*. https://doi.org/10.1016/j.snb.2018.04.108
78. Masson, J. F. (2017). Surface plasmon resonance clinical biosensors for medical diagnostics. *ACS Sensors*. https://doi.org/10.1021/acssensors.6b00763
79. Mehrotra, P. (2016). Biosensors and their applications - A review. *Journal of Oral Biology and Craniofacial Research*. https://doi.org/10.1016/j.jobcr.2015.12.002
80. Griesche, C., & Baeumner, A. J. (2020). Biosensors to support sustainable agriculture and food safety. *Trends in Analytical Chemistry*. https://doi.org/10.1016/j.trac.2020.115906
81. Tuteja, S. K., Chen, R., Kukkar, M., Song, C. K., Mutreja, R., Singh, S., et al. (2016). A label-free electrochemical immunosensor for the detection of cardiac marker using graphene quantum dots (GQDs). *Biosensors & Bioelectronics*. https://doi.org/10.1016/j.bios.2016.07.052
82. Solanki, P. R., Singh, J., Rupavali, B., Tiwari, S., & Malhotra, B. D. (2017). Bismuth oxide nanorods based immunosensor for mycotoxin detection. *Materials Science and Engineering: C*. https://doi.org/10.1016/j.msec.2016.09.027
83. Jampasa, S., Lae-ngee, P., Patarakul, K., Ngamrojanavanich, N., Chailapakul, O., & Rodthongkum, N. (2019). Electrochemical immunosensor based on gold-labeled monoclonal anti-LipL32 for leptospirosis diagnosis. *Biosensors & Bioelectronics*. https://doi.org/10.1016/j.bios.2019.111539
84. Juronen, D., Kuusk, A., Kivirand, K., Rinken, A., & Rinken, T. (2018). Immunosensing system for rapid multiplex detection of mastitis-causing pathogens in milk. *Talanta*. https://doi.org/10.1016/j.talanta.2017.10.043
85. Sun, Y., Xu, L., Zhang, F., Song, Z., Hu, Y., Ji, Y., et al. (2017). A promising magnetic SERS immunosensor for sensitive detection of avian influenza virus. *Biosensors & Bioelectronics*. https://doi.org/10.1016/j.bios.2016.09.100
86. Zhang, H., & Miller, B. L. (2019). Immunosensor-based label-free and multiplex detection of influenza viruses: State of the art. *Biosensors & Bioelectronics*. https://doi.org/10.1016/j.bios.2019.111476
87. Kaur, G., Paliwal, A., Tomar, M., & Gupta, V. (2016). Detection of Neisseria meningitidis using surface plasmon resonance based DNA biosensor. *Biosensors & Bioelectronics*. https://doi.org/10.1016/j.bios.2015.11.025
88. Saeed, A. A., Sánchez, J. L. A., O'Sullivan, C. K., & Abbas, M. N. (2017). DNA biosensors based on gold nanoparticles-modified graphene oxide for the detection of breast cancer biomarkers for early diagnosis. *Bioelectrochemistry*. https://doi.org/10.1016/j.bioelechem.2017.07.002
89. Khan, M., Khan, A. R., Shin, J. H., & Park, S. Y. (2016). A liquid-crystal-based DNA biosensor for pathogen detection. *Scientific Reports*. https://doi.org/10.1038/srep22676
90. Bollella, P., & Gorton, L. (2018). Enzyme based amperometric biosensors. *Current Opinion in Electrochemistry*. https://doi.org/10.1016/j.coelec.2018.06.003
91. Yoo, Y. J., Feng, Y., Kim, Y. H., & Yagonia, C. F. J. (2017). *Fundamentals of enzyme engineering*. Springer. https://doi.org/10.1007/978-94-024-1026-6

92. El Harrad, L., Bourais, I., Mohammadi, H., & Amine, A. (2018). Recent advances in electrochemical biosensors based on enzyme inhibition for clinical and pharmaceutical applications. *Sensors (Switzerland).* https://doi.org/10.3390/s18010164
93. Fraser, L. A., Kinghorn, A. B., Dirkzwager, R. M., Liang, S., Cheung, Y. W., Lim, B., et al. (2018). A portable microfluidic Aptamer-Tethered Enzyme Capture (APTEC) biosensor for malaria diagnosis. *Biosensors & Bioelectronics*. https://doi.org/10.1016/j.bios.2017.10.001
94. Parthasarathy, P., & Vivekanandan, S. (2018). A numerical modelling of an amperometric-enzymatic based uric acid biosensor for GOUT arthritis diseases. *Informatics Medicine Unlocked.* https://doi.org/10.1016/j.imu.2018.03.001
95. Huang, X., Xu, D., Chen, J., Liu, J., Li, Y., Song, J., et al. (2018). Smartphone-based analytical biosensors. *The Analyst, 143*, 5339–5351. https://doi.org/10.1039/c8an01269e
96. Cui, F., & Zhou, H. S. (2020). Diagnostic methods and potential portable biosensors for coronavirus disease 2019. *Biosensors & Bioelectronics, 165*, 112349. https://doi.org/10.1016/j.bios.2020.112349
97. Kaya, S. I., Karadurmus, L., Ozcelikay, G., Bakirhan, N. K., & Ozkan, S. A. (2020). Electrochemical virus detections with nanobiosensors. *Nanosensors for Smart Cities*. https://doi.org/10.1016/b978-0-12-819870-4.00017-7
98. Aziz, A., Asif, M., Ashraf, G., Azeem, M., Majeed, I., Ajmal, M., et al. (2019). Advancements in electrochemical sensing of hydrogen peroxide, glucose and dopamine by using 2D nanoarchitectures of layered double hydroxides or metal dichalcogenides. A review. *Microchimica Acta, 186*, 1–16. https://doi.org/10.1007/s00604-019-3776-z
99. Asif, M., Aziz, A., Azeem, M., Wang, Z., Ashraf, G., Xiao, F., et al. (2018). A review on electrochemical biosensing platform based on layered double hydroxides for small molecule biomarkers determination. *Advances in Colloid and Interface Science, 262*, 21–38. https://doi.org/10.1016/j.cis.2018.11.001
100. Huang, J. C., Chang, Y. F., Chen, K. H., Su, L. C., Lee, C. W., Chen, C. C., et al. (2009). Detection of severe acute respiratory syndrome (SARS) coronavirus nucleocapsid protein in human serum using a localized surface plasmon coupled fluorescence fiber-optic biosensor. *Biosensors & Bioelectronics, 25*, 320–325. https://doi.org/10.1016/j.bios.2009.07.012
101. Roh, C., & Jo, S. K. (2011). Quantitative and sensitive detection of SARS coronavirus nucleocapsid protein using quantum dots-conjugated RNA aptamer on chip. *Journal of Chemical Technology and Biotechnology, 86*, 1475–1479. https://doi.org/10.1002/jctb.2721
102. Ishikawa, F. N., Chang, H. K., Curreli, M., Liao, H. I., Olson, C. A., Chen, P. C., et al. (2009). Label-free, electrical detection of the SARS virus n-protein with nanowire biosensors utilizing antibody mimics as capture probes. *ACS Nano, 3*, 1219–1224. https://doi.org/10.1021/nn900086c
103. Park, T. J., Hyun, M. S., Lee, H. J., Lee, S. Y., & Ko, S. (2009). A self-assembled fusion protein-based surface plasmon resonance biosensor for rapid diagnosis of severe acute respiratory syndrome. *Talanta, 79*, 295–301. https://doi.org/10.1016/j.talanta.2009.03.051
104. Albano, D. R. B., Shum, K., Tanner, J. A., & Fung Y. S. (2018). BS5.3 - Piezoelectric quartz crystal aptamer biosensor for detection and quantification of SARS CoV helicase protein · AMA Science. In *17th Int. Meet. Chem. Sensors - IMCS 2018*, AMA Publications, , (pp. 211–213). https://doi.org/10.5162/IMCS2018/BS5.3.
105. Teengam, P., Siangproh, W., Tuantranont, A., Vilaivan, T., Chailapakul, O., & Henry, C. S. (2017). Multiplex paper-based colorimetric DNA sensor using pyrrolidinyl peptide nucleic acid-induced AgNPs aggregation for detecting MERS-CoV, MTB, and HPV oligonucleotides. *Analytical Chemistry, 89*, 5428–5435. https://doi.org/10.1021/acs.analchem.7b00255
106. Layqah, L. A., & Eissa, S. (2019). An electrochemical immunosensor for the corona virus associated with the Middle East respiratory syndrome using an array of gold nanoparticle-modified carbon electrodes. *Microchimica Acta, 186*, 1–10. https://doi.org/10.1007/s00604-019-3345-5

107. Hoy, C. F. O., Kushiro, K., Yamaoka, Y., Ryo, A., & Takai, M. (2019). Rapid multiplex microfiber-based immunoassay for anti-MERS-CoV antibody detection. *Sensing Bio-Sensing Research., 26*, 100304. https://doi.org/10.1016/j.sbsr.2019.100304
108. Seo, G., Lee, G., Kim, M. J., Baek, S. H., Choi, M., Ku, K. B., et al. (2020). Rapid detection of COVID-19 causative Virus (SARS-CoV-2) in human nasopharyngeal swab specimens using field-effect transistor-based biosensor. *ACS Nano, 14*, 5135–5142. https://doi.org/10.1021/acsnano.0c02823
109. Qiu, G., Gai, Z., Tao, Y., Schmitt, J., Kullak-Ublick, G. A., & Wang, J. (2020). Dual-functional plasmonic photothermal biosensors for highly accurate severe acute respiratory syndrome coronavirus 2 detection. *ACS Nano, 14*, 5268–5277. https://doi.org/10.1021/acsnano.0c02439
110. Mavrikou, S., Moschopoulou, G., Tsekouras, V., & Kintzios, S. (2020). Development of a portable, ultra-rapid and ultra-sensitive cell-based biosensor for the direct detection of the SARS-CoV-2 S1 spike protein antigen. *Sensors, 20*, 3121. https://doi.org/10.3390/s20113121
111. Li, Z., Yi, Y., Luo, X., Xiong, N., Liu, Y., Li, S., et al. (2020). Development and clinical application of a rapid IgM-IgG combined antibody test for SARS-CoV-2 infection diagnosis. *Journal of Medical Virology, 92*, 1518–1524. https://doi.org/10.1002/jmv.25727
112. Mahari, S., Roberts, A., Shahdeo, D., & Gandhi, S. (2020). eCovSens-ultrasensitive novel in-house built printed circuit board based electrochemical device for rapid detection of nCovid-19 antigen, a spike protein domain 1 of SARS-CoV-2, BioRxiv. 2020.04.24.059204. https://doi.org/10.1101/2020.04.24.059204.
113. Jiao, J., Duan, C., Xue, L., Liu, Y., Sun, W., & Xiang, Y. (2020). DNA nanoscaffold-based SARS-CoV-2 detection for COVID-19 diagnosis. *Biosensors & Bioelectronics, 167*, 112479. https://doi.org/10.1016/j.bios.2020.112479
114. Djaileb, A., Charron, B., Jodaylami, M. H., Thibault, V., Coutu, J., Stevenson, K., et al. (2020). A rapid and quantitative serum test for SARS-CoV-2 antibodies with portable surface plasmon resonance sensing. *Analytical Chemistry*. https://doi.org/10.26434/CHEMRXIV.12118914.V1
115. Zhu, X., Wang, X., Han, L., Chen, T., Wang, L., Li, H., et al. (2020). Multiplex reverse transcription loop-mediated isothermal amplification combined with nanoparticle-based lateral flow biosensor for the diagnosis of COVID-19. *Biosensors & Bioelectronics, 166*, 112437. https://doi.org/10.1016/j.bios.2020.112437
116. Asif, M., Ajmal, M., Ashraf, G., Muhammad, N., Aziz, A., Iftikhar, T., et al. (2020). The role of biosensors in coronavirus disease-2019 outbreak. *Current Opinion in Electrochemistry*. https://doi.org/10.1016/j.coelec.2020.08.011
117. Demeke Teklemariam, A., Samaddar, M., Alharbi, M. G., Al-Hindi, R. R., & Bhunia, A. K. (2020). Biosensor and molecular-based methods for the detection of human coronaviruses: A review. *Molecular and Cellular Probes*. https://doi.org/10.1016/j.mcp.2020.101662
118. Bhunia, A. K., Nanduri, V., Bae, E., & Hirleman, E. D. (2010). Biosensors, foodborne pathogen detection. In *Encyclopedia of industrial biotechnology* (pp. 1–50). John Wiley & Sons, Inc.. https://doi.org/10.1002/9780470054581.eib158
119. Liu, J., Chen, X., Wang, Q., Xiao, M., Zhong, D., Sun, W., et al. (2019). Ultrasensitive monolayer MoS 2 field-effect transistor based DNA sensors for screening of down syndrome. *Nano Letters*. https://doi.org/10.1021/acs.nanolett.8b03818
120. Nehra, A., & Pal Singh, K. (2015). Current trends in nanomaterial embedded field effect transistor-based biosensor. *Biosensors & Bioelectronics, 74*, 731–743. https://doi.org/10.1016/j.bios.2015.07.030
121. Janissen, R., Sahoo, P. K., Santos, C. A., Da Silva, A. M., Von Zuben, A. A. G., Souto, D. E. P., et al. (2017). InP nanowire biosensor with tailored biofunctionalization: Ultrasensitive and highly selective disease biomarker detection. *Nano Letters, 17*, 5938–5949. https://doi.org/10.1021/acs.nanolett.7b01803
122. Geim, A. K., & Novoselov, K. S. (2007). The rise of graphene. *Nature Materials*. https://doi.org/10.1038/nmat1849

123. Zhou, L., Mao, H., Wu, C., Tang, L., Wu, Z., Sun, H., et al. (2017). Label-free graphene biosensor targeting cancer molecules based on non-covalent modification. *Biosensors & Bioelectronics, 87*, 701–707. https://doi.org/10.1016/j.bios.2016.09.025
124. Afzal, A., Mujahid, A., Schirhagl, R., Bajwa, S. Z., Latif, U., & Feroz, S. (2017). Gravimetric viral diagnostics: QCM based biosensors for early detection of viruses. *Chem*. https://doi.org/10.3390/chemosensors5010007
125. QCM-D | Measurements | Biolin Scientific, (n.d.). https://www.biolinscientific.com/measurements/qcm-d (Accessed 23 Nov 2020).
126. Lim, H. J., Saha, T., Tey, B. T., Tan, W. S., & Ooi, C. W. (2020). Quartz crystal microbalance-based biosensors as rapid diagnostic devices for infectious diseases. *Biosensors & Bioelectronics, 168*, 112513. https://doi.org/10.1016/j.bios.2020.112513
127. Chen, J. Y., Penn, L. S., & Xi, J. (2018). Quartz crystal microbalance: Sensing cell-substrate adhesion and beyond. *Biosensors & Bioelectronics*. https://doi.org/10.1016/j.bios.2017.08.032
128. Cooper, M. A., & Singleton, V. T. (2007). A survey of the 2001 to 2005 quartz crystal microbalance biosensor literature: Applications of acoustic physics to the analysis of biomolecular interactions. *Journal of Molecular Recognition*. https://doi.org/10.1002/jmr.826
129. Fogel, R., Limson, J., & Seshia, A. A. (2016). Acoustic biosensors. *Essays in Biochemistry*. https://doi.org/10.1042/EBC20150011
130. Karczmarczyk, A., Haupt, K., & Feller, K. H. (2017). Development of a QCM-D biosensor for Ochratoxin A detection in red wine. *Talanta*. https://doi.org/10.1016/j.talanta.2017.01.054
131. Zhao, V. X. T., Wong, T. I., Zheng, X. T., Tan, Y. N., & Zhou, X. (2020). Colorimetric biosensors for point-of-care virus detections. *Materials Science for Energy Technologies*. https://doi.org/10.1016/j.mset.2019.10.002
132. Notomi, T., Okayama, H., Masubuchi, H., Yonekawa, T., Watanabe, K., Amino, N., et al. (2000). Loop-mediated isothermal amplification of DNA. *Nucleic Acids Research, 28*, 63. https://doi.org/10.1093/nar/28.12.e63
133. Nery, E. W., & Kubota, L. T. (2013). Sensing approaches on paper-based devices: A review. *Analytical and Bioanalytical Chemistry, 405*, 7573–7595. https://doi.org/10.1007/s00216-013-6911-4
134. Liana, D. D., Raguse, B., Gooding, J. J., & Chow, E. (2012). Recent advances in paper-based sensors. *Sensors, 12*, 11505–11526. https://doi.org/10.3390/s120911505
135. Tymm, C., Zhou, J., Tadimety, A., Burklund, A., & Zhang, J. X. J. (2020). Scalable COVID-19 detection enabled by lab-on-chip biosensors. *Cellular and Molecular Bioengineering*. https://doi.org/10.1007/s12195-020-00642-z
136. Ahmed, S. R., Kim, J., Tran, V. T., Suzuki, T., Neethirajan, S., Lee, J., et al. (2017). In situ self-assembly of gold nanoparticles on hydrophilic and hydrophobic substrates for influenza virus-sensing platform. *Scientific Reports*. https://doi.org/10.1038/srep44495
137. Zagorovsky, K., & Chan, W. C. W. (2013). A plasmonic DNAzyme strategy for point-of-care genetic detection of infectious pathogens. *Angewandte Chemie International Edition*. https://doi.org/10.1002/anie.201208715
138. Zhao, W., Zhang, W. P., Zhang, Z. L., He, R. L., Lin, Y., Xie, M., et al. (2012). Robust and highly sensitive fluorescence approach for point-of-care virus detection based on immunomagnetic separation. *Analytical Chemistry, 84*, 2358–2365. https://doi.org/10.1021/ac203102u
139. Lee, J., Ahmed, S. R., Oh, S., Kim, J., Suzuki, T., Parmar, K., et al. (2015). A plasmon-assisted fluoro-immunoassay using gold nanoparticle-decorated carbon nanotubes for monitoring the influenza virus. *Biosensors & Bioelectronics, 64*, 311–317. https://doi.org/10.1016/j.bios.2014.09.021
140. Zhou, J., Wang, Q. X., & Zhang, C. Y. (2013). Liposome-quantum dot complexes enable multiplexed detection of attomolar DNAs without target amplification. *Journal of the American Chemical Society*. https://doi.org/10.1021/ja3110329

141. Chen, L., Zhang, X., Zhou, G., Xiang, X., Ji, X., Zheng, Z., et al. (2012). Simultaneous determination of human enterovirus 71 and coxsackievirus b3 by dual-color quantum dots and homogeneous immunoassay. *Analytical Chemistry, 84*, 3200–3207. https://doi.org/10.1021/ac203172x
142. Tripp, R. A., Alvarez, R., Anderson, B., Jones, L., Weeks, C., & Chen, W. (2007). Bioconjugated nanoparticle detection of respiratory syncytial virus infection. *International Journal of Nanomedicine*. https://doi.org/10.2147/nano.2007.2.1.117
143. Li, Y., Jing, L., Ding, K., Gao, J., Peng, Z., Li, Y., et al. (2014). Detection of Epstein-Barr virus infection in cancer by using highly specific nanoprobe based on dBSA capped CdTe quantum dots. *RSC Advances, 4*, 22545–22550. https://doi.org/10.1039/c4ra02277g
144. Wang, X., Lou, X., Wang, Y., Guo, Q., Fang, Z., Zhong, X., et al. (2010). QDs-DNA nanosensor for the detection of hepatitis B virus DNA and the single-base mutants. *Biosensors & Bioelectronics, 25*, 1934–1940. https://doi.org/10.1016/j.bios.2010.01.007
145. Khan, M. Z. H., Hasan, M. R., Hossain, S. I., Ahommed, M. S., & Daizy, M. (2020). Ultrasensitive detection of pathogenic viruses with electrochemical biosensor: State of the art. *Biosensors & Bioelectronics*. https://doi.org/10.1016/j.bios.2020.112431
146. Felix, F. S., & Angnes, L. (2018). Electrochemical immunosensors – A powerful tool for analytical applications. *Biosensors & Bioelectronics, 102*, 470–478. https://doi.org/10.1016/j.bios.2017.11.029
147. Mahato, K., Kumar, S., Srivastava, A., Maurya, P. K., Singh, R., & Chandra, P. (2018). Electrochemical immunosensors: Fundamentals and applications in clinical diagnostics. In *Handbook of immunoassay technologies: approaches, performances, and applications* (pp. 359–414). Elsevier. https://doi.org/10.1016/B978-0-12-811762-0.00014-1
148. Kaushik, A., Yndart, A., Kumar, S., Jayant, R. D., Vashist, A., Brown, A. N., et al. (2018). A sensitive electrochemical immunosensor for label-free detection of Zika-virus protein. *Scientific Reports*. https://doi.org/10.1038/s41598-018-28035-3
149. Haji-Hashemi, H., Safarnejad, M. R., Norouzi, P., Ebrahimi, M., Shahmirzaie, M., & Ganjali, M. R. (2019). Simple and effective label free electrochemical immunosensor for Fig mosaic virus detection. *Analytical Biochemistry*. https://doi.org/10.1016/j.ab.2018.11.017
150. Valekunja, R. B., Kamakoti, V., Peter, A., Phadnis, S., Prasad, S., & Nagaraj, V. J. (2016). The detection of papaya ringspot virus coat protein using an electrochemical immunosensor. *Analytical Methods, 8*, 8534–8541. https://doi.org/10.1039/c6ay02201d
151. Tran, L. T., Tran, T. Q., Ho, H. P., Chu, X. T., & Mai, T. A. (2019). Simple label-free electrochemical immunosensor in a microchamber for detecting newcastle disease virus. *Journal of Nanomaterials*. https://doi.org/10.1155/2019/3835609
152. Mazloum-Ardakani, M., Hosseinzadeh, L., & Khoshroo, A. (2015). Label-free electrochemical immunosensor for detection of tumor necrosis factor α based on fullerene-functionalized carbon nanotubes/ionic liquid. *Journal of Electroanalytical Chemistry, 757*, 58–64. https://doi.org/10.1016/j.jelechem.2015.09.006
153. Turner, A. P. F.. (2013). Chemical society reviews biosensors: Sense and sensibility. Chemical Society Reviews.
154. Dias, A. D., Kingsley, D. M., & Corr, D. T. (2014). Recent advances in bioprinting and applications for biosensing. *Biosensors, 4*, 111–136. https://doi.org/10.3390/bios4020111
155. Kim, J., Imani, S., de Araujo, W. R., Warchall, J., Valdés-Ramírez, G., Paixão, T. R. L. C., et al. (2015). Wearable salivary uric acid mouthguard biosensor with integrated wireless electronics. *Biosensors & Bioelectronics, 74*, 1061–1068. https://doi.org/10.1016/j.bios.2015.07.039
156. Scheller, F. W., Yarman, A., Bachmann, T., Hirsch, T., Kubick, S., Renneberg, R., et al. (2014). Future of biosensors: A personal view. *Advances in Biochemical Engineering/Biotechnology, 140*, 1–28. https://doi.org/10.1007/10_2013_251
157. Wang, S., Poon, G. M. K., & Wilson, W. D. (2015). Quantitative investigation of protein–nucleic acid interactions by biosensor surface Plasmon resonance. In *Methods in Molecular Biology* (pp. 313–332). Humana Press Inc.. https://doi.org/10.1007/978-1-4939-2877-4_20

158. Zhang, Z., Liu, J., Qi, Z. M., & Lu, D. F. (2015). In situ study of self-assembled nanocomposite films by spectral SPR sensor. *Materials Science and Engineering: C, 51*, 242–247. https://doi.org/10.1016/j.msec.2015.02.026
159. Arlett, J. L., Myers, E. B., & Roukes, M. L. (2011). Comparative advantages of mechanical biosensors. *Nature Nanotechnology, 6*, 203–215. https://doi.org/10.1038/nnano.2011.44
160. Peng, F., Su, Y., Zhong, Y., Fan, C., Lee, S. T., & He, Y. (2014). Silicon nanomaterials platform for bioimaging, biosensing, and cancer therapy. *Accounts of Chemical Research, 47*, 612–623. https://doi.org/10.1021/ar400221g
161. Shen, M. Y., Li, B. R., & Li, Y. K. (2014). Silicon nanowire field-effect-transistor based biosensors: From sensitive to ultra-sensitive. *Biosensors & Bioelectronics, 60*, 101–111. https://doi.org/10.1016/j.bios.2014.03.057
162. Kunzelmann, S., Solscheid, C., & Webb, M. R. (2014). Fluorescent biosensors: Design and application to motor proteins. *EXS, 105*, 25–47. https://doi.org/10.1007/978-3-0348-0856-9_2
163. Oldach, L., & Zhang, J. (2014). Genetically encoded fluorescent biosensors for live-cell visualization of protein phosphorylation. *Chemistry & Biology, 21*, 186–197. https://doi.org/10.1016/j.chembiol.2013.12.012

Machine Learning-Enabled Biosensors in Clinical Decision Making

Srishti Verma, Rajendra P. Shukla, and Gorachand Dutta

Abstract

Healthcare digitization offers a variety of chances for minimizing human error rates, enhancing clinical results, monitoring data over time, etc. Machine learning and deep learning AI techniques play a key role in enhancing new healthcare systems, patient information and records, and the treatment of various ailments, among other health-related topics. The utilization of conventional sensor systems to decipher the environment is changing as another time for "smart" sensor frameworks arises. To create refined "brilliant" models that are custom fitted explicitly for detecting applications and melding different detecting modalities to acquire a more comprehensive understanding of the framework being observed, savvy sensor frameworks enjoy taken benefit of conventional and state-of-the-art machine learning calculations as well as contemporary PC equipment. Here is a chapter of current developments in biosensors used in healthcare that are reinforced by machine learning. First, several biosensor types are classified and a summary of the physiological data they have collected is provided. The introduction of machine learning techniques used in subsequent data processing is followed by a discussion of their usefulness in biosensors. And last, the possibilities for machine learning-enhanced biosensors in real-time monitoring,

S. Verma
School of NanoScience and Technology, Indian Institute of Technology, Kharagpur, India

R. P. Shukla
BIOS Lab-on-a-Chip Group, MESA+ Institute for Nanotechnology, University of Twente & Max Planck Centre for Complex Fluid Dynamics, Enschede, The Netherlands

G. Dutta (✉)
School of Medical Sciences and Technology, Indian Institute of Technology, Kharagpur, India
e-mail: g.dutta@smst.iitkgp.ac.in

G. Dutta (ed.), *Next-Generation Nanobiosensor Devices for Point-Of-Care Diagnostics*, https://doi.org/10.1007/978-981-19-7130-3_7

outside-the-clinic diagnostics, and on-site food safety detection are suggested. These problems include data privacy and adaptive learning capabilities.

Keywords

Artificial Intelligence (AI) · Machine Learning (ML) · Biosensor · Clinical decision making · Point-of-care

1 Introduction

The application of biosensors in clinical exercise, health monitoring, and food safety has grown in relevance in recent years due to its mobility, variety, and simplicity compared to conventional approaches, which rely on expensive, heavy, and sophisticated devices. An essential subset of sensors called biosensors is created to record biological signals and be used in the field of medicine. One description of a biosensor is "a compact analytical device incorporating a biological or biologically derived sensing element either integrated within or intimately associated with a physicochemical transducer [1]." The academic community has been more interested in biosensors in recent years. However, the google search popularity rankings for biomarkers are still low (20), demonstrating that the general public still has limited knowledge of issues pertaining to biosensors [2]. This stark discrepancy may be caused in part by the knowledge gap that must be bridged between the vast amounts of data acquired by sensors and the important information deduced from those data. Therefore, many biosensors do not meet the criteria to be considered "analytical devices" [1]. Any sensor's primary job is to identify and deliver accurate data about the object it is intended to measure.

Because of its portability, it may be able to meet growing testing demands, which might have a transformative influence on healthcare [3]. There are two types of portable biosensors included in this study, each with a different technology. The first one is paper-based biosensor known as a lateral flow test biosensor. It deals with a strip that incorporates sample application cushion, a nitrocellulose film, a conjugate cushion, and an adsorption cushion. The preimmobilized reagents at better places of the strip become dynamic and show particular highlights when the designated fluid example runs over the strip. It has a number of advantages, including improved portability, cost effectiveness [4], and rapid detection, and as a result, it is frequently used to identify diseases [5] and evaluate food safety [6]. In the food safety field, Li and Liu's team used a Raman scattering-based lateral flow assay to sensitively detect Escherichia coli. Establishing regression models based on machine learning methods allows for accurate and quantitative analysis of Escherichia coli [7].

Microfluidic-based biosensors are another type of portable biosensor. Biosensors are integrated to lab-on-a-chip structures using microfluidics to create this type of portable biosensor [8]. The development of microfluidic systems enables the analysis of small-volume samples while also reducing reagent use and sample processing time. The amalgamation of microfluidics with machine learning forms, dubbed

"intelligent microfluidics [8]," maximizes the potential of the microfluidic-based biosensor. Smartphone and smart electronics are improving, and new apps are being developed, making them increasingly appropriate for use as compact biosensors and logical instruments in medical services and food safety [9].

Another example of portable biosensors are wearable biosensors which could be divided into three classes in light of sensor arrangement and epitome comparative with the human body: on-body, garments and material based, and frill [10]. Tattoo sensors, contact focal points, and skin patches are examples of on-body biosensors that interact closely with the human body. Biomarkers present in sweat and ISF, like lactate, glucose, and electrolyte ions, are oftentimes identified with tattoo sensors. To aid in the diagnosis of dehydration, a fluorescent technique based tattoo biosensor was designed for screening of dermal interstitial fluids electrolytes [11]. Interestingly, Wiorek et al. present an epidermal fix for glucose examination in sweat that consolidates pH and temperature change [12]. Sensors that are coordinated with material wearables are known as clothing and material based biosensors [10]. These are oftentimes used to recognize wound liquid, sweat, and surrounding air. One of the most well-known models is the brilliant bandage. For real-time health monitoring, fiber-based biosensors may be a good option. They can be easily woven into textiles, perhaps allowing for improved biosensor wear experiences. Zhao et al. demonstrated wearable electrochemical biosensors based on gold fibers for sweat glucose monitoring [13]. Wearable biosensors that are loosely attached to the body or clothing are referred to as accessories [14]. The eyeglasses can all the while screen sweat electrolytes and metabolites progressively by joining metabolite-electrolyte sensors onto nose-span cement cushions. By picking the proper receptor and changing the cement cushions, different biomarkers can likewise be focused on accomplishing multianalyte detection on the eyewear stage [15].

Customary detecting frameworks frequently screen a solitary sensor yield, a gadget that screens the adjustment of the result obstruction as an element of temperature is known as thermistor. Higher data throughput will naturally result from the addition of more sensors to devices, which presents a significant difficulty in collecting and processing the vast amount of sensory input. Additionally, the exorbitant amount of information cannot be consistently labelled, processed, or analyzed using ordinary sensing devices and conventional processing methods [16]. Machine learning (ML) algorithms and theories [17] have recently made strides, opening up new possibilities and providing new perspectives on how to effectively tackle these problems of large data sets. These ML algorithms are already being used in real-world settings for things like business [18], healthcare analytics [19], and economics [20].

The capacity of ML calculations to gain and naturally separate examples and qualities from a given assortment of information, which typically needs a space master to uncover, is its critical upper hand. In light of their flexibility and toughness, ML calculations might be utilized in essentially any application that meets the central state of an erratic dataset. The developing information amounts and inadequately comprehended framework models of customary detecting advances might make these calculations viable substitutions. Top of the line "brilliant" models

made utilizing ML calculations supplant as far as possible in a conventional detecting framework. The calculations are utilized to assess, investigate, and extricate significant information from gigantic, confounded data sets. They depend on numerical and measurable procedures. The majority of "smart" systems are developing to benefit from the trend toward parallel computation that became more accessible with the development of contemporary graphics processing units (GPUs). The expense of estimation time in information examination and model preparation is enormously diminished due to the excellent equal handling limit that permits algorithmic models to dissect hundreds or even millions of data of interest without a moment's delay [21]. Before passing on the sensory measures to a trained smart ML-based model, the system preprocesses them. The smart model then processes and analyzes the sensory data according to the application's requirements. The necessities of the application and the sensor innovation conclude which of the two sorts of shrewd models are laid out for savvy sensor frameworks. The keen models might be partitioned into two gatherings in view of whether they are prepared to address classification-based issues or regression-based issues. To associate the connections between tactile information and future qualities (e.g., future blood glucose level forecast in light of past estimations) [22], a regression model employs predictive ML algorithms, though a classification-based savvy model utilizes sorting ML calculations to distinguish and isolate sensory information with discrete class marks (e.g., recognizing malignant growth and non-malignant patients from gas sensor estimations) [23]. To reveal patterns of sickness states inside that expanse of large information, ML would empower AI preparing by combining various sources from verifiable datasets of millions of patients, like clinical records, clinical imaging, omics, and wearable diagnostics [24–27]. As an outcome, enough amounts and sorts of preparing tests would be incorporated, and general access constraints to nearby datasets would be taken out as an obstruction to the improvement of solid AI-driven redid clinical decision support systems (CDSSs). The got CDSS-empowered AI calculation could then be upgraded with new information from different existing and novel devices to empower exact pre-screening and analysis as well as giving inside and out information on sickness highlights like subtype, grade, stage, and hereditary transformation to help altered therapy.

In this chapter, we have first come up with an overview of the well-known ML methods that are applied to build intelligent models in a smart sensor system with ML support for real-world sensing applications along with ability to take clinical decisions. The ML techniques are separated into two groups under this section: traditional non-neural network (non-NN) algorithms (e.g., Principal Component Analysis [PCA], linear discriminant analysis [LDA], Support Vector Machine [SVM], Hierarchical Cluster Analysis [HCA], Random Forest [RF], and Decision Trees [DT]) together with modern neural network (NN) methods (e.g., Feed Forward Artificial Neural Network [FFA-NN], Recurrent Neural Network [RNN], Convolution Neural Network [CNN]). Subsequently, we have given an overview of the novelties of smart ML-reinforced biosensor in real-world sensing benefits (Fig. 1).

The assessment closes by outlining the main paths and difficulties encountered by current research initiatives and suggesting future research possibilities where holes

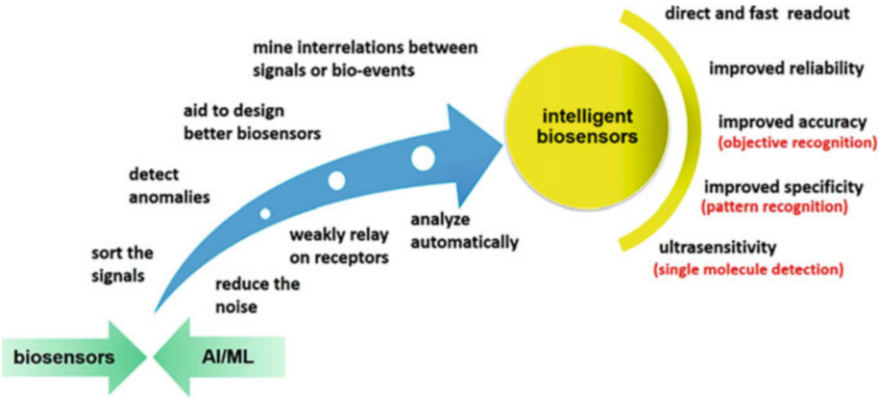

Fig. 1 Advantages ML brings to biosensors. Reproduced with permission from ref. [28] Copyright 2020 American Chemical Society. All rights reserved

exist in present endeavors. Non-NN algorithms, as a general rule, are often hard to set up and call for more physical work to calibrate ML boundaries to achieve application goals. This is because of the necessity for space skill about the qualities of a particular sensor dataset to exactly make an application-explicit non-NN brilliant model. Moreover, the elements can be "automatically" recovered by other ML algorithms or physically picked by a space expert [29].

1.1 AI-ML in Medical Sensors

Other benefits of ML in biosensors is the capacity to get great logical outcomes from boisterous and low-goal detecting information that might vigorously cover. ML can move maneuver information from biosensor in different ways: (1) Categorization: The algorithms can categorize the sensing signals into multiple groups depending on the analyte of interest. (2) Anomaly detection: The sample matrix and operating circumstances will always have an impact on biosensors. When biosensors are employed on-site, contamination can be considerably hampered. ML could inspect the signal and respond to request "does the signal appear to be correct?" It also "corrects" sensor performance discrepancies in real samples caused by biofouling and interferences. (3) Noise reduction: The sensor signals are constantly accompanied by noise. Signal obstruction, like electrical clamor, can happen on the subsecond course of events, while biosensor signals develop over seconds or minutes. (4) Pattern recognition and Object identification: Sensing data may be simply and successfully processed by utilizing ML algorithms to uncover latent objects and patterns [30, 31]. ML can automatically, directly, precisely, and quickly support biosensor readout, which is basic for on location discovery or analysis. Researchers can create optimum sensing devices faster by clustering of metamaterials, which eliminates the need for significant experimentation.

Medical sensors have simplified the operations of medical instruments while making them safer and more effective [32]. They have been developed to analyze biomarkers present in body fluids (sweat, breath, tears, urine, saliva, etc.) flowing in or out of the body for diagnosing and monitoring diseases. Inside the most recent 40 years, significant headway has been made, and a few significant upheavals have happened from lab-based cathodes to versatile biosensors and presently to wearable biosensors. Long-term monitoring of multivariate groups is now possible due to the proliferation of noninvasive portable and wearable sensors, hence largely overcoming the challenges when it comes to biosensor data collection. This could bring another revolution—AI/ML Biosensors [33]. In the first place, multitudous signal, regularly electrical and optical signs are gathered from biosensors followed by its contribution to different ML algorithms, with a few unique structures. Each signal has an alternate property that in this way prompted various information handling using ML. ML calculations play essential part in design acknowledgment and arrangement to brace biosensors in expanding applications, further developing selectivity and selectivity, and helping navigation.

Shin et al. depicted a profound learning model for beginning phase cellular breakdown in the lungs determination that was prepared using surface-improved Raman spectroscopy (SERS) signs of exosomes delivered from sound and cellular breakdown in the lung's cells, with a separation exactness of 95%. The profound learning model showed that 90.7% of the 43 patients with stage I and II malignant growth would have higher likeness to cellular breakdown in the lungs cell exosomes than the normal of the solid controls, exhibiting the expected utility of profound learning name free SERS strategies for clinical interpretation. These advances, then again, extricate wellbeing markers in an obtrusive way and don't consider constant checking or estimation of natural liquid structure. AI based intelligence empowered electrochemical biosensors coordinated with versatile and wearable dissecting electronic stages, which can give logical data utilizing an organic acknowledgment component, stand out enough to be noticed for the in situ discovery of clinical markers in different body liquids, attributable for their exceptional potential benefits of scaling down, high sensitivity, and name free estimation [34]. Kim et al. reported that utilizing ML algorithms, they were able to identify and discriminate prostate cancer with 99% accuracy using a urinary multimarker biosensor [35]. A solitary biomarker study had a typical exactness of just 62.9%, missing almost 50% of the patients. The specialists found that rising the quantity of biomarkers further developed screening viability while using random forest (RF) and neural network (NN) algorithms. ML can recognize prostate cancer growth patients with more than 99% accuracy utilizing 76 urine examples. ANN model-helped Si nanowire field effect transistors (SiNW FETs) for particular VOC identification in single-part and multicomponent circumstances were exhibited by Wang et al. [36]. Eleven VOCs, as well as their twofold and ternary blends, could be precisely identified using just a single SiNW FET sensor (as opposed to a variety of various sensors as in exemplary electronic nose techniques). Indeed, even in multicomponent combinations containing balancing atoms with physical/substance properties indistinguishable from those of the designated VOC, this technique showed great

selectivity toward explicit VOC(s). Concentration of VOC could likewise be anticipated with low blunders utilizing ANNs and a solitary SiNW FET.

2 Different Biosensors with Machine Learning

2.1 Electrochemical Biosensors

The electrochemical biosensors (EC) are one of the most common biosensors used in medical diagnosis [37–42]. The use of novel ML procedures in current EC biosensors, notwithstanding, is still in its outset. EC biosensors are not truly repeatable or stable in real sample discovery, despite the relatively extensive theoretical foundations of electrochemistry allowing description of a vast range of signals. The electrode utilized in EC biosensors fouls over the long haul, which is another element. Therefore, sensitive signals that are significantly linked with the type and quantity of analytes cannot be acquired using one-dimensional data analysis. The potential for coordinating ML with electrochemical biosensors to research how ML might be utilized to increment sensor accuracy and reliability in real sample estimations is featured by this [43–45]. Massah and coworkers employed an SVM regression model to enhance the functionality of a portable EC biosensor based on cyclic voltammetry [46]. The SVM regression model was used to extend the useful life of the EC biosensor, allowing it to continue functioning for 10 days after the enzyme has been immobilized. Different part types, including linear, polynomial, and Gaussian with various boundaries, were utilized to figure the concentration of nitrate. Their presentation was assessed utilizing the correlation coefficient (R^2) and mean squared error (MSE). The polynomial portion with the kernel boundary at $y = 0.20$ was ideal, with a MSE of 0.0016 and a R^2 of 0.93, according to the results. The SVM regression model was used to extend the useful life of the EC biosensor, allowing it to continue functioning for 10 days after the enzyme has been immobilized. Four hundred nitrates and, surprisingly, more can be found even without changing the enzyme.

By utilizing techniques like *electrochemical impedance spectroscopy (EIS)*, equivalent circuit models can be used to derive an important characteristic from EIS data with χ^2 testing. The retrieved parameters are used to provide information about the events occurring on the working electrodes. The troublesome aspect of adjusting the EIS information from electrode arrangements or solution is picking or making a similar to circuit model [49]. The equivalent circuit model examination was inadequately portrayed, especially for the small molecule-protein collaboration based EIS biosensors. Rong et al. created an SVM prototype without equivalent circuit fitting to assess the EIS data [50]. To identify the most effective machine learning model, SVM prototype with four distinct kernels—sigmoidal, polynomial, radial basis, and linear function—were contrasted. Eighty percent of 54 EIS data were arbitrarily chosen as training data, while the residual 20% were assigned to the testing information set. The training information set was classified with an accurateness of 98% using the radial base function kernel, which performed at its best. The

performance was improved by adjusting the penalty parameter (C) and nonlinear kernel coefficient (γ) to their optimum values of 10 and 0.01, respectively. There hasn't yet been any information about an EC biosensor that uses deep learning. The small number of accessible data sets may be one factor. This open doors for the utilization of deep learning in electrochemical biosensors will emerge from the improvement of arrays or multiplexed EC biosensors to assess countless real samples.

The accurateness and precision of single-molecule (SM) identification can be increased by combining it with ML. Additionally, the combination can optimize the design constraints of the electrical biosensor and quantitatively assess the capability of molecule recognition [51]. SM electrical detecting techniques can be categorized into two groups: nanopore and nanogap. They are frequently used for viral detection [52], peptide sequencing, DNA, carbohydrate, and RNA, [53–55]. However, maximum current (I_p) and current duration (t_d) signals for analytes with similar molecule volumes and border orbital energies are similar. The detection and identification of several analytes cannot be accomplished via the overlap of current signals. By applying ML techniques like SVM, RF, and CNN to analyze the current-time waveform, this problem is solved [56]. The Rotation Forest model was shown by Kawai and colleagues [48] to be able to distinguish between electrical signs and comparable microbiological forms. Other barely noticeable highlights can be recuperated for distinguishing the bacterial species (*E. coli* and *Bacillus subtilis*) notwithstanding the width td and height Ip of the ongoing waveform (Fig. 2). By fusing the time vector with the present vector, 60 features were obtained. To anticipate the leftover 18 resistive waveforms as the test, the whole collected qualities of 161 waveforms from B. subtilis and *E. coli* (a sum of 322 spikes) were utilized as training information. The discoveries showed that a solitary bacterium has a separation exactness of more noteworthy than 90%.

2.2 SERS and Other Spectra-Based Biosensors

A complex matrix can even be used to get intrinsic fingerprint information about an analyte by means of surface enhanced Raman spectroscopy (SERS). One of the most encouraging insightful strategies for fast, label-free, point-of-care, and nondestructive diagnosis is SERS sensing [57, 58]. However, the spectra of many analytes and the material in the matrix are comparable or overlap. Manually differentiating them is difficult or impossible. Hopefully, the use of ML will considerably increase SERS's efficacy. Since huge informational index variety brings the fluctuation up in predictions, that confines the ways to deal with semiquantitative analysis, the consistency of the enhancement element of the SERS substrate is vital for ML techniques [59]. With intermediate or big information sets, CNN consistently displays a higher prediction accuracy than other ML techniques [60]. CNN is presently the most often used for spectral analysis as a result [61, 62]. Ying's team published a useful manual for CNN used in the spectrum analysis [63]. To distinguish between normal and malignant cells by detecting the medium used for cell

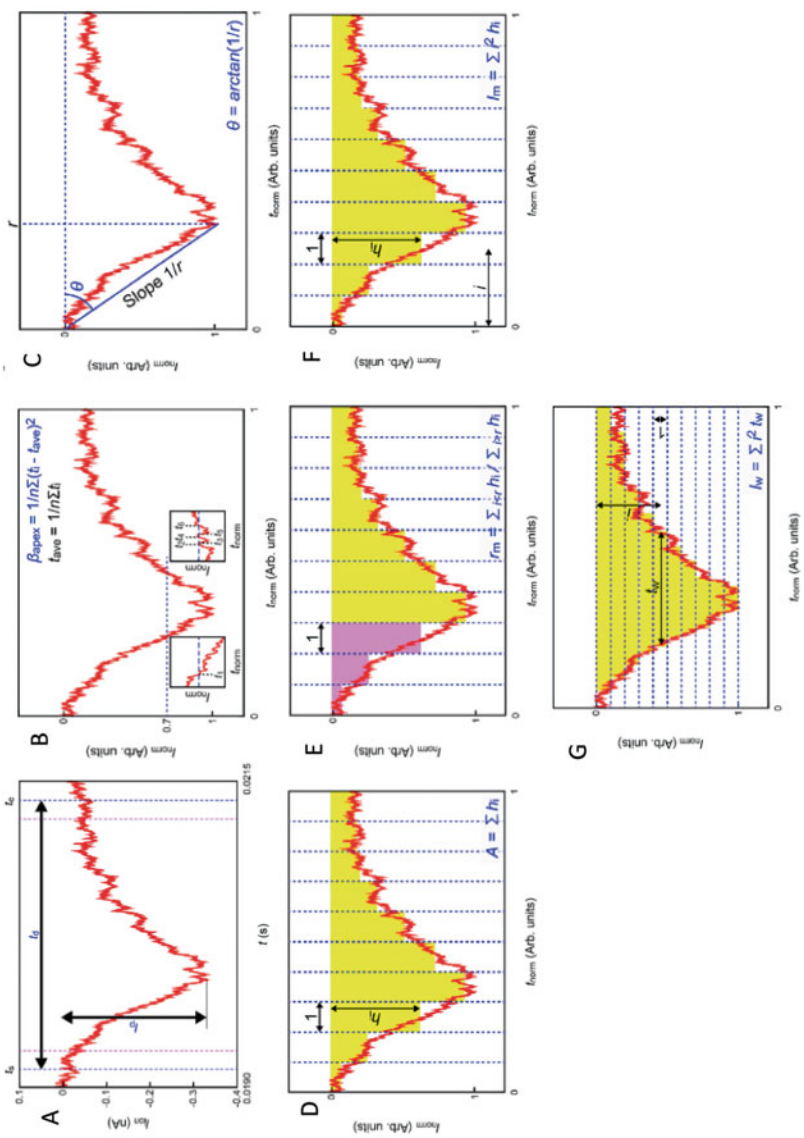

Fig. 2 Extracted multidimensional characteristics from the current-time waveform, which is reproduced with permission from Ref. [47, 48], All rights Reserved 2017 Springer Nature Limited and The American Chemical Society. Pulse height I_p and width t_d (**a**), bluntness of resistive pulse apex βapex (**b**), onset angle θ (**c**), area A (**d**), ratio r_m of area before current peak to that of behind the current peak (**e**), inertia I_m (**f**), and I_w (**g**). The multiphysics simulation of the waveform during the bacteria's passage through the nanopore biosensor was used to precisely analyze the different characteristics for differentiating between ΔfliC and wild-type *E. coli*

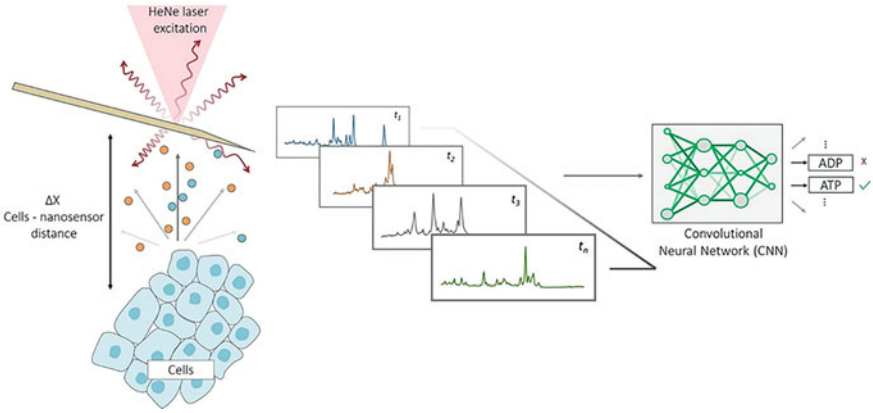

Fig. 3 Machine learning reinforced surface enhanced Raman spectroscopy nanoprobe, Reprint with permission from [59]. Copyright 2019 American Chemical Society. All Rights Reserved

growth, Erzina et al. developed an enhanced SERS-CNN approach [64]. The biomarkers were captured and the Raman signals were improved using gold multi-branched nanoparticles (AuMs) decorated with various chemical groups. In order to acquire greater resolution SERS spectra, a plasmonic coupling was also formed on the gold strident surface. The problem, though, is that the target analyte caused the interference signal to grow, which in turn reduced the detection's accuracy (Fig. 3).

To solve this obstacle, the SERS and CNN approaches were combined. The findings indicated the estimated accurateness was 100% for data justification using a comparable but modified CNN method. For single-molecule and single-cell investigation, combining SERS biosensors and ML techniques is extremely desired. It is quite intriguing that the CNN prototype, that has significantly improved the recognition accurateness, can readily distinguish between non-analyte and signal clatter. A spectral signal could also be transformed into a concentration value using the CNN model and the Langmuir isotherm deviations. Microorganisms can also be recognized by Raman spectroscopy down to the single-cell or single-particle level. More precise identification outcomes may be obtained by using ML in conjunction with a sizable microbe-related Raman data collection. A CNN model and laser tweezer Raman spectroscopy have both been used to detect different microbe class or subtypes at the solitary-cell level [65].

2.3 Colorimetric and Fluorometric Biosensor

Here we focus on biosensors that employ pictures as detecting signals, such as fluorometric and colorimetric ones. Significant attention has been generated by the automatic classification of colors and its intensity through the photos captured using biosensing. One kind of fluorometric biosensor is the digital polymerase chain reaction (dPCR). Colorimetric biosensors include the lateral flow assay,

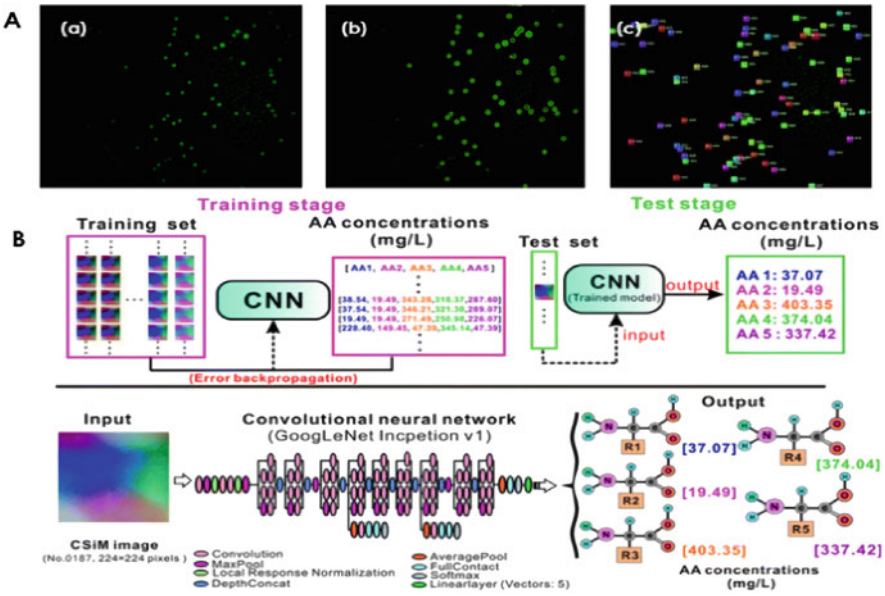

Fig. 4 (**A**) Mask R-CNN prototype and threshold separation analysis of photos with varying lighting conditions. Reproduced from reference with permission from ref. [66] Copyright 2019. The Royal Society of Chemistry. All rights reserved. (*a*) A real-world experiment's image with asymmetrical lighting. (*b*) The outcomes of segmentation by threshold. (*c*) The Mask R-CNN prototype's findings. (**B**) CNN prototype for mixed AA analysis developed. Reproduced with permission from Ref. [68] Copyright 2020. The Royal Society of Chemistry

paper-based vertical flow assay, and various colorimetric strips. For the dPCR to be used in the real application, it must be possible to recognize the positive reaction chamber in the fluorescent picture accurately and quickly. The analysis of the photos has made use of conventional techniques such as threshold segmentation, numerical clustering, and grid placement [66]. Threshold segmentation is the most popular image processing technique [67]. In each study, the threshold segmentation's settings must be adjusted. Additionally, it is restricted to the examination of photos with irregular illumination brought either by subpar camera imaging or irregular lighting. In the actual testing environment, the distribution of light intensity is never even. A low accurateness of the affirmative response chamber identification may result from this circumstance. Mask R-CNN has recently been used to accurately and automatically evaluate the photos [66]. An actual image (Fig. 4Aa) revealed that the micro-reaction compartments, including the positive one, have lesser illumination in this location on the left than in other places. The findings based on threshold separation and the suggested Mask R-CNN prototype, respectively, were displayed in Figs. 4Ab and Ac. With two misclassified spots, the threshold separation approach read out 56 illuminated spots out of 82 affirmative response compartments. The percentage of true positives was 68.29%. The created CNN prototype has potential applications in digital ELISA [69], location surface plasmon resonance imaging

[70], and fluorescent microarrays [71, 72] technologies for biological detection, in addition to the dPCR.

Colorimetric detection (quantitative) with improved accurateness and repeatability is made possible by smartphone apps and cloud-based ML prototypes [73, 74]. A colorimetric biosensor based on a smartphone was recently created to track bacterial water pollution [75]. Based on the color intensity of the biosensor pictures, CNN was used to categorize the presence or absence of bacteria. The reported strategy enhanced the accuracy of *E. coli* presence prediction to 99.99%. The detection of saliva alcohol concentrations was investigated utilizing a smartphone-based colorimetric biosensor and three distinct machine learning techniques (ANN, SVM, and LDA). Images in 4 color domain (HSV, RGB, Lab, and YUV) were assessed using ML methods. The RGB color space's green channel had the best differentiability and sensitivity, whereas the blue channel saw a significant color change. With LAB color domain as element, the ANN model performed at its best. The total categorization rate for increased concentrations was 80%, whereas it was 100% for standard concentrations [76]. The colorimetric sensor with CNN assistance can interpret the result quickly without using bulky equipment. For the measurement of mixed amino acids (AAs), a color spectral image-based approach was published in addition to the colorimetric and fluorometric image-based recognition methods [68]. LeNet, Vanilla CNN, Inception v1, SqueezeNet, and Residual Network (RestNet), six popular CNNs, were investigated. The generated Inception v1 model demonstrated advanced accuracy and better mordancy among these six CNNs algorithms. The RMSE was 10.22% and the R^2 for five AAs was 0.999 (Fig. 4B).

2.4 Cytometry Based Biosensors

There were reported many ML-based microfluidic cytometers [77, 78]. To inspect the presentation of a focal point free blood cell counting gadget that incorporates a microfluidic station and a complementary metal oxide semiconductor (CMOS) picture sensor, outrageous learning machine-based super-resolution (ELMSR) and CNN-based super-resolution (CNNSR) were utilized [77].

Four times the cell resolution was increased, and CNNSR demonstrated 9.5% higher quality than ELMSR in terms of resolution augmentation. A blood brain barrier (BBB) organ-on-a-chip was created by Oliver and colleagues to study the brain metastasis of breast cancer. A blood brain barrier (BBB) organ-on-a-chip was created by Oliver and colleagues [79] to study the brain metastasis of breast cancer. Confocal tomography was used to find cellular dynamic phenotypes and characteristics. Eight machine learning techniques were used to evaluate the pictures, including NB, neural networks, RF and NN, DT, stochastic gradient descent (SGD), and logistic regression to forecast the likelihood of brain metastasis. These ML calculations were reviewed utilizing the region under the weighted average of accuracy and review (F1), exactness (CA), and bend (AUC) (Fig. 5).

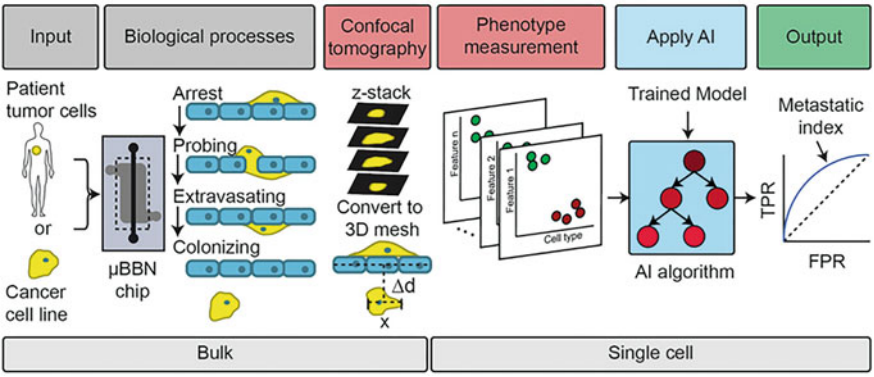

Fig. 5 ML-assisted ex vivo organ-on-a-chip model to study the metastatic spread of cancer to the brain. Reproduced with permission from Ref. [79] Copyright 2019

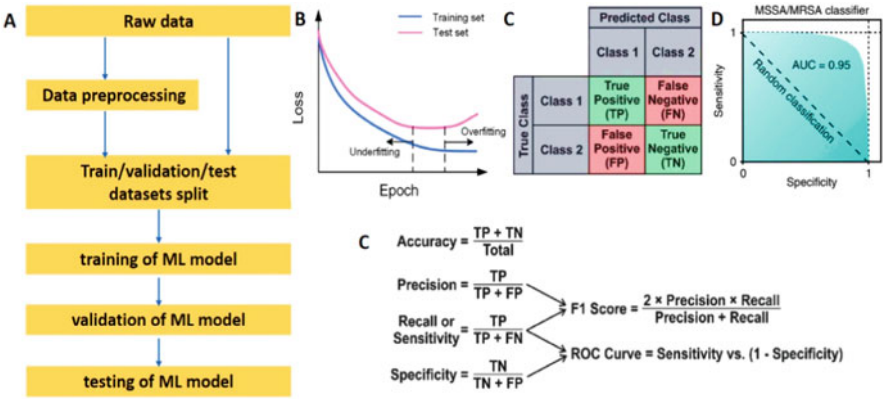

Fig. 6 (**a**) The basic methodology for ML-based data analysis. Reproduced from ref. [80] with permission. Copyright 2020. American Chemical Society. All rights reserved. (**b**) The loss curve during training. When the test set loss rises, overfitting will happen. Reproduced from ref. [81] with permission. Copyright 2019 Elsevier B.V. All rights reserved. (**c**) A representation of a confusion matrix, the formulae for the first level metrics that may be derived from it, and the second level metrics that are more effective. Reproduced from ref. [82] with permission. Copyright 2020 Elsevier B.V. A ROC curve in (**d**) Reproduced from ref. [83] with permission. Springer Nature Limited. Copyright 2019. The Authors

3 Machine Learning for Biomedical Processing

When used in the biomedical field, data processing is crucial for maximizing the amount of information that can be extracted from biosensors and converting it into messages that users can interpret (Fig. 6).

An essential move toward working on the presentation of biosensors is to lay out an acceptable relationship between the crude information and the concentration of the objective analyte as numerous biosensors base their detecting on the location of explicit analytes. The mathematical models were created manually in the conventional data analysis paradigm. Only straightforward models, like the linear prototype and the polynomial prototype, were utilized to analyze the data, and the studied data were only of low dimensions (2D and 3D). Consequently, it is crucial to create a new paradigm for data processing. We review the data processing techniques applied to biosensors during the past 6 years in this part, covering preprocessing and machine learning (ML) algorithms for biological signals [84].

3.1 Data Preprocessing

In many biosensors, processing of signal acquired is necessary to effectively carry out following processing steps. Preprocessing encompasses a variety of data modification processes, such as image analysis, data metric creation, and transformation. One or more preprocessing actions are required, depending on the properties of the raw data that was obtained. Three main preprocessing techniques are introduced here.

Baseline Correction

The goal of baseline correction is to account for drifts and so improve the responsiveness of sensors [85]. An example would be a CV. The choice and placement of baselines heavily influence the mathematical relationships that are frequently created between the concentration of the analyte of interest and the peak current. The performance of the biosensor can be enhanced with baseline correction because it makes it easier to measure the peak current. Fractional, relative, and difference baseline correction methods are available [86].

Data Standardization

Data normalization is a process that corrects for measurement disparities among arrays as well as variations in sensor scale [87], making it easier to compare results across multiple experiments.

Data Compression

One of significant parts of its goal is to likely diminish the information aspects and extraction of the most helpful elements. Principal component analysis (PCA), a solo ML approach, is much of the time utilized for information pressure. Since the early 2000s, PCA has been used to decrease the dimensions of information [88]. By computing the principal components (PCs), it achieves dimensionality reduction and decreases the information dimension to only the first few PCs. Here, PCA makes it possible to clearly visualize the data structure and makes the subsequent model creation easier [89]. The quality of the regression is impacted by the number of selected PCs. The ideal number of PCs can be found and all that results can be

acquired by sweeping the quantity of components to incorporate [90]. Another technique for reducing dimensionality is linear discriminant analysis (LDA) which is supervised, opposed to PCA, and generates vectors that optimize mean differences between the target classes [91].

4 Non-neural Algorithm

Non-NN algorithms, by and large, are harder to set up and expect for more manual work to tweak ML parameters to achieve application targets. This is because of the prerequisite for space skill about the qualities of a particular sensor dataset to definitively make an application-explicit non-NN smart model. Additionally, the element can be "automatically" extracted by other ML algorithms or manually chosen by a domain expert [92]. Non-neural ML techniques employed in biosensors to interpret biological signals, including abovementioned random forests, PCA, and LDA. Figure 7 displays the graphic representations of various algorithms. Table 1 provides a quick overview of the biosensors strengthened with non-neural methods.

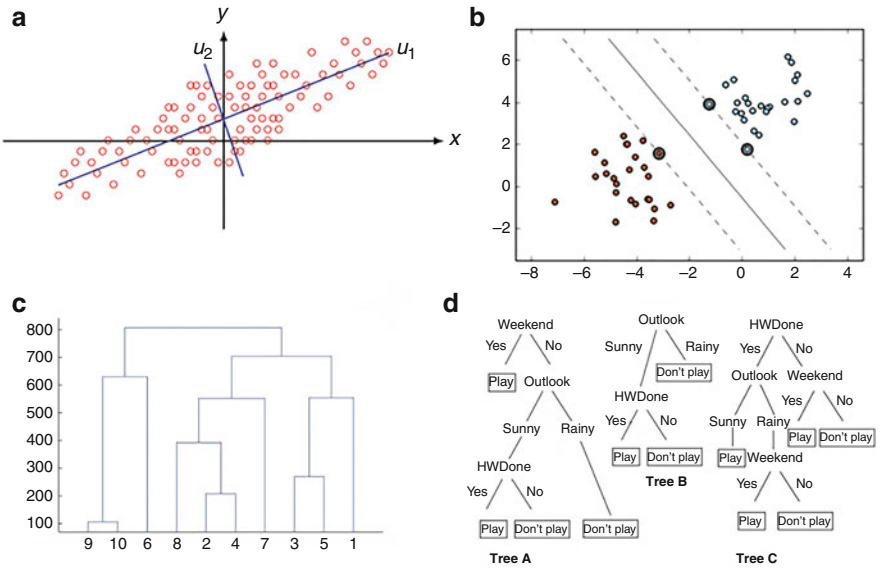

Fig. 7 Schematic illustrations of machine learning algorithms. (**a**) PCA, which is reproduced with permission from ref. [93], Springer Nature 2016, All rights reserved. (**b**) SVM, which is reproduced with permission from [94], Springer Nature 2018, All rights reserved. (**c**) HCA, which is reproduced with permission from ref.[95], John Willey and Sons 2015, All rights reserved. (**d**) Three Trees' RFs, which are reproduced with permission from Ref. [96] under the guidelines of Creative Commons Attribution License 2014, All rights reserved. The Authors. Publisher Tylor & Francis

Table 1 Non-neural algorithm reinforced biosensor

Machine learning algorithm	Target analyte	Mechanism	Collected data format	Application	Root mean square error	References
PCA, HCA, PLS	Exhaled VOCs	Electrochemical	Conductance	Diagnosis of diabetes mellitus, chronic kidney disease	3.83	[23]
HCA	Exhaled VOCs	Electrochemical	Resistance	Assess asthma in a clinical setting	–	[97]
MLR	Exhaled VOCs	Electrochemical	Resistance	Classification and diagnosis of 17 diseases	–	[98]
kNN, SVM, QDA	Food odor	Electrochemical	Resistance	Beef quality	0.519	[99]
PCA, RFs	Food odor	Electrochemical	Resistance	Internal quality of the Chinese pecans	Linoleic acid = 0.5727	[81]
PCA,k-means, SVM, DTs	Food odor	Electrochemical	Resistance	Diagnosis of potato storage disease	–	[100]
PCA, LDA, SVM	Food odor	Electrochemical	Resistance	Detection of milk adulteration	–	[101]
SVM, RF, XGBoost	Food odor	Electrochemical	Resistance	Detection of wine properties	–	[102]
PCA	Glucose, fructose	Optical	SEIRA	Detection of glucose and fructose level	–	[103]
SVM	Blood glucose	Electrochemical	Voltage	Detection of blood glucose	–	[104]
SVM	Biomarkers, biomolecules	Optical	Fluorescence intensity	Detection of lysozyme and adenosine triphosphate	ATP/ LYS = 0.12/ 0.091	[105]
RFs	Transcription factors	Optical	Fluorescence intensity	Detection of specific molecules	Phenol=2.1	[106]
PCA	Blood glucose	Electro-magnetic	Simulated transmission response	Monitoring of blood glucose level	–	[107]
PLSR	Blood	Electrochemical	Voltage	Real-time analysis of dopamine and norepinephrine	DA = 2.9 NE = 2.37	[45]

4.1 PCA and LDA

The techniques are capable of accomplishing the arrangement function of many types of signals in addition to data preparation similar to e-nose signals. Using an e-nose information, PCA was used to separate four vigor conditions with two elements: diabetes, high creatinine in vigor people, and low creatinine in vigor subjects. The e-nose identify whether the milk is tempered by formalin by working out and looking at the initial two PCs' scores, of which the concentration can be even little than 0.01% [86]. LDA was employed in the same study to differentiate between various levels of adulteration [86]. By using LDA, Ali et al. were able to clearly discriminate between three dissimilar bacterial sets in scatter plots [108].

4.2 Support Vector Machine (SVM)

The most popular clustering approach in signal processing is SVM, a supervised machine learning algorithm. In order to divide data into potential classes, SVM creates a hyperplane or collection of hyperplanes in high-dimensional space. The hyperplane has the greatest remoteness from the closest training information point of class to reduce the generalization error of the classification. For both linear and nonlinear datasets, there exist multivariate functions to determine the hyperplanes, including linear, radial basis (RBF), polynomial, and sigmoid functions. Binary classification issues can be resolved using the SVM algorithm. One input to several classification outputs can be mapped using SVMs to resolve "multiclassification" challenges [109] or to address one-to-one predictive problems [110]. The SVM technique determines the biggest divergence between the input information, those are represented as nD support vectors, and divides them into two groups as $(n–1)D$ plane called the hyperplane. With the aid of a clever mathematical "kernel trick" [110], the hyperplane splits the input vectors into groups either linearly or nonlinearly. This gap between the input vectors and the hyperplane divider is known as the margin. The more correctly the datasets can be categorized, the higher the margin gap between the groups. In order to identify various wine qualities, Liu et al. used numerous ML techniques to analyze the information gathered from metal oxide semiconductor sensors and create pinpointing models. SVM performed the best at recognizing vintages and fermentation procedures among the tested algorithms [102].

4.3 Random Forests (RFs) and Decision Trees (DTs)

Each node represents a characteristic of an instance that needs to be "tested" in the DT method, each branch represents a value that the node can expect, and each leaf represents a value distribution. DT was chosen as one of the most accurate and sensitive algorithms to assess data from a wrist-worn biosensor and demonstrated its capability to identify opioid use in real time [111]. The creation of a DT model,

however, takes a lot of work. Working with high-dimensional data is challenging. As the tree gets deeper, an individual DT frequently runs into the overfitting issue. It will obtain an excellent training outcome but may cause unacceptably high test error [102]. In numerous ML applications, ensemble approaches have demonstrated great performance. RF, boosting, and bagging are the often utilized ensemble algorithms. RF operates by creating a variety of DTs for regression and classification [112]. Overfitting, especially when the tree is deep, is one of the drawbacks of DTs. Overfitting occurs when a model tries to find a general prediction rule rather than trying to adjust the noise in the training information to boost accurateness [113]. One approach to addressing this issue is RFs. In order to prevent overfitting and restrict error growth, RFs are constructed using numerous single decision trees and aggregate their findings into a single outcome. High sensitivity was achieved by utilizing RFs to look at huge-scale simulated response information from a biosensor array for the recognizable proof of minuscule molecules [106]. The classification along with prognosis of lung cancer relies on gene expression data, and Qingyong et al. present a self-paced learning bootstrap with random forest [114].

Numerous more non-neural algorithms, like multiple linear regression [99], k-means clustering [98], and k-nearest neighbor algorithm [99] (kNN) contribute to signal process in addition to the ML methods, of biosensors.

4.4 Hierarchical Cluster Analysis (HCA)

HCA is an unsupervised technique (cluster analysis). The techniques like Euclidean distance, squared Euclidean distance, Manhattan distance, maximum distance, and Mahalanobis distance are used to perform the clustering analysis. The clustering performance depends on the use of the proper metrics. HCA creates a cluster hierarchy that is frequently seen as a dendrogram. By comparing the similarities in tyrosol content across 15 various types of beers, for instance, HCA demonstrated a strong capacity to classify the brews [115]. In order to categorize the VOC patterns of asthma patients into three groupings, HCA was also used to evaluate the data from an e-nose equipped with 32 sensors [116] (Fig. 7c). Additionally using an HCA dendrogram, Saidi et al. demonstrated that the breath profiles could be effectively grouped in accordance with the patients' states of health [23].

5 Artificial Neural Network Algorithms

The parallel computational capability of GPUs used to train NN has significantly increased over the past 10 years, which has led to a rise in curiosity in deep learning techniques [17] and its real-life applications. The idea behind an artificial neural network is to create a network of inter-woven logical computation nodes that are each independently set off by numerical capabilities and weights that are established by information input into the ANN.

5.1 Feed Forward Artificial Neural Network

Three layers make up a typical feedforward neural network (FNN) configuration: an input layer, a hidden layer, and an output layer. It is built up of interconnected neurons and is intended to resemble the human brain. Data goes in a solitary direction—from the information input layer to the hidden layer and to the output layer—in light of the fact that the structure is non-cyclic and doesn't cycle or loop (Fig. 8).

It is divided into shallow networks and deep networks depending on how many hidden layers are there. Utilizing an activation function, for example, the sigmoid function or hyperbolic tangent function, real-valued number is computed for every neuron in hidden layers from the neurons associated in the previous layer.

After the value calculated exceeds a predetermined threshold, the node will become active. Both classification and regression problems can be solved with FNN. Rens et al. used readings from five e-nose devices on 52 lung cancer patients or healthy controls to train a FNN. The generated model was then applied to score the blinded patient sets and distinguish lung cancer patients from that of vigor controls [118]. FNN was also used as a potent machine learning model to analyze data gathered from electrochemical sensors and volumetric sensors. Similar to this,

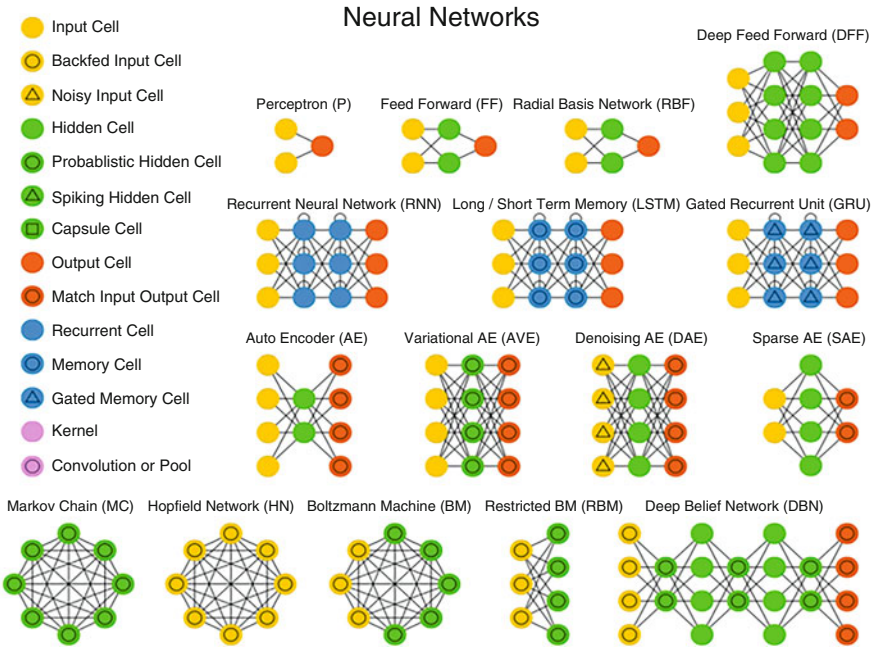

Fig. 8 Schematic of neural network structures, which is reproduced with permission [117] under the guidelines of Creative Commons Attribution License, All rights reserved, Copyright 2020. The Authors. Publisher MDPI, Basel, Switzerland

modest concentrations of very hazardous binary organophosphate combinations in milk were analyzed using FNN [119].

5.2 Recurrent Neural Network

RNN has caught researchers' interest among the various deep learning techniques in studies involving sequential data [120]. The internal recurrent n-neuron nodes of each m-recurrent hidden layer, however, function as memory elements [120]. Recurrent neuron nodes in a sequential chain can store activation data from earlier hidden states, mix it with current input state. The technique performs amazingly well with fleeting or sequential information, like prescient texts or speech recognition applications, because the link between previous items and the present input is preserved [121]. Because of their predominant presentation in model preparation, the cutting-edge RNN variations long short term memory (LSTM) and gated recurrent units (GRUs) have been widely adopted in numerous smart applications [122, 123]. Because the network topology of RNN is especially created to address past information in each repetitive round [124, 125], it is best suited for sequential data. RNN is frequently used for time-series mapping issues such as handwriting recognition (Doetsch et al., n.d.), speech recognition (Takeuchi et al.), and reinforcement learning [126, 127] because of the property of spreading previous information along time through repeating connections. To find DNA alterations, bidirectional RNN with LSTM was created [128]. Additionally, RNN-based algorithms have increased read accuracy for nanopore sequencing [129, 130].

5.3 Convolutional Neural Network

CNN is a sub-part of deep learning that excels at analyzing images, together with computed tomography (CT) [131], magnetic resonance (MR) images [132], and X-ray [133]. Typically, the CNN model has three level: (1) Convolutional level: This layer contains filters that move over preprocessed signals. Stride determines how the filter rotates the source image. After the convolution stage, the feature map can be obtained. (2) The down-sampling level, also known as the pooling layer. Convolutional layer output has to have its dimension reduced by a pooling procedure in order to avoid overfitting and reduce computational load. (3) A fully connected level: To incorporate nonlinearity into the output, Tanh, Relu, and Softmax (Costa) are typically utilized. The last decade have witnessed a number of significant developments in image processing applications, and CNN has created a number of specialized high-performance frameworks, including YOLO9000, AlexNet [134], GoogLeNet [135], U-net [136], and VGG [110]. The decomposition and conversion of the picture input propagated into the NN to a multidimensional array, from where important abstract structures are short-listed, is how a CNN outshines at processing along with analyzing images.

The abstract characteristics are then flattened and proliferated to neural network to get trained for applications based on regression or classification. To assess chemical spectra for multiplexing SERS sensing, Lussier et al. created one-dimension CNN prototype with two level convolutional, pooling, and densely linked neuron's figure for each [59]. The final output was transferred and transformed into probabilistic values using the SoftMax function. One thousand SERS spectra were obtained and were arbitrarily divided into (60%) training information, (20%) validation information, and test information. The greatest likelihood was given a positive integer value 1, while the others were given a negative integer value of 0. Preprocessing and labelling were done on the SERS spectra. Completely programmed approach for distinguishing lung cancer in the lung tissue sample through its complete slide pictures, was proposed by Matko et al. CNN is used for classification at the image patch level [137]. The execution of two CNN architectures, VGG and ResNet, is compared. Results acquired show that the CNN-based method can possibly help pathologists in the early diagnosis of lung cancer (Table 2).

6 Conclusion and Outlook

The benefits and drawbacks of the aforementioned machine learning algorithms are briefly discussed below after evaluating various machine learning techniques. SVM performs better when the dimension and sample size are bigger, but it takes longer to handle a large dataset and is not appropriate for classes that overlap. RFs make up for the overfitting flaw in single decision trees. In spite of the fact that it needs unobtrusive connections between predictions given by individual trees, it is compelling at dealing with missing information and decreasing both individual and absolute total errors. The advantages of neural networks are their high classification accuracy, great noise tolerance, and ability to approximate complex nonlinear relationships. To be more specific, it frequently needs a huge dataset, and when used in biosensors, thousands of specimens are required to achieve accurateness on par with non-neural methods. Furthermore, since we are not able to watch how problems are solved, it is challenging to explain the outcome, which undermines the validity and acceptance of the findings.

The advent and advancement of portable and wearable biosensors pave the way for in-person food safety testing, out-of-clinic diagnosis, and real-time monitoring. Using the right machine learning techniques, it is possible to efficiently analyze vast amounts of sensing information and convert it to understandable vigor information. Biosensors can identify illnesses outside of a clinic thanks to machine learning (ML). A deep neural network, for instance, has taught to categorize patients' actions and measure neurologic illness. But ML-enhanced biosensors still face a lot of difficulties, including those related to biosensor dependability and mass manufacturing, data privacy, and machine learning's capacity for adaptive learning. First, sensing performances are crucial to the machine learning-enhanced biosensor, and as machine learning is a technique to support sensor signal processing, a higher

Table 2 Neural algorithm reinforced biosensor

Machine learning algorithm	Target analyte	Mechanism	Application	Root mean square error	References
FNN	Exhaled breath	Electrical	Diagnosis of lung cancer	–	[118]
FNN	Fish sample	Electrochemical	Assessment of fish freshness	XT/HX = 1.3305/ 1.3319	[138]
FNN	Plant growth regulator and herbicide	Electrochemical	Detection of phytoinhibitor maleic hydrazide in crops	Training/ testing = 0.2724/ 0.4851	[139]
FNN	Hydroquinone, catechol	Spectrophotometric	Determination of catechol and hydroquinone	–	[140]
FNN	Binary organophosphate mixtures	Electrical	Detection of malaoxon and chlorpyriphos-oxon	–	[141]
FNN, ANFIS	Food odor	Electrical	Assessment of beef quality	0.002	[99]
BPNN	Catechol	Electrochemical	Detection of catechol in water	Training/ testing = 0.0074/ 0.0084	[142]
BPNN	Food odor	Electrical	Detection of wine properties	–	[102]
DCNN	Food odor	Optical	Assessment of food freshness	–	[143]
CNN	Bovine serum albumin	CMUT	Classify the sensor data to different propagation delay values	–	[144]
MLP, LSTM	Glucose		Healthcare monitoring system for diabetic patients	2.285	[22]

efficacy could only be attained by enhancing biosensor's dependability. Establishing smart sensor system that depends upon enormous information and algorithms is a significant barrier in terms of the tenet for data processing and storage. In neoteric years, cloud computing has been used to interpret sensor inputs since it offers superior computational power and data storage. Cloud and biosensor integration is nothing new, especially for surveil applications where the volume of information is continually growing over time. The direct connection of many sensors to the cloud is sometimes too expensive and too sluggish due to the exponential rise in the number of sensors. Edge computing has so been introduced in recent years. Instead of a single data center, edge computing enables data processing at scattered edge devices. It benefits from great computational effectiveness, rapid network processing, low cost, and more. Therefore, there is a good chance that biosensors will use this cutting-edge technology. Anytime something is connected to the internet, data privacy is always a possible concern. The healthcare sector has seen personal information leaks in recent years, raising concerns about data privacy. Together, sensor end-users, information owners, and service providers should address this problem [145]. Establishing a benign information sharing platform through advanced technologies and moral rules is of major relevance to data owners like doctors and sensor suppliers. A thorough process must be designed for product and service providers, or businesses across the board, to guarantee data protection.

The majority of ML-enhanced biosensors currently lack adaptive learning capabilities; therefore, this presents another problem. Biosensors will be able to learn from their surroundings using adaptive learning rather of only depending on manually input training sets. An adaptable model continually improves and optimizes itself by learning from the environment, in contrast to a nonadaptive system. Inaccurate results and catastrophic mistakes, that could be caused by a single-fixed model, might be less likely as a result [89]. On the other hand, adaptive learning is a solution to resolve the conflict between them since the quest of generalizability for nonadaptive ML models may result in the compromise of good local performance, especially in clinical practice [146]. With the use of machine learning (ML), these large-scale, high-dimensional datasets must be integrated and analyzed so that physical states may be classed and biomarker trajectories can be linked to clinically important outcomes [147]. Additionally, the potent skills in obtaining, analyzing, and translating enormous amounts of data will aid in addressing present problems in health sector, like grave diagnostic errors, and inefficient workflows, and set the groundwork for precision medicine [148].

As technology advances naturally, we will ultimately witness advancements in approaches, improved frameworks, and future breakthroughs in AI. There will be a snowballing need for highly effective, intelligent, precise, and sovereign smart sensor systems which process real-time risk and make decisions that could have life-or-death consequences as contemporary society plans for the inescapable advances into industrial revolution 4.0 [149]. This is clearly apparent in the realm of independent vehicles and might be applied to the assembling sectors where NN savvy machines and robots that are associated with the cloud are currently supplanting regular systems.

Acknowledgments Authors gratefully acknowledge the Start-Up Research Grant (SRG) funded by Science & Engineering Research Board (SERB) (SRG/2020/000712), Department of Science and Technology (DST)(Government of India, Ministry of Science and Technology, (Technology Development and Transfer, TDP/BDTD/12/2021/General), Indo-German Science & Technology Centre (IGSTC) (IGSTC/Call 2019/NOMIS/22/2020-21/164), and Institute Scheme for Innovative Research and Development (ISIRD) (IIT/SRIC/ISIRD/2019–2020/17), Indian Institute of Technology Kharagpur (IIT Kharagpur), India for the financial support.

References

1. Karunakaran, C., Rajkumar, R., & Bhargava, K. (2015). Introduction to biosensors. *Biosensors & Bioelectronics, 1–68*. https://doi.org/10.1016/B978-0-12-803100-1.00001-3
2. McRae, M. P., Simmons, G., Wong, J., & McDevitt, J. T. (2016). Programmable bio-nanochip platform: A point-of-care biosensor system with the capacity to learn. *Accounts of Chemical Research, 49*, 1359–1368. https://doi.org/10.1021/ACS.ACCOUNTS.6B00112
3. Jani, I. V., & Peter, T. F. (2013). How point-of-care testing could drive innovation in global health. *The New England Journal of Medicine, 368*, 2319–2324. https://doi.org/10.1056/NEJMSB1214197
4. Zhao, S., Wang, S., Zhang, S., Liu, J., & Dong, Y. (2018). State of the art: Lateral flow assay (LFA) biosensor for on-site rapid detection. *Chinese Chemistry Letters, 29*, 1567–1577. https://doi.org/10.1016/J.CCLET.2017.12.008
5. Raeisossadati, M. J., Danesh, N. M., Borna, F., Gholamzad, M., Ramezani, M., Abnous, K., et al. (2016). Lateral flow based immunobiosensors for detection of food contaminants. *Biosensors & Bioelectronics, 86*, 235–246. https://doi.org/10.1016/J.BIOS.2016.06.061
6. Mahmoudi, T., de la Guardia, M., & Baradaran, B. (2020). Lateral flow assays towards point-of-care cancer detection: A review of current progress and future trends. *Trends in Analytical Chemistry, 125*, 115842. https://doi.org/10.1016/J.TRAC.2020.115842
7. Yan, Y., Qiao, Z., Hai, X., Song, W., & Bi, S. (2021). Versatile electrochemical biosensor based on bi-enzyme cascade biocatalysis spatially regulated by DNA architecture. *Biosensors & Bioelectronics, 174*, 112827. https://doi.org/10.1016/J.BIOS.2020.112827
8. Galan, E. A., Zhao, H., Wang, X., Dai, Q., Huck, W. T. S., & Ma, S. (2020). Intelligent microfluidics: The convergence of machine learning and microfluidics in materials science and biomedicine. *Matter, 3*, 1893–1922. https://doi.org/10.1016/J.MATT.2020.08.034
9. Smith, Z. J., Chu, K., Espenson, A. R., Rahimzadeh, M., Gryshuk, A., Molinaro, M., et al. (2011). Cell-phone-based platform for biomedical device development and education applications. *PLoS One, 6*, e17150. https://doi.org/10.1371/JOURNAL.PONE.0017150
10. Steinberg, M. D., Kassal, P., & Steinberg, I. M. (2016). System architectures in wearable electrochemical sensors. *Electroanalysis, 28*, 1149–1169. https://doi.org/10.1002/ELAN.201600094
11. Kim, J., Sempionatto, J. R., Imani, S., Hartel, M. C., Barfidokht, A., Tang, G., et al. (2018). Simultaneous monitoring of sweat and interstitial fluid using a single wearable biosensor platform. *Advancement of Science, 5*. https://doi.org/10.1002/ADVS.201800880
12. Wiorek, A., Parrilla, M., Cuartero, M., & Crespo, G. A. (2020). Epidermal patch with glucose biosensor: PH and temperature correction toward more accurate sweat analysis during sport practice. *Analytical Chemistry, 92*, 10153–10161. https://doi.org/10.1021/ACS.ANALCHEM.0C02211/ASSET/IMAGES/LARGE/AC0C02211_0007.JPEG
13. Zhao, Y., Zhai, Q., Dong, D., An, T., Gong, S., Shi, Q., et al. (2019). Highly stretchable and strain-insensitive fiber-based wearable electrochemical biosensor to monitor glucose in the sweat. *Analytical Chemistry, 91*, 6569–6576. https://doi.org/10.1021/ACS.ANALCHEM.9B00152/ASSET/IMAGES/LARGE/AC-2019-001522_0004.JPEG

14. Kalimuthu, P., Gonzalez-Martinez, J. F., Ruzgas, T., & Sotres, J. (2020). Highly stable passive wireless sensor for protease activity based on fatty acid-coupled gelatin composite films. *Analytical Chemistry, 92*, 13110–13117. https://doi.org/10.1021/ACS.ANALCHEM.0C02153/SUPPL_FILE/AC0C02153_SI_001.PDF
15. Sempionatto, J. R., Nakagawa, T., Pavinatto, A., Mensah, S. T., Imani, S., Mercier, P., et al. (2017). Eyeglasses based wireless electrolyte and metabolite sensor platform. *Lab on a Chip, 17*, 1834–1842. https://doi.org/10.1039/C7LC00192D
16. Chen, M., Mao, S., & Liu, Y. (2014). Big data: A survey. *Mobile Networks Applications, 19*, 171–209. https://doi.org/10.1007/S11036-013-0489-0
17. Lecun, Y., Bengio, Y., & Hinton, G. (2015). Deep learning. *Nature, 521*, 436–444. https://doi.org/10.1038/nature14539
18. Ke, M., & Shi, Y. (2014). Big data, big change: In the financial management. *Open Journal Account, 03*, 77–82. https://doi.org/10.4236/OJACCT.2014.34009
19. Murdoch TB, Detsky AS (2013) The inevitable application of big data to health care. JAMA 309:1351–1352. doi: https://doi.org/10.1001/JAMA.2013.393.
20. Einav, L., & Levin, J. (2014). Economics in the age of big data. *Science (80-), 346*, 6210. https://doi.org/10.1126/SCIENCE.1243089/ASSET/7F3648CC-2ADD-4903-8B55-53748987B7D8/ASSETS/GRAPHIC/346_1243089_F3.JPEG
21. Arefin, A. S., Riveros, C., Berretta, R., & Moscato, P. (2012). GPU-FS-kNN: A software tool for fast and scalable kNN computation using GPUs. *PLoS One, 7*, e44000. https://doi.org/10.1371/JOURNAL.PONE.0044000
22. Alfian, G., Syafrudin, M., Ijaz, M. F., Syaekhoni, M. A., Fitriyani, N. L., & Rhee, J. (2018). A personalized healthcare monitoring system for diabetic patients by utilizing BLE-based sensors and real-time data processing. *Sensors, 18*, 2183. https://doi.org/10.3390/S18072183
23. Saidi, T., Zaim, O., Moufid, M., El Bari, N., Ionescu, R., & Bouchikhi, B. (2018). Exhaled breath analysis using electronic nose and gas chromatography–mass spectrometry for non-invasive diagnosis of chronic kidney disease, diabetes mellitus and healthy subjects. *Sensors Actuators, B Chemistry, 257*, 178–188. https://doi.org/10.1016/J.SNB.2017.10.178
24. Adir, O., Poley, M., Chen, G., Froim, S., Krinsky, N., Shklover, J., et al. (2020). Integrating artificial intelligence and nanotechnology for precision cancer medicine. *Advanced Materials, 32*, 1901989. https://doi.org/10.1002/ADMA.201901989
25. Brown, K. A., Brittman, S., Maccaferri, N., Jariwala, D., & Celano, U. (2020). Machine learning in nanoscience: Big data at small scales. *Nano Letters, 20*, 2–10. https://doi.org/10.1021/ACS.NANOLETT.9B04090/ASSET/IMAGES/LARGE/NL9B04090_0003.JPEG
26. Mahadevaiah, G., Prasad, R. V., Bermejo, I., Jaffray, D., Dekker, A., & Wee, L. (2020). Artificial intelligence-based clinical decision support in modern medical physics: Selection, acceptance, commissioning, and quality assurance. *Medical Physics, 47*, e228–e235. https://doi.org/10.1002/MP.13562
27. Nimri, R., Battelino, T., Laffel, L. M., Slover, R. H., Schatz, D., Weinzimer, S. A., et al. (2020). Insulin dose optimization using an automated artificial intelligence-based decision support system in youths with type 1 diabetes. *Nature Medicine, 26*, 1380–1384. https://doi.org/10.1038/S41591-020-1045-7
28. Cui, F., Yue, Y., Zhang, Y., Zhang, Z., & Zhou, H. S. (2020). Advancing biosensors with machine learning. *ACS Sensors, 5*, 3346–3364. https://doi.org/10.1021/acssensors.0c01424
29. Turner, C. R., Turner, C. R., Fuggetta, A., & Wolf, A. L. (1999). A conceptual basis for feature engineering. *Journal of Systems and Software, 49*, 3–15.
30. Morellos, A., Pantazi, X. E., Moshou, D., et al. (2016). Machine learning based prediction of soil total nitrogen, organic carbon and moisture content by using VIS-NIR spectroscopy. *Biosystems Engineering, 152*, 104–116. https://doi.org/10.1016/J.BIOSYSTEMSENG.2016.04.018
31. Vakilian, K. A., & Massah, J. (2018). A portable nitrate biosensing device using electrochemistry and spectroscopy. *IEEE Sensors Journal, 18*, 3080–3089. https://doi.org/10.1109/JSEN.2018.2809493

32. Wan, H., Zhuang, L., Pan, Y., & Fan, G. (2020). Biomedical sensors. In *Biomedical Information Technology* (pp. 51–79). Academic Press. https://doi.org/10.1016/B978-0-12-816034-3.00002-X
33. Yang, P., Wei, G., Liu, A., Huo, F., & Zhang, Z. (2022). A review of sampling, energy supply and intelligent monitoring for long-term sweat sensors. *NPJ Flex Electron., 61*(6), 1–13. https://doi.org/10.1038/s41528-022-00165-9
34. da Silva, P., Neves, M. M., González-García, M. B., Hernández-Santos, D., & Fanjul-Bolado, P. (2018). Future trends in the market for electrochemical biosensing. *Current Opinion in Electrochemistry, 10*, 107–111. https://doi.org/10.1016/J.COELEC.2018.05.002
35. Kim, H., Park, S., Jeong, I. G., Song, S. H., Jeong, Y., Kim, C. S., et al. (2021). Noninvasive precision screening of prostate cancer by urinary multimarker sensor and artificial intelligence analysis. *ACS Nano, 15*, 4054–4065. https://doi.org/10.1021/ACSNANO.0C06946/ASSET/IMAGES/LARGE/NN0C06946_0006.JPEG
36. Wang, B., Cancilla, J. C., Torrecilla, J. S., & Haick, H. (2014). Artificial sensing intelligence with silicon nanowires for ultraselective detection in the gas phase. *Nano Letters, 14*, 933–938. https://doi.org/10.1021/NL404335P/SUPPL_FILE/NL404335P_SI_001.PDF
37. Dutta, G. (2020). Electrochemical biosensors for rapid detection of malaria. *Materials Science for Energy Technologies, 3*, 150–158. https://doi.org/10.1016/J.MSET.2019.10.003
38. Dutta, G., & Lillehoj, P. B. (2017). An ultrasensitive enzyme-free electrochemical immunosensor based on redox cycling amplification using methylene blue. *Analyst, 142*, 3492–3499. https://doi.org/10.1039/C7AN00789B
39. Dutta, G., & Lillehoj, P. B. (2018). Wash-free, label-free immunoassay for rapid electrochemical detection of PfHRP2 in whole blood samples. *Scientific Reports, 81*(8), 1–8. https://doi.org/10.1038/s41598-018-35471-8
40. Dutta, G., Rainbow, J., Zupancic, U., Papamatthaiou, S., Estrela, P., & Moschou, D. (2018). Microfluidic devices for label-free DNA detection. *Chemosens, 6*, 43. https://doi.org/10.3390/CHEMOSENSORS6040043
41. Dutta, G., Regoutz, A., & Moschou, D. (2020). Enzyme-assisted glucose quantification for a painless lab-on-PCB patch implementation. *Biosensors & Bioelectronics, 167*, 112484. https://doi.org/10.1016/J.BIOS.2020.112484
42. Dutta, N., Lillehoj, P. B., Estrela, P., & Dutta, G. (2021). Electrochemical biosensors for cytokine profiling: Recent advancements and possibilities in the near future. *Biosensors, 11*, 94. https://doi.org/10.3390/BIOS11030094
43. Cazelles, R., Shukla, R. P., Ware, R. E., Vinks, A. A., & Ben-Yoav, H. (2020). Electrochemical determination of hydroxyurea in a complex biological matrix using MoS2-modified electrodes and chemometrics. *Biomed 2021, 9*, 6. https://doi.org/10.3390/BIOMEDICINES9010006
44. Hayun, S. B., Shukla, R. P., & Ben-Yoav, H. (2022). diffusion- and chemometric-based separation of complex electrochemical signals that originated from multiple redox-active molecules. *Polymers, 14*, 717. https://doi.org/10.3390/POLYM14040717
45. Mazafi, A., Shukla, R. P., Shukla, S. K., et al. (2018) Intelligent Multi-Electrode Arrays as the Next Generation of Electrochemical Biosensors for Real-Time Analysis of Neurotransmitters. MeMeA 2018–2018 IEEE Int Symp Med Meas Appl Proc. https://doi.org/10.1109/MEMEA.2018.8438720.
46. Massah, J., & Asefpour Vakilian, K. (2019). An intelligent portable biosensor for fast and accurate nitrate determination using cyclic voltammetry. *Biosystems Engineering, 177*, 49–58. https://doi.org/10.1016/J.BIOSYSTEMSENG.2018.09.007
47. Tsutsui, M., Tanaka, M., Marui, T., Yokota, K., Yoshida, T., Arima, A., et al. (2018). Identification of individual bacterial cells through the intermolecular interactions with peptide-functionalized solid-state pores. *Analytical Chemistry, 90*, 1511–1515. https://doi.org/10.1021/ACS.ANALCHEM.7B04950/ASSET/IMAGES/LARGE/AC-2017-049508_0004.JPEG

48. Tsutsui, M., Yoshida, T., Yokota, K., Yasaki, H., Yasui, T., Arima, A., et al. (2017). Discriminating single-bacterial shape using low-aspect-ratio pores. *Scientific Reports, 7*, 17371. https://doi.org/10.1038/S41598-017-17443-6
49. Vivier, V., & Orazem, M. E. (2022). Impedance analysis of electrochemical systems. *Chemistry Reviews*. https://doi.org/10.1021/acs.chemrev.1c00876
50. Rong, Y., Padron, A. V., Hagerty, K. J., Nelson, N., Chi, S., Keyhani, N. O., et al. (2018). Post hoc support vector machine learning for impedimetric biosensors based on weak protein–ligand interactions. *Analyst, 143*, 2066–2075. https://doi.org/10.1039/C8AN00065D
51. Taniguchi, M. (2020). Combination of single-molecule electrical measurements and machine learning for the identification of single biomolecules. *ACS Omega, 5*, 959–964. https://doi.org/10.1021/ACSOMEGA.9B03660/ASSET/IMAGES/LARGE/AO9B03660_0004.JPEG
52. Arima, A., Harlisa, I. H., Yoshida, T., Tsutsui, M., Tanaka, M., Yokota, K., et al. (2018). Identifying single viruses using biorecognition solid-state Nanopores. *Journal of the American Chemical Society, 140*, 16834–16841. https://doi.org/10.1021/JACS.8B10854
53. Di Ventra, M., & Taniguchi, M. (2016). Decoding DNA, RNA and peptides with quantum tunnelling. *Nature Nanotechnology, 11*, 117–126. https://doi.org/10.1038/NNANO.2015.320
54. Heerema, S. J., & Dekker, C. (2016). Graphene nanodevices for DNA sequencing. *Nature Nanotechnology, 11*, 127–136. https://doi.org/10.1038/NNANO.2015.307
55. Im, J. O., Biswas, S., Liu, H., Zhao, Y., Sen, S., Biswas, S., et al. (2016). Electronic single-molecule identification of carbohydrate isomers by recognition tunnelling. *Nature Communications, 71*(7), 1–7. https://doi.org/10.1038/ncomms13868
56. Albrecht, T., Slabaugh, G., Alonso, E., & Al-Arif, S. M. M. R. (2017). Deep learning for single-molecule science. *Nanotechnology, 28*, 423001. https://doi.org/10.1088/1361-6528/AA8334
57. Kasera, S., Herrmann, L. O., del Barrio, J., Baumberg, J. J., & Scherman, O. A. (2014). Quantitative multiplexing with nano-self-assemblies in SERS. *Scientific Reports, 4*. https://doi.org/10.1038/SREP06785
58. Larkin, P. J. (2017). *Infrared and Raman spectroscopy: Principles and spectral interpretation* (pp. 1–286). Elsevier.
59. Lussier, F., Missirlis, D., Spatz, J. P., & Masson, J. F. (2019). Machine-learning-driven surface-enhanced Raman scattering Optophysiology reveals multiplexed metabolite gradients near cells. *ACS Nano, 13*, 1403. https://doi.org/10.1021/ACSNANO.8B07024/ASSET/IMAGES/LARGE/NN-2018-070248_0005.JPEG
60. Dong, J., Hong, M., Xu, Y., & Zheng, X. (2019). A practical convolutional neural network model for discriminating Raman spectra of human and animal blood. *Journal of Chemometrics, 33*, e3184. https://doi.org/10.1002/CEM.3184
61. Acquarelli, J., van Laarhoven, T., Gerretzen, J., Jansen, J. J., Rijpma, A., van Asten, S., et al. (2017). Convolutional neural networks for vibrational spectroscopic data analysis. *Analytica Chimica Acta, 954*, 22–31. https://doi.org/10.1016/J.ACA.2016.12.010
62. Liu, J., Osadchy, M., Ashton, L., Foster, M., Solomon, C. J., & Gibson, S. J. (2017). Deep convolutional neural networks for Raman spectrum recognition: A unified solution. *Analyst, 142*, 4067–4074. https://doi.org/10.1039/C7AN01371J
63. Yang, J., Xu, J., Zhang, X., Wu, C., Lin, T., & Ying, Y. (2019). Deep learning for vibrational spectral analysis: Recent progress and a practical guide. *Analytica Chimica Acta, 1081*, 6–17. https://doi.org/10.1016/J.ACA.2019.06.012
64. Erzina, M., Trelin, A., Guselnikova, O., Dvorankova, B., Strnadova, K., Perminova, A., et al. (2020). Precise cancer detection via the combination of functionalized SERS surfaces and convolutional neural network with independent inputs. *Sensors and Actuators B: Chemical, 308*, 127660. https://doi.org/10.1016/J.SNB.2020.127660
65. Lu, W., Chen, X., Wang, L., Li, H., & Fu, Y. V. (2020). Combination of an artificial intelligence approach and laser tweezers Raman spectroscopy for microbial identification. *Analytical Chemistry, 92*, 6288–6296. https://doi.org/10.1021/ACS.ANALCHEM.9B04946/ASSET/IMAGES/MEDIUM/AC9B04946_M002.GIF

66. Hu, Z., Fang, W., Gou, T., Wu, W., Hu, J., Zhou, S., et al. (2019). A novel method based on a mask R-CNN model for processing dPCR images. *Analytical Methods, 11*, 3410–3418. https://doi.org/10.1039/C9AY01005J
67. Tan, C., Sun, Y., Li, G., et al. (2019) Image segmentation technology based on genetic algorithm. In ACM Int Conf Proceeding Ser Part F147955. (pp. 27–31). https://doi.org/10.1145/3316551.3318229.
68. Duan, Q., Lee, J., Zheng, S., Chen, J., Luo, R., Feng, Y., et al. (2020). A color-spectral machine learning path for analysis of five mixed amino acids. *Chemical Communications, 56*, 1058–1061. https://doi.org/10.1039/C9CC07186E
69. Rissin, D. M., Kan, C. W., Campbell, T. G., Howes, S. C., Fournier, D. R., Song, L., et al. (2010). Single-molecule enzyme-linked immunosorbent assay detects serum proteins at subfemtomolar concentrations. *Nature Biotechnology, 28*, 595–599. https://doi.org/10.1038/NBT.1641
70. Wang, Z., Huang, X., & Cheng, Z. (2018). Automatic spot identification method for high throughput surface plasmon resonance imaging analysis. *Biosensors, 8*, 85. https://doi.org/10.3390/BIOS8030085
71. Liu, Q., Fang, L., Yu, G., Wang, D., Xiao, C. L., & Wang, K. (2019). Detection of DNA base modifications by deep recurrent neural network on Oxford Nanopore sequencing data. *Nature Communications, 101*(10), 1–11. https://doi.org/10.1038/s41467-019-10168-2
72. Xiao, M., Liu, Z., Xu, N., Zhuang, L., Lu, J., Zheng, S., et al. (2020). A smartphone-based sensing system for on-site quantitation of multiple heavy metal ions using fluorescent carbon Nanodots-based microarrays. *ACS Sensors, 5*, 870–878. https://doi.org/10.1021/ACSSENSORS.0C00219/ASSET/IMAGES/LARGE/SE0C00219_0003.JPEG
73. Solmaz, M. E., Mutlu, A. Y., Alankus, G., Kılıç, V., Bayram, A., & Horzum, N. (2018). Quantifying colorimetric tests using a smartphone app based on machine learning classifiers. *Sensors Actuators, B Chemistry, 255*, 1967–1973. https://doi.org/10.1016/J.SNB.2017.08.220
74. Yetisen, A. K., Martinez-Hurtado, J. L., Garcia-Melendrez, A., da Cruz Vasconcellos, F., & Lowe, C. R. (2014). A smartphone algorithm with inter-phone repeatability for the analysis of colorimetric tests. *Sensors Actuators, B Chemistry, 196*, 156–160. https://doi.org/10.1016/J.SNB.2014.01.077
75. Gunda, N. S. K., Gautam, S. H., & Mitra, S. K. (2019). Editors' choice—artificial intelligence based mobile application for water quality monitoring. *Journal of the Electrochemical Society, 166*, B3031. https://doi.org/10.1149/2.0081909JES
76. Bae, E., Kim, H., Awofeso, O., et al. (2017). Colorimetric analysis of saliva–alcohol test strips by smartphone-based instruments using machine-learning algorithms. *Applied Optics, 56*(1), 84–92. https://doi.org/10.1364/AO.56.000084
77. Huang, X., Guo, J., Wang, X., Yan, M., Kang, Y., & Yu, H. (2014). A contact-imaging based microfluidic cytometer with machine-learning for single-frame super-resolution processing. *PLoS One, 9*, e104539. https://doi.org/10.1371/JOURNAL.PONE.0104539
78. Huang, X., Jiang, Y., Liu, X., Han, Z., Rong, H., Yang, H., et al. (2016). Machine learning based single-frame super-resolution processing for lensless blood cell counting. *Sensors (Basel), 16*. https://doi.org/10.3390/S16111836
79. Oliver, C. R., Altemus, M. A., Westerhof, T. M., Cheriyan, H., Cheng, X., Dziubinski, M., et al. (2019). A platform for artificial intelligence based identification of the extravasation potential of cancer cells into the brain metastatic niche. *Lab on a Chip, 19*, 1162–1173. https://doi.org/10.1039/C8LC01387J
80. Haick, H., & Tang, N. (2021). Artificial intelligence in medical sensors for clinical decisions. *ACS Nano, 15*, 3557–3567. https://doi.org/10.1021/ACSNANO.1C00085/ASSET/IMAGES/LARGE/NN1C00085_0006.JPEG
81. Jiang, S., Wang, J., Wang, Y., & Cheng, S. (2017). A novel framework for analyzing MOS E-nose data based on voting theory: Application to evaluate the internal quality of Chinese pecans. *Sensors and Actuators B: Chemical, 242*, 511–521. https://doi.org/10.1016/J.SNB.2016.11.074

82. Lussier, F., Thibault, V., Charron, B., Wallace, G. Q., & Masson, J.-F. (2020). Deep learning and artificial intelligence methods for Raman and surface-enhanced Raman scattering. *TrAC Trends in Analytical Chemistry, 124*, 115796. https://doi.org/10.1016/J.TRAC.2019.115796
83. Ho, C. S., Jean, N., Hogan, C. A., Blackmon, L., Jeffrey, S. S., Holodniy, M., et al. (2019). Rapid identification of pathogenic bacteria using Raman spectroscopy and deep learning. *Nature Communications, 101*(10), 1–8. https://doi.org/10.1038/s41467-019-12898-9
84. Mitra, B., Craswell, N., & Delft, B. (2018). An Introduction to Neural Information Retrieval. An Introd to Neural Inf Retr xx, No. xx:1–18. https://doi.org/10.1561/XXXXXXXXX.
85. Kiani, S., Minaei, S., & Ghasemi-Varnamkhasti, M. (2016). A portable electronic nose as an expert system for aroma-based classification of saffron. *Chemometrics and Intelligent Laboratory Systems, 156*, 148–156. https://doi.org/10.1016/J.CHEMOLAB.2016.05.013
86. Ayari, F., Mirzaee-Ghaleh, E., Rabbani, H., & Heidarbeigi, K. (2018). International journal of food properties detection of the adulteration in pure cow ghee by electronic nose method (case study: Sunflower oil and cow body fat). *International Journal of Food Properties, 21*, 1670–1679. https://doi.org/10.1080/10942912.2018.1505755
87. Jha, S. N. (2010). Nondestructive evaluation of food quality: Theory and practice. In *Nondestructive Evaluation of Food Quality: Theory and Practice* (pp. 1–288). Springer. https://doi.org/10.1007/978-3-642-15796-7
88. Kearl Pearson, F. R. S. (2010). LIII. On lines and planes of closest fit to systems of points in space. *The London, Edinburgh, and Dublin Philosophical Magazine and Journal of Science., 2*, 559–572. https://doi.org/10.1080/14786440109462720
89. Ha N, Xu K, Ren G, ,Arnan Mitchell, Jian Zhen Ou (2020) Machine learning-enabled smart sensor systems. Advanced Intelligent Systems 2:2000063. doi: https://doi.org/10.1002/AISY.202000063.
90. Rea, I., & De Stefano, L. (2019). Recent advances on diatom-based biosensors. *Sensors, 19*, 5208. https://doi.org/10.3390/S19235208
91. Martinez, A. M., & Kak, A. C. (2001). PCA versus LDA. *IEEE Transactions on Pattern Analysis and Machine Intelligence, 23*, 228–233. https://doi.org/10.1109/34.908974
92. Li, F. N. (2013). Requirements-driven software service evolution. Lect Notes Comput Sci (including Subser Lect Notes Artif Intell Lect Notes Bioinformatics) 7759 LNCS; pp. 419–425. https://doi.org/10.1007/978-3-642-37804-1_44/COVER/.
93. Vidal, R., Ma, Y., & Sastry, S. S. (2016). Principal component analysis. *Interdisciplinary Applied Mathematics, 40*, 25–62. https://doi.org/10.1007/978-0-387-87811-9_2
94. Chauhan, V. K., Dahiya, K., & Sharma, A. (2019). Problem formulations and solvers in linear SVM: A review. *Artificial Intelligence Review, 52*, 803–855. https://doi.org/10.1007/S10462-018-9614-6/FIGURES/16
95. Köhn, H.-F., & Hubert, L. J. (2015). *Hierarchical cluster analysis* (pp. 1–13). Wiley. https://doi.org/10.1002/9781118445112.STAT02449.PUB2
96. Fawagreh, K., Gaber, M. M., & Elyan, E. (2014). Random forests: From early developments to recent advancements. *2*, 602–609. http://mc.manuscriptcentral.com/tssc. https://doi.org/10.1080/21642583.2014.956265.
97. Farraia, M., Rufo, J. C., Paciência, I., Castro Mendes, F., Rodolfo, A., Rama, T., et al. (2020). Human volatilome analysis using eNose to assess uncontrolled asthma in a clinical setting. *Allergy, 75*, 1630–1639. https://doi.org/10.1111/ALL.14207
98. Nakhleh, M. K., Amal, H., Jeries, R., Broza, Y. Y., Aboud, M., Gharra, A., et al. (2017). Diagnosis and classification of 17 diseases from 1404 subjects via pattern analysis of exhaled molecules. *ACS Nano, 11*, 112–125. https://doi.org/10.1021/ACSNANO.6B04930/ASSET/IMAGES/NN-2016-04930J_M001.GIF
99. Wijaya, D. R., Sarno, R., & Zulaika, E. (2019). Noise filtering framework for electronic nose signals: An application for beef quality monitoring. *Computers and Electronics in Agriculture, 157*, 305–321. https://doi.org/10.1016/J.COMPAG.2019.01.001
100. Rutolo, M. F., Iliescu, D., Clarkson, J. P., & Covington, J. A. (2016). Early identification of potato storage disease using an array of metal-oxide based gas sensors. *Postharvest Biology and Technology, 116*, 50–58. https://doi.org/10.1016/J.POSTHARVBIO.2015.12.028

101. Tohidi, M., Ghasemi-Varnamkhasti, M., Ghafarinia, V., Bonyadian, M., & Mohtasebi, S. S. (2018). Development of a metal oxide semiconductor-based artificial nose as a fast, reliable and non-expensive analytical technique for aroma profiling of milk adulteration. *International Dairy Journal, 77*, 38–46. https://doi.org/10.1016/J.IDAIRYJ.2017.09.003
102. Liu, H., Li, Q., Yan, B., et al (2018). Bionic electronic nose based on MOS sensors array and machine learning algorithms used for wine properties detection. *Sensors 2019, 19*, 45. https://doi.org/10.3390/S19010045
103. Kühner, L., Semenyshyn, R., Hentschel, M., Neubrech, F., Tarín, C., & Giessen, H. (2019). Vibrational sensing using infrared Nanoantennas: Toward the noninvasive quantitation of physiological levels of glucose and fructose. *ACS Sensors, 4*, 1973–1979. https://doi.org/10.1021/ACSSENSORS.9B00488/ASSET/IMAGES/LARGE/SE-2019-00488K_0004.JPEG
104. Boubin, M., & Shrestha, S. (2019). Microcontroller implementation of support vector machine for detecting blood glucose levels using breath volatile organic compounds. *Sensors, 19*, 2283. https://doi.org/10.3390/S19102283
105. Saberi, Z., Rezaei, B., Rezaei, P., & Ensafi, A. A. (2020). Design a fluorometric aptasensor based on CoOOH nanosheets and carbon dots for simultaneous detection of lysozyme and adenosine triphosphate. *Spectrochimica Acta, Part A: Molecular and Biomolecular Spectroscopy, 233*, 118197. https://doi.org/10.1016/J.SAA.2020.118197
106. Kim, H., Seong, W., Rha, E., Lee, H., Kim, S. K., Kwon, K. K., et al. (2020). Machine learning linked evolutionary biosensor array for highly sensitive and specific molecular identification. *Biosensors & Bioelectronics, 170*, 112670. https://doi.org/10.1016/J.BIOS.2020.112670
107. Omer, A. E., Shaker, G., Safavi-Naeini, S., Kokabi, H., Alquié, G., Deshours, F., et al. (2020). Low-cost portable microwave sensor for non-invasive monitoring of blood glucose level: Novel design utilizing a four-cell CSRR hexagonal configuration. *Scientific Reports, 101*(10), 1–20. https://doi.org/10.1038/s41598-020-72114-3
108. Khan, S., Ali, S., & Bermak, A. (2019). Substrate dependent analysis of printed sensors for detection of volatile organic compounds. *IEEE Access, 7*, 134047–134054. https://doi.org/10.1109/ACCESS.2019.2939860
109. Li, H., Qi, F., & Wang, S. (2005). A comparison of model selection methods for multi-class support vector machines. *Lecture Notes in Computer Science, 3483*, 1140–1148. https://doi.org/10.1007/11424925_119/COVER/
110. Jordan, M. I., LeCun, Y., & Solla, S. A. (2001). IEEE Conference on Neural Information Processing Systems--Natural and Synthetic. In Advances in neural information processing systems : proceedings of the first 12 conferences.
111. Mahmud, M. S., Fang, H., Wang, H., et al. (2018). Automatic Detection of Opioid Intake Using Wearable Biosensor. Int Conf Comput Networking, Commun [proceedings] Int Conf Comput Netw Commun (pp. 784–788). https://doi.org/10.1109/ICCNC.2018.8390334
112. Shaikhina, T., Lowe, D., Daga, S., Higgins, R., & Khovanova, N. (2019). Decision tree and random forest models for outcome prediction in antibody incompatible kidney transplantation. *Biomedical Signal Processing and Control, 52*, 456–462. https://doi.org/10.1016/J.BSPC.2017.01.012
113. Etterich, T. D. (1995). Overfitting and undercomputing in machine learning. *ACM Computing Surveys, 27*, 326–327. https://doi.org/10.1145/212094.212114
114. Wang, Q., Zhou, Y., Ding, W., Zhang, Z., Muhammad, K., & Cao, Z. (2020). Random Forest with self-paced bootstrap learning in lung cancer prognosis. *ACM Transactions on Multimedia Computing, Communications, and Applications, 16*, 34. https://doi.org/10.1145/3345314
115. Cerrato-Alvarez, M., Bernalte, E., Bernalte-García, M. J., & Pinilla-Gil, E. (2019). Fast and direct amperometric analysis of polyphenols in beers using tyrosinase-modified screen-printed gold nanoparticles biosensors. *Talanta, 193*, 93–99. https://doi.org/10.1016/J.TALANTA.2018.09.093
116. Farraia, M., Cavaleiro Rufo, J., Paciência, I., Castro Mendes, F., Rodolfo, A., Rama, T., et al. (2020). Human volatilome analysis using eNose to assess uncontrolled asthma in a clinical setting. *Allergy, 75*, 1630–1639. https://doi.org/10.1111/ALL.14207

117. Leijnen, S., & van Veen, F. (2020). The neural network zoo. *Proceedings, 47*, 9. https://doi.org/10.3390/PROCEEDINGS2020047009
118. van de Goor, R., van Hooren, M., Dingemans, A. M., Kremer, B., & Kross, K. (2018). Training and validating a portable electronic nose for lung cancer screening. *Journal of Thoracic Oncology, 13*, 676–681. https://doi.org/10.1016/j.jtho.2018.01.024
119. Facure, M. H. M., Mercante, L. A., Mattoso, L. H. C., & Correa, D. S. (2017). Detection of trace levels of organophosphate pesticides using an electronic tongue based on graphene hybrid nanocomposites. *Talanta, 167*, 59–66. https://doi.org/10.1016/J.TALANTA.2017.02.005
120. Lipton, Z. C., Berkowitz, J., & Elkan, C. (2015). A critical review of recurrent neural networks for sequence learning. https://doi.org/10.48550/arxiv.1506.00019.
121. LeCun, Y., Bottou, L., Bengio, Y., & Haffner, P. (1998). Gradient-based learning applied to document recognition. *Proceedings of the IEEE, 86*, 2278–2323. https://doi.org/10.1109/5.726791
122. Cho, K., van Merriënboer, B., Bahdanau, D., & Bengio, Y. (2014). On the Properties of Neural Machine Translation: Encoder–Decoder Approaches. in *Proc SSST 2014 - 8th Work Syntax Semant Struct Stat Transl* (pp. 103–111). https://doi.org/10.3115/V1/W14-4012.
123. Hochreiter, S., & Schmidhuber, J. (1997). Long short-term memory. *Neural Computation, 9*, 1735–1780. https://doi.org/10.1162/NECO.1997.9.8.1735
124. Hanson, J., Yang, Y., Paliwal, K., & Zhou, Y. (2017). Improving protein disorder prediction by deep bidirectional long short-term memory recurrent neural networks. *Bioinformatics, 33*, 685–692. https://doi.org/10.1093/BIOINFORMATICS/BTW678
125. Ordóñez, F. J., Roggen, D., Liu, Y., et al. (2016). Deep convolutional and LSTM recurrent neural networks for multimodal wearable activity recognition. *Sensors, 16*, 115. https://doi.org/10.3390/S16010115
126. Williams, J. D., & Zweig, G. (2016). End-to-end LSTM-based dialog control optimized with supervised and reinforcement learning. https://doi.org/10.48550/arxiv.1606.01269.
127. Zoph, B., & Le, Q. V.. (2016). Neural Architecture Search with Reinforcement Learning. 5th Int Conf Learn Represent ICLR 2017 - Conf Track Proc. https://doi.org/10.48550/arxiv.1611.01578
128. Liu, H., Li, Q., Yan, B., Zhang, L., & Gu, Y. (2019). Bionic electronic nose based on MOS sensors array and machine learning algorithms used for wine properties detection. *Sensors, 19*, 45. https://doi.org/10.3390/S19010045
129. Boža, V., Brejová, B., & Vinař, T. (2017). DeepNano: Deep recurrent neural networks for base calling in MinION Nanopore reads. *PLoS One, 12*, e0178751. https://doi.org/10.1371/journal.pone.0178751
130. Rang, F. J., Kloosterman, W. P., & de Ridder, J. (2018). From squiggle to basepair: Computational approaches for improving nanopore sequencing read accuracy. *Genome Biology, 19*, 1–11. https://doi.org/10.1186/S13059-018-1462-9/FIGURES/3
131. Setio, A. A. A., Ciompi, F., Litjens, G., Gerke, P., Jacobs, C., van Riel, S. J., et al. (2016). Pulmonary nodule detection in CT images: False positive reduction using multi-view convolutional networks. *IEEE Transactions on Medical Imaging, 35*, 1160–1169. https://doi.org/10.1109/TMI.2016.2536809
132. Pereira, S., Pinto, A., Alves, V., & Silva, C. A. (2016). Brain tumor segmentation using convolutional neural networks in MRI images. *IEEE Transactions on Medical Imaging, 35*, 1240–1251. https://doi.org/10.1109/TMI.2016.2538465
133. Kallenberg, M., Petersen, K., Nielsen, M., Ng, A. Y., Diao, P., Igel, C., et al. (2016). Unsupervised deep learning applied to breast density segmentation and mammographic risk scoring. *IEEE Transactions on Medical Imaging, 35*, 1322–1331. https://doi.org/10.1109/TMI.2016.2532122
134. Krizhevsky, A., Sutskever, I., & Hinton, G. E. (2017). ImageNet classification with deep convolutional neural networks. *Communications of the ACM, 60*, 84–90. https://doi.org/10.1145/3065386

135. Szegedy, C., Liu, W., Jia, Y., et al. (2015). Going deeper with convolutions. Proc IEEE Comput Soc Conf Comput Vis Pattern Recognition 07-12-June-2015:1–9. https://doi.org/10.1109/CVPR.2015.7298594.
136. Ronneberger, O., Fischer, P., & Brox, T. (2015). U-net: Convolutional networks for biomedical image segmentation. Lect Notes Comput Sci (including Subser Lect Notes Artif Intell Lect Notes Bioinformatics). *9351*, 234–241. https://doi.org/10.1007/978-3-319-24574-4_28/COVER/.
137. Saric, M., Russo, M., Stella, M., & Sikora, M. (2019). CNN-based Method for Lung Cancer Detection in Whole Slide Histopathology Images. 2019 4th Int Conf Smart Sustain Technol Split 2019. https://doi.org/10.23919/SPLITECH.2019.8783041.
138. Zhu, Y., Liu, P., Xue, T., Xu, J., Qiu, D., Sheng, Y., et al. (2021). Facile and rapid one-step mass production of flexible 3D porous graphene nanozyme electrode via direct laser-writing for intelligent evaluation of fish freshness. *Microchemical Journal, 162*, 105855. https://doi.org/10.1016/J.MICROC.2020.105855
139. Sheng, Y., Qian, W., Huang, J., Wu, B., Yang, J., Xue, T., et al. (2019). Electrochemical detection combined with machine learning for intelligent sensing of maleic hydrazide by using carboxylated PEDOT modified with copper nanoparticles. *Mikrochimica Acta, 186*. https://doi.org/10.1007/S00604-019-3652-X
140. Boroumand, S., Arab Chamjangali, M., & Bagherian, G. (2019). An asymmetric flow injection determination of hydroquinone and catechol: An analytic hierarchy and artificial neural network approach. *Measurement, 139*, 454–466. https://doi.org/10.1016/J.MEASUREMENT.2019.03.025
141. Mishra, R. K., Alonso, G. A., Istamboulie, G., Bhand, S., & Marty, J. L. (2015). Automated flow based biosensor for quantification of binary organophosphates mixture in milk using artificial neural network. *Sensors and Actuators B: Chemical, 208*, 228–237. https://doi.org/10.1016/J.SNB.2014.11.011
142. Maleki, N., Kashanian, S., Maleki, E., & Nazari, M. (2017). A novel enzyme based biosensor for catechol detection in water samples using artificial neural network. *Biochemical Engineering Journal, 128*, 1–11. https://doi.org/10.1016/J.BEJ.2017.09.005
143. Guo, L., Wang, T., Wu, Z., Wang, J., Wang, M., Cui, Z., et al. (2020). Portable food-freshness prediction platform based on colorimetric barcode combinatorics and deep convolutional neural networks. *Advanced Materials, 32*, 2004805. https://doi.org/10.1002/ADMA.202004805
144. Pelenis, D., Barauskas, D., Vanagas, G., Dzikaras, M., & Viržonis, D. (2019). CMUT-based biosensor with convolutional neural network signal processing. *Ultrasonics, 99*, 105956. https://doi.org/10.1016/J.ULTRAS.2019.105956
145. Krittanawong, C., Rogers, A. J., Johnson, K. W., Wang, Z., Turakhia, M. P., Halperin, J. L., et al. (2020). Integration of novel monitoring devices with machine learning technology for scalable cardiovascular management. *Nature Reviews. Cardiology, 182*(18), 75–91. https://doi.org/10.1038/s41569-020-00445-9
146. Futoma, J., Simons, M., Panch, T., Doshi-Velez, F., & Celi, L. A. (2020). The myth of generalisability in clinical research and machine learning in health care. *Lancet Digital Health, 2*, e489–e492. https://doi.org/10.1016/S2589-7500(20)30186-2
147. Gambhir, S. S., Ge, T. J., Vermesh, O., Spitler, R., & Gold, G. E. (2021). Continuous health monitoring: An opportunity for precision health. *Science Translational Medicine, 13*. https://doi.org/10.1126/SCITRANSLMED.ABE5383
148. Topol, E. J. (2019). High-performance medicine: The convergence of human and artificial intelligence. *Nature Medicine, 251*(25), 44–56. https://doi.org/10.1038/s41591-018-0300-7
149. Thoben, K. D., Wiesner, S. A., & Wuest, T. (2017). "Industrie 4.0" and smart manufacturing - a review of research issues and application examples. *International Journal of Automation Technology, 11*, 4–16. https://doi.org/10.20965/IJAT.2017.P0004

Recent Progress on the Development of Chemosensors

Tiasa Das, Sanskar Jain, and Avijit Kumar Das

Abstract

Chemosensors are the chemical structures which convert chemical stimuli into responsive form that can be easily detected, such as change of colour, fluorescence, and other electronic signal. Recently, chemosensors development for detection and monitoring of gases has been growing interest due to the significant importance in environmental and biological systems. Subsequently, the development of chemosensors for detection of various gases is considered to be a significant goal in science and among the all gases, carbon dioxide (CO_2) is a major public concern due to its role in global greenhouse warming with environmental pollution. Moreover, quite critical level of CO_2 in the modern agricultural, food, environmental, oil and chemical industries is dangerous for living beings to survive such high concentration levels of CO_2. Therefore, rapid and selective detection and monitoring of CO_2 in the gaseous as well as in the liquid phases provides an incentive for development of new methods. The coverage of this book chapter is divided into different sections according to the use of different types of molecular backbones and the detection pathways.

Keywords

Chemosensors · Detection · Gases · Fluorescence · CO_2

T. Das · S. Jain · A. K. Das (✉)
Department of Chemistry, CHRIST (Deemed to be University), Hosur Road, Bengaluru, Karnataka, India
e-mail: avijitkumar.das@christuniversity.in

G. Dutta (ed.), *Next-Generation Nanobiosensor Devices for Point-Of-Care Diagnostics*, https://doi.org/10.1007/978-981-19-7130-3_8

1 Introduction

The progression of designing chemosensors has gained traction among academic chemists and biologists in fields involving supramolecular analytical chemistry [1]. Chemosensors are typically defined as chemical complexes programmed to detect chemical stimulations through the process of transforming them into a reaction that can be promptly and readily detected [2]. A wide range of chemosensors is often utilised in sensing volatile organic compounds, managing fossil fuel combustion products produced by automobile engines and industrial sources, surveilling air quality, sensing toxic gases, etc. Traditionally, these gases are detected by time-consuming and expensive chromatographic techniques such as HPLC and gas chromatography [1]. However, the need of the hour is to develop cost-effective chemosensors as they can be tremendously useful in today's world. There are a lot of volatile gases for which chemosensors are being developed throughout the world. These sensors utilise different properties of the analyte to signal its presence. In this chapter, we talk about chemosensors that are being used for the detection of carbon dioxide (CO_2).

Carbon dioxide (CO_2) is an omnipresent constituent of gas mixtures from a variety of abiotic environmental systems, including the burning of fossil fuels for electricity production, transportation, natural gas generation, and the majority of chemical processing [3]. These mechanisms have significant negative effects on the climate of the entire planet and human wellbeing, including the greenhouse effect, the rise in sea levels, and the potential diversification of subtropical deserts [4]. It has been widely acknowledged that limiting CO_2 emissions is a vital action to be undertaken globally since CO_2 is a primary greenhouse gas. Hence, the Kyoto Protocol has legally compelled several nations to control their greenhouse gas emissions [5].

As a result, one of the primary steps to lowering greenhouse gas emissions is the monitoring of CO_2. Regulating bioreactors, greenhouse agriculture, and food packaging are just a few of the many uses for CO_2 sensing. Due to the pressing need for CO_2 monitoring, several sensing techniques have been developed, including infrared spectroscopy, gas chromatography, pH, and optical chemosensors [1]. Chemosensor-based CO_2 sensing is more widely appealing to other approaches since it is quick, easy, inexpensive, and very accurate. The most common method for creating CO_2 chemosensors combines pH indicators with CO_2 capturing substances [6]. This strategy uses the dissociation of carbonic acid to protonate a signalling molecule (usually fluorescent molecules) that undergo some change which we can detect. Similarly, other strategies of detecting CO_2 utilise different properties of the gas to trigger a change in a signalling molecule which we can detect through various means [1, 7].

2 Pyrene-Based Chemosensor for Detection of CO_2

Pyrene-based Schiff base named (E)-N′-((5-(pyren-1-yl)thiophen-2-yl)methylene) nicotinohydrazide (**1**) which on interaction with fluoride anion acts as a colorimetric chemosensor for carbon dioxide as a result of the generation of anionic nitrogen, which is a strong nucleophile and hence well suited for CO_2 gas sensing [8].

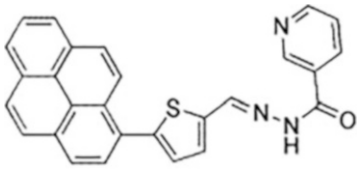

1

Compound **1** is widely utilised in anion sensing studies as it has a free NH group and has been observed to be highly selective towards fluoride anion due to its high electronegative nature and hence is utilised for colorimetric detection for the same. While conducting quantitative analysis through UV-Visible absorbance studies, it was observed that there was a significant decrease in the peak of the deprotonated **1** from 425 nm while an increase was seen in the case of the characteristic peak of 375 nm of free **1** with a spontaneous colour change of yellow to transparent as a result of this regain. The fluctuation in fluorescence spectra revealed a marked increase with a corresponding wavelength of 390 nm upon exposure to carbon dioxide gas. The CO_2 sensing mechanism follows the interaction of CO_2 with the deprotonated anime moiety which results in the formation of compound **1** -CO_2 adduct, which has a characteristic spectral profile capable of detection as a result of formation of N-C bond. This system on interaction fluoride anion has a carbon dioxide sensing detection limit of 0.4 ml.

(E)-N′-(pyren-1-ylmethylene) nicotinohydrazide (**2**) is highly sensitive and selective colorimetric type chemosensor which deals with both anion and CO_2 gas detection and consists of pyrene with the role of chromophore and nicotinic acid hydrazide as receptor [9].

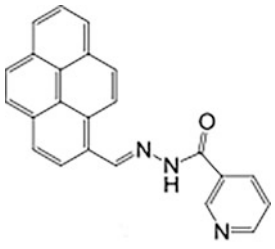

2

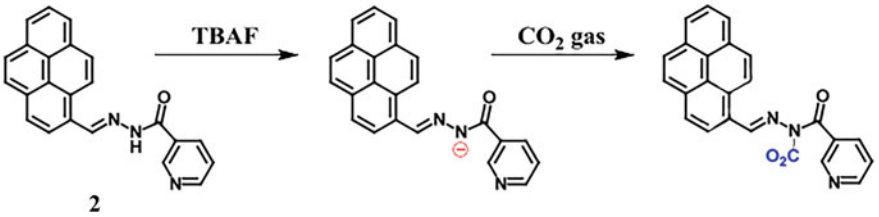

Fig. 1 Pathway of CO_2 detection by **2** (Reprinted from Ref. [9] with permission from Elsevier)

Compound **2** is considered crucial for anion detections due to the presence of free NH group and a colour change of colourless to yellow was observed in the presence of fluoride ions. Quantitative analysis through spectral studies revealed the presence of 450 nm peak as a result of the interaction between **2** and TBAF (fluoride ions). On addition of CO_2 gas, this peak is observed to decrease with pure **2** experiencing a peak of 1647 cm^{-1}, while the deprotonated **2** in presence of CO_2 gas shows a characteristic peak at 1669 cm^{-1}. The occurrence of this peak can be reasoned with the vibrations of asymmetric nature present in the NCO_2 moiety. On addition of CO_2 to **2** solution, the dark yellow colour is seen to change to transparent as the amount of CO_2 is increased.

The mechanism accepted for this system is that firstly on addition of TBAF, deprotonation of the proton in the free NH group of **2** takes place, which results in ease of interaction with fluoride ion. This, when exposed to CO_2 gas through the action of potassium carbonate on dilute HCl, it produces change in colour and the anionic form of **2** is utilised for sensing CO_2 gas with a detection limit down to 0.1 ml (Fig. 1).

3 Intra-molecular Hydrogen Bonding Stabilisation Based Fluorescent Chemosensor for Detection of CO_2

Sodium (anthracen-9-ylmethyl) glycinate (**3**) which is an amino acid based chemosensor was used as a fluorescent chemosensor with turn-on mechanism for CO_2 sensing [6]. This system further helps in differentiating fluorescent CO_2 sensors into categories of strong, intermediate, and weak through assay procedures.

On studying fluorescence spectral changes, it was observed that there was a pronounced increase in the fluorescence level after subjected to CO_2 exposure in the solution of **3** and it was linearly increasing compared to the amount of CO_2 bubbled in the solution and results in a saturated level at 0.06 ml of CO_2. The mechanism of sensing of CO_2 by chemosensor **3** is made to react with CO_2 resulting in the formation of a carbamic acid adduct or chemosensor 3-CO_2 adduct (**3′**) (Fig. 2). This adduct is extensively sustained due to the presence of strong intra-molecular hydrogen bonds which prevents the photoinduced electron transfer (PET) process which would otherwise quench the fluorescence by converting it to anthracene, and helps in enhanced fluorescence permitting highly accurate and sensitive

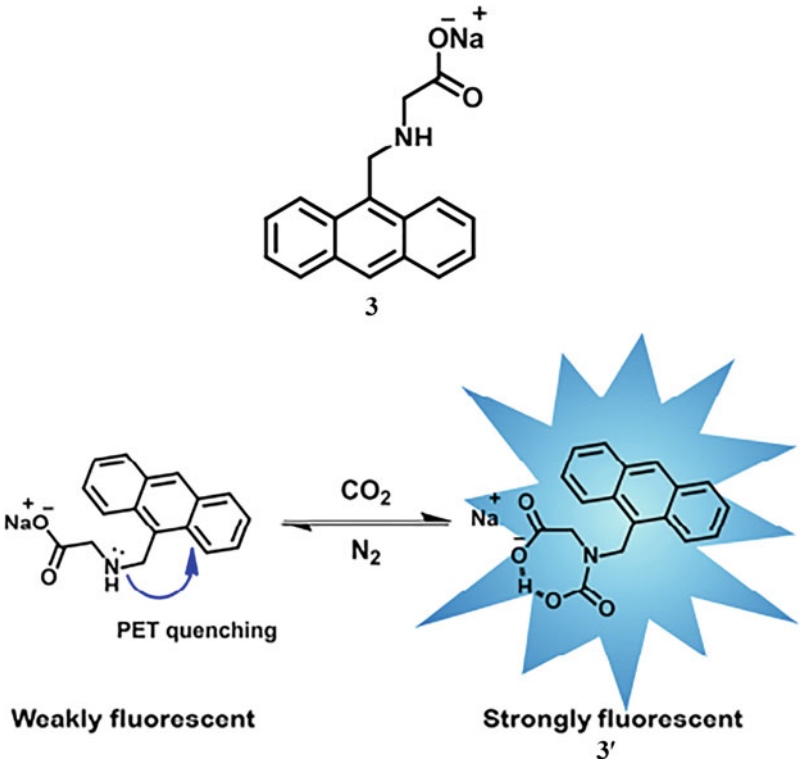

Fig. 2 *Top*: Structure of sodium (anthracen-9-ylmethyl) glycinate (**3**). *Bottom*: Pathway for CO_2 detection sodium (anthracen-9-ylmethyl) glycinate (Reprinted from Ref. [6] with permission from Elsevier)

CO_2 detection. The detection limit for chemosensor **3** for CO_2 was found to be approximately 2 ppm.

4 Squaraine-Based System for Detection of CO_2

An unsymmetrical 1,3-substituted squaraine SQ-NH_2 (**4**) was developed in accordance with the literature procedure provided by You and Gao for the purpose of fluorescent and colorimetric based CO_2 sensing by first removal of the alkenyl proton (deprotonation) by tetra-*n*-butylammonium fluoride (TBF) and then substituting a fluoride ion in its position [10].

The original UV-Vis absorbance spectra according to **4** in presence of dimethylsulfoxide (DMSO) were noted and they showed a distinct absorbance band corresponding to 539 nm. Upon addition of tetrabutylammonium salt (TBAF), the absorbance was observed to be reduced considerably and gives rise to a band corresponding to 405 nm. These fluctuations in the spectra are considered to

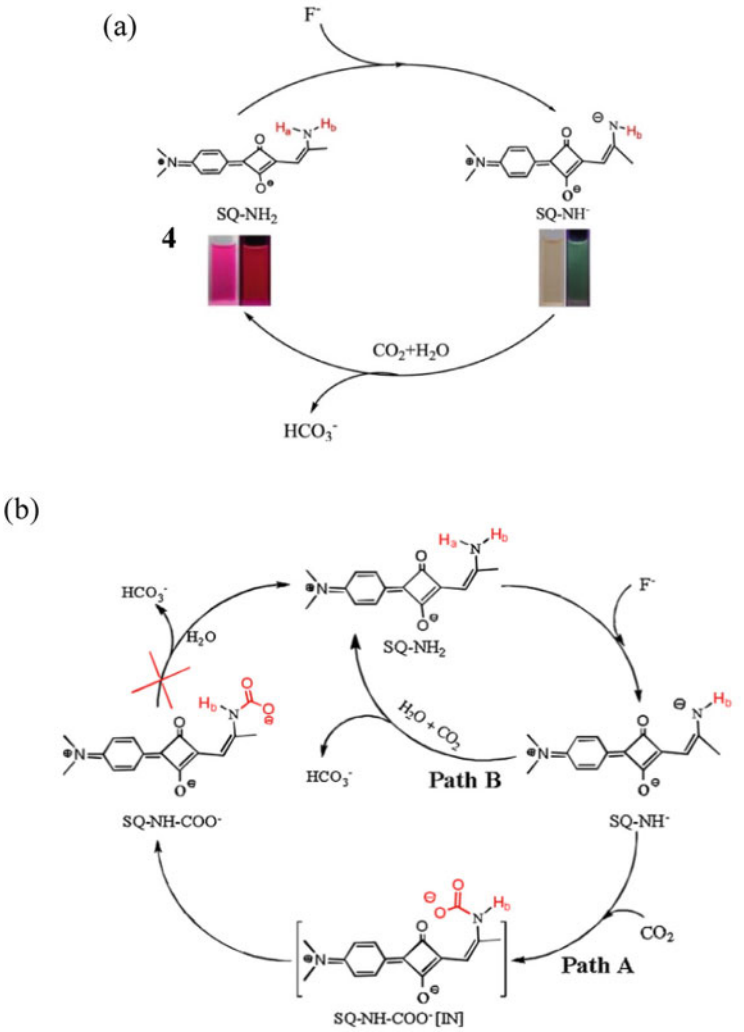

Fig. 3 (**a**) Structure of 1,3 substituted squaraine-NH_2 (SQ-NH_2, **4**) and the colour and fluorescence changes in presence of F^- and CO_2. (**b**) Pathways A and B of CO_2 detection system (Reprinted from Ref. [10] with permission from Elsevier)

be due to the deprotonation of the amino moiety by F^-. This decrease in absorbance of SQ-NH_2 (**4**) and increase in absorbance of SQ-NH^- are visible to the bare eyes due to the change in colour of the solution from red to yellow in daylight (Fig. 3a). We see a subsequent reversion of colour from yellow to red when increasing volumes of CO_2 were added to the original solution treated with TBAF. There was a similar drop in the intensity of the emission band on the addition of TBAF to SQ-NH_2 (**4**) corresponding to 611 nm and then a marked increase in new emission peak was

observed at 485 nm ultimately resulting in an isosbestic point at 575 nm. As increasing volumes of CO_2 were added, the intensity of the emission peak at 611 nm was regained, while that corresponding to 485 nm was lost. The fluorescence colour of the solution has been observed to change from red to orange-yellow through an intermediate of green-yellow on illumination with UV. There were no changes observed in emission as CO_2 volumes reached a level of saturation.

A deprotonated equilibrium reaction takes place by adding TBAF to the solution of SQ-NH_2 (**4**) and DMSO and further addition of CO_2 can lead to the revival of SQ-NH_2 (**4**) and HCO_3^- through two paths—A and B (Fig. 3b). Path A is based on the assumption of the formation of an unstable intermediate SQ-NH-COO^-, due to the strong nucleophilic attack on CO_2 by SQ-NH^- and the ultimate regain of SQ-NH_2 (**4**) and bicarbonate ion on reaction with moisture. Path B utilises the basic property of SQ-NH^- which generates the nucleophilic attack of H_2O resulting in the same product formation. It was observed through DFT calculations that Path B was a more feasible mechanism of CO_2 sensing through the SQ-NH_2 (**4**) sensor. Both the detection limits of pure CO_2 gas in the fluorescent and colorimetric systems were calculated to be 39 ppm and 38 ppm, respectively.

5 α-Cyanostilbene-Based Fluorescent Chemosensor for Detection of CO_2

(Z)-3-(4-(3-Aminopropoxy)phenyl)-2-(4-nitrophenyl)acrylonitrile (**5**) having a primary amine exhibited enhanced fluorescence due to aggregation-induced emission (AIE) for CO_2 detection in a solution [11].

The fluorescence intensity of **5** was measured by dynamic light scattering (DLS) and the average particle diameter was observed to be 86.99 nm and 774.1 nm of the aggregates before and after exposure to CO_2. Further fluorescence spectral studies showed a fluctuation of 365 nm to 565 nm after CO_2 bubbling into the ligand **5** solution. Both the studies point to an enhanced fluorescence as a result of magnified aggregation due to CO_2 exposure. The mechanism for the sensing of CO_2 by chemosensor **5** is that carbamic acid is formed as a result of reaction of CO_2 with the primary amine present in **5** resulting in generation of salt bridges due to the consequent reaction between carbamic acid and other amine molecules (Fig. 4).

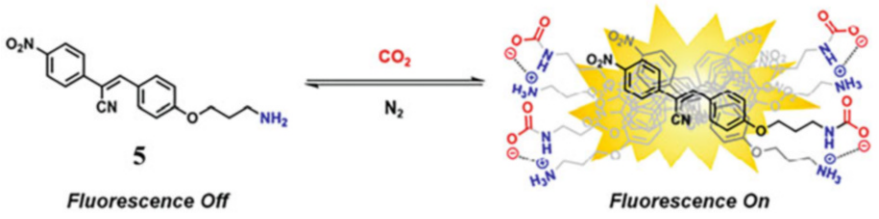

Fig. 4 Structure of **5** and pathway of detection of CO_2 (Reprinted from Ref. [11] with permission from Elsevier)

Henceforth, we notice an amplified fluorescence due to congregation instigated by electrostatic reaction between carbamate and ammonium salts due to the increase in size of the aggregates of **5**. This system **5** is reversible in nature as if we bubble N_2 and CO_2, there is a decrease in fluorescence due to moderation of fluorescence. The detection limit of chemosensor **5** for CO_2 was observed to be approximately 26 ppm.

6 pH Indicator-Based Sensors for CO_2

CO_2 readily undergoes hydration to form carbonic acid from its gaseous form. The carbonic acid form dissociates partially to hydrogen carbonate and releases a proton. As the first ionisation is partial and the dissociation constant is low ($K_a = 2.5 \times 10^{-4)}$, it forms a weak acid. The reaction is given in Fig. 5.

Most pH indicator-based sensors for CO_2 rely on the weak acidity to detect it as the sensor molecule reacts with the proton to cause a change. Most commonly used is the 1-hydroxypyrene-3,6,8-trisulfonate (**6**) molecule that is fluorescent, but it gets protonated which turns its fluorescence off (Fig. 6). Hence the usual fluorescent intensity lessens. This sensor is sensitive for amounts less than that present in the atmosphere (387 ppm) with a detection limit of 80 ppm [7].

Another common molecule Diketopyrrolo-pyrrole (**7**) is extensively used as a chemosensor for CO_2 [12]. The molecule acts as the core for various sensors that get protonated and deprotonated in the presence of H^+ conferred by dissociation of carbonic acid (Fig. 7). The deprotonated form gives a blue colour while in presence of CO_2 and they give fluorescence of deep red to orange.

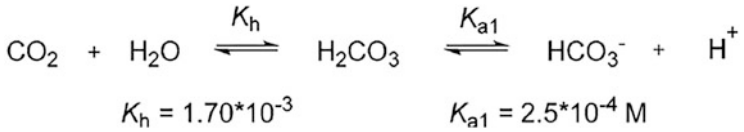

Fig. 5 Reaction of CO_2 with H_2O

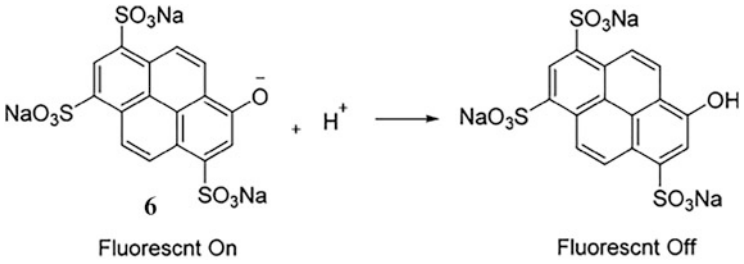

Fig. 6 Structures of pH indicator (**6**) as a CO_2 sensor (Reprinted from Ref. [7] with permission from American Chemical Society)

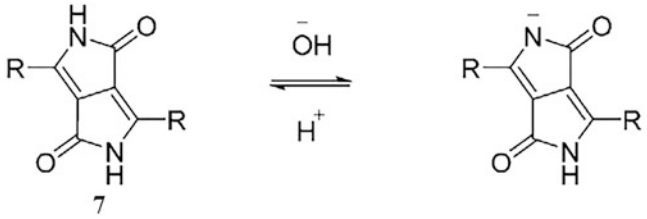

Fig. 7 Protonation and deprotonation of **7** sensor (Reprinted from Ref. [12] with permission from American Chemical Society)

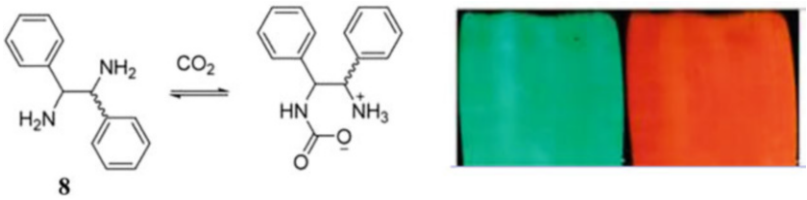

Fig. 8 Reaction of chiral dopants with CO_2 (Left) and colour change from green to orange on exposure to CO_2 (Right) (Reprinted from Ref. P13] with permission from American Chemical Society)

7 Amine-Based Sensors for CO_2

CO_2 is a weak electrophile which reacts with a basic amine group to form a carbamate salt. Using this reaction, various sensors were developed by introducing an amine group to fluorescent molecules. The presence of amine group would reduce fluorescence because of PET (photoinduced electron transfer) which was again liberated when CO_2 would react with it forming the salt turning the fluorescence on. A sensor (**8**) was developed by using optically pure chiral diamines which would react with CO_2 forming carbamate [13]. The sensor showed a strong colour change from orange to green on exposure to CO_2 (Fig. 8).

Another strategy involved photophysical effect in which the fluorescence varies as the physical properties of the solution containing the sensor change. CO_2 in amine solutions like dipropylamine (DPA) (**10**) forms carbamate ionic liquid (CIL) causing a net increase in viscosity and polarity (Fig. 9b).

Molecules like hexaphenylsilole (**9**) emit low fluorescence initially but release high fluorescence in aggregate forms. This effect is called aggregation-induced emission (AIE) (Fig. 9a). As CO_2 increases the viscosity of the solution, there's a logarithmic increase in the fluorescence values which can help in quantitative estimation of the gas across the entire range (0–100%) with an Π_{max} at 480 nm [14].

In a similar fashion, another sensor **11** was developed that used a sulphonate derivative of Tetraphenylethylene (TPE) as the probe [15]. A polymer with amine functional group present (such as chitosan) was developed for the same.

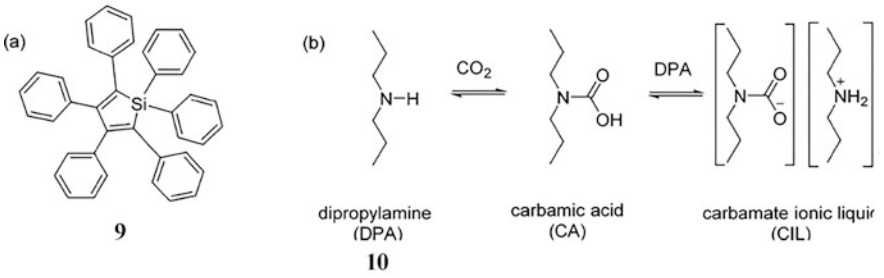

Fig. 9 (**a**) Structure of Hexaphenylsilole (**9**). (**b**) Formation of CIL from DPA (**10**) and CO_2 (Reprinted from Ref. [14] with permission from Wiley)

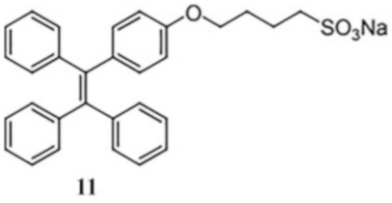

This probe **11** is non fluorescent at 6% THF-Water. As CO_2 releases H^+ ions, the free -NH_2 groups of the polymer become positively charged, attracting the negatively charged probe. Through AIE, the fluorescence is activated as the rotation of the molecules remain locked. The characteristic fluorescence wavelength is at 460 nm which shows linear increase from 5 uM to 50 uM of analyte with detection limit 0.00127 hPa.

8 Deprotonation-Assisted Sensors for CO_2

In this strategy, a fluoride ion induces deprotonation of the amine moiety which would then react with CO_2. The basic principle behind the reaction is that a strong anion can cause an active proton in the sensor's amine to be lost, making it a nucleophile. This allows CO_2 to bind with it to form a complex that can decompose to give our original sensor molecule back. This reaction is accompanied by a change in fluorescence. Yoon et al. developed a sensor by combining tetrapropyl benzobisimidazolium salts to a precursor molecule of N-heterocyclic carbene (NHC) constructing tetrapropylbenzo-bis(imidazolium) hexafluorophosphate (**12**) [16] (Fig. 10). The molecule showed the highest absorption at the wavelength of 290 nm. But on addition of fluoride ions, the absorption band shifted to 344 nm. On subsequent addition of CO_2, the magnitude of absorption at 290 nm as well as the

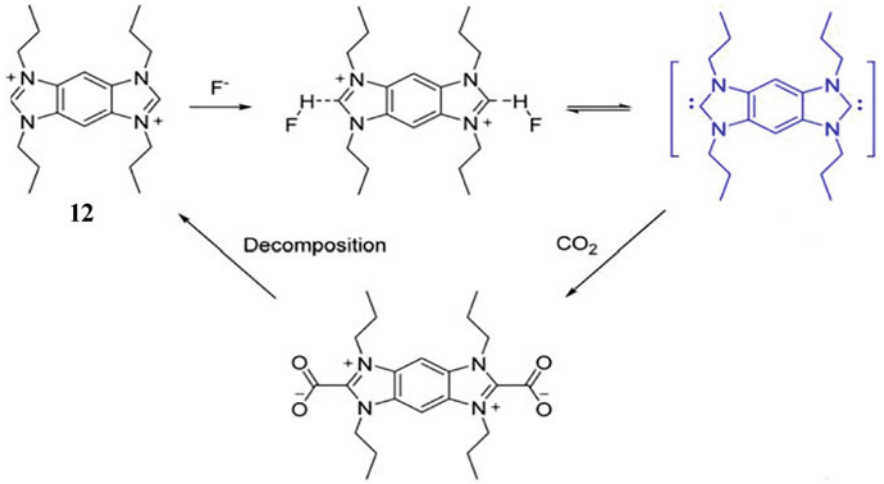

Fig. 10 Reaction of **12** with CO_2 (Reprinted from Ref. [16] with permission from American Chemical Society)

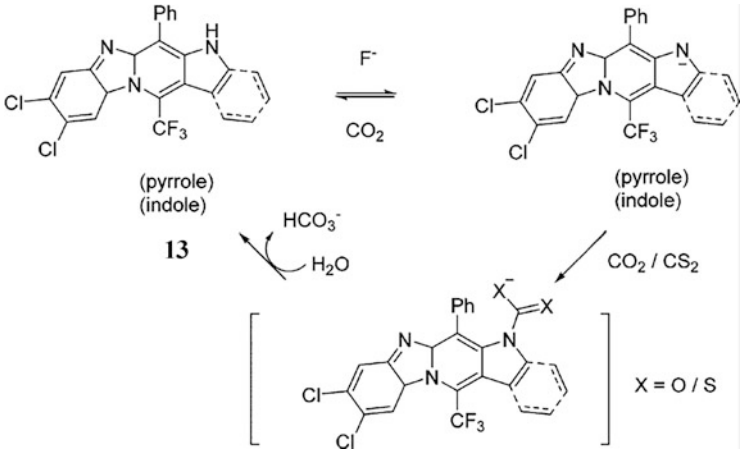

Fig. 11 Proposed reactions of **13** with F^- and then either CO_2 or CS_2 (Reprinted from Ref. [17] with permission from Elsevier)

corresponding fluorescence emission started increasing in a linear fashion with the concentration of CO_2.

Using similar strategies, Yoon et al. developed a sensor **13** using pyrrole and indole as starting points with N conjugated to them [17]. They could create a sensor that would show distinct shift in absorption and emission band as well as intensity of emission upon reacting with F^- which are then subsequently restored as CO_2 is made to react with it (Fig. 11). The upper detection limit of the sensor **13** for CO_2 is 0.41 μM.

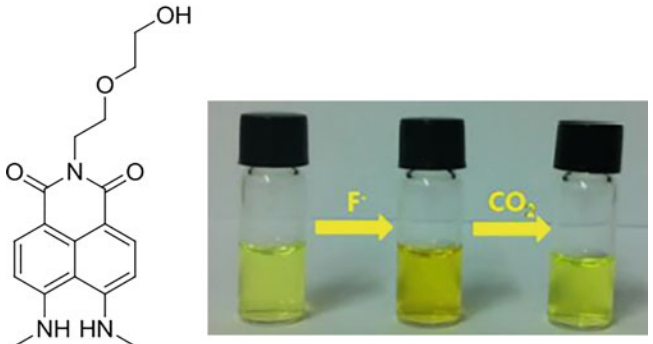

14

Fig. 12 Structure of Naphthalimide derivative (Left) and colour change displayed by sensor **14** by interacting with F^- and CO_2 (Right) (adapted from references 18)

Another sensor N-[2-(2-hydroxyethoxy)ethyl]-4,5-di{[(2-methylthio)ethyl] amino}-1,8-naphthalimide (**14**) using the same principle was developed by Yoon et al. based on naphthalimide derivative [18]. The sensor **14** itself showed absorption at 445 nm which would undergo red shift on addition of anions such as CN^- and F^-. This red shift was then reversed by the addition of CO_2 with the detection limit being 2.04×10^{-7} M (Fig. 12).

9 Chemosensors Based on Functional Material for Detection of CO_2

A multitude of chemical sensors **15** based on nanomaterial such as polymers and porous silica materials have been developed based on PDA (polydiacetylene) wherein the sensing mechanism would be driven by the reaction between CO_2 and the primary amines present forming carbamate anions [19]. (Fig. 13). These would then interact with the imidazolium cations of PDA in the presence of TEA characterised by the development of a new absorption peak near 540 nm accompanied by decreased intensity of original absorption maxima of PDA at 623 nm. Hence the colour changes from blue to red as complementary wavelengths are emitted.

Another strategy involved using a porous polymer and a reporting molecule distyrylbenzene (DBZ) which was introduced in the nano channels of the polymer [20]. The polymer-DBZ conjugate showed selective adsorption for CO_2. After which the polymer and DBZ undergo a coupled transformation reported by DBZ through a shift from a weak-green fluorescence to blue fluorescence. The polymer-DBZ

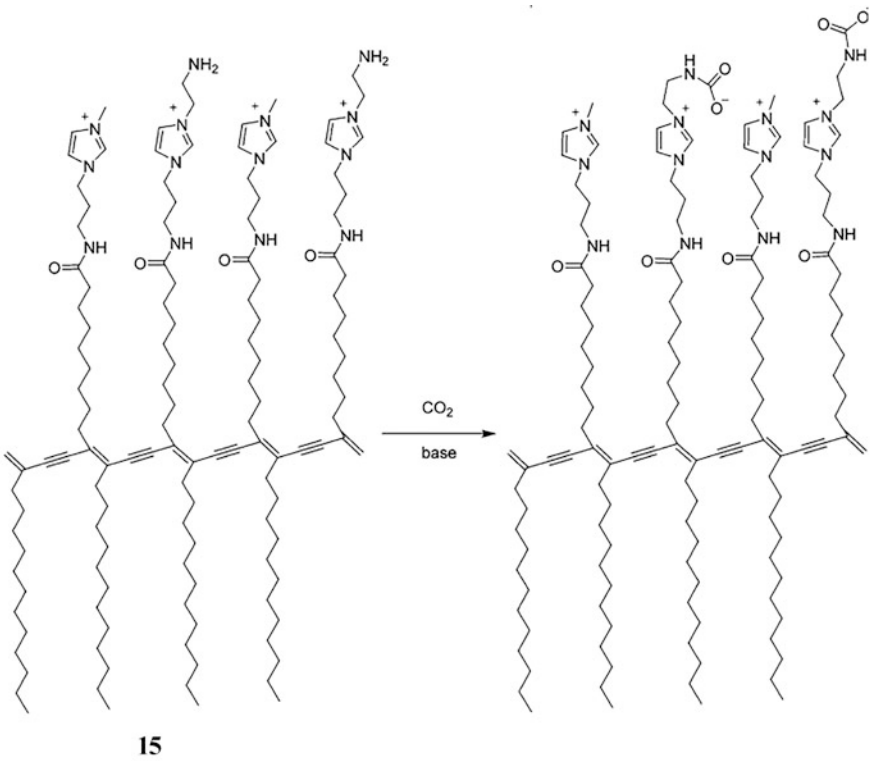

Fig. 13 CO_2 detection through sensor **15** in presence of TEA as base (Reprinted from Ref. [19] with permission from American Chemical Society)

complex could also differentiate between CO_2 and acetylene which show similar chemical properties.

10 Chemosensors Based on Metal-Oxide Semiconductors for Detection of CO_2

Semiconductors have seen an explosion in their use for detection of various gases. Their response times, detection limits as well as recovery time are better compared to other sensors. For CO_2, various semiconductors have been developed such as LaOCl-SnO_2 nanowire. Since LaOCl is a p-type semiconductor and SnO_2 is a n-type, there is a junction formation which extended the electron depletion. LaOCl also catalyses the reaction between CO_2 and adsorbed entities forming polydentate carbonates and hydroxyl carbonates further reducing the resistance of the wire. This was used as the response to the presence of CO_2. This sensor could detect CO_2 between the limits of 250–4000 ppm with a response time between 3 and 20 s. Operating temperature for the detection is a bit high at 500 °C. Another study

involving ultra-thin nanofilm of La_2O_3 could detect CO_2 with levels as low as 100 ppm with an upper limit of 250 ppm at room temperature [21].

Like nanowires, thin films made of $BaTiO_3$-CuO semiconductor were also developed to detect CO_2. The response is a change in resistance and capacitance which could be detected in 10 min at 300 °C. However, since the reaction happens on the surface, it is theorised that thicker films will give results faster. The detection limit of a thin film of 400 nm width is 500–10,000 ppm [22].

Another strategy involved construction of microspheres of Gd_2O_3 of diameter between 0.7 and 2.5 μm. These microspheres could detect the presence of 1% CO_2 repeatedly at 470 °C. Using a similar strategy, microspheres of Nd_2O_3 were constructed which could detect CO_2 between the limits of 100–250 ppm at an operating temperature of 400 °C with a response time of 3.6 s [23].

11 Conclusions and Outlook

Methods for the detection and quantification of CO_2 gases using various specific fluorescent chemosensors are necessary based on the studies by understanding and monitoring a variety of environmental and biological phenomena. In this book chapter we have highlighted various studies for detection of CO_2 along with a detailed discussion of the design strategies, sensing performances, mechanisms, and applications. The discussion of this topic was divided into sections which focus on fluorescent organic molecules, metal-oxide semiconductors, functional materials, pH indicator-based sensors, etc. However, although numerous chemosensors for CO_2 have been developed and applied in biological studies, still a high demand to construct the chemosensors displaying high selectivities, sensitivities, and biocompatibilities and that can be utilised for real-time imaging and nondestructive detection of CO_2.

References

1. Zhou, X., Lee, S., Xu, Z., & Yoon, J. (2015). Recent Progress on the development of Chemosensors for gases. *Journal of the American Chemical Society, 115*, 7944.
2. Chen, X., Pradhan, T., Wang, F., Kim, J. S., & Yoon, J. (2012). Fluorescent chemosensors based on spiroring-opening of xanthenes and related derivatives. *Chemical Reviews, 112*, 1910–1956.
3. Smolander, M., Hurme, E., & Ahvenainen, R. (1997). Leak indicators for modified-atmosphere package. *Trends in Food Science and Technology, 8*, 101–106.
4. Tian, T., Chen, X., Li, H., Wang, Y., Guo, L., & Jiang, L. (2013). Amidine-based fluorescent chemosensor with high applicability for detection of CO2: A facile way to "see" CO2. *The Analyst, 138*, 991–994.
5. Lashof, D. A., & Ahuja, D. R. (1990). Relative contributions of greenhouse gas emissions to global warming. *Nature, 344*, 529.
6. Seungyoon, S., Jongseo, K., Park, K.-H., KyuAhn, C., & Rhee, C.-H. (2015). Intra-molecular hydrogen bonding stabilization based-fluorescent chemosensor for CO2: Application to screen relative activities of CO2 absorbents. *Dyes and Pigments, 123*, 125–131.

7. Royce, N. D.-S., Jin, J., Mechery, S. J., Sampathkumaran, U., & Owen, T. W. (2010). Fluorescent-dye-doped Sol−Gel sensor for highly sensitive carbon dioxide gas detection below atmospheric concentration. *Analytical Chemistry, 82*, 593–600.
8. Gowri, A., Khamrang, T., Velusamy, M., Kathiresan, M., Kumar, M. D., Jaccob, M., & Kathiravana, A. (2020). Pyrene based chemosensor for carbon dioxide gas – Meticulous investigations and digital image based RGB analysis. *Sensors and Actuators Reports, 2*, 100007.
9. Gowry, A., Veeraragavana, V., Kathiresanb, M., & Kathiravan, A. (2019). A pyrene based colorimetric chemosensor for CO2 gas detection triggered by fluoride ion. *Chemical Physics Letters, 719*, 67–71.
10. Jianqi, S., Yea, B., Xiaa, G., Zhaoa, X., & Wang, H. (2016). A colorimetric and fluorescent chemosensor for the highly sensitive detection of CO2 gas: Experiment and DFT calculation. *Sensors & Actuators, B: Chemical, 233*, 76–82.
11. Mincheol, S., Seungyoon, J., & Min, K. (2019). A simple turn-on fluorescent chemosensor for CO2 based on aggregation-induced emission: Application as a CO2 absorbent screening method. *Dyes and Pigments, 162*, 978–983.
12. Schutting, S., Borisov, S., & Klimant, I. (2013). Diketo-Pyrrolo-pyrrole dyes as new colorimetric and fluorescent pH indicators for optical carbon dioxide sensors. *Analytical Chemistry, 85*, 3271–3279.
13. Han, Y., Pacheco, K., Bastiaansen, C. W. M., Broer, D. J., & Sijbesma, R. P. (2010). Optical monitoring of gases with cholesteric liquid crystals. *Journal of the American Chemical Society, 132*, 2961–2967.
14. Ning, Z. Z., Chen, Q., Zhang, Y., Yan, S., Qian, Y., Cao, H., & Tian. (2017). Aggregation-induced emission (AIE)-active starburst Triarylamine fluorophores as potential non-doped red emitters for organic light-emitting diodes and Cl2 gas chemodosimeter. *Advanced Functional Materials, 18*, 3799–3807.
15. Khandare, D. G., Joshi, H., Banerjee, M., Majik, M. S., & Chatterjee, A. (2015). Fluorescence turn-on chemosensor for the detection of dissolved CO2 based on ion-induced aggregation of tetraphenylethylene derivative. *Analytical Chemistry, 87*, 10871–10877.
16. Guo, Z., Song, N. R., Moon, J. H., Kim, M., Jun, E. J., Choi, J., & Yoon, J. (2012). A benzobisimidazolium-based fluorescent and colorimetric chemosensor for CO2. *Journal of the American Chemical Society, 134*, 17846–17849.
17. Lee, M., Moon, J. H., Swamy, K., Jeong, Y., Kim, G., Choi, J., & Yoon, J. (2014). A new bis-pyrene derivative as a selective colorimetric and fluorescent chemosensor for cyanide and fluoride and anion-activated CO2 sensing. *Sensors & Actuators, B: Chemical, 199*, 369–376.
18. Lee, M., Jo, S., Lee, D., Xu, Z., & Yoon, J. (2015). A new naphthalimide derivative as a selective fluorescent and colorimetric sensor for fluoride, cyanide and CO2. *Dyes and Pigments, 120*, 288–292.
19. Xu, Q., Lee, S., Cho, Y., Kim, M. H., Bouffard, J., & Yoon, J. (2013). Polydiacetylene-based colorimetric and fluorescent chemosensor for the detection of carbon dioxide. *Journal of the American Chemical Society, 135*, 17751–17754.
20. Yanai, N., Kitayama, K., Hijikata, Y., Sato, H., Matsuda, R., Kubota, Y., & Kitagawa, S. (2011). Gas detection by structural variations of fluorescent guest molecules in a flexible porous coordination polymer. *Nature Materials, 10*, 787–793.
21. Trung, D. D., Toan, L. D., Hong, H. S., Lam, T. D., Trung, T., & Van Hieu, N. (2012). Selective detection of carbon dioxide using laocl-functionalized SNO2 nanowires for air-quality monitoring. *Talanta, 88*, 152–159.
22. Herrán, J., Mandayo, G., Ayerdi, I., & Castaño, E. (2008). Influence of silver as an additive on batio3–CUO thin film for CO2 monitoring. *Sensors & Actuators, B: Chemical, 129*, 386–390.
23. Michel, C. R., López-Contreras, N. L., & Martínez-Preciado, A. H. (2013). Gas sensing properties of Gd2O3 microspheres prepared in aqueous media containing pectin. *Sensors & Actuators, B: Chemical, 177*, 390–396.

Medical Device and Equipment Sector in India: Towards Sophisticated Digital Healthcare Systems—An Overview

P. K. Paul

Abstract

Healthcare Sector in India is changing rapidly with different types of advancement including introducing latest systems and technologies. Latest Information Technology and Computing Systems have changed entire arena of traditional medical and healthcare operations. Subsystems of IT such as Networking, Website Systems, Database Systems, and Software Systems radically change the scenario. Medical and healthcare segment tremendously changed in last decade and as a result huge gap is noted in current demand and supply systems of medical and allied devices in India. At the same time this gap gives a wonderful opportunity in developing and manufacturing medical devices. Very recently many medical device manufacturers from domestic and international market are engaged in developing and marketing devices in India. The medical devices are growing and there are tremendous growths in the sector by individual efforts, joint initiatives, multinational companies, etc. Government policies and financial changes are also important to note for the significant growth in medical device sector in India. Due to different reasons India is the top 20 markets in the world as far as medical devices are concerned. This chapter is focused on medical devices especially on Indian market. Growth, various changes, market scenario, and policies are also depicted in this work.

Keywords

Healthcare sector · Digitalization · Medical devices · Medical instruments · ICT Healthcare · Indian economy

P. K. Paul (✉)
Department of CIS, Raiganj University (RGU), Raiganj, India

G. Dutta (ed.), *Next-Generation Nanobiosensor Devices for Point-Of-Care Diagnostics*, https://doi.org/10.1007/978-981-19-7130-3_9

1 Introduction

Medical and healthcare sector as growing therefore outsourcings in medical devices are also noticeable. This sector has significant growth in recent past especially in last decade and present growth indicates that it will gain in coming decade with greater speed. Recently several changes are made in the areas of joint initiative, agreements, loan, licensing, and so on [1, 2]. Government of India recently changes the norms and policies for betterment, India based manufacturing, transparency, investment from outside India, and so on. In the year 2022, the market in this sector was 10.6 Billion USD and expected to reach 37% CAGR at 50 Billion USD in the year 2025. Comprising with Indian and foreign companies including small and medium sector, India is moving towards a best destination in Medical Device sector and Industry. Among some significant changes important are focusing Research and Development, Training and Skill Development, hundred percent FDI for medical devices to boost the market [3–5]. According to the report, the medical and surgical appliances sector stood at 2.23 US Dollar in between April, 2000 and June, 2021. Furthermore it is expected that within 2025 the diagnostics and allied sector may grow at a CAGR of 13.5%. Some of the important and promising areas of the healthcare and medical equipment sector are as follows:

- Medical, Healthcare and allied Infrastructure
- Designing and Developing Surgical Instruments
- Medical Systems and Imaging Systems
- Electromedical Equipment
- Orthopedic Appliances
- Prosthetic Appliances
- Cancer Diagnostics including Clinical Informatics practice
- In developing Ophthalmic Instruments as well as Appliances
- Advancing Orthodontic Equipment as well as Dental Implants
- Point of Care Testing and Diagnostic Devices
- Digital Healthcare System including telemedicine
- Medical Records and Healthcare Data Management [6–8]

2 Objectives

The present paper entitled "Medical Device and Equipment Sector in India: Towards Sophisticated Digital Healthcare Systems—*An Overview*" is a conceptual one and it deals with following aim and objective:

- To learn about the basic of the Digital Healthcare Systems especially in India.
- To know about the Scenario of Medical Device Sector in India with focused areas.
- To learn about the growing opportunities in healthcare and medical sector.

- To know about the policies, challenges, and issues in Medical Device sector in India including probable solutions.
- To get an idea of market size, growth, and export industry of medical devices in India.
- Medical devices investments and their details are also important in this context.

3 Methods

Present work is a conceptual in nature and prepared based on review of literature. Medical device and industry is an interdisciplinary topic therefore review of the documents done in the areas of medical devices, healthcare informatics and therefore Health and Medical related journals, thesis are analyzed and reported. In addition to these, Health and Medical related journals Business, Commerce, and Management related journals have been analyzed and reported in preparation of this work.

4 Scenario of Medical Device Sectors in India

Medical Device Industry in India is booming even there are huge challenges in global market. Due to some of the advantages and opportunities, Medical Devices industry is rising in India viz. limited HR and labor cost, advanced technical expertise, funding from different government bodies, finance from the associations, easiness in accessories in product development, etc. And as a result of new product development, outsourcing of the manufactured medical devices becomes easy. Day by day different multinational companies and firms are looking to suit their requirements and it is further to grow in the coming years. The Drugs and Cosmetics Amendment Bill, 2013 is important and this norms and bill play important role in growing medical devices, equipments, and products related to the diagnostics [9–11]. This bill also plays an important role in detaching medical devices and drug development too. This bill also helps the local manufacturers to compete on a global scale. The changes in medical and healthcare development sector are rapidly noticeable in last few decades and as a whole it helps in revenue and employment. The elderly population in India about 100 billion with the growing rate of the population is 1.6% per year. The economic growths, awareness, and market penetration of the health insurance are changing entire industry (Table 1).

According to the study of India Brand Equity Foundation (IBEF), the Indian healthcare Industry already reached 190 billion in 2020 and it may reach up to 370 billion USD within 2024–2025. The increasing demand regarding specialized healthcare needs leads growth in medical devices, clinical trials, telemedicine services and as a result medical equipment market has also been increased. The expansion of the medical and healthcare sector has catched more and large investment and here furthermore new entrants backed by private equity investors. According to the Global Burden of Disease Study (GBD) shown by the Lancet Journal, India has ranked 145th (out of 195 countries) regarding healthcare index.

Table 1 Some of the popular medical devices and instruments

List of medical devices			
Ablation device	Bone cements	MRI	Orthopedic implants
Catheters	Contraceptives	Dialysis machine	PET Equipments
Disposal hypodermic needles	Heart valves	Blood pressure monitor	X ray machine
Drug eluting stents	IV cannula	Glucometer	Digital thermometer
CT scanners	Surgical dressing	Cardiac stents	Scalp vein set

India's healthcare access and quality (HAQ) index score has improved in recent years, increasing from 44.8 (out of 100) in 2015 to 67.3 in 2020. The COVID-19 has also changed the entire investing scenario of healthcare sector not only in India but also in entire world [12, 13]. India spends only 1.2% of total GDP in healthcare and medical sector and it is expected to reach 2.5% by 2025 and as a whole overall healthcare and medical device sector is therefore likely to change more [14, 15].

5 Growing Opportunities in Medical Device in India

The advancement of technologies specially Computing has changed entire arena of healthcare and medical systems. The matching delivery mechanism has changed system and there are different changes noticeable in healthcare sector such as construction, equipments, financing and all these directly and indirectly touch with medical device sector in India. Supplying equipments as well as medical consumable is offering tremendous opportunities for the United States and some countries to offer healthcare related companies to offer healthcare equipments. India is growing market and becoming leading destination in high-tech diagnostic services. Several investments in healthcare segment are eye-catching in recent past. Health insurance companies are also involving much and as a result indirectly also help in healthcare and medical device industry. In healthcare sector, some of the other growth includes kits related to the testing and diagnostics, hand-made equipments, operating room simulations, etc. In healthcare market about 50% belongs to importing. On other hand, portable and handheld devices and equipments such as testing devices of blood pressure, blood sugar, oxygen level, etc. are also rising and fastest in India [16, 17]. Around 45 million diabetics is active in India and the number is also increasing and study reveals it may touch 70 million by 2025. And as a result the health-related issues are increasing and rising medical device related market also growing. Some of the healthcare device and allied aspects are described as under.

5.1 Medical Devices Sector and Growth

Medical device and instruments market is expected to reach 10 billion USD and India imports about 80% of the medical and healthcare devices. For the equipments such as cancer related diagnostics, medical imaging, ultrasonic scans, and also Polymerase chain reaction (PCR) systems and technologies etc. this import related aspects could be considered as worthy. And India depends on abroad for importing many medical devices and instruments. Healthcare and modern hospitals chains are also importantly growing in India such as Apollo, Fortis, Manipal, Hinduja, Max, etc. as a result medical tourism industry is also growing and altogether results in more medical devices and its utilizations. As far as medical tourism is concerned it is now contributed USD 2 billion in the medical and healthcare market. Compared to other sector in medical and healthcare sector barriers to the entry are low, and non-tariff barriers and the expansion of the price controls to the medical devices have forced market projection. During last 25 years the economy of the country is noticeable and therefore India tends to be a price competitive market. The production Linked Incentive scheme initiated by the Government of India (GoI) considered as important regarding developing medical device manufacturing in India rather importing [18, 19].

5.2 Health Insurance

In recent past, medical and healthcare sector is booming rapidly and in India health insurance is also increasing with very limited payment. As per scenario 2% covered by private health insurance organization and 15% covered by Government organizations/bodies. Several private insurance companies entered the market with opportunities in cashless treatment too. Thus the treatments in the healthcare are increasing and indirectly it is increasing the medical device uses [20, 21].

5.3 Hospital and Medical Infrastructure

Healthcare services are offered by the primary, secondary as well as tertiary care centers in India. Previously it is considered that only two categories serve the healthcare sector viz. government bodies and ministries, and private bodies and organization. The medical infrastructure market is rapidly increasing each year (about 15%) and private sector planning more on new age, modern and super specialty hospitals and medical centers. It is important to note that India is facing chronic shortage of healthcare related systems and infrastructure specially in the second and third tier towns and also in rural and sub-urban areas. According to the experts, India needs about 1.75 million more hospital beds within 2025 and this is creating an opportunity for foreign companies for the establishment of the sector due to FDI (Foreign direct investment). It is worthy to mention that Indian healthcare growth is expected to touch 130 USD billion with 2022–2023.

5.4 Biotech and Digital Healthcare Sector

Medical Device market is also growing in India and fastest due to emergence of Biotech sector. It represents a diverse opportunity for the international organizations and firms. As per latest study it has been noted that about 800 companies comprise market size of 5–7 billion USD, and internationally India shares 2% of the biotech Industry. As far as clinical trials, contract research and manufacturing is concerned India has significance. It is worthy to mention that digital healthcare segment is growing and during COVID 19 period the significant growth can be noted. During the period the aspects of telemedicine have significantly changed and people are adapting new health technologies and intelligent solutions to reduce barriers of hospitals and patients. Telemedicine nowadays consists with modern technologies such as Artificial Intelligence, Machine Learning, Cloud Computing, and Big Data Technologies. Leading hospitals and Healthcare sector such as Apollo, Fortis, Manipal, Hinduja, and Max have adopted different telemedicine services and modern technologies in this regard. NITI Aayog in association with the Ministry of Health and Family Welfare has developed different models, guidelines, and framework regarding ICT practice in healthcare and needful for the registered medical practitioners [22, 23]. Physician can now be able in remote and virtual consultancy under the guidance of National Medical Commission (NMC). India is heavily suffering with availability of medical infrastructure and a rural Indian has to travel 62 miles for getting affordable healthcare services. In COVID period use of digital healthcare technologies initiative by the GOI is considered as worthy and valuable [24, 25].

5.5 Refurbished Medical Equipment

As far as Indian capital cost is concerned, Indian manufacturers as well as investors engaged in reducing the capital costs. And also refurbished medical laboratory related devices and instruments for preparing Indian markets. Most of such machines are being used in top-of-the-line hospitals, corporation, multispecialty and super specialty hospital and diagnostics centers. Many international companies and organizations are doing their business and also selling medical laboratory systems and devices for the Indian market. Increasingly Indian hospitals and similar organizations are demanding continuous service and spare parts refurbishments, equipments maintenance in India. India gives restrictions on already used medical and healthcare devices and equipments. In India there is a provision of importing medical devices prepared and used in other countries provided there should be minimum 5 years of lifespan with a licensing and declaration. Furthermore without permission of the Director of Foreign Trade (DGET) it is not possible to sale, transfer, and dispose medical and healthcare equipments. It is important to note that parts, accessories, and tools can be given for the import, maintenance as well as operation up to 15%.

5.6 Policies and Regulations Governing Healthcare Instruments and Devices

The policies and regulations regarding healthcare devices are also being governed by the Government of India and this is being pursued by the Drugs and Cosmetics Act of 1940. Furthermore several categories of implantable devices are being control under the provision of Medical Device Rules, 2017. In India, medical devices are being categorized into following [18, 26]:

- *Class A:* In this category device with low risk basically considered such as surgical dressings, alcohol swabs.
- *Class B:* This category belongs to medical devices having moderate risks such as needle kits, cervical drains, etc.
- *Class C:* There are certain devices having moderate high risk, and among such devices important are bone cement, catheters, etc.
- *Class D:* Such devices are considered and required in high risk such as coronary stents, Bioresorbable Vascular Scaffold (BVS) System, angiographic guide wire, embolic filter system, etc.

All these devices are being finally categorized by the Government of India in January, 2020. Here devices include instruments, implants, software, etc. There are certain norms and regulations already adopted by the Government in regard to regulations, and laws. Government of India in the year 2017 introduced price controls on cardiac stents, reducing market price of 70% lower than that of prevalent market rate.

Medical Devices are also being listed by the National List of Essential Medicines (NLEM), and as of now 37 medical devices are listed within Drugs and Cosmetics Act. Later Government of India levied 5% ad-valorem health cess regarding importing of different devices such as medical devices, dental devices, surgical devices, and veterinary devices. In addition to these, devices like orthopedic knee implants which were previously exempted from customs duties and later the same have been withdrawn from the duty exemption.

It is also important to note that regarding price control of Oxygen concentrators (OCs) the National Pharmaceutical Pricing Authority (NPPA) issued an order with Trade Margin Rationalization (TMR). Last Year (2021) Indian Certification for Medical Devices (ICMED) scheme was added by the joint initiative of the Quality Council of India (QCI) and Association of Indian Medical Device. This initiative is fruitful in the verification of the quality, safety as well as benefit of the medical and healthcare devices. Furthermore new rules are to be introduced in re-approval of the manufacturing and importing licenses, etc.

6 Medical Devices, India and Future Growth

Medical Device market is moving gradually and it was in the year 2015 valued at USD 3.5 billion and increasing day by day. As per the development of the economic, healthcare, and social systems, the medical devices market is also growing rapidly and considered as important parameters in foreign manufactures. Medical Device as well as sophisticated medical technology is supported by the foreign experts. Medical tourism including luxury healthcare market is increasing and this results specialized, high-tech medical equipment. Surgical instruments including cancer diagnostics systems and equipments are in demand. Some of the equipments viz. orthopedic and prosthetic are also in need. Devices are belongs to the imaging, orthodontic as well as dental implants which are rising in different areas in addition to the traditional electro medical equipment [5, 20]. In India some of the areas are being considered as medical cluster and among them important are as follows (as depicted in Fig. 1 with highlighted color):

Fig. 1 Popular States in Medical Device cluster in India

- Gujarat
- Maharastra
- Karnataka
- Haryana
- Andhra Pradesh
- Tamil Nadu

6.1 Market Size and Export Scenario

As far as market share is concerned India considered within 20 markets for the medical devices and instruments. The devices market is increasing 37% CAGR and expected to reach 50 billion US Dollar in 2025 from Rs. 75,611 crore in the year 2025. With the initiation of Government of India Medical Device sector is getting strengthening and here in research and development areas too investment considered as worthy. Furthermore 100% FDI is allowed for medical devices including medical and surgical appliances. In between 2020 and 2025 it is estimated that diagnostic imaging may be expand at a CAGR of 13.5% and wearable market will grow 93.8%.

India has a 75–80% import dependency on medical devices, with exports at Rs. 14,802 crore (US$2.1 billion) in 2019 and is expected to increase at a CAGR of 29.7% to reach Rs. 70,490 crore (US$10 billion) in 2025. It is worthy to note that to increase export of medical devices in the country some of the initiatives are noted from the part of Indian Ministry of Health and Family Welfare (MOHFW), and CDSCO, i.e., Central Drugs Standard Control Organization. Among the projects and initiatives few important include:

- Re-evaluating schedule MIII (which is a draft on medical goods manufacturing practices).
- Implementation of the facility requirements including system for the export labeling.
- Assessing clinical evaluation including adverse reporting clarifications.

The scenario is changing rapidly in changing the norms, regulations, and governance for the proper growth and development.

6.2 Growth and Challenges in Medical Device Sector in India

In India not all the Medical Devices are governed by the regulations, only certain product categories are having such regulations. It is to worthy to note that India has some of the obstacles for the manufacturers from India and that need to overcome using different strategies. Indian manufacturers are also suffering with the competition of low cost Chinese products, and there is a need of changes in norms and regulations. Furthermore for the foreign manufacturers like American, European, and Japanese companies proper and balanced regulations need to adopt. Globally

Medical Device market is predicted to reach about US Dollar 400 within next year. Medical device market in India in the year 2013 was 6.3 billion USD and it was about 7% to 8% of overall healthcare budget/spending in India, whereas pharmaceutical share 18%. Since the per capita spending is limited even of US Dollar 3, Government of India feels FDI is the best solutions for the domestic development. Medical Device sector is growing and within 2025 the industry is projected to have value of US Dollar 50 billion. As healthcare systems, hospitals are rising therefore sophisticated medical instruments are in demand. The outlook of the medical device industry will change significantly due to allowing 100% FDI in the medical devices outsourcing. Since in the past there was no regulatory framework and incentives for the development of the devices in India therefore the changed norms and new regulatory frameworks and 100% FDI has an impact in the market. As previously there was high tax rates imposed therefore it was difficult to implement medical device marketing and manufacturing units in India but the scenario has changed significantly. Due to internal high tax it was difficult to establish physical setups in India therefore indirect business was only solutions. Internationally many countries now list India become a favorite destination. United States of America (USA) is representing largest market for the outsourcing. Due to HR and adorable technical solutions Asian countries considered as most perfect destination for medical and allied devices production. Asian countries mainly India and China considered as cost effective and quality medical device manufacturers in OEMs. According to the market research firm GlobalData medical device Industry is projected to reach with a growth rate of 7% in between 2021 and 2025, and the same can be successfully reached by different projects and initiatives such as Atmanirbhar Bharat Abhiyaan, promotion of medical devices parks scheme [5, 27]. Therefore the medical device sector can be enriched into a desirable sector only by adopting the following:

- Establishing better and healthy eco-system, with increasing export systems, developing medical informatics strategies.
- Planning and establishing medical device licensing, regulations, suitable frameworks, etc.
- More and more medical tourism sector will also be beneficial for the local product development and manufacturing competencies.
- Tax relief, development of the special economic zone also considered as worthy and beneficial in boosting of the medical device sector.
- In addition to these, boosting local developer should be supported by the accessibility and affordability of the medical devices [10, 22].

Medical Devices and healthcare market in India compared with other countries is different but tremendously developing than the neighbor countries and most of the Asian countries. India's total spending of healthcare is 93 billion USD, whereas total healthcare spending in the USA is 3 trillion USD and even China spends 574 billion USD. Therefore in contrast with the sharing of per capita investment India shares 4.7% of the GDP, whereas the USA and China share 17.1% and 5.5%, respectively.

Elements	India	USA	China
Population	1,251,695,584	321,368,864	1,367,485,388
Healthcare Expenditure	93 Billion USD	3 Trillion USD	574 Billion USD
Healthcare cost (% of GDP)	4.7%	17.1%	5.5%
Healthcare cost per capita	75 USD	9403 USD	420 USD
Healthcare sharing	Govt.30% & Private 70%	Govt. 48% & Private 52 %	Private 44%
Medical device market size	3.5 billion USD	147.7 billion USD	8.7 billion USD

Fig. 2 Depicted healthcare expenditure and related facts of India, USA, and China

As far as Healthcare expenditure per capita is concerned India holds 75 billion USD, whereas the USA is 9403 billion USD and China 420 Billion USD. Here Fig. 2 is depicted the aspects of the healthcare in detail.

According to the study it is also important to note that the market size for the medical device is US Dollar 3.5 billion in India, whereas market share of the USA is 147.7 billion USD and in China the share is 8.7 billion USD. Medical Device market is changing due to incentives too, in the month of May, 2020 Government of India declared detailed investment plans about 4.9 billion USD over the period of 5 years, and these funds may be utilized over a period of 5 years. Furthermore said investment is only acceptable if investment is offered in manufacturing in medical devices. Some of the notable achievements and initiatives of the Medical Devices market in India by the private sector in recent past are as follows [2, 23]:

- Cipla, a leading pharmaceutical company has launched pneumotach system based, portable wireless spiromete called “Spirofy” in the year 2021. Same year 2021 witness of launching of portable hydrogen generating machine called “udazH” for private utilizations by the Serene Envirotech Pvt. Ltd. With this machine two users can utilize the device at a time.
- Leading electronic appliance company Microtek in the year 2021 also jumped into the medical device manufacturing with projected devices as oxygen concentrators, monitors for the purpose of blood pressure, oximeters, digital and infrared thermometers, etc. Same year Innovation Imaging Technologies Pvt. Ltd. established a state of the art facility center in India (Bangalore) for the development of the 240 laboratories (catheterization) within 1 year and therefore it is treated as important initiative for the development of the cardiology-related diseases in India.
- Last year another achievement gained by the HDM where they had supplied 500 million 0.5 ml AD syringes for healthy, smooth vaccination drive.

- DRHP in association with the SEBI has projected to invest Rs. 1500 crore for the medical and healthcare sector. Similarly Medtronic India in same year (2021) has collaborated with Stasis Health for Medical Infrastructure development.
- Siemens Healthnieers, a leading healthcare technology organization initiated to start development unit in Gujarat including collaboration with Synthetic MR, with a new license agreement [2, 5].
- India got Australia-India Council grant for conducting pre-clinical testing required for the purpose of neurosurgery. Additionally to have first medical tools manufacturing unit at Noida, it is projected to prepare by the investment of Rs. 5000 crore.
- Government of Punjab is also recently planned to have Medical Device Manufacturing plant with proposed cost Rs. 180 crore. Government of Tamil Nadu is also planning to establish Medical device park with estimated cost of Rs. 430 crore.
- In Maharastra too proposed investment of Rs. 150 crore to be received by the healthcare company in-vitro diagnostic. Additionally, advanced technology solutions for the testing of COVID-19, TB, HIV, Dengue are being planned.
- Japanese Healthcare Organization Omran Healthcare is planning to extend healthcare manufacturing units in existing locations of their operations and also enhanced services at Warangal with an expected turnover of Rs. 220 crore.

These are basic and recently planned initiative regarding the development of the medical device manufacturing units in India. The Indian Council of Medical Research (ICMR) in collaboration with IITs planned to establish Centres of Excellence (CoE) with the aim of developing products as per Make-in-India product development. In 2021 some of the activities also considered as notable viz. government's plans on new drugs, cosmetics, manufacturing on medical devices, under PLI scheme 13 companies also granted development of the medical devices for enhancing country's own medical devices. Government's initiative (in the year 2014) on "Make in India" campaign regarding the development of the medical devices is treated as valuable. Indian Government had also took initiative for the medical device park in India of Rs. 5000 crore. Furthermore, medical park has also been proposed with investment of Rs. 500 crore in Uttar Pradesh; and this initiative is taken very recently in the month of July, 2021. Public Procurement Order (PPO) was also an important step by the Department of Pharmaceuticals (DoP) for improving medical devices manufacturing of country's own. Under the Legal Metrology Act, the import of the devices such as nebulizers and oxygen concentrators becomes easy and smooth. As a whole the medical informatics companies such as Siemens, Allengers, Wipro-GE Healthcare, Nipro, Sahajanand, Involution Healthcare, and Integrits Health are going to invest Rs. 729 crore and going to generate about 2000 jobs according to the market research organization. National Medical Devices Promotion Council establishment also considered as valuable in regard to developing local manufacturing of the medical devices. In addition to different state government's move Government of Andhra Pradesh has also taken an important move of establishing Andhra Pradesh MedTech Zone (APMTZ) [19, 28]. This is

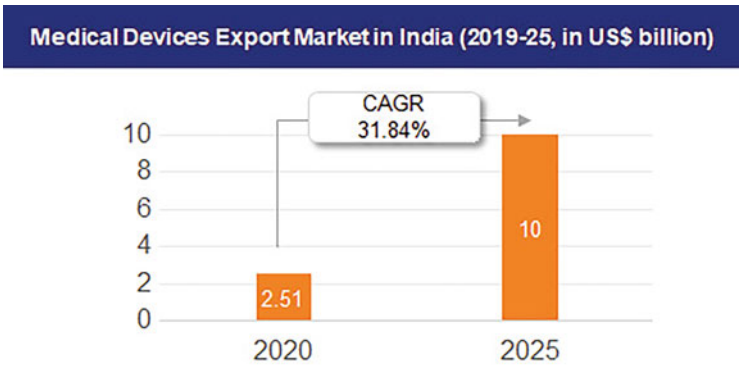

Fig. 3 Possible medical device growth by 2025 (Source: IBEF)

specially planned for the developing scientific facilities, laboratories, and also manufacturing units in Vishakhapatnam. According to the financial organization and market research venture IBEF the medical device export market in India is expected to increase at US Dollar 2.1 billion and CAGR of 31.84% as depicted in Fig. 3.

7 Conclusion

Medical Device is growing significantly during last decade and there is an important gap in India for the current demand and requirement of the medical devices in India and as a result different initiatives have been taken by various stakeholders. Today many healthcare organizations are getting opportunities for developing medical devices in India itself and even import also become easy. India is considered within 20 markets in developing and sale of the medical devices and instruments and it is expected to grow at 37% CAGR. The composition of medical device organizations in India is small, mid, and large; all. Government of India is engaged with different industrial, research, and academic activities of medical devices so that market can be boosted up more and more. 100% FDI in Medical devices no doubt would be worthy in developing the concerned market. It is also expected that the diagnostic market will reach of 13.5% in India.

References

1. Aileni, R. M., Pasca, S., & Valderrama, C. (2015, October). Cloud computing for big data from biomedical sensors monitoring, storage and analyze. In *2015 Conference Grid, Cloud & High Performance Computing in Science (ROLCG)* (pp. 1–4). IEEE.
2. Lahiry, S., Sinha, R., & Chatterjee, S. (2019). Medical device regulation in India: What dermatologists need to know. *Indian Journal of Dermatology, Venereology and Leprology, 85*(2), 133–137.

3. Haleem, A., & Javaid, M. (2019). Additive manufacturing applications in industry 4.0: A review. *Journal of Industrial Integration and Management, 4*(04), 1930001.
4. Jarosławski, S., & Saberwal, G. (2013). Case studies of innovative medical device companies from India: Barriers and enablers to development. *BMC Health Services Research, 13*(1), 1–8.
5. Zhao, G., Wang, H., & Liu, G. (2015). Advances in biosensor-based instruments for pesticide residues rapid detection. *International Journal of Electrochemical Science, 10*(12), 9790–9807.
6. Dang, A., & Sharma, J. K. (2019). Economics of medical devices in India. *Value in Health Regional Issues, 18*, 14–17.
7. Maresova, P., Penhaker, M., Selamat, A., & Kuca, K. (2015). The potential of medical device industry in technological and economical context. *Therapeutics and Clinical Risk Management, 11*, 1505.
8. Yang, Y., & Gao, W. (2019). Wearable and flexible electronics for continuous molecular monitoring. *Chemical Society Reviews, 48*(6), 1465–1491.
9. Gomez, A. L., Venkatesh, N. D., & Neelakandan, N. (2020). A comparative study of medical device regulations in India: Before and after the implementation of medical device rules 2017. *Research Journal of Pharmacy and Technology, 13*(9), 4423–4429.
10. Shah, S. G. S., Robinson, I., & AlShawi, S. (2009). Developing medical device technologies from users' perspectives: A theoretical framework for involving users in the development process. *International Journal of Technology Assessment in Health Care, 25*(4), 514–521.
11. Zhao, G., Guo, Y., Sun, X., & Wang, X. (2015). A system for pesticide residues detection and agricultural products traceability based on acetylcholinesterase biosensor and internet of things. *International Journal of Electrochemical Science, 10*(4), 3387–3399.
12. Kamble, S., Gunasekaran, A., & Dhone, N. C. (2020). Industry 4.0 and lean manufacturing practices for sustainable organisational performance in Indian manufacturing companies. *International Journal of Production Research, 58*(5), 1319–1337.
13. Windmiller, J. R., & Wang, J. (2013). Wearable electrochemical sensors and biosensors: A review. *Electroanalysis, 25*(1), 29–46.
14. Kumar, V. (2018). Regulatory regime on Indian medical device industry—A way forward. *Innoriginal International Journal of Science, 5*(3), 5–7.
15. Waqas, M., Dong, Q. L., Ahmad, N., Zhu, Y., & Nadeem, M. (2018). Critical barriers to implementation of reverse logistics in the manufacturing industry: A case study of a developing country. *Sustainability, 10*(11), 4202.
16. Markan, S., & Verma, Y. (2017). Indian medical device sector: Insights from patent filing trends. *BMJ Innovations, 3*(3), 167.
17. Wong, C. K., Ho, D. T. Y., Tam, A. R., Zhou, M., Lau, Y. M., Tang, M. O. Y., et al. (2020). Artificial intelligence mobile health platform for early detection of COVID-19 in quarantine subjects using a wearable biosensor: Protocol for a randomised controlled trial. *BMJ Open, 10*(7), e038555.
18. Winterhalter, S., Zeschky, M. B., Neumann, L., & Gassmann, O. (2017). Business models for frugal innovation in emerging markets: The case of the medical device and laboratory equipment industry. *Technovation, 66*, 3–13.
19. Zhang, Y., Qiu, M., Tsai, C. W., Hassan, M. M., & Alamri, A. (2015). Health-CPS: Healthcare cyber-physical system assisted by cloud and big data. *IEEE Systems Journal, 11*(1), 88–95.
20. Javaid, M., & Haleem, A. (2019). Industry 4.0 applications in medical field: A brief review. *Current Medicine Research and Practice, 9*(3), 102–109.
21. Shah, S. G. S., & Robinson, I. (2007). Benefits of and barriers to involving users in medical device technology development and evaluation. *International Journal of Technology Assessment in Health Care, 23*(1), 131–137.
22. Rao, G. S. U. (2013). "Made in India": How's that for an indigenous medical device? *Indian Journal of Neurosurgery, 2*(02), 151–153.
23. Ye, S., Feng, S., Huang, L., & Bian, S. (2020). Recent progress in wearable biosensors: From healthcare monitoring to sports analytics. *Biosensors, 10*(12), 205.

24. Bhat, B. B., Prabhu, P. P., Lobo, M. J., & Kamath, B. V. (2019). Medical device industry in India: Past to present. *Research Journal of Pharmacy and Technology, 12*(12), 5959–5962.
25. Wang, R., & Jia, J. (2020). Design of intelligent martial arts sports system based on biosensor network technology. *Measurement, 165*, 108045.
26. Zaripova, V. M., & Petrova, I. Y. (2016). Information technology of concept design of biosensors. *Indian Journal of Science and Technology, 9*(1), 1–11.
27. Rane, S. B., & Kirkire, M. S. (2016). Analysis of barriers to medical device development in India: An interpretive structural modelling approach. *International Journal of System Assurance Engineering and Management, 7*(3), 356–369.
28. Paul, P. K. (2021). Biosensor and healthcare Vis-à-Vis cloud computing and IoT: Towards sophisticated healthcare development—An overview. In *Modern techniques in biosensors* (pp. 253–273). Springer.

Application of Radiopharmaceuticals in Diagnostics and Therapy

Priya Sarkar, Shivani Khatana, Bimalendu Mukherjee, Jai Shukla, Biswajit Das, and Gorachand Dutta

Abstract

Radiopharmaceuticals are biologically active molecules with a radioisotope attached to them. Radiopharmaceuticals have both diagnostic and therapeutic applications. The radioisotope present within the radiopharmaceuticals emits radiations which are detected by the radiation detectors and are used to produce an image to diagnose a particular disease, the process of production of images of organs or tissues of interest by using radiopharmaceuticals is called scintigraphy. ^{99m}Tc is most widely used radioactive tracer for most of the nuclear medicine procedures, often referred as workhorse of nuclear medicine. Radioactive tracers, mostly ^{99m}Tc may be used in diagnosis and prognosis of coronary artery diseases. Myocardial perfusion imaging may be considered for patients with defective stress test as it's non-invasive technique before angiography. In order to understand the metastatic potential of cancer growth, metabolic studies along with detection staging is extremely helpful. Radioactive tracers are used for tumour imaging and ^{67}Ga is the most sensitive. Radiopharmaceuticals may now be a good alternative which have been used to study the liver, which are giving impactful results, ^{99m}Tc-labelled IDAs may be considered as new hepatobiliary agents, which offer better clinical information than any other diagnostic modalities available. For several other diagnostic purpose, radioactive tracers are used as Fe tracers that are useful for several haematopoiesis studies, results may give us brief understanding about the exact cause of Fe-deficiency anaemia.

Authors Priya Sarkar, Shivani Khatana, and Bimalendu Mukherjee contributed equally to this work.

P. Sarkar · S. Khatana · B. Mukherjee · J. Shukla · B. Das · G. Dutta (✉)
School of Medical Science and Technology (SMST), Indian Institute of Technology Kharagpur, Kharagpur, India
e-mail: g.dutta@smst.iitkgp.ac.in

G. Dutta (ed.), *Next-Generation Nanobiosensor Devices for Point-Of-Care Diagnostics*, https://doi.org/10.1007/978-981-19-7130-3_10

It is found that Cobalt tracers have more sensitivity in diagnosing pernicious anaemia. For therapeutic purpose, most common radioisotope is ^{131}I, used to treat thyroid cancer and hypothyroidism. Radiotherapy, which generally regarded as a treatment of cancer, uses high dosages of radiation to kill cancerous cells, also pain in bone metastasis can be treated non-invasively by radiotherapy. Among therapeutic application, radioimmunotherapy is also used which involves the use of radiolabelled antibody with radionuclide in the treatment.

Keywords

Radioactive tracers · PET · SPECT · Myocardial perfusion imaging · Radiation therapy · Radioimmunotherapy

1 Introduction

Biologically active compounds with a radioisotope attached to it are known as radiopharmaceuticals. They can bind with specific targets like organs, tissues, or cells within the human body. Their uses in clinical practice are increasing day by day. Radiopharmaceuticals application lies in providing functional information at the molecular and cellular level non-invasively which helps in the identification of health conditions and therapy of diseases [1]. Radiopharmaceuticals are radioactive compounds that are used to diagnose and treat the various diseases. Radiopharmaceuticals have two components—a radionuclide and a pharmaceutical. Schematic view of the two major components of radiopharmaceuticals is shown in Fig. 1. The biologically active molecule can be thought of as a vehicle that drives the radioisotope inside our body to a specific tissue or organ of our interest. The process of production of images of organs or tissues of interest by using radiopharmaceuticals is called scintigraphy. In the preparation of

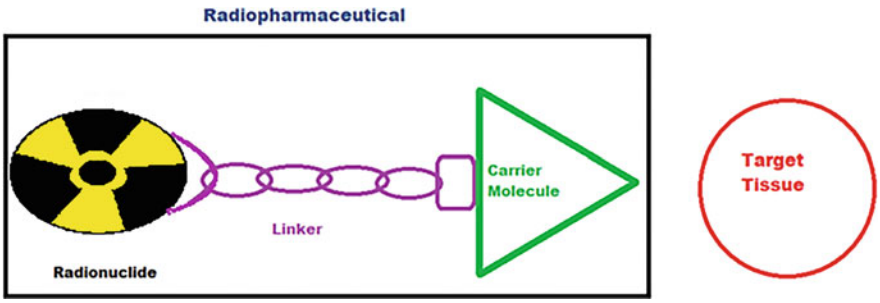

Fig. 1 Radiopharmaceutical consists of a radionuclide (radioactive element), that uses for external scan, linked to a non-radioactive element with the help of a linker, that acts as a carrier molecule which directs the radionuclide to the target tissue or organ

radiopharmaceuticals, first a pharmaceutical is chosen according to favoured localization in the given organ as its purpose is to direct the radionuclide to the location that need to be diagnosed or treated and to obtain images. Then a radionuclide is tagged with that chosen pharmaceutical so that after administration of the radiopharmaceuticals to the patient, radiations are emitted from it which can be detected or used to provide image by a radiation detector [2]. Tissue blood flow and metabolism, protein–protein interactions, expression of cell receptors in normal and abnormal cells, cell–cell interactions, neurotransmitter activity, cell trafficking and homing, tissue invasion, and programmed cell death are some of the functional information for investigations that can be obtained from these imaging techniques. These details are important for examining both healthy and disease-related states, and they also assist clinicians in determining how well a particular treatment is working [1].

There are several ways to administer radiopharmaceuticals to a patient, including through injection, oral administration (in the form of pills), or insertion into the cavity in the body [3, 4]. The radiopharmaceuticals drugs which are used for diagnostic purposes are short-lived radiotracers. Radiopharmaceuticals that are used for diagnostic purposes accommodate small amount of radiation as compared to those that are used in treatment. Diagnostic radiopharmaceuticals enable the doctors and researchers to non-invasively see the biochemical activities inside the human body, to diagnose the disease and which treatment is best suited for the patient and also help them to monitor patient's response to treatment [5]. An imaging modality such as Positron Emission Tomography (PET) or Single Photon Emission Computed Tomography (SPECT) is used to study the activity inside the organ after the patient receives a radioactive dosage for the diagnostic process [6]. Radiopharmaceuticals emit radiation and based on this can be used for diagnosis and therapy, depending on what type of radiation it emits. Generally, if gamma-ray particles are emitted then it is used for diagnosis, whereas if beta or alpha particles are emitted then it will use for therapeutic purposes [7]. There are some characteristics that have to be considered while selecting radiopharmaceuticals for clinical purposes:

- For diagnostic purposes, radiopharmaceuticals should have short half-life so that it decays quickly to safely diagnose the disease of the patient and also limit the radiation doses. The list of radionuclides with their corresponding half-lives are given in Table 1.
  Due to high penetration power as compared to the alpha and beta decay, gamma rays have a less destructive effect on the human body, and therefore, the majority of radionuclides that generate gamma radiation are employed in imaging with a gamma camera for diagnosis. The different types of radiation and their corresponding radiation power is shown in Fig. 2.
- Beta emission increases the radiation dose due its low penetration power, therefore mostly those radionuclides have been used for diagnosing that generate gamma rays with enough energy to easily leave the body and need to have a short half-life to reduce the radiation dose.

Table 1 Different types of radionuclide with their half-life

Radionuclide	Half-life	References
Fluorine-18	109.8 min.	[8]
Technetium-99 m	6 h	[9]
Lead-212	10.6 h	[10]
Copper-67	15 h	[11]
Samarium-153	1.93 days	[12]
Holmium-166	26.8 h	[13]
Thallium-201	73.1 h	[14, 15]
Gallium-67	78.3 h	[16]
Xenon-133	5.27 days	[17]
Iodine-131	8 days	[18]
Chromium-51	27.7 days	[19]
Strontium-89	50.6 days	[20]
Phosphorus-32	14.26 days	[21]
Yttrium-90	64.2 h	[22]

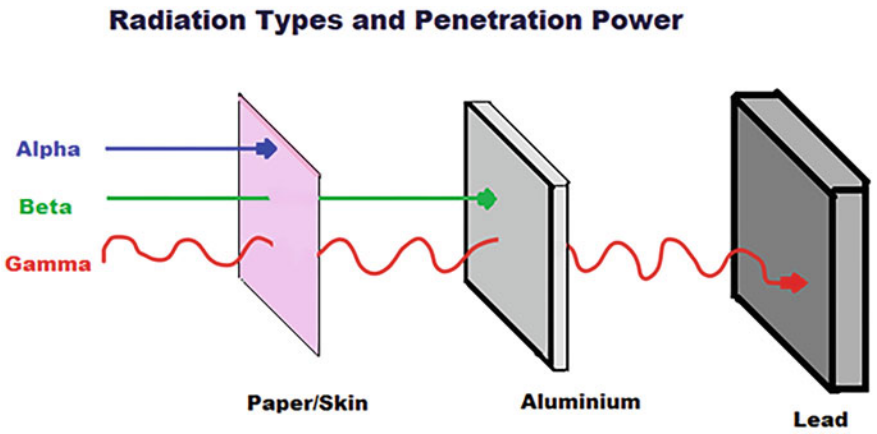

Fig. 2 Different radiation types and their penetrating power

- For radiopharmaceuticals, there should be high specific activity to properly localize to the target site.
- To protect healthy tissue and organ from being exposed to damaging radiation, radiopharmaceuticals should reach to the intended target tissue or organ swiftly and precisely.

  The stability of radiopharmaceuticals is also very important to consider in diagnostic applications as the stability of radioisotopes can be effected by pH, temperature, and light. If these factors are not taken under consideration during the diagnostic imaging it can result into undesirable results, such as decreased quality of image, and undesirable distribution of radiation [2, 7, 23].

2 Monitoring of Tissues and Organs by Radiopharmaceuticals

The main advantage of radiopharmaceuticals is their radioactivity that allows non-invasive external monitoring of the target tissue or organ with very small effect on the biological activities in the body [2, 24]. For diagnosis, when the radiopharmaceuticals are given to the patient, it is continuously monitored by an imaging device such as gamma camera. These imaging systems include SPECT and PET imaging, computed tomography-PET, micro-PET, and micro-computerized axial tomography [2]. When a single gamma ray is directly emitted, SPECT cameras are used to identify nuclides; however, when a pair of gamma rays are emitted, PET cameras are utilized [2, 5].

2.1 Single Photon Emission Computed Tomography (SPECT)

The SPECT scan technique creates three-dimensional images by utilizing radionuclides that display the blood flow path to tissues and organs. By using a scintillation camera different image of varying orientations around the patient are collected which are developed through tomographic reconstruction approach. The major clinical applications of SPECT are in brain scanning, cardiac perfusion imaging, and liver scanning. A radioactive tracer is injected into the bloodstream before the SPECT scan which eventually emits gamma ray and gets detected by the computed tomography (CT) scanner. The collected information from the emitted radiations of the gamma rays is evaluated by the computer and displayed on CT cross-sections which are organized to create a three-dimensional representation of the human brain. The radionuclides used as a tracer in SPECT are Xenon-133, Technetium-99m, Flourine-18, and Thallium-201. As SPECT imaging technology exhibits excellent sensitivity but falls short of computed tomography's high anatomic resolution, dual integrated systems have been developed by merging CT and SPECT which will carry out both functional and anatomical image respectively in a given scan. SPECT is different from PET scan as the radionuclide tracer used in this technique stays in the bloodstream unlike being absorbed to the neighbouring tissues, hence it helps to limit and narrow down the images to that zone where blood flows [25, 26].

2.2 Positron Emission Tomography (PET)

Positron emission tomography (PET) is a method used to measure the metabolic process of cells of body tissues and visualize the biochemical changes associated with it. It uses small amount of radionuclide and gamma camera system. Consequently, it combines biochemical analysis and nuclear medicine. In this method, a particle accelerator called a cyclotron is employed to create unstable atoms with an excess of protons that decay back to neutral neutrons by producing positrons (the

antiparticle of the electron). Within a short range, the emitted positron collides with electron generating high energy and momentum and that gets converted to two oppositely directed gamma rays with 511 keV of energy. The detector detects these two gamma rays that forms the image. The advantage of this technique is that it emits gamma rays at 511 keV of fixed energy and as a result it will eventually help for the instrument in optimization process by fixing the value for detection at this energy. Though a major challenge for PET technique lies due to very short half-lives of cyclotron produced, positron emitter like ^{15}O has 2.07 min half-life [26].

3 Diagnostic Applications of Radiopharmaceuticals

Departments of nuclear medicine are crucial in the administration of radiopharmaceuticals used in patient diagnosis. The main objective of nuclear medicine is to provide valuable details about the activities or functioning of the human body and that help the doctors to diagnose the disease state of the patient [27]. Diagnostic radiopharmaceuticals are used to examine the functioning of various organs of the body such as brain, liver, kidneys, lungs, stomach, heart, in tumour imaging, in diagnosis and studying of cancer, estimate bone growth, and to adapt other diagnostic procedures that are required for the treatment of the patient. It may help in early identification of the disease or disease state of a patient so that proper treatment is given to the patient [6]. The list of radiopharmaceuticals with various diagnostic applications is given in Table 2.

3.1 Uses of Technetium-99m

Technetium-99m is the radionuclide that is most frequently employed in diagnostic radiopharmaceuticals, because of its following ideal characteristics required in diagnostic applications of radiopharmaceuticals:

- ^{99m}Tc has a 6-h half-life, which is brief enough to analyse the target tissue or organ while simultaneously minimizing the radiation dosage to the patient.
- There is emission of gamma rays in ^{99m}Tc decay process and low-energy electrons are emitted, therefore again reduce the radiation dose and also the energy of gamma rays is low, therefore it easily escapes the human body.

^{99m}Tc commonly used in a number of diagnostic imaging scans that are used to diagnose various disease states such as infections, injuries, tumours, heart diseases, thyroid and kidney abnormalities, and also used in guiding some cancer procedures such as in tumour detection in lung cancer [6, 24, 34]. The major organ systems imaged by Technetium-99m are shown in Fig. 3.

Table 2 List of diagnostic applications of radiopharmaceuticals

Radionuclide	The diagnostic use	References
Technetium-99m	Used in diagnosis of amyloid heart disease and in PET scans in myocardial perfusion imaging	[28, 29]
Flourine-18	Used in PET to assess alterations in glucose metabolism in bone tumour	[30]
Holmium-166	Used in diagnosis of liver cancer	[13]
Iodine-131	Used in studying the function of thyroid gland in treatment of thyroid cancer or in hyperthyroidism	[18]
Gallium-68	Used in PET scans to diagnose cardiac, respiratory pathologies and in Alzheimer's disease	[16, 31]
Chromium-51	Used for labelling red blood cells and for diagnosis of gastrointestinal bleeding	[19]
Potassium-42	Used in tumour localization and studies of renal blood flow	[32]
Xenon-133	Used in imaging of lungs and evaluate pulmonary function	[17]
Thallium-201	Used in the diagnosis of coronary artery disease and parathyroid hyperactivity	[15]
Selenium-75	Used for scanning pancreas to study the production of digestive enzymes	[33]

3.2 Radiopharmaceuticals Used for Diagnosis of Cardiovascular Diseases

In the entire world, cardiovascular disease (CVD) is one of the leading causes of death [35]. The cardiologists of the early twenty-first century have access to a wide range of imaging modalities, but situations not so few years ago. The only effective heart imaging technology available at the start of the 1970s was an intrusive procedure called cardiac catheterization. Since the development of nuclear cardiology investigations, it led the way to the non-invasive assessment of cardiac disease. Radionuclide ventriculography (RNV) was the first non-invasive method in assessing left ventricular (LV) function and it established nuclear cardiology as a clinical discipline [36].

Myocardial Perfusion Imaging (MPI) or Myocardial Perfusion Scintigraphy (MPS)

Inorganic compounds such as ^{13}N-ammonia ($^{13}N\text{-}NH_3$) and ^{15}O-water ($^{15}O\text{-}H_2O$) may be used for cardiac perfusion imaging [37]. It is an important diagnostic technique which can be used for detection and prognosis of coronary artery disease. Thallium-201 Chloride or ^{99m}Tc radioisotope as tracers may use for the process. Test is performed in order to understand the blood flow at rest and during stress, thereby defining flow-limiting epicardial coronary stenoses and sometimes microvascular disease. Three radiopharmaceuticals are used routinely in clinical procedures for myocardial perfusion scintigraphy: Thallium-201 (^{201}Tl) as Thallous chloride, Technetium-99m (^{99m}Tc) Sestamibi, and (^{99m}Tc) Tetrofosmin, these tracers are

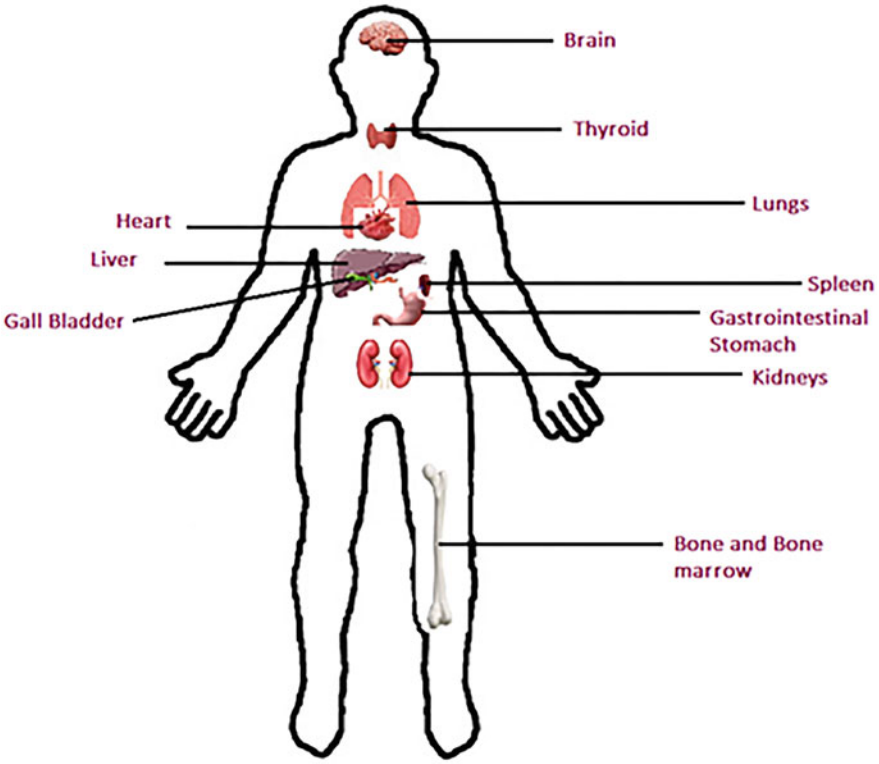

Fig. 3 Imaging done by ^{99m}Tc that is used in diagnostic applications

also available for SPECT myocardial perfusion imaging (MPI). Several PET tracers can be used to assess myocardial perfusion, these include ^{82}Rb, ^{13}N-NH_3, and ^{15}O-water [36], and the advantages of MPI is shown in Fig. 4.

3.3 Radiopharmaceuticals Used for Study of Liver and Diagnosis of Diseased Condition

Tests to analyse liver functions have been mostly done by clinical laboratory diagnostic procedures, mostly invasive for a significant number of years. Apart from these, radiographic imaging procedures are also utilized which involve oral cholecystography and intravenous cholangiography are few to mention, although it serves the purpose, but most of them are invasive techniques involving a certain amount of risk and discomfort to the patient, also as these techniques use contrast media, which may cause other problems in patients as well. Radiopharmaceuticals now have been used to study the liver, which are giving interesting results [38]. Radiopharmaceuticals which can localize within the hepatobiliary

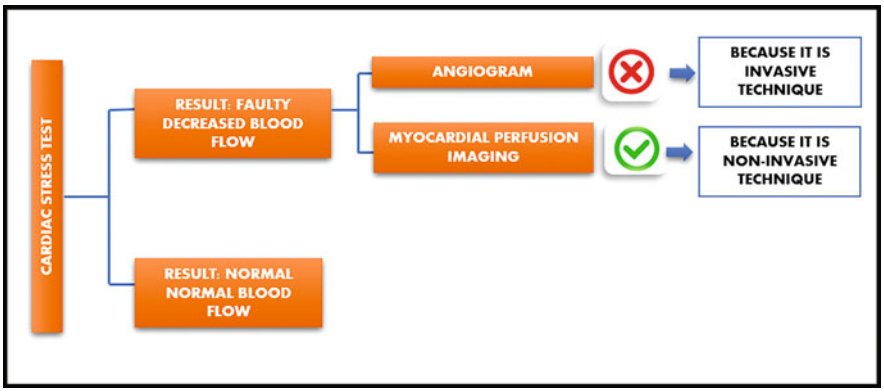

Fig. 4 Advantage of myocardial perfusion imaging as it is non-invasive

(HB) system are used for non-invasive diagnostic imaging modality, that can help in evaluation of several difficult clinical problems related to HB disorders [39]. In jaundice, ^{99m}Tc-para-butyIIDA concentrated more in the liver than ^{99m}Tc-HIDA, on comparing between two agents in the same patient [40]. Comparing among two ^{99m}Tc-HIDA and ^{99m}Tc-p-butyl-IDA Liver radioactivity decreased significantly after 10 min with HIDA compared to 35 min with p-butyl-IDA [41].

3.4 Radiopharmaceuticals Used in the Diagnosis of Cancer

To Detect Cancerous Growth in the Body: Metabolic Study Using FDG

Cancer is a condition where when cells division goes out of control. More amount of glucose is consumed by cancerous cells than any normal cell, this is also considered as one of the hallmarks of cancer cells. The Warburg effect is the main reason behind the shift in energy production. Fluorine-18-fluorodeoxyglucose (FDG)-PET utilizes this feature to distinguish between normal and cancerous cells, based on consumption of glucose. FDG build-up in cancer cells can notify us about aberrant mitochondrial function, which is seen in a variety of cancer cells. Different rates of glucose use can help us identify the presence and spread of tumours, as well as distinguish between malignant and benign tumours. Metastases give us information about the severity of the disease, which helps physicians for TNM(Tumour,node,metastasis) staging of tumour and determining therapeutic strategies.

Tumour Imaging

Gallium-67 is the radioactive tracer that is most frequently utilized. Hodgkin's disease staging can be done using Gallium-67, which has an 87% sensitivity. But lower sensitivity is achieved in the case of detection of non-Hodgkin's lymphomas. Galium-67 has the highest positive rate in detecting bronchogenic carcinomas. Its sensitivity rate for detecting lung cancer is 67%. There is proof that ^{67}Ga is at least complimentary to lymphangiography, if not more sensitive, in the staging of

lymphoma. But ^{67}Ga cannot reliably identify adenocarcinomas that originate in the gastrointestinal system as its sensitivity is very low at only about 40%, so in this case, adenocarcinoma of the gastrointestinal tract is detectable with significantly increased sensitivity using various chelates of bleomycin, such as ^{111}In-Bleo, ^{99m}Tc-Bleo, and ^{57}Co-Bleo. According to certain research, ^{111}In-Bleo is less sensitive than ^{57}Co-Bleo and ^{99m}Tc-Bleo at detecting tumours [42].

3.5 Radiopharmaceuticals Used for Diagnosis in Kidney Diseases

The evaluation of renal function has a significant deal of potential for nuclear medicine. Quick, dependable, and accurate answers to physicians' questions are now possible because of the numerous straightforward techniques that have been suggested as well as recent advancements in renal radiopharmaceuticals and computer software. Functional metrics like the Effective Renal Plasma Flow (ERPF) and Glomerular Filtration Rate (GFR) can be measured using radiopharmaceuticals. Of the several agents approved by GFR, Technitium-99 m-DTPA, as well as Chromium-51-EDTA, is primarily utilized in clinics. Due to its radiochemical and biological characteristics, the first agent is quite reliable, but only the latter can be utilized when imaging is needed. There are two substances that the renal tubules actively secrete that can be used to estimate ERPF [43, 44].

3.6 Radiopharmaceuticals for Diagnosis of Haematopoietic Disorders

Isotopes of iron are the most common tracer which are used in haematopoiesis studies. Other most common tracers are ^{111}In (linked to transferrin) and ^{99m}Tc-colloids, which are also used in haematopoiesis studies. ^{52}Fe is found to provide better results as tracer in recognition of erythropoiesis. ^{99m}Tc-labelled leukocytes or ^{99m}Tc-labelled antibodies may be used in study of circulating and progenitor white cells. Iron-deficiency anaemias may be caused because of several reasons which may be malnutrition or malabsorption, abnormal or extreme blood loss, so exact cause can be found out with radioactive ^{59}Fe, ^{55}Fe as tracer and stable ^{54}Fe, ^{57}Fe iron isotopes. The results may be interpreted to give a guidance for dietary supplementation [45]. Red cell survival, blood volumes, and other factors of iron metabolism have been investigated with ^{51}Cr, ^{125}I, and ^{59}Fe radioisotopes and the data obtained has been reported to provide clarification of the nature of the anaemia and also demonstrated the haemolytic and erythropoietic role of the spleen in others with splenomegaly. It was reported that results helped in further evaluation of various blood disorders [46]. With the development of the cyanocobalamin (^{57}Co, ^{58}Co) tracer, tests for vitamin B-12 deficiency in cases of pernicious anaemia or malabsorption have improved sensitivity and so it has upgraded scope [45].

3.7 Radiopharmaceuticals for Diagnosis of Lung Disorders

Lung scintigraphy is a popular non-invasive technique for measuring the air and blood supply to the lungs, and it helps to rule out pulmonary embolism (blood clots in lungs). In this technique radionuclide, ^{99m}Tc is mainly used. Lung scintigraphy also called VQ (Ventilation-perfusion) lung scan can be divided into two parts which include firstly the use of intravenous injection to inject radionuclide ^{99m}Tc along with protein aggregates for imaging which helps in further evaluation of blood flow (perfusion), and secondly, small ^{99m}Tc-labelled aerosol particles are breathed in to measure the airflow in the lungs (Ventilation) and then compared with blood flow (perfusion), [47]. The standard radioactive labels used in VQ lung scan are Xenon-133 and ^{99m}Tc-diethylene-triamine-pentaacetate (DTPA) although aerosolized form of Technetium 99 m hydroxy methylene diphosphonate (^{99m}Tc-HDP) is proven to be used as an alternative radiopharmaceutical substitute for Xenon-133 and ^{99m}Tc-diethylene-triamine-pentaacetate (DTPA). Also, ^{99m}Tc-HDP usage is much cost-effective compared to the use of ^{99m}Tc-DTPA, though the perfusion images obtained for different orientations were found to be same for both ^{99m}Tc-HDP and ^{99m}Tc-DTPA [48].

4 Therapeutic Applications of Radiopharmaceuticals

Radiopharmaceuticals that involve alpha and beta decays are used in therapeutic applications. The therapeutic radiopharmaceutical dose is administered to the patient and kept in the targeted tissue or organ and in this way, therapeutic radiopharmaceuticals destroy the affected tissues [49] Therapeutic radiopharmaceuticals are radiolabelled molecules that are designed to deliver the dose to specific diseased location. Certain radionuclides involve alpha and beta decays which undergo emission of radiations that can destroy the diseased tissues [24]. With this application, therapeutic radiopharmaceuticals are used in therapy of many cancers and tumours and other diseases. Therapeutic radiopharmaceuticals provide either palliative or curative treatment [24]. Therapeutic radiopharmaceuticals are designed in such a way that bind selectively to specific biochemical protein receptor at the diseased site. They are designed to specifically target and destroy the cancerous cells without affecting normal healthy tissues and cells [5]. Some of the radionuclides with their therapeutic applications are summarized in the following Table 3.

4.1 Delivery of Radionuclides by Nanocarriers

Radionuclides play a vital role in nuclear imaging of cells and internal radiotherapy, so it is necessary for the targeted delivery of radionuclide on the site of interest. Though targeted radionuclide therapy has been used for a long time with the help of peptides and monoclonal antibodies, it has showed low therapeutic index and toxic

Table 3 Therapeutic applications of radiopharmaceuticals

Radionuclide	Therapeutic applications	Reference
Iodine-131	Used for treatment of Graves' disease (hyperthyroidism and thyroid cancer)	[50]
Holmium-166	Used for treatment of liver tumour	[13]
Yttrium-90	Used for treatment of hepatocellular carcinoma, non-Hodgkin's lymphoma	[51, 52]
Phosphorus-32	Used for treatment of polycythemia vera	[22]
Lutetium-177	Used for treatment of neuroendocrine therapy	[53]
Radium-223	Used for treatment of bone metastases	[54]
Rhenium-186	Used for pain relief in bone metastases	[55]
Strontium-89	Used for pain relief in prostate cancer	[56]
Erbium-169	Used in relief of arthritis pain	[20]
Samarium-153, Phosphorus-32	Used for pain relief in bone metastasis	[57]

side effects. It becomes extremely important to deliver the radionuclides at the target location at ideal concentration with the lowest possible toxicity and highest possible therapeutic index. Here comes the role of nanocarriers especially in cancer diagnostics and therapeutics which ensures high drug bioavailability, good biocompatibility, and targeted delivery of the radiopharmaceutical to the tumour cells. Due to very less size of nanocarriers ranging from 1 to 100 nm, it has a number of benefits, including improved permeability and retention of radionuclides and medications by passive targeting to the leaky tumour tissues [58]. Radionuclides can be loaded to nanocarriers by broadly two methods: (1) By using bifunctional chelating agent which chelates radionuclide and gets chemically conjugated to the nanocarrier, or (2) by using physical encapsulation of the radionuclide inside the nucleus or cavity of the nanocarrier [26]. There are several number and classification of nanocarriers that act as radiopharmaceutical delivery systems such as iron oxide nanoparticles, polymeric nanoparticles, dendrimers, carbon nanotubes, and quantum dots [58]. There are essentially four distinct ways to radiolabel nanomaterials with radionuclides: adsorption, trapping, chelation (which is frequently used for radionuclides with a metallic character), and covalent bond formation (which is frequently used for radionuclides without a metallic character) [59].

Polymeric Nanoparticles

Polymers are class of natural or synthetic macromolecules which forms by the covalent union of monomers to form linear or branched chain. Choosing of right type of monomer is very crucial for the synthesis of polymer because each of them will show different physical and chemical properties. As polymers have great synthetic versatility, they provide a lot of options for the researchers to customize them according to the need. Hence the usage of polymeric nanoparticles for drug delivery systems is very relevant. The radionuclide either may be anchored to the surface of the polymeric nanoparticle via chelating ligands which are decorated on

the surface of the polymeric nanoparticle or inside its core via encapsulation process. Among several number of clinically and pre-clinically tested nanoparticles, polymeric nanoparticles carrying radionuclides possess great advantages. Because they provide high payloads of radionuclides, help to form proper image, and show non-invasive therapy. Lots of radionuclides have been used for the synthesis of radioactive polymeric nanoparticles. It has been reported that ^{111}In-labelled polymeric nanoparticles possess wide use for understanding the biodistribution of nanoparticle [60]. There are several types of polymeric nanoparticles for carrying radionuclides that comprise of liposomes, micelles, nano emulsions, etc. For ocular therapy implementation of intravitreal implants is one of the options for sustained drug delivery in the posterior zone of ocular globe, but it requires painful methods like numerous injection and surgeries. So, to overcome these hurdles biodegradable polymers are used for targeted delivery of drug which provides effective dosage at the site of action and shows high solubility along with high bioavailability and sustained release of drug [61]. Radionuclides like ^{99m}Tc, ^{111}In, ^{186}Re, and ^{188}Re are used for tumour, blood pool, and lymph node imaging where micelle (type of polymeric nanoparticle) is used as the carrier. Micelle nanocarrier is very advantageous because of its ease of preparation and having hydrophilic polymer shell that reduces RES (reticuloendothelial system) uptake [26].

Inorganic Nanoparticles

Inorganic nanoparticles consist of metals and metal oxides having high-density electronic states that can be modified by changing the size and form of the inorganic nanoparticles. Biodegradable magnetic iron oxide microparticles made of poly (lactic acid), magnetite (Fe_3O_4), and ^{90}Y were one of the first agents used for targeted radiotherapy. Along with that ^{186}Re and ^{188}Re were used by encapsulating with magnetic microspheres for tumour radiotherapy [26]. Platinum-derived compounds like carboplatin and cisplatin have high chemotherapeutic activity. Though use of these compounds increases the chances of DNA damage because Pt derived compounds initially disrupts DNA repairing mechanism and along with that applying of radiation leads to further damage of DNA [62]. A bidentate metal chelating ligand known as 8-hydroxyquinoline has vast medicinal applications like anticancer properties and antimicrobial activities. It is used in the FDA-approved neutral-charge complex [^{111}In][In(oxine)3] that radiolabels leukocytes to image infection and inflammation. [^{111}In]In^{3+} is a common SPECT isotope having a half-life of 2.8 days which decays to release two low-energy gamma rays by electron conversion and also emits Auger–Meitner electrons of interest in theranostics [63]. Also carbon-based nanomaterials (CNMs) are well known for their excellent physicochemical properties. They function as a suitable carrier to deliver optimum amounts of radionuclides and also targeted by anchoring of molecular recognition ligands. There are variety of CNMs including nanodiamonds, fullerenes, and graphene which are explored for the improvement of targeted delivery of radionuclides [59].

Dendrimers

Nanocarriers which contain homogenous and monodisperse structure having radially symmetrical inner core and outer shell structure are termed as dendrimers. Due to their many biological traits, incuding their capacity for self-assembly, chemicals stability, polyvalency, low cytoxicity, and solubility. Its centre core atom or collection of atoms serves as the first node in its chemical structure. And from that core branches of other atoms called dendron formation occurs through a variety of chemical reactions [64]. The advantages of using dendrimers include incorporation of multivalent radionuclides and low PDI value which improves biodistribution. Various radionuclides are labelled along with dendrimers due to their unique structural features. Bifunctional chelators chemically conjugated on the surface of the dendrimers are used to label with radionuclides via chelation property. 1,4,7,10-Tetraazacyclododecane-1,4,7,10-tetraacetic acid (DOTA) is one of the popular chelating substances that is covalently bonded to the dendrimer's surface to load ^{67}Gd (III), a non-radioactive metal, for MR imaging. Along with that some radionuclides like ^{125}I, ^{76}Br, and ^{131}I can be labelled via the chloramine T method with the addition of tyrosine into dendrimers [65]. Criscione et al. showed that conjugation of triiodinated moieties and ^{99m}Tc on the surface of G4 PAMAM dendrimers can be made for the application of SPECT/CT [66]. Still some radionuclides like ^{18}F cannot be carried through dendrimers because of its complicacy, low radiochemical yield, and harsh chemical reaction conditions [26, 67, 68]. Hence new strategies should be employed for radiolabelling of ^{18}F also to dendrimers. Along with that positive charge of dendrimers may cause toxicity, as surface charge of cell membrane is negative which will be eventually ruptured by dendrimers due to formation of nanopores on the cell surface. So due to these challenges for usage of dendrimer, scientists started modifying several chemical modifications on the outer periphery of the nano molecule to decrease the cytotoxicity side effect. It is reported that dendrimers anchored with PEGylated groups, acetyl groups, and carbohydrates decrease the cell cytotoxicity effect into much lower amount [69].

5 Role of Electrochemical Sensors for Detection of Radiopharmaceuticals

An electrochemical sensor is a device that can detect a particular chemical/biological analyte quantitively via three different techniques which includes potentiometry, voltammetry, and amperometry. It has several advantages over other sensors because of its high selectivity, specificity, short response time, cost-effective, point of care application, and most importantly simple measurement procedure. Since most of the radiopharmaceuticals reported contain electroactive redox centres, electrochemical sensors play a major role for continuous, direct in vivo monitoring of radiopharmaceuticals inside the body of test animals. Sensors are developed for radiopharmaceuticals for the determination of chemical form of the species that targets a particular region of organ [70]. Theresa Lee et al. developed a chemical

electrochemical sensor for in vivo measurement of radiopharmaceutical analogue for the first time. They have developed a microelectrode carbon-fibre based electrochemical sensor which has outer coating of polymeric Nafion gel that helps in monitoring of a specific chemical species $[Re(DMPE)_3]^+$ where DMPE is 1,2-bis (dimethylphosphino)ethane, a non-radioactive analogue of the prototype cationic lipophilic ^{99m}Tc imaging agent $[^{99m}Tc(DMPE)_3]^+$ in the heart of a live rat. $[Re(DMPE)_3]^+$ is detected by the following oxidation when the potential of the sensor is scanned from −200 to 400 mV:

$[Re(DMPE)_3]^+ \blacktriangledown [Re(DMPE)_3]^{2+} + 1e^-$ [71].

On comparison of voltametric oxidation peak currents of the Re complex at Nafion modified electrode and bare electrode, the former one showed an increment of current up to 100 times than the latter one. Other than electrochemical sensor, fibre optic absorbance sensors are also reported. As some radiopharmaceuticals do not show fluorescence property eventually for them, an absorbance sensor is used to monitor the concentration and oxidation states of radiopharmaceuticals. An example of heart imaging agent analogue is trans-$[Re(p\text{-}SC_6H_4CH_3)_2(DMPE)_2]PF_6$ which is detected by the usage of fibre optical sensor [70].

6 Radiotherapy

Radiotherapy is a treatment of cancer such as breast cancer, liver cancer, thyroid cancer, lung cancer, and ovarian cancer, in which high dosages of radiation are used to kill cancerous cells. Radiotherapy kills cancerous cells or slows down their growth by damaging the DNA of those cells, so that they stop dividing or die and then, these died cells are broken down and body will remove them [72–74]. Radiotherapy does not kill cancerous cells immediately, but it takes time of some days or weeks of treatment [72]. Currently, intensity modulated radiotherapy (IMRT) along with image-guided radiotherapy (IGRT) are the two radiotherapy techniques most frequently used to treat cancer. The major benefit of IMRT is the reduction of late side effect. IGRT provides information about the size, shape, and location of malignant cells as well as the cells and tissues that surround them [74].

6.1 Treatment of Thyroid Diseases

Iodine-131(^{131}I) is used for the treatment of thyroid diseases (for both benign and malignant). It mainly used for the treatment of hyperthyroidism or Graves' disease (cause of hyperthyroidism) and thyroid cancer. Radioactive Iodine (RAI) therapy is used for the treatment of hyperthyroidism and thyroid cancer [6, 49]. In treatment of hyperthyroidism, ^{131}I radionuclide destroys the follicle cells by the emission of beta particles and thus controls or stops the growth as well as activities of the thyroid cells. In this way, overactive thyroid returns to its normal function [49]. In thyroid

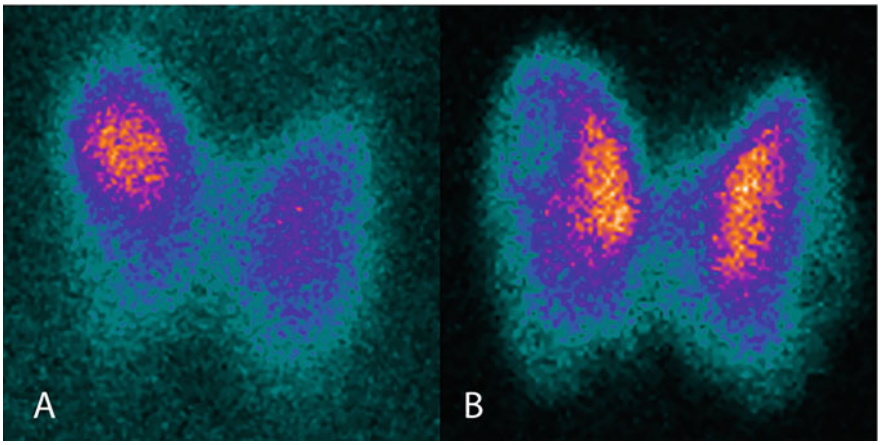

Fig. 5 Thyroid scintigraphy before and after RAI therapy. (**a**) ^{123}I scintigraphy before RAI, showing focally increased uptake in the toxic adenoma. (**b**) ^{99m}Tc scintigraphy after RAI, showing diffusely increased uptake, except in the area of the previously treated toxic adenoma. Reprinted with permission from ref. [75], published by frontiers under the guidelines of the Creative Commons Attribution License (CC BY). All rights reserved, Copyright 2022

cancer, radiolabelled Iodine-131 selectively targets the tissue of thyroid gland with the emission of alpha particle that destroys the tumour tissues [23]. Radiolabelled ^{131}I-131 can be given to the patient either orally or by injection [23].

Thyroid scintigraphy images prior to and following RAI treatment are shown in Fig. 5.

6.2 Treatment of Metastatic Bone Pain

Various cancers like prostate, lung, breast, thyroid, and kidney, most often prostate and breast cancer are associated with bone pain [49]. Bone metastasis can lead to pain, hypercalcemia, and fractures [23, 49]. Treatment of bone metastasis includes radiotherapy, chemotherapy, using drugs and surgery [23, 49]. The metastatic bone pain can be treated non-invasively by radiotherapy. The radiotherapy is highly effective for bone pain relief and also results in reduction of tumour cells [23, 49]. Samarium-153, Phosphorus-32, Radium-223, rhenium-186, and Strontium-89 are the most widely used radionuclides in radiotherapy for palliative treatment of bone metastasis [23, 49, 76]. Samarium-153, Phosphorus-32, and Strontium-89 are used in treatment of bone metastasis due to the emission of beta-particle. After the administration intravenously, Strontium-89 chloride behaves as calcium and is concentrated in bone [23, 24]. The part of Strontium-89 that is not concentrated in the bone, excreted through kidney and gastrointestinal system (National Cancer Institute).

6.3 Treatment of Non-Hodgkin's Lymphoma

Radioimmunotherapy is used in the treatment of non-Hodgkin's lymphoma which involves the use of radiolabelled antibody with radionuclide [24, 51, 77, 78]. Schematic of radioimmunotherapy is shown in Fig. 6.

Radiopharmaceuticals Iodine-131 radiolabelled tositumomab (Bexxar) and B-cell non-Hodgkin lymphoma is treated with Yttrium-90 ibritumomab tiuxetan (Zevalin) [24, 49, 51, 77, 78]. I-131 tositumomab radiolabelled by the oxidation of radioactive iodine with iodogen and its solution contained additives that limit radiolysis [29]. Tositumomab is a monoclonal antibody that has high affinity for the CD20 antigen on the surface of B-lymphocytes which inhibit the tumour growth [49, 51].

6.4 Treatment of Hepatocellular Carcinoma

Hepatocellular carcinoma is the most common type of primary liver tumour [49]. Radioembolization is used in the treatment of hepatocellular carcinoma which involves the injection of microspheres particles that are loaded with radionuclide with the help of transarterial method [49, 52, 79, 80]. This treatment is based on the principle that liver tumour cells derive blood supply from hepatic artery while the cells of healthy liver from the portal vein [49, 79]. Yttrium-90 microspheres are specifically directed to tumour cells by arterial route, so that these tumour cells are exposed to high radiation dose with a very little effect of radiation on healthy liver [49, 81]. Currently there are two forms of microspheres available for ^{90}Y which includes TheraSphere (glass microspheres) and SIR-Spheres (resin microspheres) [49, 79, 80].

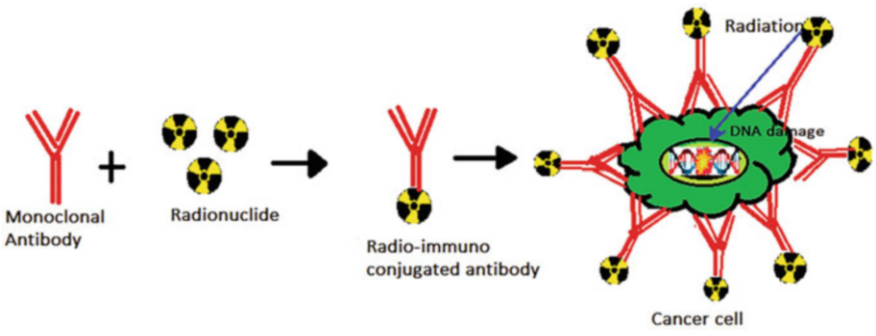

Fig. 6 Radioimmunotherapy involves the use of radio-immuno conjugate monoclonal antibody to target cancerous cell

6.5 Treatment of Neuroendocrine Tumours

Neuroendocrine tumours can develop in both gastrointestinal system and lungs but most commonly it occurs in gastrointenstinal system [49, 82]. Generally, neuroendocrine tumours can be developing in intestine, pancreas, stomach, and lungs [49]. Currently, ^{177}Lu-dotatate and both ^{131}I–metaiodobenzylguanidine (MIBG) and ^{123}I-MIBG are used in the treatment of neuroendocrine tumours [6, 49, 82]. ^{177}Lu-dotatate is used in the treatment of gastroenteropancreatic neuroendocrine tumours. With the beta-rays emission, ^{177}Lu-dotatate treats the tumour. The ^{177}Lu-dotatate treatment is applied for a series of 4 or 5, for about 2 months period [6, 49, 82].

With some neuroendocrine tumours, such as pheochromocytoma, neuroblastoma, and carcinoid tumour, MIBG selectively targets the neuroendocrine cells because of its structural similarity to the neurotransmitter norepinephrine. ^{131}I or ^{123}I-MIBG is more effective in the treatment of pheochromocytoma and neuroblastoma but less effective in paraganglioma (when pheochromocytoma found outside of adrenal glands is called paraganglioma) and carcinoid tumour. By the beta-rays emission, ^{131}I-MIBG targets the neuroendocrine tumours [49, 82, 83].

7 Conclusion

Radiopharmaceuticals may be efficiently used for the diagnosis as well as therapeutic purpose to diagnose several diseases. The best part of using radioisotopes for imaging is that they are non-invasive, specific and body is exposed to considerably low dose of radiation. The future target is used to find radiopharmaceutical with improved sensitivity to detect disease at very early stage. Out of all the major challenges, one encounter regarding expanding nuclear medicine for diagnostics is to handle these radioisotopes safely by following strict radiation safety protocols to safeguard from any hazards. And most of these isotopes are short lived so another challenge lies in transporting them quickly from the production site to the health centres in rural region where connectivity is not as good and most of these procedures are costly with respect to use for patients in developing countries as their production, quality control, transportation, and storage of these isotopes require special attention, so these diagnostic tests are comparatively less popular. In both diagnosis and treatment, nanocarriers function as a medication delivery mechanism by employing radiopharmaceuticals, and they are essential for the precise transport of radiopharmaceuticals to the site of action. Though there are several challenges for each type of nanocarriers like limited control over size, number and site of radiolabel chelation which may hamper the reproducibility of results and controlling of cytotoxicity and polydispersity of nanocarriers are a matter of concern.

Acknowledgments Authors gratefully acknowledge the Start-Up Research Grant (SRG) funded by Science & Engineering Research Board (SERB) (SRG/2020/000712), Department of Science and Technology (DST) (Government of India, Ministry of Science and Technology, (Technology Development and Transfer, TDP/BDTD/12/2021/General), Indo-German Science & Technology Centre (IGSTC) (IGSTC/Call 2019/NOMIS/22/2020-21/164), and Institute Scheme for Innovative Research and Development (ISIRD) (IIT/SRIC/ISIRD/2019–2020/17), Indian Institute of Technology Kharagpur (IIT Kharagpur), India for the financial support.

References

1. IAEA: Diagnostic Radiopharmaceuticals Diagnostic radiopharmaceuticals, radioactive drugs for diagnosis | IAEA. https://www.iaea.org/topics/diagnostic-radiopharmaceuticals. (Accessed 30 Jul 2022).
2. Payolla, F. B., Massabni, A. C., & Orvig, C. (2019). Radiopharmaceuticals for diagnosis in nuclear medicine: A short review. *Eclética Química Journal, 44*, 11–19. https://doi.org/10.26850/1678-4618EQJ.V44.3.2019.P11-19
3. IBM Micromedex Radiopharmaceutical (Oral Route) Description and Brand Names - Mayo Clinic. https://www.mayoclinic.org/drugs-supplements/radiopharmaceutical-oral-route/description/drg-20070231
4. Moffitt Radiopharmaceuticals | Moffitt | Moffitt. https://moffitt.org/treatments/radiation-therapy/radiopharmaceuticals/
5. Centre for Probe Development and Commercialization Centre for Probe Development and Commercialization.. https://www.imagingprobes.ca/
6. World Nuclear Association Radioisotopes in Medicine | Nuclear Medicine - World Nuclear Association. https://world-nuclear.org/information-library/non-power-nuclear-applications/radioisotopes-research/radioisotopes-in-medicine.aspx
7. Moravek Inc. Characteristics of Radiopharmaceuticals. https://www.moravek.com/characteristics-of-radiopharmaceuticals/
8. Alauddin, M. M. (2012). Positron emission tomography (PET) imaging with 18F-based radiotracers. *American Journal of Nuclear Medicine and Molecular Imaging, 2*, 55.
9. The Supply of Medical Isotopes. OECD. (2019).
10. McNeil, B. L., Robertson, A. K. H., Fu, W., Yang, H., Hoehr, C., Ramogida, C. F., et al. (2021). Production, purification, and radiolabeling of the 203Pb/212Pb theranostic pair. *EJNMMI Radiopharmacy and Chemistry, 6*, 6. https://doi.org/10.1186/S41181-021-00121-4
11. Hao, G., Mastren, T., Silvers, W., Hassan, G., Öz, O. K., & Sun, X. (2021). Copper-67 radioimmunotheranostics for simultaneous immunotherapy and immuno-SPECT. *Scientific Reports, 11*, 1. https://doi.org/10.1038/s41598-021-82812-1
12. Sciacca, F. (2020). Samarium-153. Radiopaedia.org. https://doi.org/10.53347/RID-74414.
13. Smits, M. L. J., Nijsen, J. F. W., van den Bosch, M. A. A. J., Lam, M. G., Vente, M. A., Huijbregts, J. E., et al. (2010). Holmium-166 radioembolization for the treatment of patients with liver metastases: Design of the phase I HEPAR trial. *Journal of Experimental & Clinical Cancer Research, 29*. https://doi.org/10.1186/1756-9966-29-70
14. Geraci, M. J., Brown, N., & Murray, D. (2012). Thallium-201 for cardiac stress tests: Residual radioactivity worries patients and security. *The Journal of Emergency Medicine, 43*, e439. https://doi.org/10.1016/J.JEMERMED.2011.05.093
15. Poudyal, B., Shrestha, P., & Chowdhury, Y. S. (2022). *Thallium-201*. StatPearls.
16. Bailey, D. L., Sabanathan, D., Aslani, A., Campbell, D. H., Walsh, B. J., & Lengkeek, N. A. (2021). RetroSPECT: Gallium-67 as a long-lived imaging agent for Theranostics. *Asia Oceania Journal of Nuclear Medicine and Biology, 9*, 1. https://doi.org/10.22038/AOJNMB.2020.51714.1355
17. Murphy, A., & Jones, J. (2010). Xenon-133. Radiopaedia.org. https://doi.org/10.53347/RID-12395.

18. Pineda, J. D., Lee, T., Ain, K., Reynolds, J. C., & Robbins, J. (1995). Iodine-131 therapy for thyroid cancer patients with elevated thyroglobulin and negative diagnostic scan. *The Journal of Clinical Endocrinology and Metabolism, 80*, 1488–1492. https://doi.org/10.1210/JCEM.80.5.7744991
19. PubChem Chromium-51 | Cr - PubChem. https://pubchem.ncbi.nlm.nih.gov/compound/Chromium-51
20. Zhang, W., Zhao, W., Jia, Z., & Deng, H. (2013). Strontium-89 therapy for the treatment of huge osseous metastases in prostate carcinoma: A case report. *Experimental and Therapeutic Medicine, 5*, 608–610. https://doi.org/10.3892/ETM.2012.807/HTML
21. PubChem Phosphorus-32 | H3P - PubChem. https://pubchem.ncbi.nlm.nih.gov/compound/Phosphorus-32
22. Memon, K., Lewandowski, R. J., Riaz, A., & Salem, R. (2013). Yttrium 90 microspheres for the treatment of hepatocellular carcinoma. *Recent Results in Cancer Research, 190*, 207–224. https://doi.org/10.1007/978-3-642-16037-0_14
23. Alsharef, S., Alanazi, M., Alharthi, F., Qandil, D., & Qushawy, M. (2020). Review about radiopharmaceuticals: preparation, radioactivity, and applications. *International Journal of Applied Pharmaceutics, 12*, 8–15. https://doi.org/10.22159/IJAP.2020V12I3.37150
24. Mohammad, A. K., Masoodi, M. H., & Farooq, S. (2015). Medical uses of Radiopharmaceuticals. *PharmaTutor., 3*(8), 24–29.
25. Mayfield Brain & Spine. (2019). SPECT scan | Single Photon Emission Computed Tomography. https://mayfieldclinic.com/pe-spect.htm. (Accessed 27 July 2022).
26. Mitra, A., Nan, A., Line, B., & Ghandehari, H. (2006). Nanocarriers for nuclear imaging and radiotherapy of cancer. *Current Pharmaceutical Design, 12*, 4729–4749. https://doi.org/10.2174/138161206779026317
27. Open Medscience Radiopharmaceuticals used in medical imaging | Open Medscience.
28. Falk, R. H., Lee, V. W., Rubinow, A., Hood, W. B., Jr., & Cohen, A. S. (1983). Sensitivity of technetium-99m-pyrophosphate scintigraphy in diagnosing cardiac amyloidosis. *The American Journal of Cardiology, 51*, 826–830. https://doi.org/10.1016/S0002-9149(83)80140-4
29. The Supply of Medical Isotopes. (2019). https://doi.org/10.1787/9b326195-en.
30. Kole, A. C., Nieweg, O. E., Hoekstra, H. J., van Horn, J. R., Koops, H. S., & Vaalburg, W. (1998). Fluorine-18-fluorodeoxyglucose assessment of glucose metabolism in bone tumors. *Journal of Nuclear Medicine, 39*, 1027.
31. Dittrich, R. P., de Jesus, O. (2022) Gallium Scan. Definitions. https://doi.org/10.32388/7947iw.
32. PubChem Potassium-40;potassium-42 | K2 - PubChem.
33. Blau, M., & Bender, M. A. (1962). Se75-selenomethionine for visualization of the pancreas by isotope scanning. *Radiology., 78*, 974. https://doi.org/10.1148/78.6.974
34. Adams, C., Banks, K. P. (2021) Bone Scan. The Meniscus (pp. 91–95). https://doi.org/10.1007/978-3-642-02450-4_12.
35. Roth, G. A., Forouzanfar, M. H., Moran, A. E., Barber, R., Nguyen, G., Feigin, V. L., et al. (2015). Demographic and epidemiologic drivers of global cardiovascular mortality. *The New England Journal of Medicine, 372*, 1333–1341. https://doi.org/10.1056/NEJMOA1406656
36. Manabe, O., Kikuchi, T., Scholte, A. J. H. A., El Mahdiui, M., Nishii, R., Zhang, M.-R., et al. (2018). Radiopharmaceutical tracers for cardiac imaging. *Journal of Nuclear Cardiology, 25*, 1204. https://doi.org/10.1007/S12350-017-1131-5
37. Schindler, T. H., Marashdeh, W., & Solnes, L. (2016). Clinical application of myocardial blood flow quantification in CAD patients. *Annals of Nuclear Cardiology, 2*, 84–93. https://doi.org/10.17996/ANC.02.01.84
38. Chervu, L. R., Nunn, A. D., & Loberg, M. D. (1982). Radiopharmaceuticals for hepatobiliary imaging. *Seminars in Nuclear Medicine, 12*, 5–17. https://doi.org/10.1016/S0001-2998(82)80025-1
39. Chervu, L. R., Joseph, J. A., Chun, S. B., Rolleston, R. E., Synnes, E. I., Thompson, L. M., et al. (1988). Evaluation of six new 99mTc-IDA agents for hepatobiliary imaging. *European Journal of Nuclear Medicine, 14*, 441–445. https://doi.org/10.1007/BF00252386

40. Rosenhall, L., Shaffer, E. A., Lisbona, R., & Pare, P. (1978). Diagnosis of hepatobiliary disease by 99mTc-HIDA cholescintigraphy. *Radiology, 126*, 467–474. https://doi.org/10.1148/126.2.467
41. Agha, N. H., Al-Hilli, A. M., Dahir, N. D., Al-Hissoni, M. S., Jasim, M. N., Miran, K. M., et al. (1986). Long-term clinical investigation of the hepatobiliary agents: 99mTc-HIDA and 99m-Tc-p-butyl-IDA. *Nuklearmedizin, 25*, 181–187. https://doi.org/10.1055/S-0038-1624339/ID/JR1624339-16
42. Wang, H., Naghavi, M., Allen, C., Barber, R. M., Bhutta, Z. A., Carter, A., et al. (2016). Global, regional, and national life expectancy, all-cause mortality, and cause-specific mortality for 249 causes of death, 1980–2015: A systematic analysis for the global burden of disease study 2015. *The Lancet, 388*, 1459–1544. https://doi.org/10.1016/S0140-6736(16)31012-1/ATTACHMENT/092770C9-1B7B-4CF3-9349-655862684147/MMC3.MP4
43. Hamoudeh, M., Kamleh, M. A., Diab, R., & Fessi, H. (2008). Radionuclides delivery systems for nuclear imaging and radiotherapy of cancer. *Advanced Drug Delivery Reviews, 60*, 1329–1346. https://doi.org/10.1016/J.ADDR.2008.04.013
44. Mäcke, H. [Radiopharmaceuticals in kidney diagnosis] - PubMed. https://pubmed.ncbi.nlm.nih.gov/2024106/. Accessed 30 Jul 2022.
45. Shreeve, W. W. (2007). Use of isotopes in the diagnosis of hematopoietic disorders. *Experimental Hematology, 35*, 173–179. https://doi.org/10.1016/J.EXPHEM.2007.01.027
46. Knox-Macaulay, H. H. M. (1989). Radioisotope investigations of haematological disorders (excluding sickle cell disease) in Sierra Leone. *African Journal of Medicine and Medical Sciences, 18*, 75–81.
47. Dr Ian Jong VQ Scan - InsideRadiology. https://www.insideradiology.com.au/vq-scan/. (Accessed 27 Jul 2022).
48. Prasad, K., & Young, C. (2016). Technetium 99m hydroxymethylene diphosphonate as an alternative ventilation agent in pulmonary ventilation perfusion scans for use during periods of standard ventilation agent shortage. *Journal of Nuclear Medicine*. *57*, 1275LP–1275.
49. Nitipir, C., Niculae, D., Orlov, C., Barbu, M. A., Popescu, B., Popa, A. M., et al. (2017). Update on radionuclide therapy in oncology. *Oncology Letters, 14*, 7011–7015. https://doi.org/10.3892/OL.2017.7141/HTML
50. Mumtaz, M., Lin, L. S., Hui, K. C., & Khir, A. S. M. (2009). Radioiodine I-131 for the therapy of graves' disease. *The Malaysian Journal of Medical Sciences, 16*, 25.
51. Sartor, O. (2004). Overview of samarium Sm 153 lexidronam in the treatment of painful metastatic bone disease. *Reviews in Urology, 6*, S3.
52. Lee, J. H., Lee, T., & Choi, J. W. (2016). Nano-biosensor for monitoring the neural differentiation of stem cells. *Nanomaterials, 6*. https://doi.org/10.3390/NANO6120224
53. Parmentier, C. (2003). Use and risks of phosphorus-32 in the treatment of polycythaemia vera. *European Journal of Nuclear Medicine and Molecular Imaging, 30*, 1413–1417. https://doi.org/10.1007/S00259-003-1270-6/TABLES/2
54. Maqsood, M. H., Din, A. T. U., & Khan, A. H. (2019). Neuroendocrine tumor therapy with Lutetium-177: A literature review. *Cureus, 11*. https://doi.org/10.7759/CUREUS.3986
55. Shirley, M., & McCormack, P. L. (2014). Radium-223 dichloride: A review of its use in patients with castration-resistant prostate cancer with symptomatic bone metastases. *Drugs, 74*(5), 579–586. https://doi.org/10.1007/S40265-014-0198-4
56. Graham, M. C., Scher, H. I., Liu, G. B., Yeh, S. D., Curley, T., Daghighian, F. et al. Rhenium-186-labeled hydroxyethylidene diphosphonate dosimetry and dosing guidelines for the palliation of skeletal metastases from androgen-independent prostate cancer - PubMed. https://pubmed.ncbi.nlm.nih.gov/10389913/. (Accessed 30 Jul 2022).
57. Ott H, I B, Gh f (1977) la Synoviorthese des Articulations Digitales de la main a l'erbium 169. Parametres Influencant les Resultats Cliniques a Moyen Terme. La Synoviorthese des Articulations Digitales de la Main a l'erbium 169 Parametres Influencant les Resultats Cliniques a Moyen Terme.

58. Ting, G., Chang, C.-H., Wang, H.-E., & Lee, T.-W. (2010). Nanotargeted radionuclides for cancer nuclear imaging and internal radiotherapy. *Journal of Biomedicine and Biotechnology, 2010*, 17. https://doi.org/10.1155/2010/953537
59. Jaymand, M., Davatgaran Taghipour, Y., Rezaei, A., Derakhshankhah, H., Abazari, M. F., Samadian, H., et al. (2021). Radiolabeled carbon-based nanostructures: New radiopharmaceuticals for cancer therapy? *Coordination Chemistry Reviews, 440*, 213974. https://doi.org/10.1016/J.CCR.2021.213974
60. Wu, S., Helal-Neto, E., dos Matos, A. P. S., Jafari, A., Kozempel, J., Silva, Y. J. A., et al. (2020). Radioactive polymeric nanoparticles for biomedical application. *Drug Delivery, 27*, 1544–1561. https://doi.org/10.1080/10717544.2020.1837296/FORMAT/EPUB
61. Begines, B., Ortiz, T., Pérez-Aranda, M., Martínez, G., Merinero, M., Argüelles-Arias, F., et al. (2020). Polymeric nanoparticles for drug delivery: Recent developments and future prospects. *Nanomaterials, 10*, 1–41. https://doi.org/10.3390/NANO10071403
62. Puntes, V. (2016). Design and pharmacokinetical aspects for the use of inorganic nanoparticles in radiomedicine. *British Journal of Radiology, 89*, 20150210. https://doi.org/10.1259/BJR.20150210/FORMAT/EPUB
63. Southcott, L., & Orvig, C. (2021). Inorganic radiopharmaceutical chemistry of oxine. *Dalton Transactions, 50*, 16451–16458. https://doi.org/10.1039/D1DT02685B
64. Abbasi, E., Fekri Aval, S., Akbarzadeh, A., Milani, M., Nasrabadi, H. T., Joo, S. W., et al. (2014). Dendrimers: Synthesis, applications, and properties. *Nanoscale Research Letters., 9*, 247.
65. Zhao, L., Zhu, M., Li, Y., Xing, Y., & Zhao, J. (2017). Radiolabeled dendrimers for nuclear medicine applications. *Molecules.* https://doi.org/10.3390/molecules22091350
66. Criscione, J. M., Dobrucki, L. W., Zhuang, Z. W., Papademetris, X., Simons, M., Sinusas, A. J., et al. (2011). Development and application of a multimodal contrast agent for SPECT/CT hybrid imaging. *Bioconjugate Chemistry, 22*, 1784–1792. https://doi.org/10.1021/BC200162R
67. Liu, Y., & Welch, M. J. (2012). Nanoparticles labeled with positron emitting nuclides: Advantages. *Methods, and Applications., 23*, 671. https://doi.org/10.1021/bc200264c
68. Devaraj, N. K., Keliher, E. J., Thurber, G. M., Nahrendorf, M., & Weissleder, R. 18F labeled nanoparticles for in ViWo PET-CT imaging. *Bioconjugate Chemistry.* https://doi.org/10.1021/bc8004649
69. Janaszewska, A., Lazniewska, J., Trzepí Nski, P., Marcinkowska, M., & Klajnert-Maculewicz, B. (2019). Cytotoxicity of dendrimers. *Biomolecules, 9*. https://doi.org/10.3390/biom9080330
70. Heineman, W. R., Swaile, B. H., Blubaugh, E. A., Landis, D. A., Seliskar, C. J., & Deutsch, E. (1993). Chemical sensors for radiopharmaceuticals. *Radiochimica Acta, 63*, 199–204. https://doi.org/10.1524/RACT.1993.63.SPECIAL-ISSUE.199
71. Theresa Lee, M. B., Seliskar, C. J., Heineman, W. R., & McGoron, A. J. (1997). Drug news Persp. *International Journal of Radiation Applications and Instrumentation Part B Nuclear Medicine and Biology, 45*, 6434–6435.
72. Akgun, E., Ozgenc, E., & Gundogdu, E. (2021). Therapeutic applications of radiopharmaceuticals: An overview overview of radiopharmaceuticals used in treatment. *Journal of Pharmaceutical Sciences, 46*, 93–104.
73. Jiang, L., Schipper, M. L., Li, P., & Cheng, Z. (2009). 123I-labeled metaiodobenzylguanidine for diagnosis of neuroendocrine tumors. *Reports in Medical Imaging, 2*, 79–89. https://doi.org/10.2147/RMI.S4529
74. Symonds, R. P. (2001). Radiotherapy. *BMJ, 323*, 1107–1110. https://doi.org/10.1136/BMJ.323.7321.1107
75. Rouiller, N., Nicod Lalonde, M., & Sykiotis, G. P. (2022). Anti-thyroglobulin antibodies as a possible risk factor for graves' disease after radioiodine treatment for toxic nodular goiter: Case report. *Frontiers in Nuclear Medicine, 2*. https://doi.org/10.3389/FNUME.2022.858062
76. National Cancer Institute Radiation Therapy for Cancer - NCI. https://www.cancer.gov/about-cancer/treatment/types/radiation-therapy

77. Macklis, R. M., & Pohlman, B. (2006). Radioimmunotherapy for non-Hodgkin's lymphoma: A review for radiation oncologists. *International Journal of Radiation Oncology Biology Physics., 66*, 833–841. https://doi.org/10.1016/J.IJROBP.2006.05.030
78. Pandit-Taskar, N., Batraki, M., & Divgi, C. R. (2004). Radiopharmaceutical therapy for palliation of bone pain from osseous metastases. *The Journal of Nuclear Medicine •, 45*, 1358.
79. Semaan, S., Makkar, J., Lewis, S., Chatterji, M., Kim, E., & Taouli, B. (2017). Imaging of hepatocellular carcinoma response after 90Y radioembolization. *AJR Am J Roentgenol., 209*, W263–W276. https://doi.org/10.2214/AJR.17.17993
80. Tomblyn, M., & Moffi, H. L. (2012). Radioimmunotherapy for B-cell non-Hodgkin lymphomas from the Department of Radiation Oncology at the. *Cancer Control, 19*, 196.
81. Lee, S. L. (2012). Radioactive iodine therapy. *Current Opinion in Endocrinology, Diabetes, and Obesity, 19*, 420–428. https://doi.org/10.1097/MED.0B013E328357FA0C
82. Curanosticum Thyroid diagnostics and therapy - Praxis für Nuklearmedizin PET-CT Zentrum. https://www.curanosticum.de/en/services/thyroid-diagnostics-and-therapy/. (Accessed 30 Jul 2022).
83. Kayano, D., & Kinuya, S. (2018). Current consensus on I-131 MIBG therapy. *Nuclear Medicine and Molecular Imaging, 52*(4), 254–265. https://doi.org/10.1007/S13139-018-0523-Z